GEOLOGICA ULTRAIECTINA

Mededelingen van de
Faculteit Aardwetenschappen
Universiteit Utrecht

No. 121

PROVENANCE AND DISPERSAL OF SAND-SIZED SEDIMENTS

Reconstruction of dispersal patterns and sources of sand-sized sediments by means of inverse modelling techniques

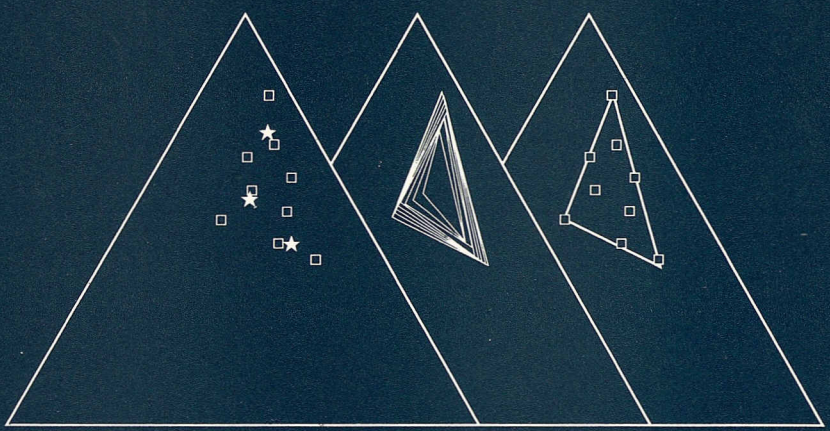

G. J. Weltje

GEOLOGICA ULTRAIECTINA

Mededelingen van de
Faculteit Aardwetenschappen
Universiteit Utrecht

No. 121

PROVENANCE AND DISPERSAL OF SAND-SIZED SEDIMENTS

Reconstruction of dispersal patterns and sources of sand-sized sediments by means of inverse modelling techniques

G. J. Weltje

27-022

CIP-GEGEVENS KONINKLIJKE BIBLIOTHEEK, DEN HAAG

Weltje, Gerardus Johannes

Provenance and dispersal of sand-sized sediments : reconstruction of dispersal patterns and sources of sand-sized sediments by means of inverse modelling techniques / Gerardus Johannes Weltje. - Utrecht : Faculteit Aardwetenschappen, Universiteit Utrecht. - (Geologica Ultraiectina, ISSN 0072-1026 ; no. 121)
Proefschrift Universiteit Utrecht. - Met lit. opg. - Met samenvatting in het Nederlands.
ISBN 90-71577-75-9
Trefw.: zand / geodynamica

PROVENANCE AND DISPERSAL OF SAND-SIZED SEDIMENTS

Reconstruction of dispersal patterns and sources of sand-sized sediments by means of inverse modelling techniques

HERKOMST EN VERSPREIDING VAN ZANDIGE SEDIMENTEN

Reconstructie van distributiepatronen en bronnen van zandige sedimenten met behulp van inverse modelleertechnieken

(met een samenvatting in het Nederlands)

PROEFSCHRIFT TER VERKRIJGING VAN DE GRAAD VAN DOCTOR
AAN DE UNIVERSITEIT UTRECHT
OP GEZAG VAN DE RECTOR MAGNIFICUS,
PROF. DR. J.A. VAN GINKEL
INGEVOLGE HET BESLUIT VAN HET COLLEGE VAN DECANEN
IN HET OPENBAAR TE VERDEDIGEN
OP MAANDAG 16 MEI 1994 DES MORGENS TE 10.30 UUR

door

GERARDUS JOHANNES WELTJE
geboren op 24 oktober 1962 te Eindhoven

Promotor: Prof. Dr. D. Eisma

Co-promotor: Dr. P.L. de Boer

.... Lo abrí al azar. Los caracteres me eran extraños. Las páginas, que me parecieron gastadas y de pobre typografía, estaban impresas a dos columnas a la manera de una biblia. [.....] Volví [una página]; el dorso estaba numerado con ocho cifras. Llevaba una pequeña ilustración, como es de uso en los diccionarios: un ancla dibujada a la pluma, como por la torpe mano de un niño. Fue entonces que el desconocido me dijo:
- Mírela bien. Ya no la verá nunca más.
Había una amenaza en la afirmacíon, pero no en la voz. Me fijé en el lugar y cerré el volumen. Inmediatamente lo abrí. En vano busqué la figura del ancla, hoja tras hoja.....

Jorge Luis Borges - El libro de arena (1975)

.... I opened it at random. The characters were strange to me. The pages, which were worn and typographically poor, were laid out in double columns, as in a bible. [.....] I turned a page; the overleaf was numbered with eight digits. It also bore a small illustration, like the kind used in dictionaries: an anchor drawn by pen and ink, as if by a child's clumsy hand.
It was at this point that the stranger said:
- Look at it closely. You'll never see it again.
There was a threat in his words, but not in his voice. I memorized the spot and closed the book. Immediately, I reopened it. In vain, I looked for the illustration of the anchor, page by page.....

Jorge Luis Borges - The book of sand (1975)

Dankwoord

Mijn promotor, Prof. Dr. D. Eisma, bedank ik voor zijn opbouwende kritiek en wetenschappelijke ondersteuning bij de totstandkoming van dit proefschrift.

Ik ben bijzonder veel dank verschuldigd aan mijn co-promotor, Dr. P.L. de Boer, die mij gestimuleerd heeft om de methodologische aspecten van het onderzoek nadrukkelijk vorm te geven. Als onderzoeksbegeleider wist hij relativeringszin te koppelen aan enthousiasme voor de sedimentaire geologie, hetgeen voor mij erg inspirerend en waardevol is geweest.

De prettige sfeer bij de Afdeling Sedimentologie heeft in niet geringe mate bijgedragen aan de totstandkoming van dit proefschrift. Ik bedank hiervoor mijn collega's Dr. J.H. Baas, Dr. N. Molenaar, Drs. W. Nijman, Drs. A.P. Oost, Dr. M.A. Pool, Dr. G. Postma, Drs. M. Prins, Drs. J.H. ten Veen en Dr. J.J.P. Zijlstra.

De aard van mijn onderwerp noopte mij met grote regelmaat om de periferie van de sedimentaire geologie te verkennen. Mijn dank gaat uit naar een groot aantal collega's op de Faculteit Aardwetenschappen, die mij hun specialistische kennis ter beschikking stelden en met wie ik op plezierige wijze van gedachten heb gewisseld.

In het bijzonder wil ik noemen Drs. J.A. van Dam, Dr. F.J. Hilgen, Prof. Dr. J.E. Meulenkamp, Dr. E.J. Rohling, Dr. W.J. Zachariasse en Prof. Dr. G.J. van der Zwaan (Stratigrafie/Paleontologie), Dr. W. Spakman en Prof. Dr. M.J.R. Wortel (Geofysica), Dr. C.A. Langereis en Prof. Dr. J.D.A. Zijderveld (Paleomagnetisme), Dr. G. Frapporti en Dr. S.P. Vriend (Geochemie), en Dr. R.L.M. Vissers (Structurele Geologie). Hun belangstelling, opbouwende kritiek en nuttige adviezen hebben mij zeer geholpen.

Drs. N.M.M. Janssen (Paleobotanie/Palynologie) leverde met zijn palynologische analyses een onmisbare bijdrage aan hoofdstuk 5 van dit proefschrift.

Voor vakkundige monsterpreparatie, laboratoriumanalyses en technische ondersteuning bedank ik de medewerkers van het Laboratorium Sedimentologie (mevr. J.M.M. Reith, dhr. H. Wijland en dhr. T. Zalm), het Laboratorium Paleontologie (dhr. G.J. van 't Veld en dhr. G.C. Ittmann) en de Afdeling Gesteentepreparatie (dhr. J.W. de Groot, dhr. J. Drenth, mevr. I. Nussgen en dhr. O.H. Stiekema).

De staf van de Bibliotheek Faculteit Aardwetenschappen (mevr. A.W.H. Jansen-Corbeek, dhr. W. van Hattem, dhr. J.C. Jansen, mevr. A. van Rhee-van der Heide, dhr. M.W.J.M. Stelling en dhr. F. Verdaasdonk) bedank ik voor het opsporen van literatuur in binnen- en buitenland; de medewerkers van de Audiovisuele Dienst (dhr. F.J. Quint, mevr. B.J.M. Benders, dhr. J.J. Bergenhenegouwen, dhr. R. Meije, dhr. I.M. Santoe en dhr. A. Trappenburg) voor het vervaardigen van de vele tekeningen en foto's in het proefschrift.

Ik ben veel dank verschuldigd aan Drs. B.J. Westerop, die het manuscript heeft gecorrigeerd en redactioneel advies heeft geboden.

De voortdurende belangstelling van familie, vrienden en kennissen voor mijn wel en wee heeft de minder aangename kanten van het werk een stuk aangenamer gemaakt. Op bepaalde momenten in de afgelopen jaren heb ik mij met moeite aan de indruk kunnen onttrekken dat men in de "buitenwereld" het verrichten van een promotieonderzoek als een weinig begeerlijke taak beschouwt. Het was dus nodig om mij "op te vrolijken", waarvoor dank. De heilzame werking van de SRHC bijeenkomsten, welke tot doel hadden om op hoog niveau van gedachten te wisselen over een breed scala van maatschappelijk relevante onderwerpen, mag in dit verband zeker niet ongenoemd blijven.

Mijn ouders hebben mij een kritische houding ten aanzien van ogenschijnlijk vanzelfsprekende zaken bijgebracht, een eigenschap die ik in de afgelopen jaren ten volle heb proberen te benutten. Ik ben hen bijzonder dankbaar voor hun niet aflatende steun.

Mijn grootste dank gaat uit naar Marike Poldervaart, voor het blijmoedig tolereren van mijn obsessieve aandacht voor het promotieonderzoek, alsmede haar "fieldwork assistance", wetenschaps-filosofische inbreng en morele ondersteuning. Dit product van een onderzoek dat mij dwong om vijf jaar lang mijn "kop in het zand te steken" draag ik aan haar op.

CONTENTS

Samenvatting 11

Introduction and summary 13

1. History of provenance studies and data analysis in sedimentary petrography 17

2. Compositional variation of siliciclastic sands 29

3. End-member modelling of compositional data: numerical-statistical algorithms for solving the mixing problem in sedimentary provenance studies 47

4. Unravelling mixed provenance of coastal sands: the Po delta and adjacent beaches of the northern Adriatic Sea as a test case 87

5. Oligocene to Early Miocene sedimentation and tectonics in the southern part of the Calabrian-Peloritan Arc (Aspromonte, southern Italy): a record of mixed-mode piggy-back basin evolution 121

6. End-member modelling as a tool for tracing Paleogene thrust-wedge evolution in the southern part of the Calabrian-Peloritan Arc (Sicily, Italy) 149

7. High-frequency detrital signals in Eocene fan-delta sandstones of mixed parentage (South-Central Pyrenees, Spain): a reconstruction of chemical weathering in transit 165

8. Astronomically induced palaeoclimatic oscillations reflected in Pliocene turbidite deposits on Corfu (Greece): implications for the interpretation of higher-order cyclicity in ancient turbidite systems 183

References 190

Curriculum Vitae 208

Publications based on this PhD Thesis

Chapter	Reference
0.1-1.2	Weltje, G.J., von Eynatten, H., 2004. *Sedimentary Geology*, 171, 1-11.
1.3-1.6	Weltje, G.J., 2002. *Earth-Science Reviews*, 57, 211-253.
2	Weltje, G.J., Meijer, X.D., de Boer, P.L., 1998. *Basin Research*, 10, 129-153.
3	Weltje, G.J., 1997. *Mathematical Geology*, 29, 503-547.
4	Weltje, G.J., 1995. In: *Geology Of Deltas* (Oti, M.N., Postma, G., Eds.), Balkema, Rotterdam, p. 181-202.
5	Weltje, G.J., 1992. *Basin Research*, 4, 37-68.
6	[Unpublished]
7	Weltje, G.J., van Anssenwoude, S.O.K.J., de Boer, P.L., 1996. *Journal of Sedimentary Research*, 66, 119-131.
8	Weltje, G.J., de Boer, P.L., 1993. *Geology*, 21, 307-310.

Errata

p. 31, Fig. 1: "treshold" should read "threshold" (2x); p. 32, Fig. 2: data point at (0.0,4.5) should be eliminated; p. 33, Fig. 3: should be labeled "A" (upper) and "B" (lower); p. 34, Fig. 4: should be labeled "A" (upper) and "B" (lower)

p. 75, Table number should be "3" instead of "1"

p. 103, Fig. 6 shows incorrect values for sparite, micrite, and bioclasts; p. 109, Table 4: horizontal line between "Reno" and "Lamone" is missing; p. 116, Table 6: "original" and "new" should be switched

p. 163, "ST" in caption to Fig. 7 should read "ST/AS"

p. 207: "Woronov" should read "Woronow" (3x)

Samenvatting

Dit proefschrift is gewijd aan de kwantitatieve analyse van de samenstelling van zandige sedimenten (zand en zandsteen). De mineralogisch-petrografische samenstelling van zand is systematisch bestudeerd vanaf de tweede helft van de negentiende eeuw, met als doel de herkomst (*"provenance"*) van het materiaal te achterhalen. De ontwikkeling van kwantitatieve "herkomstmodellen" staat nog steeds in de kinderschoenen, ondanks de respectabele ouderdom van de sediment-petrografie. Dit is voor een belangrijk deel te wijten aan de complexiteit van het proces van sedimentvorming, maar het weerspiegelt eveneens de betrekkelijk geringe aandacht voor kwantitatieve methoden waarmee de herkomst van sedimenten op objectieve wijze kan worden gereconstrueerd.

In het eerste deel van dit proefschrift (hoofdstuk 1 en 2) wordt een overzicht gegeven van de historische ontwikkeling van sediment-petrografische studies en worden veel gebruikte kwantitatieve analysemethoden kort en kritisch besproken (hoofdstuk 1). Daarna wordt een overzicht gepresenteerd van de belangrijkste factoren die van invloed zijn op de petrografische samenstelling van zand en op de veranderingen in de samenstelling die optreden ten gevolge van verwering, transport en sedimentatie (hoofdstuk 2). Twee extreme typen sedimentaire bekkenvullingen worden onderscheiden: Type 1 bekkenvullingen, waarin verschillen in sedimentsamenstelling primair worden veroorzaakt door menging van materiaal uit meerdere bronnen; Type 2 bekkenvullingen bestaan uit sedimenten die afkomstig zijn uit één bron, die sediment levert waarvan de samenstelling varieert ten gevolge van veranderingen in de mate van verwering. Voor beide situaties zijn specifieke kwantitatieve analysemethoden ontwikkeld. Deze methoden worden behandeld en vervolgens toegepast op een aantal voorbeelden in de volgende delen van het proefschrift.

Het tweede deel van het proefschrift (hoofdstuk 3 en 4) is gewijd aan de analyse van compositionele variatie in type 1 bekkenvullingen met behulp van lineaire mengmodellen. De waargenomen samenstellingsvariatie kan met behulp van een inverse modelleertechniek worden uitgedrukt als het resultaat van menging van materiaal uit een minimaal aantal sedimentbronnen. De numerieke en statistische achtergronden van deze methode worden uitgebreid besproken in hoofdstuk 3. De benodigde informatie voor een objectieve reconstructie van de herkomst van sedimenten bestaat uit de berekende samenstellingen van de sedimenten die werden geleverd door de bronnen (de "eindleden" van het mengmodel) en de verhoudingen waarin deze sedimenten zijn gemengd. Met dit model wordt de samenstelling van ieder monster zo goed mogelijk benaderd. De brongebieden van fossiele bekkens zijn in het algemeen onbekend. In zulke gevallen kan aan de hand van het ruimtelijke patroon van berekende mengverhoudingen worden voorspeld uit welke richtingen sediment werd aangevoerd en langs welke wegen het binnen het bekken werd verspreid. In hoofdstuk 4 worden de uitkomsten van deze modelleertechniek getoetst aan de hand van een analyse van recente strandzanden uit een gebied in Noord-Italië waarvan de recente geschiedenis en de huidige situatie goed bekend zijn (de Po delta en aangrenzende kustgebieden van de Adriatische Zee). De resultaten van dit experiment laten zien dat de inverse modelleertechniek van grote betekenis kan zijn voor de reconstructie van fossiele bekkens en hun achterland.

Een reconstructie van de herkomst van sedimenten als hulpmiddel bij paleotectonisch onderzoek wordt behandeld in het derde deel van het proefschrift (hoofdstuk 5 en 6) aan de hand van een voorbeeld uit de Calabrees-Peloritaanse Boog (Zuid-Calabrië en Sicilië, Italië). De vroeg-Tertiaire geschiedenis van dit gebied wordt gereconstrueerd in hoofdstuk 5, met behulp van veldgegevens en data uit de literatuur. De gereconstrueerde bekkenontwikkeling in Zuid-Calabrië sluit goed aan bij de veronderstelde ontwikkeling van de Calabrees-Peloritaanse dekbladstapel die het substraat vormt van de bestudeerde bekkens. In hoofdstuk 6 wordt de groeiwijze van de dekbladstapel op Sicilië in groter detail gereconstrueerd. De compositionele ontwikkeling van de vroeg-Tertiaire bekkenvullingen, die in en op de dekbladstapel voorkomen, wordt geanalyseerd met het mengmodel. Uit de resultaten van het model blijkt dat de groeiwijze van de dekbladstapel nauw aansluit bij de in hoofdstuk 5 gereconstrueerde bekkenontwikkeling.

Het laatste deel van het proefschrift (hoofdstuk 7 en 8) is gewijd aan de analyse en interpretatie van hoog-frequente signalen in bekkenvullingen langs actieve marges (de type 2 bekkenvullingen genoemd in hoofdstuk 2). In hoofdstuk 7 wordt de samenstelling van sediment in een Eocene puinwaaier in de zuidelijke Pyreneeën (Spanje) in detail geanalyseerd. Menging van sediment uit verschillende bronnen blijkt samen te gaan met variaties in de mate van verwering in het achterland. In hoofdstuk 8 wordt het belang van een goede tijdscontrole voor het onderscheid tussen de effecten van klimaatsfluctuaties en die van zeespiegelbewegingen geïllustreerd aan de hand van de analyse van een Plioceen turbidietsysteem op Corfu (Griekenland). De sedimentaanvoer en het groeipatroon van dit turbidietsysteem lijken vrijwel uitsluitend te zijn bepaald door regionale paleoklimatologische factoren. Deze twee voorbeelden laten zien hoe subtiele variaties in de samenstelling van zandsteen kunnen worden gebruikt bij de reconstructie van hoog-frequente veranderingen in fossiele sedimentaire systemen.

INTRODUCTION AND SUMMARY

1. Sedimentary provenance studies

Sand is loose, non-cohesive granular material. By definition, the grains or framework elements of sand range between 0.0625 (1/16) and 2.0 mm in diameter (4 to -1 ϕ on the base-two logarithmic grade scale). However, definitions of sand as a deposit - apart from the size term - are diverse. No generally accepted usage is apparent from a review of the literature with regard to the permissible proportions of oversized or undersized material in sand. The term sandstone is restricted to consolidated sands. In general, no reference is made to their composition or genesis (Pettijohn et al., 1972). The terminology adopted in this study follows similar conventions: the notions "sand" and "sandstone" are used to indicate loose and consolidated granular materials in the sand-size range, respectively, without reference to composition and genesis. The term "sand-sized sediment" is used to encompass both "sand" and "sandstone".

Sand-sized sediments consist largely of detrital grains, derived from mechanical and chemical weathering of (crystalline) parent rocks. The initial compositional and textural characteristics of sand-sized detritus are modified by attrition and sorting during transport, when the sediments are carried away from the source area. Chemical weathering during temporary storage, and mixing with sediments from other sources may further obscure the original characteristics, especially when dispersal pathways are complex and involve recycling of previously deposited sediments. After deposition and burial, sediment properties are commonly affected by diagenetic processes. The ultimate properties of a sand-sized sediment thus reflect the parent lithology and the history of modifications by weathering, transport, deposition, and diagenesis.

The intent of provenance studies is to reconstruct and to interpret the history of a sediment from the initial erosion of a parent rock to the final burial of its detritus, i.e., to unravel the "line of descent" or "lineage" of the sediment under investigation. Literally, the French word "provenance" means "origin" or "source". In sedimentary petrology, the term provenance has been used to encompass all factors related to the production of sediment, with specific reference to the composition of the parent rocks and the physiography of the source area from which the sediment is derived (Pettijohn et al., 1972).

The ultimate goal of provenance studies is to deduce the characteristics of source areas from measurements of compositional and textural properties of sediments, supplemented by information from other lines of evidence. "*A solution of the problem of provenance will immeasurably increase our understanding of the paleogeography of a region, enabling us to locate and identify possible source lands. We may also be able to trace the movement of materials and thus say something about paleocurrents and paleoslopes. The combination of source and paleocurrents leads to inferences of tectonics and climate, the primary controlling influences on sedimentary mineralogy*" (Pettijohn et al., 1987).

If "rules" governing the production of sediments can be identified, the amount and the compositional-textural properties of sediments produced under given tectonic and climatic conditions can be predicted. However, the current state of affairs in sedimentary provenance studies does not yet allow for such predictions. The development of quantitative provenance models, which relate vertical and/or lateral compositional trends within basin fills to the tectonic evolution of a source terrain, to changing sediment dispersal patterns, and/or to palaeoclimatic fluctuations, is still in its infancy.

The complex relationships of source and sediment cannot be fully explained, even in cases where both have been studied extensively, because a lot of information is invariably lost by the wide spectrum of compositional and textural modifications which affect a sediment along the pathway from source to basin. The complexity of these modifications imposes certain limits on our capability to predict the characteristics of source areas from the properties of their products, just like *"...we cannot tell all we want to know of a sand grain's origin from its composition alone, any more than we can deduce political history from human physiology"* (Siever, 1988).

In spite of the many difficulties associated with the subject of sediment provenance, a large number of studies on characteristics of sand-sized sediments has allowed to formulate general theories of provenance and of factors that control compositional modifications. Examples of such theories are the relation between sand(stone) composition and global tectonics (cf. Dickinson, 1985, 1988), the climatic-physiographic control on sand(stone) composition (cf. Basu, 1985a; Suttner & Dutta, 1986), and the relation between parent lithologies and quartz-grain subpopulations of sand-sized sediments (cf. Basu et al., 1975; Basu, 1985b). Such general theories of sediment provenance do not necessarily provide the "correct" answer to each specific question, but serve as a baseline for interpreting differences between observations and predictions based on theoretical considerations.

The sediment-forming process has been discussed in detail by Ibbeken & Schleyer (1991) in a comprehensive study of provenance and mass balance at an active plate margin in Calabria, southern Italy. The objective of this quantitative study was to predict compositional and textural properties of river-mouth sediments on the basis of a thorough investigation of drainage-basin characteristics. The authors captured the essence of modern provenance research, by concluding that *"...if we gather adequate data about a mountainous area being eroded, we should be able to predict certain features of the resulting river-mouth sediments. [...] nobody expects these predictions to be verified by nature, but the interpretation of the differences between the predicted and the real sediment should improve our understanding of provenance"* (Ibbeken & Schleyer, 1991).

2. Scope and outline of the thesis

Sedimentary provenance studies attempt to link spatial and temporal patterns of compositional variation in basin fills to the evolution of source areas. The aim of this thesis is to propose a general framework for the study of spatial and temporal patterns of compositional variation of sand-sized sediments by means of quantitative methods. A number of techniques is presented which aim at providing a concise summary and/or

explanation of compositional variation observed in natural sedimentary systems. This field of research is sometimes referred to as "provenance modelling".

The usefulness of a quantitative "provenance model" is largely determined by the extent to which the general mathematical form of the model reflects the presumed underlying mechanism(s) of compositional variation, as inferred from field and laboratory studies. Furthermore, the model should be as simple as possible. Because much of the provenance information is invariably lost by compositional modifications in transit, and there is no real hope of reconstructing the "actual" source area characteristics, parsimonious models which are capable of providing a simple explanation of the observed phenomena are preferred over more complex models. The use of more complex models should be considered only if a simple model fails to provide a mathematically and/or geologically feasible description of compositional variation within the sedimentary system under study.

The provenance modelling techniques presented in this thesis are applied to a variety of problems in the field of sedimentary geology, in order to evaluate their general usefulness for basin and source reconstructions. A multidisciplinary approach to geological reconstructions is emphasized throughout the thesis, in order to stress the importance of a successful integration of provenance studies with other fields of basin analysis.

The **first part (chapters 1 & 2)** consists of an introduction to the field of sedimentary petrography and provenance studies. The historical development of provenance studies is briefly summarized, followed by an overview of methodological aspects of data acquisition and data analysis. Subsequently, compositional modifications of sand-sized sediments are discussed within the context of a sedimentary cycle in order to provide a frame of reference for quantitative provenance interpretations. The nature of compositional modifications and their relative importance in various geological settings, expressed in terms of their effects on "petrographic framework composition" allows to distinguish two extreme cases of compositional variation in sedimentary basin fills: (1) Basin fills derived from multiple sources, in which linear compositional modifications induced by physical mixing are the principal determinants of the observed variation; (2) Basin fills derived from a single source, in which non-linear compositional modifications induced by physical and chemical weathering are the principal determinants of the observed variation. Numerical-statistical modelling techniques developed for solving problems associated with these two situations, as well as selected applications to recent and fossil cases, are discussed in subsequent parts.

In the **second part (chapters 3 & 4)**, an inverse modelling approach is presented for recasting observed compositional variation of sedimentary basin fills into a linear mixing model. The mixing model provides a quantitative estimate of the minimum number of sediment sources, their compositional characteristics, and their proportional contributions to each observation. A description of the observed compositional variation in terms of a mixing model allows to partition the basin fill into subpopulations of sediments shed by different sources, whose (paleo)geographic locations can be predicted on the basis of the spatial mixing pattern. The performance of the inverse model is evaluated by applying it to a well-constrained test case: modern beach sands of the Po-delta front and adjacent parts of the Northern Adriatic coast (Italy). The availability of data on the actual fluvial input, present longshore drift patterns and the late Holocene coastal evolution in this area allows for rigorous testing of model predictions. The results of this experiment suggest that the

inverse modelling approach is a powerful tool for reconstructing sediment dispersal paths and source-area characteristics.

An application of provenance modelling to paleotectonic reconstructions is discussed in the **third part (chapters 5 & 6)**. It is based on a case history of basin evolution in a complex geodynamic setting: the Calabrian-Peloritan Arc (southern Italy). The Late Oligocene to Early Miocene sedimentation and deformation history of this active margin has been reconstructed by combining sedimentological, stratigraphical and structural field data with information from the literature (chapter 5). In chapter 6, a mixing model of tectonically controlled compositional evolution and sediment dispersal in Late Eocene to Early Miocene thrust-sheet-top basins on Sicily is combined with stratigraphic and structural data in order to propose a scenario of Paleogene thrust-wedge evolution in the southern part of the Calabrian-Peloritan Arc. This scenario provides additional support for the tectono-sedimentary reconstruction presented in the previous chapter.

The **fourth part (chapters 7 & 8)** is devoted to the analysis and interpretation of high-frequency detrital signals in fossil depositional systems. The origin and preservation of such signals in active-margin settings is discussed within a framework provided by climatic fluctuations, sea-level fluctuations, and tectonics. Eocene fan-delta sediments from the South-Central Pyrenees (Spain) are used to illustrate the patterns of variation arising from the combined effects of mixing and weathering in the source area (chapter 7). The importance of high-resolution time control for the interpretation of compositional and lithological variation in turbidite sequences is discussed with reference to a Pliocene turbidite system on Corfu (Greece) in chapter 8. The results of these two studies indicate that high-frequency palaeo-environmental changes can be reconstructed by careful analysis of sandstone framework composition.

CHAPTER 1

HISTORY OF PROVENANCE STUDIES AND DATA ANALYSIS IN SEDIMENTARY PETROGRAPHY

1. Studies of accessory minerals

The notion that the origin of sand can be deduced from the mineralogical properties of its constituents dates back to the end of the nineteenth century. During this pioneering phase of sedimentary petrology, attention was paid primarily to the accessory minerals of sands, whose specific gravities are greater than those of the major framework constituents. These "heavy" minerals form usually less than one percent of the volume of sand-sized sediments, but there are over thirty translucent species of common occurrence (Morton, 1985). The relatively high number of heavy-mineral species and their often characteristic paragenesis have always made them a popular tool for provenance studies.

According to Boswell (1933), mineralogical investigations made prior to 1870 were entirely descriptive. The first attempts to trace heavy minerals of recent beach and river sands to their parent rocks were made by Ludwig (1874), Meunier (1877), and Michel Lévy (1878). The study of heavy minerals in fossil sediments started with the work of Thürach (1884). Retgers (1895) was the first to make explicit suggestions as to the use of heavy minerals for determining ancient drainage directions and other palaeogeographic features.

The objective of the earliest provenance studies was to determine the parent rocks of single minerals or mineral varieties (cf. Thürach, 1884). Detailed inventories were made of the accessory minerals of igneous and metamorphic rocks in order to trace particular heavy minerals to their sources. A theoretical framework for these investigations was formulated by Brammall (in Milner, 1922), who proposed the concept of the "*distributive province*", defined as "*..the environment embracing all rocks, igneous, metamorphic and sedimentary, contributing to the formation of contemporaneously accumulated sediment*" (Milner, 1962). Distributive provinces were delineated on the basis of criteria such as the presence or absence of diagnostic mineral varieties. The studies of Brammall (1928) and Groves (1931) are classical examples of the use of heavy minerals for the reconstruction of sediment dispersal from well known source areas. In the same period, Boswell (1915, 1916) and Illing (1916) pioneered the use of heavy minerals for lithostratigraphic correlation purposes.

The quantitative study of heavy-mineral assemblages began with the work of Fleet (1926), who introduced the method of counting grains in order to make the determination of the relative frequency of mineral occurrences more objective. Edelman (1931, 1933) strongly advocated a quantitative assessment of the entire heavy-mineral assemblage for provenance studies and correlation purposes, rejecting the qualitative (presence-absence) criteria on which the concept of the distributive province was based. His principal objection against this concept was that the proportional contribution of a distributive province to a sediment body could have been negligible, in view of the fact that its recognition may depend on the presence of an extremely rare diagnostic mineral. Instead, he proposed the concept of the

"*sedimentary petrological province*", defined as "*..a distinctive, homogeneous sediment body which constitutes a natural unit in terms of age, origin and geographical distribution*" (Edelman, 1933). The latter concept was used successfully in a series of monographic studies on the distribution of Quarternary sands of the North Sea Basin (Edelman, 1933; Van Baren, 1934; Baak, 1936). It subsequently gained wide acceptance as a basic element of classification in provenance studies of heavy-mineral assemblages (Hubert, 1971; Suttner, 1974; Morton, 1985).

In the 1930's and 1940's it was recognized that factors other than provenance exert fundamental controls on the composition of heavy-mineral assemblages. The reliability of subsurface correlation by heavy minerals was questioned as the evidence of hydrodynamic and diagenetic controls (selective transport, weathering and "intrastratal solution") on the composition of heavy-mineral assemblages accumulated (e.g. Pettijohn, 1941). This notion, coupled with the development of biostratigraphic correlation and geophysical logging techniques, resulted in a decline in popularity of applied heavy-mineral research (Hubert, 1971; Morton, 1985).

However, the usefulness of heavy minerals as provenance indicators of recent sediments remains undisputed. The analysis of long-term dispersal patterns has turned out to be a useful tool for monitoring the infill of sedimentary basins and the evolution of their source areas, as shown by studies carried out from the 1950's onwards in a variety of modern basins (e.g. Van Baren & Kiel, 1950; Van Andel & Poole, 1960; Pilkey, 1963; Van Andel, 1950, 1964; Hubert & Neal, 1967; Pigorini, 1968; Eisma, 1968; Davies & Moore, 1970; Gazzi et al., 1973; Stanley et al., 1975; Milliman & Summerhayes, 1975; Flores & Shideler, 1978; Clemens & Komar, 1988; Mezzadri & Saccani, 1989). In a similar fashion, careful studies of fossil heavy-mineral assemblages have continued to provide information for palaeogeographic reconstructions, as illustrated by Füchtbauer (1964), Wildi (1985), Stattegger (1987), Bernouilli & Winkler (1990), and Winkler & Slaczka (1992).

Recent developments in provenance studies indicate a revitalisation of heavy-mineral research, particularly in the form of "varietal" studies. In "varietal" studies, use is made of a single family of grains, which displays a sufficiently wide range of geochemical compositional variability to allow the distinction of various subpopulations within the sediments being studied. Garnets have been used most frequently for this purpose (e.g., Morton, 1985). The reason for this renewed interest is that sophisticated analytical methods for the study of individual grains have become available in recent years. The advantage of such "varietal" studies is that differences between heavy-mineral assemblages introduced by factors other than provenance (e.g., chemical stability, size, shape, specific gravity) are minimized. Current trends in heavy-mineral research, as summarized by Morton (1985), Suttner (1989), and Haughton et al. (1991), include the use of electron microprobe analysis for investigating the compositional range of heavy mineral populations, and the use of radiometric dating techniques of single grains.

2. Studies of principal framework grains

Provenance studies of major framework constituents began with the investigation of quartz varieties by Sorby (1880). Judd (1886) first recognized the influence of climate on the

preservation of feldspars. These early studies were expanded by Mackie (1899a, b), who established criteria for the recognition of quartz derived from igneous and metamorphic rocks, and the use of feldspars as indicators of contemporaneous climate. In the same period, Retgers (1895) studied the feldspars of the Dutch dune sands in order to decipher their provenance. In spite of these early investigations, there was little interest in the study of major framework components of sand-sized sediments during the first decades of the twentieth century, when stratigraphic heavy-mineral studies flourished. It was widely believed that "*..the lighter constituents do not provide a sufficient variety of minerals to yield any criteria of stratigraphical importance; quartz and feldspars are ubiquitous and that is about all that can be said*" (Solomon, 1932). In the same period, Cayeux (1906, 1929), Goldman (1915), Gilligan (1920), and Dake (1921) carried out the first thin-section studies of sandstones in which particular attention was paid to the major framework constituents.

The quantitative investigation of the bulk mineralogy of sands started in the 1930's with the studies of Trowbridge & Shepard (1932), Van Baren (1934), and Russell (1937). In the 1940's, Krynine and Pettijohn proposed the first versions of the sandstone classification schemes which are still being used (Klein, 1963; Okada, 1971). Krynine also strongly advocated the importance of tectonic control on the compositional and textural properties of sandstones, inspired by the ideas of his teacher Shvetsov (Folk, 1980). The interest in the bulk mineralogical and textural properties of sand-sized sediments increased strongly during the subsequent decades, partly as a result of the declining popularity of heavy-mineral studies. In the 1960's, framework mineralogy was used to infer parent-rock assemblages and weathering conditions in the source areas of fossil sediments. However, many of these inferences were based on scanty evidence or on generalisations which had not been substantiated by a thorough investigation of modern analogues (Blatt, 1967; Pettijohn et al., 1972; Suttner, 1974).

As the geosynclinal theory was replaced by the paradigm of plate tectonics in the late 1960's (Mitchell & Reading, 1986), provenance studies received new impulses through the work of Dickinson (1970), who established clearcut operational definitions for different grain types in order to make quantitative detrital modes reproducible. Subsequently, Dickinson & Suczek (1979) and Dickinson & Valloni (1980) convincingly demonstrated that the modal composition of sand-sized sediments is largely determined by plate-tectonic setting, confirming earlier suggestions of Crook (1974) and Schwab (1975). The appeal of this apparently simple method for identification of ancient plate-tectonic settings led to an enormous interest in the study of sandstone framework mineralogy and the rapid buildup of a petrographic database (Breyer, 1983; Valloni, 1985; Dickinson, 1985, 1988). Although this theory has turned out to be well suited for the reconstruction of long-term plate motions and geotectonic settings of sedimentary basins, it does not provide the resolution needed for provenance reconstructions on smaller temporal and spatial scales (Ingersoll, 1990).

The influence of climate and relief in the source area on the composition of recent fluvial sands has been studied systematically since the 1970's. The relevance of these studies for palaeoclimatic interpretations is beginning to be recognized now that attention focusses on (global) climatic changes, as demonstrated by the increasing number of papers on this subject (summarized by Basu, 1985a; Dutta, 1992). Another important development in recent years has been the trend towards the use of stable isotope data, bulk chemical

compositions and trace elements for provenance determinations (Suttner, 1989; Haughton et al., 1991). Much of the progress made in the past decade is the result of a multidisciplinary approach and the use of increasingly sophisticated methods of data acquisition.

3. Data acquisition in sedimentary petrography

Optical analysis of thin sections has been the principal method of data acquisition in provenance studies. Following generally accepted procedures, the petrographic composition of sand-sized sediments is estimated by point-counting 200 to 500 grains in a thin section, and assigning each grain to a category within the mineralogical-petrographical classification system used. Different "schools" of sedimentary petrologists have evolved over the past decades. Each developed its own point-counting method and classification criteria for the quantification of sand(stone) composition. Two methods have been used widely and are discussed in more detail below: the "Indiana" method and the "Gazzi-Dickinson" method. The main difference between these methods is the procedure used for the classification of coarse-crystalline polymineralic grains. The relative strengths and weaknesses of both methods have been discussed extensively in a series of papers by Ingersoll et al. (1984, 1985a, 1985b), Suttner & Basu (1985), Decker & Helmold (1985) and Zuffa (1980, 1985).

The "**Indiana school**" regards the composition of sand(stone) as a complex function of provenance, transport history, and modifications during and after deposition (cf. Suttner, 1974). According to this view, grain-size changes are invariably accompanied by compositional modifications, as clasts decrease in size and change in petrographic composition during mechanical and chemical weathering. It is therefore not surprising that the Indiana point-counting method is best suited to the quantification of compositional modifications that occur during weathering and transport. Ternary framework compositions are commonly expressed in terms of QFR percentages, where R stands for "rock fragments". A rock fragment is defined as a grain consisting of two or more phases or crystals where (1) no single phase is >90% of the total area of the grain as observed in a thin section (commonly applicable to very fine or fine sand grains), or (2) at least the two phases or crystals are both >0.0625 mm in size (commonly applicable to medium or coarse sand grains). An exception to this rule is made for polycrystalline quartz, which is regarded as a monomineralic rock fragment (Suttner et al., 1981). A specific size range must be selected for the point-counting analysis, as this classification procedure maximizes the dependence of the calculated composition on the grain-size considered.

The "**Gazzi-Dickinson school**" emphasizes the use of petrographic techniques for the reconstruction of original detrital compositions, and assumes that the mineralogical composition of sands is primarily controlled by the nature of the parent rocks. The Gazzi-Dickinson point-counting method was developed independently by Gazzi (1966) and Dickinson (1970). Ternary framework compositions are commonly expressed as QFL percentages, where L stands for "aphanitic lithic fragments". The Gazzi-Dickinson method differs from the Indiana method because monomineralic grains or crystals of sand size (phaneritic: >0.0625 mm) that occur within larger rock fragments are assigned to the category of the monomineralic grain rather than

to the category of the larger rock fragment. Only fine-grained (aphanitic: <0.0625 mm) polymineralic fragments are classified as lithics, because such grains can be recognized throughout the sand-size range (cf. Boggs, 1968). The bulk composition of a sand-sized sediment measured according to the Gazzi-Dickinson conventions is unaffected by breakage of coarse-grained (phaneritic) rock fragments into monomineralic grains of sand size. This procedure minimizes the dependence of the calculated composition on grain size, and it enables the direct comparison of poorly sorted sands or sands with different modal grain sizes. It has become the standard methodology for the determination of palaeotectonic settings from sandstone compositions.

Classification criteria for monocrystalline grains, fine-grained (aphanitic) polymineralic grains, and quartz varieties are common to both methods. Operational definitions for the latter categories have been proposed by Gazzi (1966), Dickinson (1970), Wolf (1971), Basu et al. (1975), Graham et al. (1976), Basu (1985b), Dorsey (1988), Johnsson (1990b), Valloni (1985; in Ibbeken & Schleyer, 1991), Garzanti (1991), and Di Giulio & Valloni (1992). A classification scheme encompassing all grain types occurring in sands and sandstones has been developed by Zuffa (1980, 1985, 1987, 1991). In addition to the non-carbonate extrabasinal (NCE) grains commonly considered in provenance studies, this extended classification scheme also includes carbonate extrabasinal (CE), non-carbonate intrabasinal (NCI), and carbonate intrabasinal (CI) grains. The extended scheme is especially suitable for the detailed description and analysis of spatial and temporal relations in mixed siliciclastic-carbonate sands (e.g., Fontana et al., 1989; Garzanti, 1991). It can be used in conjunction with both point-counting methods.

Petrographic data acquisition by means of thin-section analysis is extremely time-consuming and can only be carried out by specialists. Consequently, petrographic datasets are generally small and sensitive to "operator bias", which limits their usefulness for the quantitative analysis of sedimentary basin fills. Current developments in sedimentary provenance studies aim at eliminating this problem by improving the existing data-acquisition technology. Methods have been developed which enable the automated acquisition of large amounts of chemical/mineral data (cf. Minnis, 1984; Harvey & Lovell, 1992), whereas other developments are aimed at the analysis of individual grains instead of grain populations (Suttner, 1989; Haughton et al., 1991).

A distinct advantage of geochemical analysis over point-counting is that the chemical composition of sand(stone) can be expressed in terms of (a limited number of) well-defined variables, such as major and minor elements or oxides. In addition, geochemical analysis of sands is much more rapid and can be carried out routinely. The main disadvantage is that the bulk chemistry of sands cannot be easily interpreted in terms of provenance, unlike their petrographic composition. At present, the interpretative value of mineralogical and textural information obtained by petrographic analyses is not yet matched by a sufficiently large geochemical database to allow for reliable "automated" provenance interpretations (Bhatia, 1983; Pettijohn et al., 1987). However, studies by Bhatia (1983), Van de Kamp & Leake (1985), Johnsson & Stallard (1989), Johnsson & Meade (1990), and Kroonenberg (in press) indicate that bulk chemical analysis of sands is a promising method for characterizing parent lithologies and temporal weathering trends (*chronosequences*).

Chemical elements combine to form minerals; the latter, in turn, form rocks. Raw compositional data used in sedimentary provenance studies thus represent different levels of information within a compositional hierarchy. This hierarchy provides a useful frame of reference for data acquisition and analysis, because many problems in sedimentary provenance studies are related to the "conversion" of information from a lower to a higher level (or *vice versa*). Low-level information about sediment composition, based on geochemical analysis, can be routinely obtained, but cannot be routinely converted into information about the mineralogical composition of a sediment, or information about the parent lithologies of a sediment in the absence of *a priori* knowledge. The high-level information obtained by a careful examination of polymineralic fragments in thin section allows for much more detailed provenance interpretations, but it implies a time-consuming analysis that cannot be easily automated. A practical application of quantitative sedimentary provenance studies to the field of basin analysis requires some form of compromise between these two extremes, based on the trade-off between the desire for high-level information on the one hand, and ease of (automated) data acquisition on the other.

4. Compositional data analysis in provenance studies

Petrographic or geochemical compositions of sediments are the principal data type used in provenance studies. Compositional data are commonly expressed as proportions, percentages, or parts per million, and thus sum to a constant value (1, 100 or 10^6). In addition, they are non-negative by definition, implying that in a system of N components, the value of the N-th component is automatically fixed by the sum of the other N-1 components. This means that compositional data are constrained: they are not free to take on any value or to vary independently, and consequently, they are not amenable to analyses by common statistical methods designed for use with unconstrained data (Chayes, 1960).

The difficulty of interpreting compositional data is well illustrated by the following trivial example: "*...if one analyzes the contents of a jar half-filled with sand and finds, by a random sample, that it contained (by volume) about 20% quartz, 30% feldspar, 40% rock fragments, and 10% miscellaneous constituents, then, if the volume of the jar were doubled by addition of grains of pure quartz, a second random sample would reveal that the jar contains 60% quartz, 15% feldspar, 20% rock fragments, and 5% miscellaneous. Feldspar, rock fragments, and miscellaneous constituents appear pairwise positively correlated and all three appear negatively correlated with the quartz abundance. Also, all four [components] have shifted mean values despite the fact that only the quartz content of the jar changed...*" (Woronov, 1991c).

A fundamental (but often neglected) property of compositional data is that the forced adjustment of all components in response to a change in a single component does not reflect any physical process, but is simply an artifact of the constant-sum constraint. A composition therefore provides information only about the relative, not the absolute values of its components. There is an intrinsic dependency among the compositional variables, and no component of a composition can ever be studied in isolation. Any appropriate statistical analysis must treat a composition as a whole by using multivariate methods, instead of regarding the compositional variables as a set of univariate measurements (Aitchison, 1989).

Unfortunately, appropriate statistical methods for analyzing compositional data have been extremely slow to emerge. These difficulties have been ignored or wished away by some earth scientists, who have been using standard statistical methods for analyzing compositional data, leading statisticians to conclude that "*...right up to the present day, there has been no other form of data analysis where more confusion has reigned and where more improper and inadequate statistical methods have been applied...*" (Aitchison, 1986). Others warned their collegues for some of these statistical pitfalls, but failed to provide alternatives. Consequently, the unresolved difficulties of compositional data analysis were taken by many as a license to avoid statistical tests altogether.

The above considerations cast a serious doubt on the interpretative value of univariate estimates of location, dispersion, and association, i.e., the "means", "standard deviations", and "correlations" widely used in sedimentary petrology to summarize the characteristics of compositional data suites.

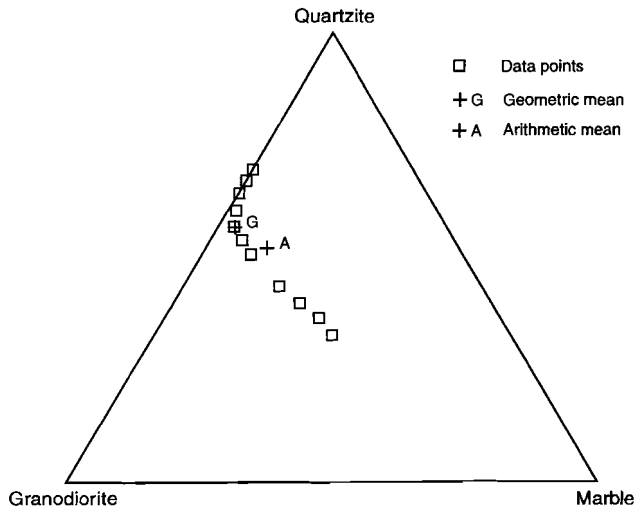

Figure 1. Pattern of compositional variation produced by progressive modification of conglomerate-clast assemblage in tumbling-barrel experiment (data recalculated from Abbott & Peterson, 1978).

The vector of univariate arithmetic means represents a hypothetical composition that would be obtained by mixing equal proportions of all compositions from which it has been calculated. It can thus be regarded as a useful measure of location, provided that the observed compositional variability reflects physical mixing or an analogous process. If the observed variability reflects another type of process, the univariate arithmetic mean composition may be very atypical of the data set. In such cases, the vector of univariate arithmetic means cannot be regarded as a typical example of a hypothetical observation, and clearly fails to provide a useful measure of central tendency of the data. This situation is illustrated for a set of three-part compositions in the ternary diagram of Fig. 1. The arithmetic mean falls outside of the range of compositions which cluster about a curved line

in ternary space (cf. Philip & Watson, 1988a; Aitchison, 1989). An alternative measure of central tendency is the composition obtained by imposing the constant sum constraint on the univariate geometric means. This "geometric mean" performs much more satisfactory in cases such as that illustrated in Fig. 1, because it does represent a typical example of a hypothetical observation (cf. Aitchison & Shen, 1984; Aitchison, 1989). If the observed compositional variation reflects physical mixing or an analogous process, both measures of location provide similar estimates.

Univariate estimates of dispersion, loosely referred to as "standard errors", "standard deviations", or "confidence intervals", have been used extensively in provenance studies. Such measures of dispersion are typically represented by hexagons centred about the arithmetic means of data sets displayed on ternary diagrams. The principal shortcoming of these univariate measures of dispersion is that they do not take into account the covariance structure of the data, because they are based on the incorrect assumption that each component varies independently of the other components. Consequently, their physical and statistical meaning are obscure (Philip et al., 1987). The construction of "true" confidence intervals in ternary diagrams based on the trinomial distribution is discussed in a series of papers by Watson & Nguyen (1985), Watson (1987), and Medak & Cressie (1991). Another parametric approach has been discussed by Aitchison & Shen (1984) and Aitchison (1986). A nonparametric method for calculating location and dispersion estimates in ternary diagrams was proposed by Philip & Watson (1988a, 1988b, 1988c) and Watson & Philip (1989). The latter paper evoked a vigorous dispute about measures of compositional variability (Aitchison, 1990, 1991a, 1991b, 1992; Watson, 1990, 1991).

If a series of random numbers is pairwise recalculated to a constant sum, the variables of the resulting two-part compositions will show a perfect negative correlation ($r=-1.0$), which in no way reflects the random nature of the original values from which the compositions have been generated. This effect is less obvious for compositions with a larger number of components, but the perceived association between compositional variables is always affected by the constant sum constraint. Moreover, unique measures of dispersion and association cannot be defined for raw compositional variables. The variances and covariances of all compositional variables are changed by exclusion of a single component from each composition, and recalculation of the remaining components to a constant sum. In spite of the doubtful *interpretative* value of measures of dispersion and association of raw compositional variables, it should be stressed that they can be of considerable *descriptive* value (analogous to the vector of univariate arithmetic means in case of physical mixing, as discussed above). For example, a strong correlation between two components of a composition is a *fact*, that can be used to predict the value of one component given the value of another. Many standard numerical techniques can therefore be used for summarizing compositional variability (e.g., Davies & Ethridge, 1975), as long as measures of dispersion and association are not interpreted in rigorous physical terms (Miesch, 1980). This impediment was neglected in early attempts to model the petrology of detrital sediments by means of principal components analysis (Griffiths, 1966; Griffiths & Ondrick, 1969). The same criticism applies to the use of various "factor-analytic" procedures aimed at clarifying inter-variable relationships (so-called R-mode methods), as well as attempts to model the variability of single components of compositional data by means of time series analysis (e.g., Stattegger, 1986).

5. Q-mode analysis in provenance studies

Central problems in the field of sedimentary provenance studies are the empirical classification of observations, and the assignment of observations to predefined compositional classes. These problems are closely related to the apportionment of sediments to their respective sources, the so-called partitioning or mixing problem. "*...In its broadest aspect, the problem of provenance can be considered as a problem of accounting - making an inventory of the different types of grains contributed by different source rocks. To this, one should add the problem of the same kinds of grains coming from different source rocks...*" (Pettijohn et al., 1987). If a number of sediment sources sheds the same types of grains in different proportions, and the proportional contributions of these sources are allowed to vary randomly, complex patterns of variation can be produced. Under such circumstances, the strength of association between a pair of compositional variables cannot even be regarded as an informative *description* of variability, unless it can be assumed that both variables represent "unique" grain types (or chemical elements), i.e., variables characteristic of a single source.

A solution of the partitioning problem thus requires a different look at compositional variability, focussed on the relationships between observations (Q-mode), instead of the relationships between compositional variables (R-mode). A suite of sandstone samples from a single sedimentary basin can be regarded as a series of mixtures of sediments supplied by an unknown number of sources with unknown compositional characteristics. A provenance reconstruction thus requires an assessment of the number of sediment sources and their compositional characteristics, i.e., the low-level petrographic information must be converted into high-level provenance information. This problem is identical to that of estimating mineral composition from geochemical compositions of rock specimens in the absence of *a priori* knowledge. In sedimentary provenance studies, unmixing has been performed by means of vector analysis (Imbrie & Van Andel, 1964; Pigorini, 1968) and its successor, extended Q-mode "factor" analysis (e.g., Flores & Shideler, 1978; Stattegger, 1987; Mezzadri & Saccani, 1989). A new strategy for solving the partitioning problem is discussed in chapter 3.

Empirical classification of observations by means of Q-mode cluster analysis (e.g., Cavazza, 1989; Stattegger & Morton, 1992) has been used for delineating groups within compositional datasets. Discriminant function analysis, an assignment technique which makes use of an *a priori* classification of observations, has enjoyed substantial use in provenance studies (e.g., Middleton, 1962; Kelley & Whetten, 1969; Davies & Ethridge, 1975; Pingitore & Shotwell, 1976; Ingersoll, 1978, 1990; Potter, 1978; Bhatia, 1983; Pirkle et al., 1985; Gergen & Ingersoll, 1986; Packer & Ingersoll, 1986; Darby, 1990; Molinaroli et al., 1991). Discriminant function analysis can be used as a descriptive tool without relying too heavily on statistical assumptions with regard to the sampling distribution of compositional variables. However, this does not mean that its application to compositional data analysis is without difficulty. Although discriminant function analysis treats the data in a multivariate way, it is a parametric technique, which requires that the compositional variables follow a multivariate normal distribution. Because compositional data fail to meet this requirement, the results of discriminant function analysis should be interpreted with great caution (Butler, 1982; Aitchison, 1986; Rock, 1988).

6. Logratio transformation of compositional data

A practical parametric approach to the statistical analysis of compositional data was developed in the 1980's (Aitchison, 1986, and references therein). Aitchison proposed a logratio transformation of the raw compositional variables as a means to eliminate the constant-sum constraint. Logratios of compositional data, i.e., variables of the form $\log(x/y)$, where x and y represent two components of the same composition, are free to take on any value and are often normally distributed. Furthermore, two logratios which do not share the same components are free to vary independently (so-called subcompositional independence). The logratio transformation also enables the definition of a unique covariance structure. These logratio properties imply that the whole range of "standard" multivariate statistical techniques can be easily adapted to the analysis of compositional data.

Until now, applications of the logratio transformation to petrographic data have been relatively scarce. Butler & Woronov (1986) scrutinized the dataset of Dickinson & Suczek (1979) in order to delineate spurious correlations induced by the constant-sum constraint. Their results suggest that the compositional trend within the "magmatic arc provenance" field of Dickinson & Suczek (1979) could equally well represent an artifact produced by imposing the constant-sum constraint on a set of independent variables, implying that it has no geological significance. Zhou et al. (1991) applied a row-centred form of the logratio transformation (see Chapter 3 of this thesis for definition) to grain-size distributions, in order to establish a multivariate classification of shelf sediments by means of principal component and cluster analyses. The logratio approach provided a clear and easily interpretable result. Results of the same analyses carried out on the raw compositional variables were much more difficult to interpret, clearly demonstrating the superiority of the logratio approach.

A fundamental problem of compositional data analysis, that cannot be resolved by mathematical manipulations, is the fact that the behaviour of a single variable cannot be studied in "isolation". Therefore, techniques especially suitable for the analysis of compositional data have been developed, based on the methodology of Aitchison. One of these, which could be of great use in provenance studies, is a method for identifying the source of compositional shifts across data suites (Woronov, 1990; Woronov & Love, 1990). By systematically comparing all logratios which can be formed from two sets of compositions, this technique allows to identify logratios which display similar trends (i.e., increase, equality, or decrease from one dataset to another) relative to a fixed component (the common divisor y mentioned above). A similar technique is used in chapter 7 to compare two sets of sandstone compositions.

Current developments in sedimentary petrology focus primarily on the improvement of data acquisition techniques. This may reflect a widespread conviction that many problems encountered in provenance studies cannot be resolved by analysis of petrographical data which have been gathered by means of "conventional" methods. However, few sedimentary petrographers have been actively engaged in the development of numerical and statistical techniques aimed at extracting more provenance-related information from petrographic data. In view of the increasingly sophisticated data-acquisition technology, the development of a theoretical framework and appropriate numerical-statistical models for deductive reasoning and testing of hypotheses becomes more and more important. There is no reason to assume

that pattern recognition in petrographic, mineral, or geochemical data will become easier if larger data sets are available. On the contrary, problems of provenance interpretation tend to increase with larger data sets (cf. Ibbeken & Schleyer, 1991). The development of more sophisticated data processing techniques thus forms an essential part of provenance studies, because it enables sedimentary geologists to fully enjoy the benefit of current developments in data-acquisition technology.

CHAPTER 2

COMPOSITIONAL VARIATION OF SILICICLASTIC SANDS

1. Observed compositional modifications in sedimentary systems

The compositional and textural properties of a sand-sized sediment reflect its parent lithologies and the cumulative effects of modifications which have taken place between the initial erosion of the parent rocks and the final burial of their detritus. The compositional evolution of sand-sized sediments is most conveniently discussed in the context of a sedimentary cycle. A sedimentary cycle is defined as "*...beginning with derivation of detritus from a lithified parent rock and ending with lithification of the derived detritus. Sediment in temporary residence on a bar or on a floodplain, even for thousands of years, but not buried and lithified is not considered to be passing through a second cycle*" (Suttner et al., 1981). The sedimentary cycle can be "unrolled" to form an "ideal" sedimentary system, in which the major sedimentary environments are present. The framework composition of sand-sized sediments is affected by modification processes in each successive sedimentary environment along the pathway between the source area and the basin of deposition.

Although many provenance studies describe the products of sedimentary processes in great detail, they provide comparatively little information about the producers, the source areas (Ibbeken & Schleyer, 1991). The following overview of compositional modifications in the "ideal" sedimentary system attempts to summarize the results of petrographic field studies in a limited number of well-known modern environments. Methods and scales of observation used in these studies are far from uniform, permitting only a qualitative summary of their main conclusions. Compositional modification of framework mineralogy in glacial (Slatt & Eyles, 1981) and aeolian (Chandler, 1988) environments, which is largely of a physical nature, has not been discussed. The "ideal" sedimentary system is made up of a series of environments in which the following processes operate:

Orogenic source areas: coarse-grained siliciclastic sediments are generated by mechanical weathering in mountainous areas; chemical weathering is volumetrically less important (Ruxton, 1970; Johnsson, 1990; Bull, 1991; Ibbeken & Schleyer, 1991; Dutta, 1992).

Proximal alluvial environments (high-gradient systems): principal modifications are attributable to mechanical destruction and selective transport (Plumley, 1948; Morris & Fan, 1962; Pittman, 1969; Bradley, 1970; Cameron & Blatt, 1971; Pearce, 1971; Moss, 1972; Schumm & Stevens, 1973; Shukis & Ethridge, 1975; Abbott & Peterson, 1978; Davies et al., 1978; McBride & Picard, 1987; Ibbeken & Schleyer, 1991), and to mixing of sediments from lower-order tributary streams (Shukis & Ethridge, 1975; Blatt, 1978; Ibbeken & Schleyer, 1991); chemical weathering can be locally important, depending on climatic conditions and residence time of detritus in this part of the sedimentary system (Bradley, 1970; Basu, 1976, 1985a; Mahaney & Halvorson, 1986; Grantham & Velbel, 1988; Bull, 1991).

Alluvial-delta plain environments (low-gradient systems): compositional modifications due to selective transport and mixing of sediments from higher-order tributary streams, and chemical weathering during temporary storage are the main causes of compositional variation (Russell, 1937; Pollack, 1961; Hayes, 1962; Krook, 1969; Whetten et al., 1969; Cleary & Conolly, 1971; Mann & Cavaroc, 1973; Self, 1975; Breyer & Bart, 1978; Harrell & Blatt, 1978; Potter, 1978; Mack, 1981; Franzinelli & Potter, 1983, 1985; Konta, 1988; Blasi & Manassero, 1990; Johnsson & Meade, 1990; Savage & Potter, 1991; Johnsson et al., 1991).

Coastal environments: compositional variability is attributable to selective transport and mechanical destruction induced by waves and currents, and to mixing of sediments from different sources by longshore transport (Hsü, 1960; Field & Pilkey, 1969; Gazzi et al., 1973; Davies & Ethridge, 1975; Rice et al., 1976; Komar, 1977; Mack, 1978; Sedimentation Seminar, 1988; Ito & Masuda, 1989; Best & Griggs, 1991; Osborne & Yeh, 1991). Chemical weathering is locally important (Savage et al., 1988).

Deep marine environments: compositional variability reflects mixing and selective transport of sediments from various (intrabasinal and extrabasinal) sources (Damuth & Fairbridge, 1970; Davies, 1972; Kelling et al., 1975; Valloni, 1985; Gergen & Ingersoll, 1986; Packer & Ingersoll, 1986; Saccani, 1987; Zuffa, 1987; Fontana et al., 1989; Marsaglia, 1991).

2. Climatic-physiographic controls on sand composition

The initial composition of sand-sized detritus supplied to a sedimentary system is determined by the nature of the parent rock(s) and by the climatic and physiographic conditions in the source area. The primary controls on the initial composition of sand-sized detritus are the mineralogical composition, texture, and grain size of the parent rocks (e.g., Dutta, 1992). Parent rocks are transformed into sand-sized detritus by mechanical and chemical weathering. The total extent of weathering, i.e., the extent to which the composition of detrital sediments deviates from the composition of their parent rocks is controlled by the rate of weathering, and by the residence time of detritus in the weathering environment. These factors are commonly labelled as "climate" (i.e., precipitation and temperature) and "relief" (i.e., slope angle), respectively (Basu, 1985a; Grantham & Velbel, 1988; Johnsson & Stallard, 1989; Dutta, 1992). In its simplest form, a weathering index for detritus can thus be represented by (cf. Grantham & Velbel, 1988):

$$\mathbf{WI} = \mathbf{C} \times \mathbf{R}$$

where
WI = weathering index ("predicted" extent of weathering)
C = rate of weathering ("climate")
R = residence time ("relief")

According to this relationship, the compositional variability of sands derived from the same parent rocks reflects changing climatic and/or physiographic conditions. However, sands of similar composition can be produced under different climatic and tectonic conditions,

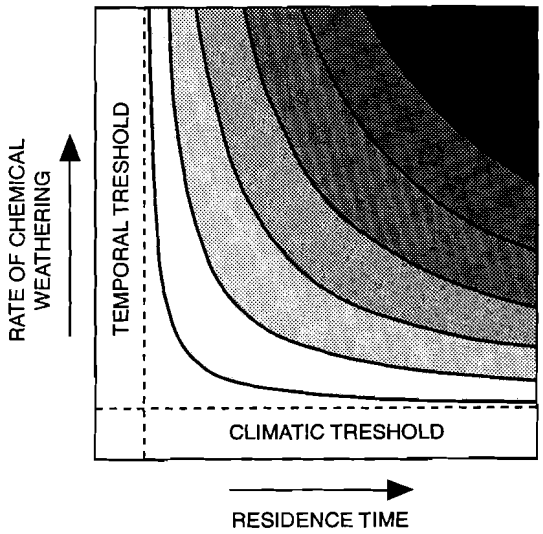

Figure 1. The extent of weathering as a function of the rate of weathering ("climate") and the residence time of detritus in the weathering environment ("relief").

provided that similar parent rocks are exposed in the source areas. This general concept is illustrated in Fig. 1.

Table 1. Calculation of weathering index for first-cycle fluvial sands.

SEMI-QUANTITATIVE WEATHERING INDEX			PHYSIOGRAPHY (relief)		
			high (mountains)	moderate (hills)	low (plains)
			0	1	2
CLIMATE (precipitation)	(semi-)arid & mediterranean	0	0	0	0
	temperate subhumid	1	0	1	2
	tropical humid	2	0	2	4

The climatic-physiographic control on sandstone composition has been clearly recognized in drainage areas with a low relief and a humid tropical climate, where first-cycle quartz arenites are produced from a variety of parent rocks (Franzinelli & Potter, 1983; Johnsson et al., 1988). At the other end of the spectrum are areas in which the composition of sand

is controlled by the nature of the parent rocks, because detritus is produced under conditions below so-called temporal or climatic tresholds. Production of sand below the temporal treshold is restricted to mountainous areas, where residence times of sand-sized detritus in soils are too short for appreciable chemical weathering to take place, even under humid tropical conditions (Ruxton, 1970). Production of sand below the climatic treshold takes place in arid and semi-arid regions, where substantial chemical weathering of sand-sized detritus is inhibited by a lack of precipitation (Slatt & Eyles, 1981; Girty, 1991).

In order to check the validity of this concept, a compilation of the results obtained from the analysis of modern lower-order stream sands derived from single lithologies under different climatic and physiographic conditions (Mann & Cavaroc, 1973; Mack, 1981; Franzinelli & Potter, 1983; Basu, 1976, Young, 1976 in Basu, 1985a; Tortosa et al., 1989) was made (see Appendix I). The grain-size fraction and point-counting method used in these studies are similar: all analyses were carried out with the "Indiana method" (see chapter 1 for definition) on medium-sized sands (1 to 2 ϕ units). A semi-quantitative weathering index was calculated according to the formula given above (Table 1). The index reflects the estimated climatic and physiographic conditions in the lower-order fluvial drainage basins of the sand suites, and ranges from 0 to 4.

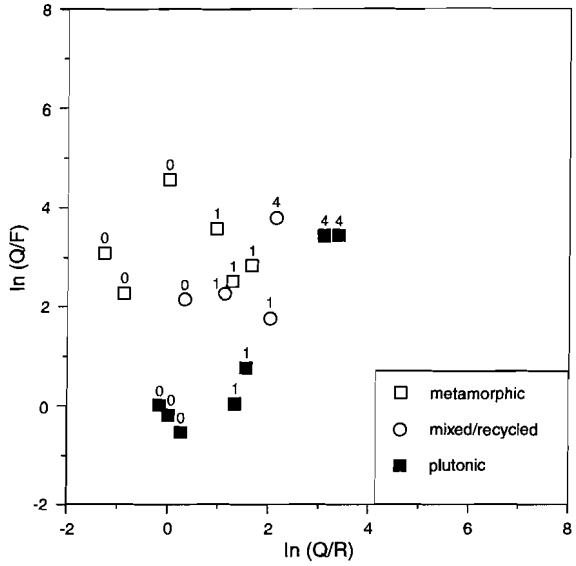

Figure 2. Parentage and weathering index of lower-order fluvial sands (data in Appendix I).

Subsequently, a bivariate plot of compositional data was constructed, using the logratio transformed QFL% data (see chapter 1 for definition), to which the weathering index of each sample suite was added. The results of this exercise, shown in Fig. 2, convincingly demonstrate the validity of the concept of climatic-physiographic control on sandstone composition. Sands of plutonic and metamorphic parentage display consistent compositional trends associated with an increasing extent of chemical weathering. The compositional trends recorded within plutonic and metamorphic sands correlate well with the weathering condition predicted on the basis of the estimated climatic and physiographic data.

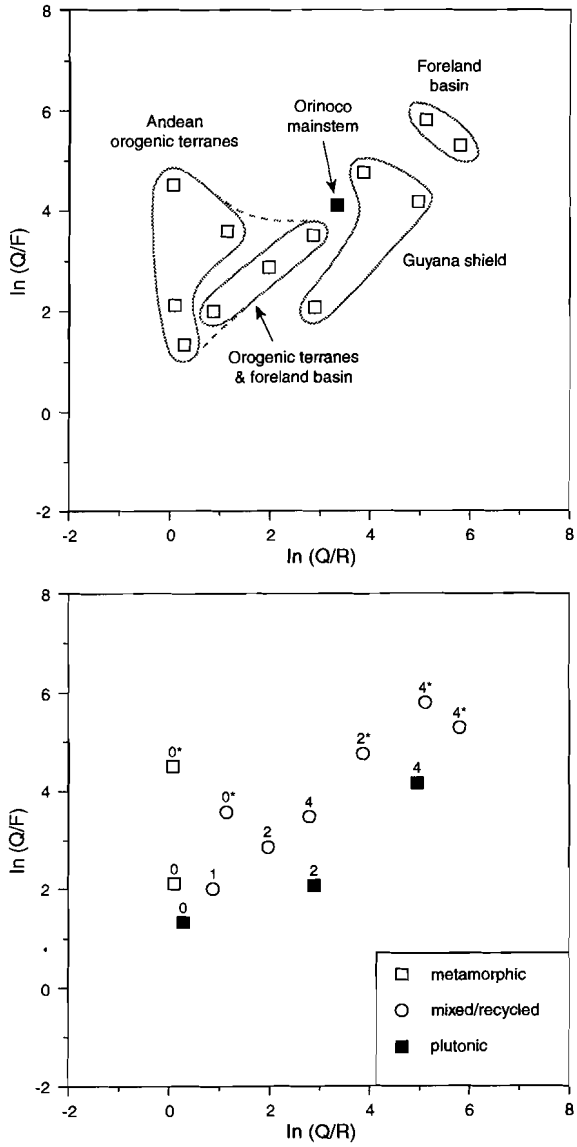

Figure 3. Sands from the Orinoco River Basin. A: Major morphotectonic provinces. B: Parentage and weathering index (data in Appendix II). Asterisks mark effects of recycling.

In larger fluvial drainage basins, the climatic-physiographic signature of lower-order monolithologic source areas is generally obscured by mixing of sediments derived from different parent lithologies and by weathering in transitional storage areas (low-gradient alluvial systems). The weathering index of the sediments from higher-order fluvial basins thus partly reflects the climatic-physiographic conditions and the size of the transitional source area, and it may also include effects attributable to recycling of ancient sediments.

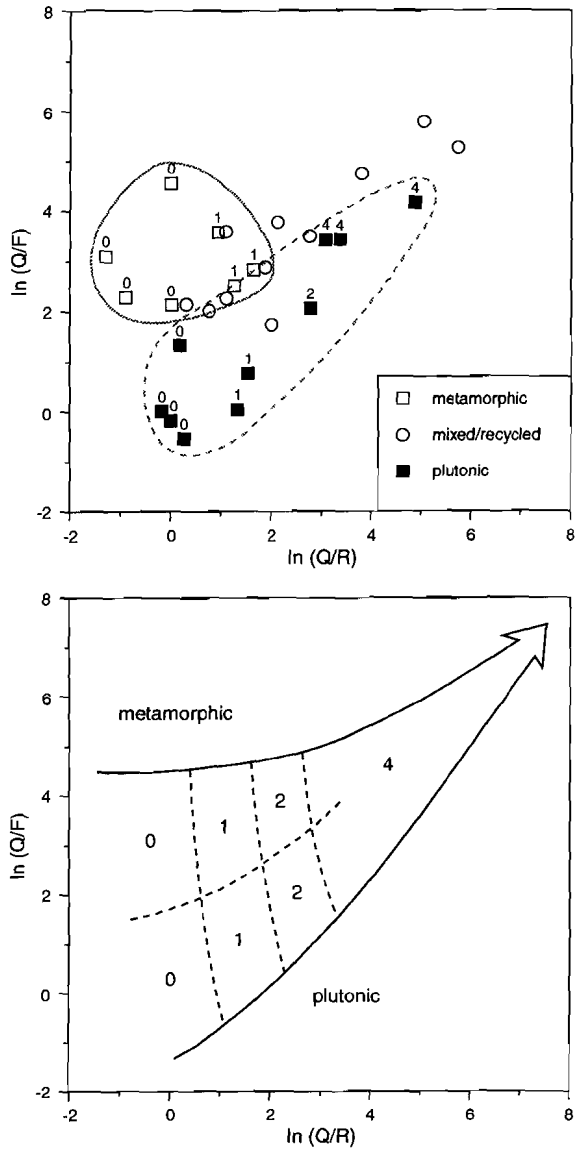

Figure 4. A: Compilation of data listed in Appendices I and II. B: Idealized temporal/spatial weathering trend, showing relation of composition to parentage and weathering conditions.

The compositional variability of fluvial sands in the Orinoco River drainage basin (Johnsson et al., 1991) clearly shows the complications of predicting source-area characteristics from sands supplied by large rivers. The dataset of Johnsson et al. (1991) is summarized in Fig. 3 (and Appendix II). Fig. 3A shows that the compositional variation encountered in the Orinoco River drainage Basin reflects a broad range of climatic-physiographic conditions and parent lithologies. The compositional evolution of sediments derived from the orogenic source areas, which subsequently cross the entire length of the foreland basin, is very

similar to the range of variation displayed by lower-order monolithologic stream sands (Fig. 2). This indicates that similar compositional trends recorded within a single basin fill can be interpreted as time series or *chronosequences*. Sediments derived from the Guayana Shield display a considerable range of compositional variation, attributable to contrasting relief and the local presence of sedimentary rocks in this source area. The effect of recycling is especially prominent in sands from smaller rivers that drain only the foreland basin. All of these compositional signals converge to the average composition of the Orinoco mainstem. Fig. 3B shows the same sandstone suites with their corresponding weathering indices (Table 1). The effects of recycling are clearly present in the sand suites marked with an asterisk, whose weathering indices are too low with respect to their compositions (in comparison with first-cycle sands). Only a limited number of monolithological sand suites can be identified. The composition of a sample of nearly pure quartz arenite from the Orinoco River mouth would merely reflect prolonged weathering in the humid tropical lowlands. Residence times of sands in the lower reaches of the Orinoco Basin are too long and the rate of chemical weathering is too high to preserve a record of climatic-physiographic conditions in the source areas.

Fig. 4A shows a scattergraph in which the data of Figs. 2 and 3B are combined. Sands of monolithological metamorphic and plutonic parentage define a clear trend, characterized by an increasing extent of weathering, coupled with an increasing value of the weathering index. This trend is depicted in Fig. 4B. Mack & Jerzykiewicz (1989) demonstrated that sands derived from andesitic rocks, which are practically devoid of sand-sized quartz grains, display an equally consistent compositional trend.

3. Overview of quantitative provenance models

At present, there are three widely used approaches to the prediction of source area characteristics from framework composition of coarse-grained sediments:

A. Regional palaeoclimate model:

Attempts to identify palaeoclimate conditions in ancient source areas have been made by comparing fossil sandstones to a "standard" provided by recent sands of similar parentage, as exemplified in Fig. 4B (Young et al., 1975; Mack & Suttner, 1977; Suttner et al., 1981; Suttner & Dutta, 1986; Mack & Jerzykiewicz, 1989; Velbel & Saad, 1991). This approach to palaeoclimatic reconstructions is not without difficulty. It follows from the concept of climatic-physiographic control that the extent of chemical weathering under given climatic conditions largely depends on the time during which detritus is exposed to the weathering environment. This implies that palaeoclimatic conditions can only be inferred if the residence time of detritus in the (transitional) source area can be estimated. Such estimates must be based on the presumed relief and the distance from the source, which may be difficult to assess in the absence of a detailed palaeogeographic reconstruction. Another problem is the presumed parentage of the fossil sandstone under investigation, that may not have been identical to that of the modern sand taken as an "absolute standard". Moreover, changing parent lithologies due to progressive denudation in the source area may seriously influence long-term detrital records.

Application of this method to larger basins is hampered by effects of mixing and recycling, as discussed above for the Orinoco River drainage basin (cf. Johnsson et al., 1991). Therefore, subtle climatic contrasts cannot be identified with certainty. Velbel & Saad (1991) argued that spatial and temporal averaging of sandstone compositions in hillslope reservoirs limits the temporal resolution of the detrital signal, so that only long-term palaeoclimatic trends associated with plate motions (cf. Suttner & Dutta, 1986) are discernible in the detrital record of lower-order drainage basins. As a result of these complications, the temporal resolution provided by this method is too low for detecting climatic fluctuations on the relatively short timespans considered by earth scientists studying the evolution of Quaternary landforms in response to climatic change (cf. Bull, 1991).

B. **Global tectonic model:**

The objective of this model is to predict the plate-tectonic setting of sedimentary basins from ternary subcompositions of sand(stone) suites. On the much larger spatial and temporal scale of global sediment dispersal systems, the principle of climatic-physiographic control also applies, but the picture is simplified because parent lithology and relief can be regarded as a function of the plate-tectonic setting of source areas and sedimentary basins. On a continent-scale, sand(stone) composition is thus largely controlled by the interaction of tectonics and climate (Dickinson & Suczek, 1979; Dickinson, 1985, 1988; Potter, 1978, 1986; Valloni, 1985; Dutta, 1992). Various types of active-margin settings can be recognized on the basis of parent lithologies, because a high relief promotes short residence times in orogenic source areas. The lack of relief in passive margin settings generally results in strongly weathered detritus. These rules do not always apply. For instance, sands from the passive margin of Argentina (Potter, 1986; Blasi & Manassero, 1990) resemble those of an active margin, due to a lack of compositional modification under arid climatic conditions in the relatively small-sized continental drainage systems.

Empirical models based on this large-scale concept are supported by a large petrographic data base (summarized by Dickinson, 1985, 1988; Valloni, 1985) and perform very well, as demonstrated by recent studies of Gergen & Ingersoll, 1986; Packer & Ingersoll, 1986; Dorsey, 1988; DeCelles & Hertel, 1989; Lundberg, 1991; Marsaglia, 1991; Marsaglia & Ingersoll, 1992). The method was developed for (and is successful in) reconstructing the long-term source area evolution and large-scale plate-tectonic settings. A correct use of the plate-tectonic provenance model requires the averaging of sandstone suites collected on large temporal and spatial scales, in view of the small-scale compositional variability of sands attributable to local factors (Ingersoll, 1990; Ingersoll et al., 1993). However, the robustness of this averaging approach is bought at a high price: more than half of all modern fluvial sand is probably of mixed plate-tectonic provenance (Dickinson, 1988).

C. **Local unroofing model:**

The objective of this method is to predict the unroofing history of a source area from the vertical compositional variation of syntectonic conglomerates (Graham et

al., 1986; DeCelles, 1988; Pivnik, 1990; DeCelles et al., 1991). It is the only technique based on simulation or "forward modelling": Compositions which match the observed variation are generated by conceptually "eroding" and "mixing" known parent lithologies. The technique follows a "trial and error" method for reconstructing the unroofing history. Additional constraints on the model are provided by retro-deformation techniques from structural geology, such as the construction of partially restored cross-sections by means of "equal area balancing" (DeCelles et al., 1991). The method requires a considerable amount of *a priori* knowledge of source area lithology and physiography. So far, it has been used to model thrust-generated conglomerate-clast assemblages derived from sedimentary parent rocks, because such clasts can be unequivocally tied to lithologic or stratigraphic units in the source area. A conceptually similar approach was used by Ibbeken & Schleyer (1991) as part of an extensive study aimed at predicting the composition of river-mouth sediments from a careful reconstruction of rock-specific erosion rates in a series of drainage basins along an active plate margin in southern Calabria (Italy).

4. Analysis of compositional modifications

The observed compositional variation among and within sand(stone) suites in sedimentary systems can be attributed to a variety of processes. The compositional and textural properties of sediments are affected by selection, mixing, and mechanical breakage of grains during transport, and chemical-mineralogical transformations during chemical weathering. All of these modifications are selective: the extent to which selection occurs depends on the range of physical and chemical properties of the the grain population under investigation (i.e., durability, chemical stability, size, shape, and specific gravity). During transport, each grain behaves differently, depending on its size, shape, and specific gravity. It is well-known that grain-size distributions are affected by selective transport and deposition (e.g., Komar, 1977; Bardsley, 1978; Dacey & Krumbein, 1979; McLaren, 1981; McLaren & Bowles, 1985; Paola et al., 1992). The same applies to the other bulk physical properties, such as shape and density distributions.

In the hypothetical case of an ideal fluvial system with no tributaries that is fed by a single source, all of the observed spatial variation of bulk physical and textural properties can be attributed to selective transport if no mechanical or chemical weathering occurred in the system being studied, and if the initial characteristics of the sediment supplied to this ideal system did not vary. In this case, mean transport rates will be different for each size/shape/density class within the grain population, and all of the observed spatial variation of bulk sediment properties can be attributed to varying proportional contributions of each size/shape/density class to the sediment. Consequently, the chemical and petrographical composition within each size/shape/density class must be the same at every location. Selective transport alone does not affect the ratios of grain types belonging to a single size/shape/density class, because selection within a subpopulation of grains cannot occur if all elements behave in an identical manner during transport.

The concept of framework composition employed by the "Gazzi-Dickinson school" (described in chapter 1) is based on ratios of classes of principal framework grains, i.e., grains with similar shape and specific gravity (quartzose grains, feldspars, and polymineralic

grains). Effects of shape and density selection are minimized by discarding certain classes of grains with deviating properties, such as platy micaceous grains and accessory "heavy" minerals. In addition, the definition of framework composition generally applies to ratios of principal framework elements within a narrow range of grain sizes. All of these restrictions aim at minimizing effects of size, shape and density selection, which may have taken place during transport of the sediment. Following the Gazzi-Dickinson conventions, the "framework composition" of sands is defined in terms of ratios of principal framework elements with similar shape and specific gravity within a narrow range of grain sizes.

The analysis of compositional modification can be simplified considerably if it is accepted that compositional variations attributable to size, shape, and density selection can be largely eliminated by quantifying framework compositions of sand-sized sediments according to the guidelines set out above. This proposition is not unreasonable, as shown by Ingersoll et al. (1984) and Zuffa (1985), who demonstrated that framework compositions of different grain-size classes of the same sediments, determined according to the Gazzi-Dickinson conventions, form tight clusters in QFL-space. It may be expected that framework compositions determined according to the Gazzi-Dickinson conventions are equally robust with respect to small variations of shape and specific gravity within the subpopulation of grains considered. It follows that the principal framework composition of a sediment shed by a single source can be represented by a single point in QFL-space, regardless of its sampling location, provided that all of the observed variation in bulk physical properties reflects the effects of selective transport and deposition.

The elimination of selective transport and deposition leaves three possible mechanisms of compositional variation within a single size/shape/density class: mechanical weathering (breakage of grains without chemical-mineralogical modification), chemical weathering (chemical-mineralogical transformation and dissolution), and physical mixing of sediments from various sources. These variations of framework composition can be classified in terms of selective and non-selective modifications.

A. Selective modifications: weathering

The class of principal framework grains can be subdivided into various types of minerals and polymineralic lithic fragments. Each grain type is characterized by its own chemical and mechanical stability, that will determine the rate at which it will dissolve, decompose, or disaggregate under given environmental conditions. Selective modifications, such as chemical and mechanical weathering, treat each type of framework grain differently, and will cause changes to the ratios of framework elements. On account of their selective nature, mechanical and chemical weathering are non-linear functions of the compositional variables. Selective modifications can be identified under (natural) laboratory conditions as distinctly curved trends in compositional space. Compositional patterns attributable to chemical weathering can be recognized in sediments which have undergone *in situ* modifications. They are most pronounced in sediments of monolithologic parentage (e.g., soils and saproliths in first-order fluvial drainage basins). However, similar effects may be observed in more distal parts of sedimentary systems, where sediments from various sources have been sufficiently homogenized by mixing, prior to being subjected to *in situ* modification. Two examples of curved compositional trends resulting from

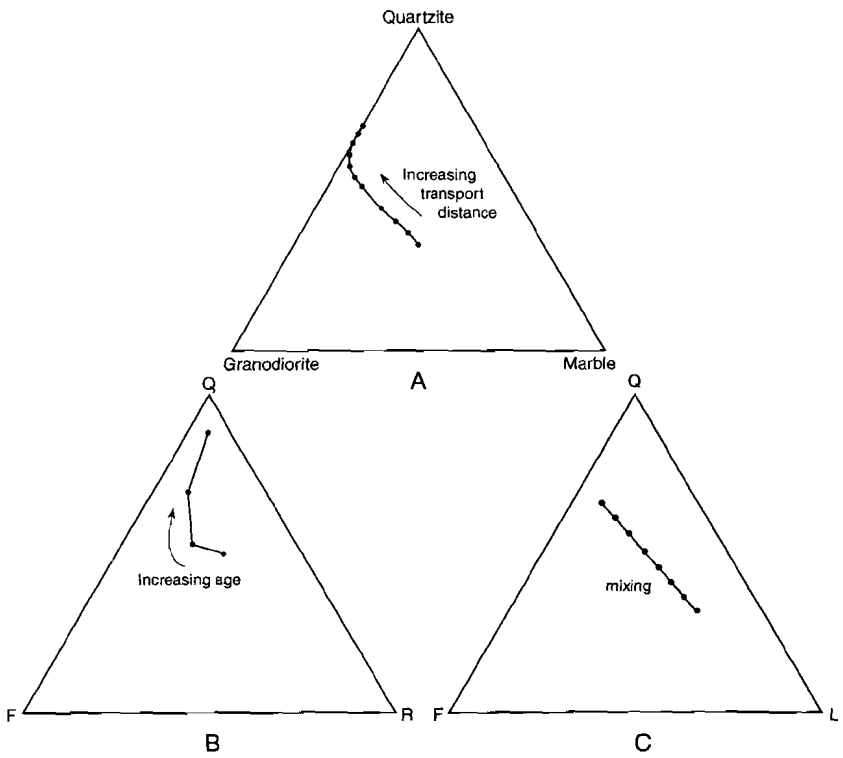

Figure 5. A: Abrasion of conglomerate-clast assemblage (Abbott & Peterson, 1978). B: Weathering chronosequence of fluvial sands in point bar (Johnsson & Meade, 1990). C: Mixing of two "source compositions".

progressive non-linear modifications by mechanical weathering (Abbott & Peterson, 1978) and chemical weathering (Johnsson & Meade, 1990) are depicted in the ternary diagrams of Fig. 5A and 5B, respectively.

B. Non-selective modifications: mixing

Physical mixing of sediments from compositionally distinct sources induces strictly linear trends in compositional space, because all principal framework grains of similar size, shape, and density are treated in the same way during the transport process. For example, all possible mixtures of two compositions can be represented by a straight line segment in a three dimensional QFL-space (Fig. 5C), whereas mixing of sediments from three distinct sources produces a triangular field in QFL-space that is enclosed by the "source compositions" (Fig. 6A). Linear mixing in sedimentary systems is a primary cause of compositional variation on widely different scales. On the smallest scale, compositional variation of detrital sediments carried by first order streams reflects contributions of different parent rocks. On a larger scale, compositional variation of sands in large fluvial systems reflects the mixing of sediments delivered by its "second order" tributary streams. Patterns of

compositional variation in the shallow marine environment can be attributed to mixing and dispersal of sediments from various river systems ("third order"). A considerable proportion of the observed compositional variation in sandstone suites is thus determined by hierarchical tributary structures, that can be recognized from the uplands in which sediments are produced to the ocean basins in which they are eventually deposited. Along this pathway, local compositional signals are diluted by the addition of materials derived from different sources, until a more or less stable compositional signal has been generated. Examples of this "mixing hierarchy" are presented by DeCelles & Hertel (1989), Johnsson (1990a), and Ingersoll et al. (1993).

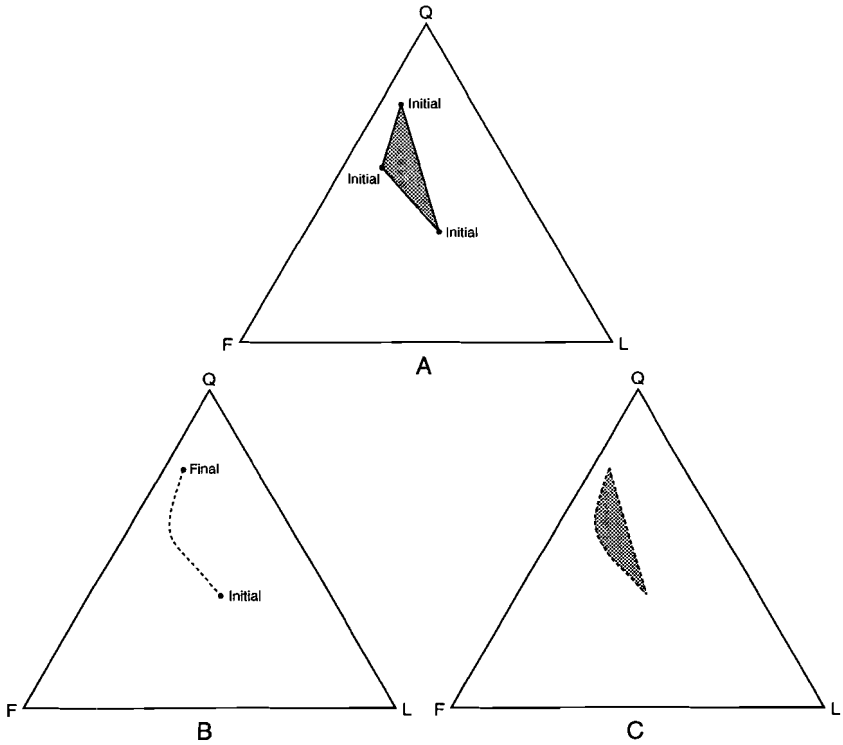

Figure 6. A: Mixing of three "source compositions". B: Pattern of compositional variation in soil profile (weathering chronosequence). C: New pattern of sediment compositions after transport and mixing.

The points raised above imply that the perceived effects of a modification process depend to a large extent on the range of physical properties displayed by the subpopulation of grains under study. This has important consequences for the analysis and modelling of compositional modifications. Certain modifications, which behave in a non-linear way with respect to the bulk properties of sediments can be regarded as linear if we restrict our observations to framework-grain populations with similar physical properties (size/shape/-density). This should allow to distinguish linear modifications due to physical mixing from

non-linear modifications due to mechanical and chemical weathering. Compositional modifications of a single size/shape/density class of framework grains in the different environments of the "ideal" sedimentary system are summarized in Table 2.

Table 2. Modifications of principal framework composition in the "ideal" sedimentary system.

Sedimentary environments	Non-linear modifications	Linear modifications
Orogenic source areas	mechanical weathering	-
Proximal alluvial environments	mechanical weathering chemical weathering	physical mixing
Alluvial-delta plain environments	chemical weathering	physical mixing
Shallow marine environments	mechanical weathering	physical mixing
Deep marine environments	-	physical mixing

5. Linear models of compositional variation

In a sedimentary system, selective and non-selective modifications usually go together. This is obvious from the fact that breakage of grains is particularly common during transport in high-gradient streams (e.g., Cameron & Blatt, 1968; McBride & Picard, 1987; Ibbeken & Schleyer, 1991). Far less obvious is the distinction between weathered sediments before and after transport. For instance, a series of observations arranged along a vertical profile through a soil and saprolith into an unweathered polymineralic parent rock is expected to show a non-linear compositional trend attributable to *in situ* weathering, represented by the curved line segment in Fig. 6B. As soon as this weathering residue is stripped from the bedrock surface, and enters the sedimentary (fluvial) system, its spatial pattern of compositional variation will change due to physical mixing of materials derived from various levels in the original soil profile. The new pattern of compositional variation displayed after transport will consist of a roughly triangular area delimited by the original trend and the straight line between the two extreme compositions (Fig. 6C). In this particular case, the resulting pattern of compositional variation is virtually indistinguishable from that of the ternary mixing system depicted in Fig. 6A.

Based on these considerations, one might argue that compositional variation in many natural sedimentary systems can be adequately *described* by a linear mixing model. However, the fact that a linear mixing model can be fitted to the data does not automatically imply that the observed variation indeed reflects physical mixing. An example of a non-linear system that can be adequately described (but not explained) by a linear mixing model is the feldspar solid-solution series. This geochemical-mineralogical system shows two superimposed patterns of binary "mixing" (i.e., albite-plagioclase and albite-potassium feldspar), which together form a ternary "mixing" system that can be displayed in a ternary

diagram. The peculiar distribution of admissible "mixing proportions" within the ternary diagram indicates that the compositional variation is unlikely to reflect random physical mixing, because "mixtures" of potassium feldspar and plagioclase are not allowed.

In practice, the spatial distribution of "mixing proportions" in the area under investigation and the geological reasonableness of the "source compositions" should be taken into account in order to determine if the observed variation can indeed be attributed to physical mixing. The mathematical background and a number of applications of linear mixing models will be discussed in detail in the following chapters.

6. Analysis of high-frequency detrital signals

Valuable information about rates of chemical weathering has been obtained from the analysis of "weathering rinds" on conglomerate clasts (Colman, 1981, 1986; Colman & Dethier, 1986; Whitehouse et al., 1986; Bull, 1991). This method is now widely used for relative and absolute dating of Quaternary alluvium. The rate of change of most rock-weathering features decreases with time; typical initial growth rates of weathering rinds on volcanic and sedimentary clasts are of the order of 0.1 mm/kyr (Colman, 1986). Modifications of principal framework composition by chemical weathering are much more rapid, due to the larger surface/volume ratio of sand-sized sediments. Significant compositional maturation of sands under humid tropical weathering conditions occurs in less than 6 kyr (Johnsson & Meade, 1990), and it may take no more than 30 to 40 kyr to wipe out the parent-rock signal completely (Kroonenberg, in press). *In situ* weathering of plutonic detritus in cold subhumid mountainous drainage basins results in a significant increase of quartz/feldspar ratios (from 1.0 in parent rocks to 2.0 in soils) over a period of less than 5 kyr (Mahaney & Halvorson, 1986). The above observations strongly suggest that first-cycle sands take less than 10 kyr to reach a significant degree of compositional maturation under a wide range of climatic conditions. High-frequency detrital signals (with wavelengths of 10 to 100 kyr) are also generated in areas where regular alternations of arid and semi-arid, or arid and subhumid conditions prevailed, as demonstrated by analyses of Quaternary conglomerate-clast assemblages (Bull, 1991) and Pleistocene high-resolution aeolian clay-mineral records (Krissek & Clemens, 1991).

Sediments move down alluvial systems in distinct pulses (Johnsson et al., 1991). Extensive studies of Quaternary fluvial systems and hillslope sediment reservoirs demonstrate that sediment fluxes have been strongly influenced by short-term climatic changes in the range of 10 to 100 kyr. In general, the timing of climatically induced aggradation and degradation events in alluvial systems seems to be in step with variations in the Earth's orbital parameters, although responses are complex and differ in number from region to region, reflecting climatic, tectonic, and lithologic controls of the time needed to replenish hill slope sediment reservoirs after stripping events (Bull, 1991). The evolution of hillslope reservoirs is largely dictated by self-enhancing feedback mechanisms which preclude a rapid alternation between stages of denudation and stages of colluvial aggradation and soil formation. It has therefore been suggested that high-frequency compositional signals are unlikely to be generated in hillslope reservoirs (Velbel & Saad, 1991). The data of Ibbeken & Schleyer (1991) indeed show that physical mixing of sediments in high-gradient alluvial systems is extremely efficient.

The situation is quite different in more distal reaches of the subaerial sedimentary system. The limited data available suggest that sand grains spend most of their time in inactive parts of the alluvial system, and very little time in transport (Schick et al., 1987a, 1987b; Johnsson et al., 1991; Heller et al., 1992). Consequently, the major source of compositional modification in low-gradient drainage basins of large river systems, coastal plains, and delta plains is *in situ* weathering during times of temporary storage (Krook, 1969; Cleary & Conolly, 1971; Savage et al., 1988; Johnsson & Meade, 1990). It seems likely that high-frequency signals should originate in a low-gradient alluvial system, where sediments from different sources have been homogenized, relief is low and residence times are long in comparison with the upper reaches of the alluvial system.

However, the fact that high-frequency signals are generated in many sedimentary systems does not imply that such signals are also preserved. "Fresh" sands derived from a hillslope reservoir are mixed with *in situ* weathered sands derived from reworking within the alluvial system (Cleary & Conolly, 1971; Franzinelli & Potter, 1983; Johnsson et al., 1991). The ultimate composition of sediments which have crossed the entire length of a drainage basin thus depends on the extent of *in situ* weathering, and the degree of mixing with previously deposited sediments. The preservation of high-frequency detrital signals thus largely depends on the rate of mixing (temporal averaging), which is a function of sediment supply and subsidence rate. Tectonically active margins are potentially suitable locations for the preservation of high-frequency detrital signals, because sediment supply and subsidence rates are generally high, and physical mixing due to reworking of sand bodies in the low-gradient alluvial system is minimal (cf. Heller et al., 1992).

As discussed previously, non-linear compositional trends generated by *in situ* weathering may be completely obscured by physical mixing. A prerequisite for the positive identification of weathering signals is that the sediment supplied to a low-gradient alluvial system has attained compositional stability by temporal and spatial averaging due to physical mixing upstream, prior to being subjected to *in situ* modifications. Such sediments are (at least conceptually) derived from a single, compositionally stable source, and the observed compositional variability should primarily reflect varying degrees of modifications in transit, attributable to changing climatic and/or physiographic conditions. The efficiency of mixing in lower-order drainage basins (Ibbeken & Schleyer, 1991) suggests that this requirement is fulfilled in many high-gradient feeder systems.

Current methods of estimating palaeoclimate conditions from sandstone composition suffer from various drawbacks: (1) *A priori* knowledge of parentage is required: sediments must be derived from known monolithologic parent rocks; (2) *A priori* knowledge of tectonic relief and distance from the source is required in order to assess the residence time of detritus. These limitations indicate that current methods can only be used with confidence in lower-order drainage basins. However, temporal resolution of detrital signals generated in such basins is inferred to be small due to the averaging of sand(stone) composition in hillslope reservoirs, whereas long-term palaeoclimate estimates from sandstone compositions could be seriously in error due to changing provenance in response to progressive denudation in the source area. It is therefore suggested that palaeo-environmental studies of sandstone composition should focus on the analysis of *short-term climatic-physiographic changes* recorded in sedimentary systems fed by a compositionally stable source.

An approach along these lines requires far less *a priori* knowledge of parent lithologies and residence time. It cannot provide an "absolute" estimate of palaeoclimate conditions, but it does allow to detect high-frequency signals, which reflect the dynamics of the system in response to short-term palaeo-environmental changes. If high-frequency signals are indeed preserved in basin fills, the systematic analysis of such palaeoclimatic-physiographic signatures should allow to refine the interpretation of short-term variability in fossil sedimentary systems. This, in turn, should narrow the gap between the observed dynamics of (sub)recent geomorphic systems and the interpretation of pre-Quaternary basin fills.

7. Basic patterns of compositional variation in basin fills

The review of compositional modifications and principal controls on the framework composition of sand-sized sediments presented in this chapter suggests that patterns of compositional variation in basin fills can be subdivided into two extreme types:

Type 1: Basin fills derived from multiple sources, in which linear compositional modifications induced by physical mixing are the principal determinants of the observed spatial (and/or temporal) compositional variation.

Type 2: Basin fills derived from a single source, in which non-linear compositional modifications induced by chemical weathering are the principal determinants of the observed temporal (and/or spatial) compositional variation.

In reality, few basin fills can be unambiguously assigned to one of both categories. For instance, the entire fill of a large basin along an active margin may be satisfactorily described in terms of type 1 for a series of time slices, whereas a detailed study of the sediments supplied by one of its sources over a considerable period of time is likely to indicate a type 2 pattern. Numerical and statistical modelling techniques have been developed for solving problems associated with these two cases, according to the guidelines set out above. These methods and their application to recent and fossil basin fills are discussed in subsequent chapters. The analysis of type 1 basin fills is discussed in chapters 3, 4 and 6. A type 2 basin fill is analysed in chapter 8, and a "hybrid" case is presented in chapter 7.

Appendix I

SANDS FROM VARIOUS LOWER-ORDER FLUVIAL DRAINAGE BASINS

Reference	No.	PL	C	R	WI	Q(%)	F(%)	R(%)	ln(Q/F)	ln(Q/R)
Basu (1976)	51	P	0	1	0	31.9	38.5	29.6	-0.189	0.072
Tortosa et al. (1989)	22	P	0	0	0	29.0	50.0	21.0	-0.545	0.323
Tortosa et al. (1989)	11	P	0	0	0	32.0	32.0	36.0	0.000	-0.118
Basu (1976)	37	P	1	1	1	59.9	28.1	12.1	0.758	1.599
Mann & Cavaroc (1973)	2	P	1	1	1	45.2	43.7	11.1	0.034	1.403
Franzinelli & Potter (1983)	21	P	2	2	4	92.9	3.0	4.0	3.423	3.135
Franzinelli & Potter (1983)	13	P	2	2	4	93.9	3.1	3.1	3.423	3.423
Tortosa et al. (1989)	8	M	0	0	0	22.0	1.0	77.0	3.091	-1.253
Young (1975) in Basu (1985a)	?	M	0	1	0	29.0	3.0	68.0	2.269	-0.852
Mack (1981)	6	M	1	1	1	71.0	2.0	27.0	3.570	0.967
Mann & Cavaroc (1973)	2	M	1	1	1	80.5	4.8	14.7	2.828	1.702
Young (1975) in Basu (1985a)	?	M	1	1	1	74.0	6.0	20.0	2.512	1.308
Mann & Cavaroc (1973)	2	S	1	1	1*	76.8	13.6	9.6	1.733	2.075
Franzinelli & Potter (1983)	33	S	1	0	0*	54.8	6.5	38.7	2.140	0.348
Franzinelli & Potter (1983)	9	S	1	1	1*	70.5	7.4	22.1	2.259	1.160
Franzinelli & Potter (1983)	12	S	2	2	4*	87.9	2.0	10.1	3.773	2.163

PL		PARENT LITHOLOGY:	WI		WEATHERING INDEX: WI = C x R
	P	plutonic and high-grade metamorphic		0	unweathered
	M	low to high-grade metamorphic		1	slightly weathered
	S	sedimentary (2nd cycle mixed P-M)		2	moderately weathered
				4	intensely weathered
		upper case: exclusive or dominant		*	
		lower case: subordinate			indicates sediment recycling
C		CLIMATE:	R		RELIEF:
	0	(semi-)arid and mediterrancan		0	high (mountains)
	1	temperate subhumid		1	moderate (hills)
	2	tropical humid		2	low (plains)

Appendix II

FLUVIAL SANDS FROM ORINOCO RIVER DRAINAGE BASIN (Johnsson et al., 1991)

Morphotectonic provinces		No.	PL	C	R	WI	Q(%)	F(%)	R(%)	ln(Q/F)	ln(Q/R)
Orogenic terranes	Caribbean Mountains	16	Mp	1	0	0	48.4	5.7	45.9	2.136	0.054
	Northern Merida Andes	10	Pm	1	0	0	48.4	12.7	38.9	1.338	0.220
	Southern Merida Andes	6	S	1	0	0*	73.7	2.0	24.3	3.598	1.109
	Cordillera Oriental	13	SM	1	0	0*	50.2	0.5	49.3	4.522	0.019
Orogenic terranes & Foreland basin	proximal Llanos (< 100 km)	26	SMP	1	1	1*	63.3	8.5	28.2	2.005	0.807
	middle Llanos (100-200 km)	10	Smp	2	1	2*	83.2	4.6	12.2	2.885	1.921
	distal Llanos (> 200 km)	6	Smp	2	2	4*	91.7	2.8	5.5	3.500	2.807
Foreland basin	Western Llanos	7	S	2	2	4*	99.1	0.3	0.6	5.796	5.103
	Eastern Llanos	13	S	2	2	4*	99.2	0.5	0.3	5.282	5.793
Guayana Shield	elevated (no cover)	43	P	2	1	2	84.4	10.7	4.9	2.061	2.840
	elevated (sed. cover)	11	Sp	2	1	2*	97.1	0.8	2.1	4.763	3.847
	lowland	15	P	2	2	4	97.8	1.5	0.7	4.171*	4.933
Orinoco mainstem	(averaged)	44	SMP	2	2	4*	95.0	1.6	3.4	4.114	3.326

CHAPTER 3

END-MEMBER MODELLING OF COMPOSITIONAL DATA: NUMERICAL-STATISTICAL ALGORITHMS FOR SOLVING THE MIXING PROBLEM IN SEDIMENTARY PROVENANCE STUDIES

1. THE MIXING PROBLEM

1.1 Introduction

Detrital sediments generally consist of many different types of particles. Sands, for example, can be extremely heterogeneous materials, on a microscopic scale as well as the much larger scale of an entire sedimentary basin. In many cases, the spatial heterogeneity of sands can be conveniently described in terms of a *linear mixing model*. Data sets which conform to this model can be expressed as *mixtures of a fixed number of end members*. It is a trivial exercise to predict the composition of any mixture if we know the compositions of the end members, and their proportional contributions. Unfortunately, the opposite occurs more frequently in practice: compositional variation is assumed to reflect mixing, but the exact nature of the mixing process is unknown. The *mixing problem* manifests itself whenever it is required to recast observed compositional variation among a series of observations in terms of a mixing model. A general solution to the mixing problem is crucial to the advancement and wider application of sedimentary provenance studies in basin analysis. Estimating the parameters of a mixing process and apportioning mixtures of sediments to their respective sources is a prerequisite for the reconstruction of source-area evolution and sediment-dispersal patterns. These, in turn, contain valuable information about the interplay of tectonic and climatic controls on basin infill.

In this paper, numerical and statistical methods for solving the mixing problem will be presented. A brief overview of the historical developments in this field is followed by a detailed account of the basic algebra and computational procedures. Special attention will be given to the assumptions required for inversion of compositional data, and their implications for the resulting mixing models. A synthetic data set of nine sandstone compositions, expressed in terms of the principal framework constituents quartz, feldspar, and lithic (polymineralic) fragments, has been used to illustrate some of the basic aspects of mixing models (Table 1). Many of the concepts and computational procedures can be clarified by referring to a *geometric vector model*. This limits the number of compositional variables in these examples to three. However, the same algebraic concepts apply to data sets consisting of any number of components. All algebraic symbols used have been listed in Appendix I.

1.2 The geometric vector model

Compositions can be represented by vectors from the origin $\boldsymbol{O}$ to a set of coordinates $\boldsymbol{X}$, which define directions in the positive orthant of p-dimensional space (e.g. Imbrie & Purdy, 1962; Imbrie & Van Andel, 1964; Philip & Watson, 1988b). The constant sum of the

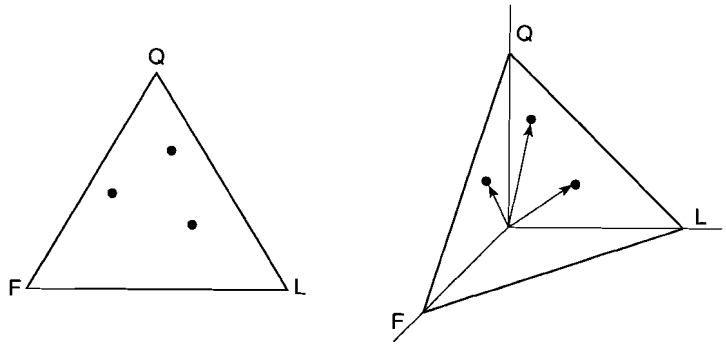

Figure 1. Geometric vector model of compositional data with three components. The tips of all composition vectors are confined to a two-dimensional simplex: the ternary diagram.

compositional variables, usually 1, 100, or 10^6 (for measurements recorded as proportions, percentages, or parts per million, respectively), accounts for the fact that the tips of all composition vectors are confined to a (p-1)-dimensional hyperplane or simplex (e.g. Aitchison, 1986). For example, framework compositions of sands are generally expressed in terms of their percentual quartz, feldspar, and lithic content (QFL%). Such compositions can be represented by vectors from the origin to a set of QFL-coordinates in 3-dimensional space. All possible composition vectors within that space are confined to a 2-dimensional simplex: the ternary diagram traditionally used in sedimentary provenance studies to display compositional data (Fig. 1). The vertices of this ternary diagram are usually thought of as variables that represent a set of orthogonal reference axes, but they can also be regarded as hypothetical observations made up of pure constituents. These hypothetical observations are the *reference vectors* or *end members* of the ternary diagram, from which all possible compositions can be generated by mixing. The ternary diagram thus outlines a *mixing space*, in which the most extreme compositions are the end members. In a geometrical sense, the end-member vectors are the *vertices* of this mixing space.

Table 1. Synthetic data set of nine sandstone compositions, defined in terms of principal framework constituents. The data set was constructed by mixing of the first three compositions.

Label	Quartz (%)	Feldspar (%)	Lithics (%)
Obs. 1	80.0	5.0	15.0
Obs. 2	50.0	30.0	20.0
Obs. 3	40.0	15.0	45.0
Obs. 4	65.0	17.0	18.0
Obs. 5	60.0	10.0	30.0
Obs. 6	57.0	20.0	23.0
Obs. 7	52.0	15.0	33.0
Obs. 8	44.0	21.0	35.0
Obs. 9	68.0	10.0	22.0

Any sandstone composition represented on a ternary diagram can be interpreted as a mixture of theoretical end members consisting of mineralogically pure sands (made up of 100% quartz, 100% feldspar, and 100% lithic grains, respectively). For instance, a synthetic data set (Table 1) is depicted in Fig. 2A as a series of mixtures of these pure constituents. The corresponding mixing model is given in Table 2. Not much has been gained in terms of explanatory power by fitting this mixing model to the data. The model cannot be interpreted in terms of physical mixing, because it employs *virtual end members*: sands made up of pure feldspar and lithic grains do not occur in nature. But many other mixing models could be defined which are capable of reproducing the data exactly with a completely different set of end members.

The synthetic data set of Table 1 was constructed from the first three observations, which have been mixed in various proportions to generate the other six compositions. A mixing model with the first three observations as end members is shown in Fig. 2B and Table 2. The second model can be interpreted in terms of physical mixing, because it employs *realistic end members*, i.e., extreme compositions actually observed. The new mixing model of the dataset is much more informative for those interested in provenance of sandstone than the former. According to this new model, the observed compositional variation can be attributed to the mixing of three compositionally "extreme" types of sandstone, termed arkosic arenite, quartz arenite, and lithic arenite, respectively. The change from the first to the second mixing model is accomplished by a *coordinate transformation*. In this case, the frame of reference has been transformed by replacing the orthogonal reference vectors with a subset of vectors from the dataset (and changing the mixing proportions accordingly). The geometric mixing model can be generalized to an algebraic mixing model, which can be used to represent mixing systems with any number of compositional variables.

1.3 The general mixing model

Compositional data are generally cast into the form of a matrix $\boldsymbol{X}$, with n rows representing observations, and p columns representing variables. The compositional variables are non-negative, and each row of the data matrix sums to a constant c, usually 1, 100, or 10^6 (for measurements recorded as proportions, percentages, or parts per million, respectively).

$$\sum_{j=1}^{p} x_{ij} = c \qquad x_{ij} \geq 0 \tag{1}$$

If compositional variation among a series of measured specimens results from a physical mixing process, each row of the matrix of compositional data $\boldsymbol{X}$ is a non-negative linear combination of the q rows of $\boldsymbol{B}$, a matrix of end-member compositions. The matrix $\boldsymbol{M}$ represents the proportional contributions of the end members to each observation. In matrix notation, this perfect mixing can be expressed as

$$\boldsymbol{X} = \boldsymbol{MB} \tag{2}$$

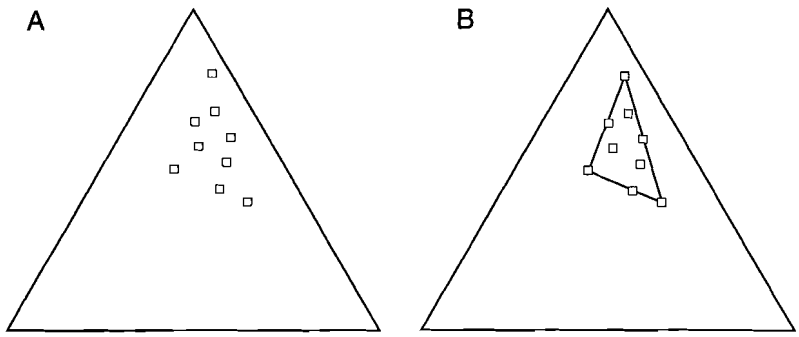

Figure 2. Ternary diagrams showing the data set of Table 1. A: standard ternary representation. B: representation of the data as mixtures of "extreme" observations.

Table 2. Two mixing models of the synthetic data. The first model is the commonly used ternary representation; the second model employs a subset of "extreme" observations as end members.

FIRST MIXING MODEL				SECOND MIXING MODEL			
End-member contributions:				End-member contributions:			
Obs. no.	EM 1	EM 2	EM 3	Obs. no.	EM 1	EM 2	EM 3
1	0.80	0.05	0.15	1	1.00	0.00	0.00
2	0.50	0.30	0.20	2	0.00	1.00	0.00
3	0.40	0.15	0.45	3	0.00	0.00	1.00
4	0.65	0.17	0.18	4	0.51	0.47	0.02
5	0.60	0.10	0.30	5	0.50	0.00	0.50
6	0.57	0.20	0.23	6	0.29	0.53	0.18
7	0.52	0.15	0.33	7	0.26	0.17	0.57
8	0.44	0.21	0.35	8	0.00	0.40	0.60
9	0.68	0.10	0.22	9	0.67	0.11	0.21
Mean	0.57	0.16	0.27	Mean	0.36	0.30	0.34
End-member compositions:				End-member compositions:			
Label	Q (%)	F (%)	L (%)	Label	Q (%)	F (%)	L (%)
Pure Q	100.0	0.0	0.0	Obs. 1	80.0	5.0	15.0
Pure F	0.0	100.0	0.0	Obs. 2	50.0	30.0	20.0
Pure L	0.0	0.0	100.0	Obs. 3	40.0	15.0	45.0

subject to the following non-negativity and constant-sum constraints:

$$\text{(3)} \qquad \sum_{k=1}^{q} m_{ik} = 1 \qquad m_{ik} \geq 0$$
$$\sum_{j=1}^{p} b_{kj} = c \qquad b_{kj} \geq 0$$

Although this representation is acceptable from an algebraic point of view, it does not account for the fact that perfect mixing cannot be demonstrated in practice, due to sampling and measurement errors in $\boldsymbol{X}$. Therefore, the assumption is made that the data matrix $\boldsymbol{X}$ is made up of a systematic part $\boldsymbol{X'}$, attributable to perfect mixing, and a matrix of error terms $\boldsymbol{E}$, representing non-systematic contributions to $\boldsymbol{X}$. We will assume that the errors are relatively small and $\boldsymbol{X'}$ "closely" resembles $\boldsymbol{X}$. By definition, the rows of $\boldsymbol{X'}$, the estimated matrix of perfect mixtures, consist of non-negative linear combinations $\boldsymbol{M}$ of q end-member compositions $\boldsymbol{B}$:

$$\text{(4)} \qquad X' = X - E$$
$$X' = MB$$

The range of each variable in $\boldsymbol{X'}$ cannot exceed that of the corresponding variable in the end members $\boldsymbol{B}$, due to the non-negativity constraint on $\boldsymbol{M}$. In other words, the end-member matrix must contain the extreme values of each variable. By definition, the rows of $\boldsymbol{X'}$ are also subject to the constant-sum constraint, and therefore

$$\text{(5)} \qquad \sum_{j=1}^{p} x'_{ij} = c \qquad x'_{ij} \geq 0$$
$$\sum_{j=1}^{p} e_{ij} = 0$$

The above considerations lead to the following mathematical formulation of the general mixing model (subject to the constraints listed above):

$$\text{(6)} \qquad X = MB + E$$

A linear mixing model provides an efficient and informative summary of the "structure" of a compositional dataset whenever physical mixing or an analogous process is assumed to be the dominant cause of variation among a series of observations. With the help of this *forward model*, the composition of each sample from a given area or sediment body can be explained in terms of mixing, and the range of admissible values for any of the compositional variables can be predicted. Attention will now be focussed on methods for solving the *inverse problem*, i.e., the problem of estimating the parameters of such models from a series of observations. Methods for solving the mixing problem have been historically conceived as *unmixing* (Ehrlich & Full, 1987; Williams et al., 1988).

1.4 Inverse modelling strategies

Unmixing strategies may differ widely, depending on the extent of *a priori* knowledge available to the researcher. Two cases can be distinguished, based on the mathematical form of the inverse problem. The history and principles of both methods are briefly discussed in the following sections.

(1) The end members are known *a priori*, i.e., the number of end members and their compositions is assumed to determine $\boldsymbol{B}$ exactly. Methods for solving this problem are referred to as *linear unmixing*.
(2) Nothing is known about the end members and the mixing model must be based on the data only. Methods for solving this problem are referred to as *bilinear unmixing*.

2. LINEAR UNMIXING

2.1 Normative partitioning

Normative partitioning was one of the first linear unmixing methods developed in igneous petrology and geochemistry. The objective of this technique is to recast the chemical compositions of igneous rocks and solid solution series of mineral groups such as feldspar, pyroxene, and garnet into proportional contributions of a set of (theoretical) end-member minerals. Partitioning according to the CIPW norm (Cross et al., 1902; Kelsey, 1965) has been employed widely by igneous petrologists. The mineral composition of an igneous rock specimen according to the CIPW norm is obtained by assigning the major oxides to one of the theoretical end-member minerals in an order reflecting the presumed order of crystallisation from the parent magma. This subtractive partitioning approach requires considerable *a priori* knowledge of the geological system under consideration. Not only does it require knowledge of the number of end members and their chemical compositions, but it also relies on the assumption that the composition of a rock specimen can be adequately represented by an assemblage of theoretical end-member minerals, i.e., that the presumed crystallisation indeed took place and equilibrium conditions were established.

In general, such assumptions are of limited value for the normative partitioning of sediments, which may contain a wide range of minerals that are unstable under atmospheric conditions. The opposite view, i.e., that detrital sediments are made up of a "chance medley" of minerals (Blatt, 1967), is probably more realistic. It explains why normative partitioning of sedimentary rocks has met with limited success (Imbrie & Poldervaart, 1959; Miesch, 1962; Nicholls, 1962; Garrels & Mackenzie, 1971). Nevertheless, recasting geochemical compositions of sediments into contributions of "standard" minerals, analogous to the CIPW norm, is still regarded as a useful tool for comparative purposes. Recently developed normative partitioning methods for sediments allow for greater flexibility, by taking into account the observed variation within single end members, and/or variations in the number of chemical components actually measured (e.g. Heath & Dymond, 1977; Cohen & Ward, 1991; Merodio et al., 1992).

2.2 Normative partitioning by least squares

The application of matrix algebra to petrogenetic problems led to an important generalisation of normative partitioning procedures (Perry, 1967; Chayes, 1968; Bryan et al., 1969). The use of least squares estimation procedures enables the objective minimization of differences between measured compositions and calculated normative compositions, eliminating the need for *a priori* knowledge of the crystallisation order of minerals. Many different versions of least squares partitioning have been proposed in petrology and geochemistry (Gray, 1973; Reid et al., 1973; Albarède & Provost, 1977; Stormer & Nicholls, 1978; Provost & Allègre, 1979; LeMaitre, 1979, 1981; Russell, 1986; Woronov, 1991a). Variations between these least squares estimation procedures arise from the methods used to implement sum-to-one (i.e., mass conservation) constraints on the system, and from different criteria for weighing the presumed analytical errors.

As in normative partitioning, *a priori* knowledge of the number of end members and the end-member compositions reduces the unmixing procedure to solving a set of linear equations. In least squares partitioning the number of compositional variables p exceeds the number of end members q (equality of these two numbers implies that an exact solution can be computed). The basic least squares problem is formulated as follows:

The system of linear equations

$$\boldsymbol{B}^T\boldsymbol{m}^T \approx \boldsymbol{x}^T \tag{7}$$

is solved for $\boldsymbol{m}$ by means of the normal equations

$$\boldsymbol{m}^T = (\boldsymbol{B}\boldsymbol{B}^T)^{-1}\boldsymbol{B}\boldsymbol{x}^T \tag{8}$$

The least squares estimate of each normative composition is then given by

$$\boldsymbol{x}' = \boldsymbol{m}\boldsymbol{B} \tag{9}$$

A major drawback of this approach is that least squares minimization of the differences between observed and normative compositions may result in negative contributions $\boldsymbol{m}$ of one or more end members, and consequently, negative components of the estimated normative composition $\boldsymbol{x}'$. This unfavourable result has been encountered in various sediment-partitioning experiments (e.g. Pearson, 1978; Hodgson & Dudeney, 1984; Herron, 1986; Harvey & Lovell, 1992). Alternative algorithms, such as *non-negative least squares* (e.g. Lawson & Hanson, 1974; Menke, 1984), *quadratic programming* (Chatterjee et al., 1989), or *linear programming* (e.g. Wright & Doherty, 1970; Banks, 1979) can be used to produce mathematically feasible (i.e., non-negative) solutions to $\boldsymbol{m}$ in cases where the ordinary least squares approach fails to provide such results. All of the above-mentioned techniques require that the end-member compositions are known exactly, or have been measured without errors. However, if the composition of the mixture to be partitioned has

also been determined accurately, unrealistic least squares solutions must reflect incorrect assumptions regarding the number of end members and/or the end-member compositions. Therefore, a mathematically feasible solution obtained by imposing non-negativity constraints on the mixing parameters by means of constrained least squares approximation or linear programming does not necessarily imply a correct choice of end members.

3. BILINEAR UNMIXING

3.1 The explicit mixing problem

Unmixing is much more difficult if no *a priori* information about the number of end members and/or their compositions is available, as in many sedimentary provenance studies. In such cases, the mixing problem is stated in explicit form, indicating that all mixing parameters must be estimated from the data. A solution to the explicit mixing problem for a given data set requires estimation of the following parameters (defined as in equations 2 to 6):

- $\boldsymbol{X'}$ (the "perfect mixture" compositions)
- $\boldsymbol{E}$ (the non-systematic contributions to the data)
- q (the number of end members)
- $\boldsymbol{B}$ (the end-member compositions)
- $\boldsymbol{M}$ (the end-member contributions to each "perfect mixture")

The explicit mixing problem can be solved in two steps. According to equation 4, the data matrix must be partitioned into "signal" and "noise", before the "signal" can be expressed as the product of two matrices $\boldsymbol{M}$ and $\boldsymbol{B}$. The second step of modelling end-member compositions and mixing proportions from the estimated matrix of "perfect mixtures" is then reduced to solving a bilinear problem. The bilinear problem cannot be solved uniquely by inverse methods, because there may be an infinite number of mixing models that fit a given set of data within tolerable error, and the particular combination of mixing parameters which actually produced the data cannot be reconstructed. However, estimates of the mixing parameters that satisfy additional constraints on the solution can be identified. One of these solutions will be referred to as the "optimal" solution of the mixing problem under consideration.

3.2 Vector analysis

The first unmixing method aimed at resolving the explicit mixing problem was introduced to geology by Imbrie (1963) under the name of *vector analysis*, although it is commonly referred to as *(extended) Q-mode factor analysis*. The latter denomination is rather misleading, in view of the fact that the methods and objectives of unmixing have little in common with those of factor analysis as developed in the social sciences. In its initial form, Q-mode factor analysis was intended as a classification tool aimed at resolving a series of observations into linear combinations of a small number of theoretical observations or *factors* (Burt, 1937). *Vector analysis* can be regarded as an augmented form of factor analysis in which final results are given in terms of actual observations judged to be significant end members in the spectrum of diversity under study (Imbrie, 1963; Imbrie &

Van Andel, 1964; Manson & Imbrie, 1964). The concepts and methods of vector analysis are discussed in detail by Jöreskog et al. (1976), who refer to it as the *Imbrie Q-mode method.*

The vector analysis concept of Imbrie and co-workers was expanded by Miesch (1976a, b, c, 1980, 1981), which resulted in the first generally applicable algorithms for unmixing of compositional data. Unmixing is accomplished by two computer programs, EXTENDED CABFAC and QMODEL (Klovan & Miesch, 1976). The program EXTENDED CABFAC is a modified version of the Q-mode factor analysis program CABFAC (Klovan & Imbrie, 1971). The program QMODEL incorporates certain procedures from an earlier vector analysis program COVAP (Manson & Imbrie, 1964). The EXTENDED CABFAC-QMODEL algorithm can be used to develop mixing models without *a priori* knowledge of the number and compositions of the end members. It relies on the assumption that feasible estimates of the "true" end members, in the form of observations of extreme composition, are contained within the data set being analyzed. Unmixing by means of vector analysis often fails to produce a satisfactory mixing model if this assumption is not met, due to the lack of explicit non-negativity constraints (cf. equations 3 and 5) on the factor model. In practice this may lead to unrealistic mixing models with negative values of $\boldsymbol{X'}$, $\boldsymbol{M}$, and $\boldsymbol{B}$.

This problem was partly overcome by Full et al. (1981), who developed the EXTENDED QMODEL algorithm for deducing the compositions of "external" end members from the multidimensional geometry of a dataset. EXTENDED CABFAC-EXTENDED QMODEL (Full et al., 1981) can be used to develop models with non-negative mixing proportions $\boldsymbol{M}$ if feasible estimates of the "true" end members have not been sampled and no *a priori* knowledge of their compositions is available. A further refinement to this method was introduced by Full et al. (1982). The general outline of these QMODEL methods is discussed in Ehrlich & Full (1987) and Williams et al. (1988). Unfortunately, negative values of $\boldsymbol{X'}$ and $\boldsymbol{B}$ cannot be fully eliminated by the QMODEL algorithms. Similar objections can be raised against two other methods aimed at deducing the compositions of "external" end members from the factors provided by the EXTENDED CABFAC program, proposed by Clarke (1978) and Leinen & Pisias (1984). These two methods generally produce non-negative end-member compositions $\boldsymbol{B}$, but do not take into account possible negative values in $\boldsymbol{X'}$ or $\boldsymbol{M}$.

3.3 Alternative approaches

Alternative approaches to the explicit mixing problem have been developed to eliminate the problem of negative values in $\boldsymbol{X'}$, $\boldsymbol{M}$, and $\boldsymbol{B}$, which could not be solved by vector analysis. *Linear programming* techniques aim at minimizing the error terms $\boldsymbol{E}$ subject to non-negativity constraints on $\boldsymbol{M}$ and $\boldsymbol{B}$ (Dymond, 1981; Dymond et al., 1984; Owen, 1987). These techniques may yield satisfactory results, although they have a number of disadvantages in comparison with the vector analysis approach. Three principal objections can be raised against the use of linear programming techniques for solving the inverse mixing problem: (1) Minimization of the absolute error sum for each composition does not in general produce the "best" estimates of the mixtures $\boldsymbol{X'}$ (Renner, 1988, 1993a, b). (2) Furthermore, the mixing proportions $\boldsymbol{M}$ which are generated by these algorithms are non-negative by definition, obscuring the possibility that some of the end members $\boldsymbol{B}$ may not

represent extreme compositions (Renner, 1988; Renner et al., 1989). (3) Finally, the number of end members q must be known *a priori*, or estimated by means of other methods.

An unmixing method proposed by Ripley (1990) employs a *convex hull algorithm* for determining possible end-member compositions. By definition, a convex hull must contain all of the data points (e.g., Hadley, 1961). A mixing model based on this approach is extremely sensitive to the presence of a single data point of extreme composition, which may not even belong to the mixing process of interest. This end-member estimation procedure is far from robust, and will fail to provide a satisfactory mixing model if such outliers are present.

Renner (1988) presented alternatives to some of the vector analysis procedures developed by Klovan & Imbrie (1971), Miesch (1976a), Klovan & Miesch (1976), and Full et al. (1981). The unmixing algorithm of Renner (1988) proceeds in much the same way as the vector analysis method, although many of the potential pittfalls of the factor model have been eliminated by the use of constrained least squares estimation. The compositions of possible end members are determined by *least squares regression*, subject to non-negativity constraints on $\boldsymbol{X'}$, $\boldsymbol{M}$, and $\boldsymbol{B}$. Renner (1991) also proposed a statistical test for estimating the number of end members, based on the logratio transformation of compositional variables (cf. Aitchison, 1986), in order to supplement the estimation procedure developed by Miesch (1976a; 1980).

Van der Heijden (in press) recently pointed out that the unmixing techniques developed in the earth sciences are similar to the *Latent budget model* used in the social sciences for analysing time-allocation. The objective of latent-budget analysis is to describe the time budgets of (groups of) individuals as non-negative linear combinations of a fixed number of hypothetical or latent time budgets. Model parameters are estimated by means of a maximum likelihood criterion, under the assumption that the observations are independent and follow a multinomial distribution (De Leeuw & Van der Heijden, 1988; De Leeuw et al., 1990; Van der Heijden et al., 1992). Although the parametric form of the latent budget model closely resembles that of the mixing model, the required assumption of statistical independence is not realistic in the context of provenance reconstructions. In fact, the compositional data sets used in provenance studies should fulfill the opposite requirement, because reconstructions of spatial and temporal patterns of compositional variation in sedimentary basin fills are largely based on the dependence of neighbouring and/or successive observations in the absence of *a priori* knowledge.

4. A NEW BILINEAR UNMIXING ALGORITHM

The inverse modelling approach presented in this paper is based on a fundamentally revised concept of vector analysis, as developed by Imbrie (1963), Imbrie & Van Andel (1964), Klovan & Imbrie (1971), Klovan & Miesch (1976), Miesch (1976a, 1980), and Full et al. (1981, 1982). The concept of vector analysis advocated by these authors still includes a number of computational procedures that originated with factor analysis (such as row-normalisation of input data, the use of communalities for assessing goodness of fit, the use of Varimax rotation, and selection of initial extremes by iterative oblique projection). The relevance of this "factor analytic" approach to unmixing has been questioned (Full &

Ehrlich, 1986; Renner, 1988; Renner et al., 1989). The objectives of unmixing have in fact very little in common with those of factor analysis, in spite of their superficial methodological resemblance. Furthermore, the application of "factor analytic" procedures and terminology to the mixing problem has proved to be a major source of semantic confusion among earth scientists (Jöreskog et al., 1976; Miesch, 1976a; Davis, 1986). In the course of the present investigation, none of the "factor analytic" procedures turned out to be critical to the unmixing analysis. Therefore, all reference to factor analysis has been avoided, by discarding the obsolete "factor analytic" procedures, and by replacing them with more appropriate alternatives if necessary.

The two-stage modelling approach common to all least squares unmixing algorithms developed so far has been retained. A significant improvement over previous versions of vector analysis is the consistent use of constrained least squares estimation, which prevents the occurrence of negative values in the end members as well as in the estimated mixture compositions. In the first modelling stage, the mixing space is defined by partitioning the data into $\boldsymbol{X'}$ and $\boldsymbol{E}$ ("signal" and "noise"). This partitioning problem has a unique solution for each number of end members. The "best" solution is chosen in order to fix $\boldsymbol{X'}$ and q. Some of the methodological refinements suggested by Miesch (1980) and Renner (1988, 1991) have been included in modified form, in order to improve parameter estimation in the first modelling stage. The bilinear problem of estimating $\boldsymbol{M}$ and $\boldsymbol{B}$ is solved in the second modelling stage by means of iterative optimizations in the estimated mixing space. A new iterative algorithm for reconstructing feasible end-member compositions has been developed for this purpose. The algorithm is more robust than previously published methods, and has better convergence properties. Flexibility during the second modelling stage is guaranteed by taking into account the trade-off between two apparently contradictory properties of an "ideal" solution: a fully non-negative estimate of $\boldsymbol{M}$ and a "conservative" estimate of $\boldsymbol{B}$. The latter is non-negative by definition. If required, a final model is constructed which obeys all of the constraints discussed in section 1.3. A detailed discussion of this general solution is provided in the next sections.

5. DECOMPOSITION OF THE DATA SET

5.1 The weighted least squares criterion

The mixing models presented in Fig. 2 and Table 2 represent cases in which the number of end members q equals the number of variables p. There is no particular reason for this assumption in most applications of unmixing. On the contrary, the number of end members, q, is one of the parameters which must be estimated from the data. Fig. 3 shows some examples of different mixing systems in ternary diagrams. The "shape" of the data set is related to the number of end members: in a geometric representation of mixing, the tips of the end-member vectors define the vertices of a $(q\text{-}1)$ dimensional *mixing polytope* located in p-space. For example, when $q = 2$, the mixing polytope is a line segment; when $q = 3$, it is a plane triangle; when $q = 4$, it is a tetrahedron. A tetrahedron cannot be adequately represented in a ternary diagram, as shown in Fig. 3c. The end-member contributions to each data point are not uniquely determined in the latter case, because four end-member compositions are not *linearly independent* in a three-dimensional space. End members

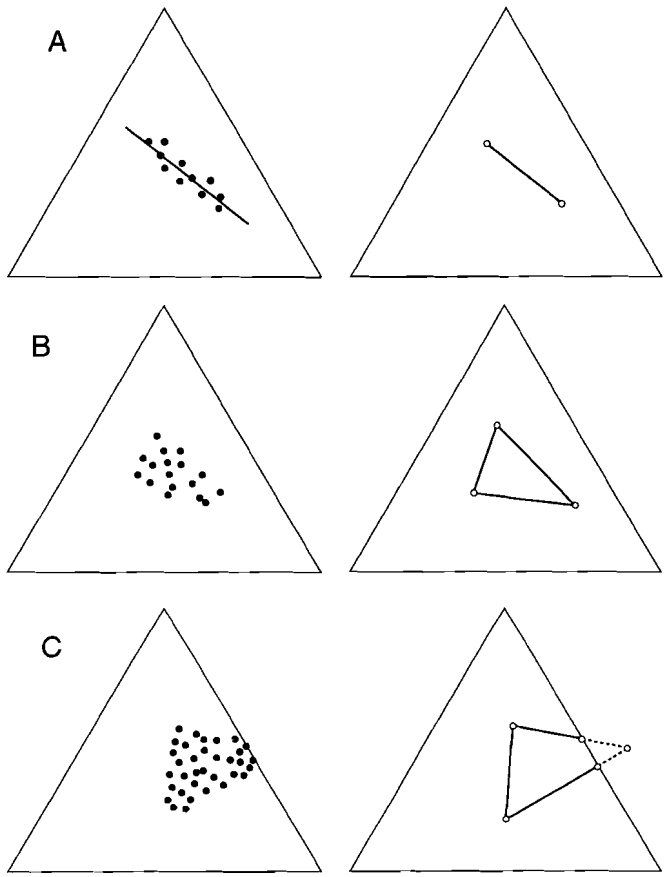

Figure 3. Mixtures of various numbers of end members. A: two end members with superimposed noise. B: three end members. C: four end members; assumption of linear independence does not hold.

which can be expressed as linear combinations of a subset of the other end members do not increase the number of dimensions occupied by the data set. In other words, the "shape" or "dimensionality" of the data in p-space indicates which number of linearly independent vectors spans the mixing polytope. As shown in Fig. 3c, the requirement of linear independence limits the maximum number of end members that can be distinguished to p. There is no reason why the actual number of end members in natural mixing systems should be limited to p. However, in such cases the number of end members cannot be estimated.

In general, the data can only be reproduced exactly by a linear model with p linearly independent reference vectors or end members. If we would choose any number of end members less than p, the data cannot be reproduced exactly, unless the data are free of errors. The latter assumption is not very realistic, and therefore, the following rule is adopted: *If it is accepted that a "small" proportion of the compositional variability reflects*

non-systematic contributions to the data, the number of end members is allowed to be less than p. If for some reason, the number of end members is judged to be less than p, the data cannot be reproduced exactly by the mixing model, and we must estimate $\boldsymbol{X'}$, the matrix of "true" mixtures, from $\boldsymbol{X}$. Since $\boldsymbol{X}$ is assumed to be compositionally "close" to $\boldsymbol{X'}$, this raises the question of quantifying the difference between compositions.

According to the vector model, the difference between two compositions i and n can be expressed as the cosine of the angle $\boldsymbol{\theta}$ between two vectors, the "coefficient of proportional similarity" (Imbrie & Purdy, 1962; Butler, 1979; Philip & Watson, 1988):

(10)
$$\cos \theta_{in} = \frac{\sum_{j=1}^{p} x_{ij} x_{nj}}{\sqrt{\sum_{j=1}^{p} x_{ij}^2 \sum_{j=1}^{p} x_{nj}^2}}$$

The angle between these two vectors ($\boldsymbol{\theta}_{in}$) in degrees is given by:

(11)
$$\theta_{in} = \frac{180}{\pi} \arccos \theta_{in}$$

The angle between two composition vectors can vary between 0^0 ($\cos \boldsymbol{\theta} = 1.0$; perfect similarity) and 90^0 ($\cos \boldsymbol{\theta} = 0.0$; perfect dissimilarity or orthogonality). If the observation vectors are normalized to unit length (i.e., projected onto a unit hypersphere), the sum of angles between each normalized vector $\boldsymbol{X}$ and its estimate $\boldsymbol{X'}$ is proportional to the sum of squared distances in p-space, as indicated by equation 12:

(12)
$$\sum_{i=1}^{n} \sum_{j=1}^{p} (x_{ij} - x'_{ij})^2$$

Minimization of this expression provides the "least squares" estimate of $\boldsymbol{X}$, i.e., an estimate that is "compositionally most similar" to the original data, given the constant-sum contraint (LeMaitre, 1979; Renner, 1988; Renner et al., 1989). A geometric interpretation of the least squares approximation of composition vectors is depicted in Fig. 4.

As a result of least squares approximation, the magnitude of the standard deviation of each variable x_j is inversely proportional to its residual sum of squares. In other words, the variables with the largest standard deviations will tend to be more closely accounted for by a least squares solution $\boldsymbol{X'}$. This may not be in accordance with the (assumed) properties of the dataset and/or the analytical precision of the measuring equipment (Miesch, 1976a, 1980; Hamann & Herzfeld, 1991).

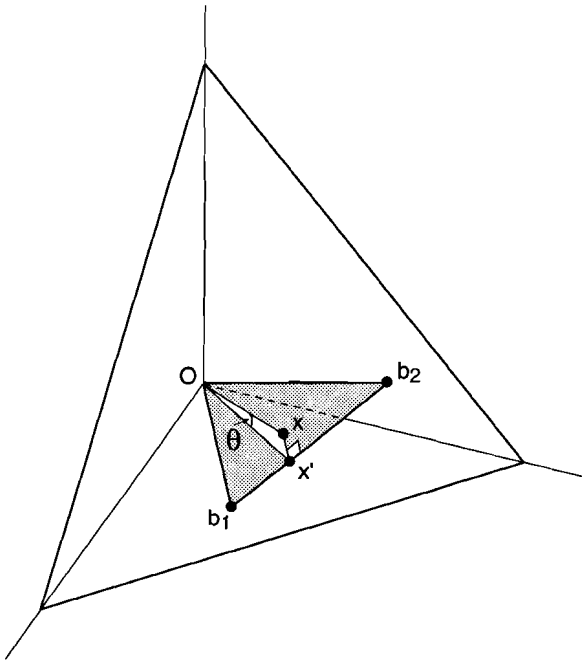

Figure 4. Orthogonal projection of observation x onto the mixing space b_1b_2. Vector x' provides the best estimate of x (angle θ is at a minimum).

If desired, the "weight" of each variable can be adjusted by scaling the columns of $\boldsymbol{X}$ prior to the computation of least squares estimates (Manson & Imbrie, 1964; Klovan & Imbrie, 1971; Miesch, 1976a):

(13)
$$w_{ij} = \frac{x_{ij} - h_j}{g_j - h_j}$$

Depending on the choice of g_j and h_j, the columns of $\boldsymbol{X}$ can be scaled so as to have certain desired characteristics. No scaling is performed when g_j=1.0 and h_j=0.0 (Under these circumstances $\boldsymbol{W}$=$\boldsymbol{X}$). Scaling of the columns of $\boldsymbol{X}$ to have means all equal to 0.5 and specified weights (i.e., standard deviations) can be achieved by other choices of g_j and h_j. The procedure for deriving these constants has been described in detail by Miesch (1980). Scaling of the variables to proportions of the column ranges (g_j=$max(x_j)$; h_j=$min(x_j)$), or to proportions of the column maxima (g_j=$max(x_j)$; h_j=0) has been used frequently. In both cases, the range of each scaled variable w_j is restricted to the interval [0.0,1.0], and the residual sum of squares of each column of $\boldsymbol{W}$' will be of the same order of magnitude. The least squares approximation of the scaled data matrix $\boldsymbol{W}$ enables the calculation of a *weighted least squares estimate* of the original data matrix $\boldsymbol{X}$.

5.2 Resolving the scaled data into linear form

The mixing process can be modelled under the assumption that the actual end-member vectors are *linearly independent*, i.e., that the rank or "dimensionality" of $\boldsymbol{B}$ equals the number of end members (see Fig. 3). By definition, this would also determine the rank of $\boldsymbol{X}$ (or its scaled version $\boldsymbol{W}$), since every observation must consists of a linear combination of the end members. In reality, errors are always present in $\boldsymbol{X}$ and its exact rank equals the number of variables p. Estimating the number of linearly independent end members needed to "closely" approximate the scaled data is thus equivalent to estimating the approximate rank of $\boldsymbol{W}$ (Renner, 1988). The rank of $\boldsymbol{X}$ is unaffected by scaling procedures such as those of equation 13, because they do not involve the subtraction of column means (Miesch, 1980). However, they do affect the approximate rank of $\boldsymbol{W}$, because the scaling procedure influences the magnitudes of residual "sum of squares" of the columns.

The scaled data are resolved into a linear combination of p mutually orthogonal vectors, in order to determine the exact rank of $\boldsymbol{W}$:

$$w_{ij} = a_{i1} f_{j1} + a_{i2} f_{j2} + ... + a_{ik} f_{jp}$$

or, in matrix notation:

(14) $$\boldsymbol{W} = \boldsymbol{A}\boldsymbol{F}^T$$

The matrix $\boldsymbol{F}$ contains the eigenvectors (principal components), a new set of mutually orthogonal reference axes for the p-dimensional cluster of observations. The eigenvectors are linear combinations of the scaled variables. The coordinates of the datapoints in this new frame of reference are represented by $\boldsymbol{A}$, the matrix of scaled loadings. The eigenvectors $\boldsymbol{F}$ can be calculated directly from the (nxp) scaled data matrix $\boldsymbol{W}$, but also from one of its cross-products, the (nxn) major product moment $\boldsymbol{W}\boldsymbol{W}^T$, or the ($pxp$) minor product moment $\boldsymbol{W}^T\boldsymbol{W}$.

For most data sets, p is much smaller than n, and the eigenvectors are obtained from the minor product moment $\boldsymbol{W}^T\boldsymbol{W}$ (Klovan & Imbrie, 1971) by means of an *eigenvector decomposition* or a *singular value decomposition* (e.g. Jöreskog et al., 1976; Press et al., 1989):

(15) $$\boldsymbol{W}^T\boldsymbol{W} = \boldsymbol{F}\boldsymbol{L}\boldsymbol{F}^T$$

Because $\boldsymbol{F}$ is columnwise orthonormal, the calculation of the matrix of scaled loadings $\boldsymbol{A}$ reduces to:

(16) $$\boldsymbol{A} = \boldsymbol{W}\boldsymbol{F}$$

The eigenvectors of $\boldsymbol{W}$ are positioned so as to account for maximum variance, in decreasing order of magnitude, as indicated by the associated (pxp) diagonal matrix of eigenvalues $\boldsymbol{L}$:

(17) $$l_{11} \geq l_{22} \geq \ldots \geq l_{jj} \geq \ldots \geq l_{pp}$$

The cumulative proportion of the total variance of $\boldsymbol{W}$ which is described by the first q eigenvectors ($q < p$) equals

(18) $$\frac{\sum_{k=1}^{q} l_k}{\sum_{j=1}^{p} l_j}$$

The number of non-zero eigenvalues thus equals the number of mutually orthogonal axes (dimensions) required to reproduce $\boldsymbol{W}$ exactly. In practice, p eigenvectors are usually needed to reproduce $\boldsymbol{W}$ exactly, although the first q eigenvectors may account for most of the "sum of squares" of $\boldsymbol{W}$ (cf. equation 18). Elimination of the (p-q) eigenvectors associated with the smallest eigenvalues corresponds to an orthogonal projection of the scaled datapoints onto a q-dimensional hyperplane ($q < p$). This projection minimizes the distortion of the geometric relationships between the observations, because the angles between each row of $\boldsymbol{W'}$ and $\boldsymbol{W}$ are minimal (cf. equation 12 and Fig. 4).

In other words, $\boldsymbol{W}$ is replaced by its least squares estimate $\boldsymbol{W'}$ (e.g. Jöreskog et al., 1976; Renner, 1988):

(19) $$W' = [A_p][F_p]^T$$

The reduced set of q eigenvectors is referred to as $\boldsymbol{F}_p$, the principal axes matrix. The value of q refers to the "dimensionality" of $\boldsymbol{W'}$, which is assumed to reflect the number of linearly independent end members in the mixing model. In many applications, a relatively small number of eigenvectors is sufficient to arrive at a close approximation of $\boldsymbol{W}$, and consequently, $\boldsymbol{X}$.

5.3 Calculation of constrained approximations to the data

The scaling procedure outlined in equation 13 must be reversed in order to obtain the weighted least squares estimate of the raw data $\boldsymbol{X}$ from the linear representation of $\boldsymbol{W}$ for every possible value of q ($2 \leq q \leq p$). This inverse transformation, which was defined by Miesch (1976a), is accomplished by calculating a scale factor s for each reference axis:

(20) $$s_k = \frac{c - \sum_{j=1}^{p} h_j}{\sum_{j=1}^{p} f_{jk}(g_j - h_j)}$$

The scale factors are used to rescale each element of the reference axes $\boldsymbol{F}$ to the original units of measurement (subject to the constant-sum constraint):

(21) $$f_{jk}^{*} = s_k f_{jk}(g_j - h_j) + h_j$$

and the elements of the loadings matrix $\boldsymbol{A}$ are rescaled accordingly (each row is automatically adjusted so as to sum to one):

(22) $$a_{ik}^{*} = \frac{\frac{a_{ik}}{s_k}}{\sum_{k=1}^{q} \frac{a_{ik}}{s_k}}$$

In this manner, a weighted least squares approximation $\boldsymbol{X'}$ can be generated for each value of q ($2 \leq q < p$):

(23) $$X' = [A_p^{*}][F_p^{*}]^T$$

Due to the lack of non-negativity constraints on the weighted least squares approximation, some of the elements of $\boldsymbol{X'}$ may be negative, which is undesirable when dealing with compositional data. This problem can be avoided by the use of constrained least squares approximation (e.g., Lawson & Hanson, 1974; Menke, 1984; Renner, 1993b). Each row of $\boldsymbol{X'}$ that is not entirely non-negative must be replaced by its nearest non-negative neighbour on the (q-1) dimensional hyperplane defined by the rescaled principal axes. This *least distance programming* problem is defined as follows:

(24) $$[F_p^{*}]\ [a_p^{*}]^T \approx [x']^T$$

subject to:

(25) $$[F_p^{*}]\ [a_p^{*}]^T \geq 0$$

The additive errors, $\boldsymbol{E}$, corresponding to each non-negative $\boldsymbol{X'}$ which has been calculated according to the above procedures can be derived from equation 4. The matrices $\boldsymbol{X'}$ and $\boldsymbol{E}$ are thus automatically fixed by the choice of q, the number of end members in the mixing model, and do not depend upon the choice of end-member compositions (Miesch, 1976a).

6. GOODNESS OF FIT OF THE LINEAR REPRESENTATION

6.1 Goodness of fit statistics

The choice of q, the number of linearly independent end members in the mixing model, is a crucial step in the unmixing procedure. Because the "true" number of end members and

the errors associated with $\boldsymbol{X}$ are unknown, q can only be estimated by a comparison of the constrained linear approximations $\boldsymbol{X}'$ for different values of q ($2 \leq q < p$) to the original data $\boldsymbol{X}$. The cumulative proportion of the total "sum of squares" of $\boldsymbol{W}$ retained by discarding the (p-q) eigenvectors associated with the smallest eigenvalues (equation 18) can be regarded as a useful criterion for determining a reasonable maximum value of q, but it does not provide any specific information about the goodness of fit of the rows (observations) or columns (variables) of $\boldsymbol{X}'$. The goodness of fit of a linear model $\boldsymbol{X}'$ must be evaluated by means of different measures, which serve as guidelines to determine the "best" choice of q, or to improve the linear representation $\boldsymbol{X}'$ for a given value of q. The following three measures are currently available:

Angular deviations: The angular deviation of each estimated composition vector indicates the degree to which an observation can be approximated by mixing of q end members (Renner, 1988). The angular deviation (in degrees) is defined as the angle $\boldsymbol{\theta}$ between a composition vector and its estimate (cf. equations 10 and 11). When $q = p$, all angular deviations are equal to 0.0°. The *mean angular deviation* across all composition vectors, defined as

$$\bar{\theta}_{x\text{-}x'} = \frac{1}{n} \sum_{i=1}^{n} \theta_{x\text{-}x'} \tag{26}$$

is taken as an overall measure of the goodness-of fit of the estimated observations to the data. Renner (1988) suggested that observations which are characterized by gross angular deviations in (e.g. more than three times the mean angular deviation) should be excluded from the data, because they may not have taken part in the mixing process by which the

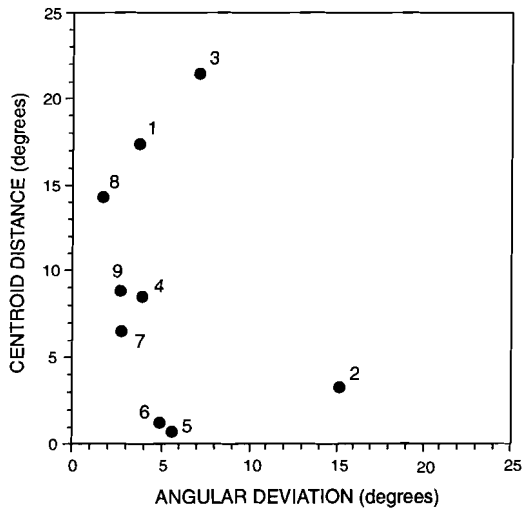

Figure 5. Scatter graph of centroid distance vs. angular deviation for two end-member approximation of data set in Table 1. Data point 2 is regarded as an outlier in this mixing system.

dataset was presumably generated. The exclusion of these observations from the analysis will generally improve the quality of a linear representation to a small extent.

The end-member compositions of the mixing model to be constructed depend largely on the positions of extreme observations in $\boldsymbol{X'}$, because the non-negativity constraint on $\boldsymbol{M}$ requires that the end-member vectors $\boldsymbol{B}$ enclose all of the observations. It is thus especially important to identify and exclude *extreme* observations which are poorly reproduced by a model with q end members, in order to minimize the risk of forcing the model to accept such aberrant data points, which may not even belong to the mixing system of interest. Extreme compositions can be identified by calculating the angle between each observation and the arithmetic mean composition of the data $\boldsymbol{X'}$ (cf. equations 10 and 11). This angle is termed the *centroid distance*. An observation may be excluded from the data when its angular deviation and centroid distance are both large. The construction of scatter graphs of centroid distance vs. angular deviation facilitates the identification of such outliers. An example of a scatter graph for a representation of the synthetic data set of Table 1 with two end members is shown in Fig. 5.

Coefficients of determination: The coefficient of determination measures the proportion of the variance of each variable accounted for by a mixing model of q end members (Miesch, 1976a, b). The coefficient of determination is defined as the squared correlation coefficient of a column of $\boldsymbol{X}$ and its corresponding estimate $\boldsymbol{X'}$, and is calculated as follows:

$$r_j^2 = \frac{d_{x_j}^2 - d_{(x_j - x_j')}^2}{d_{x_j}^2} \tag{27}$$

The *mean coefficient of determination* across the variables is taken as an overall measure of the goodness-of-fit of the model to the data. When $q = 1$, all coefficients of determination are equal to 0.0, and all compositional variation is assumed to reflect perturbations of a single composition. When $q = p$, all coefficients of determination are equal to 1.0. If the coefficient of determination of a variable is less than 0.5 (equivalent to a linear correlation coefficient of 0.7), this variable cannot be adequately reproduced by mixing of q end members (Renner et al., 1989, Renner, 1991). A poor representation may indicate that the number of end members must be increased if the observed variation of this variable is considered to reflect mixing. An alternative option would be to increase the "weight" of variables that are considered to be highly significant by selecting different scaling constants (equation 13).

In general, a low coefficient of determination is to be expected for any variable that is present in roughly equal proportions in some specimens and absent in others, suggesting that it did not take part in the mixing process. In such cases, the linear representation can be improved by dropping this variable from the analysis (and restoring the constant rowsum c), or by amalgamation of this variable onto another. "Factor-variance" diagrams can be constructed to show the coefficients of determination of each variable for various numbers of end members (Miesch, 1976a, 1976b, 1980). An example of a "factor-variance" diagram for the synthetic data set of Table 1 is shown in Fig. 6.

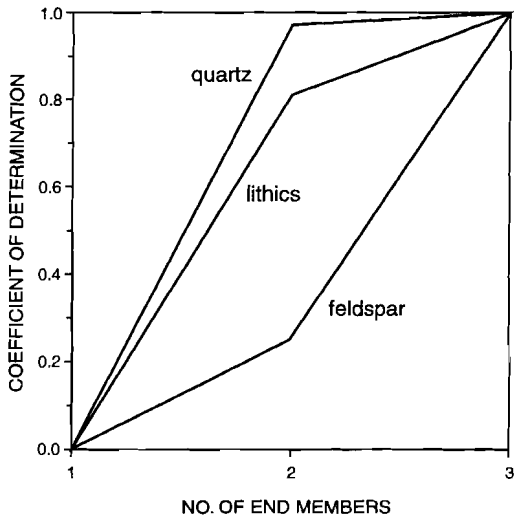

Figure 6. "Factor-variance" diagram of the data set of Table 1. Three end members are required to approximate all of the variables; a two end-member model fails to account for the observed variation.

Distribution of logratio-residuals: Well-behaved residuals are an important, but often neglected validation criterion of inverse models. A fundamental problem in unmixing is that the distribution of residuals $\boldsymbol{E}$ cannot be described by a Gaussian model, due to the constant row-sum constraint on the compositional variables (equation 1). Aitchison & Shen (1984) suggested that a non-linear transformation of the data to logratios of the original variables will change their distribution to a multivariate (p-1) dimensional Gaussian form under the assumption that errors in the original variables conform to a *multiplicative* perturbation model. Unfortunately, mixing is a linear function of the original compositional variables, and can only be modelled by assuming that the errors are *additive* (cf. equations 4 or 6). The use of least squares estimation does not explicitly require a multivariate Gaussian error distribution, but the squared distance measure employed by this method may cause outliers to have an undesirably large effect on the solution (e.g. Zhou, 1987). However, in applications of unmixing, the location of the hyperplane spanned by the reference vectors does not appear to be affected significantly by the exclusion of a small number of outliers (Renner, 1988), in spite of considerable variability of the eigenvector coefficients (cf. Trochimczyk & Chayes, 1977). This apparent robustness is corroborated by the cumulative sum of the normalized eigenvalues derived from the singular value decomposition (equation 18), which tends to be stable.

The above discussion implies that we cannot evaluate the error matrix $\boldsymbol{E}$ directly, in any other manner than by inspection of the magnitudes of the residuals (which has already been carried out implicitly by computation of the angular deviations and possible exclusion of observations). Renner (1991, 1993a) suggested that the residuals of $\boldsymbol{X'}$ can be remodelled in order to investigate if the linear representation conforms to the multiplicative error model of Aitchison & Shen (1984). According to this model, there are plausible theoretical

grounds for anticipating a univariate normal distribution among a linear combination of the logratio-residuals of each variable, provided that the differences between $\boldsymbol{X}$ and $\boldsymbol{X'}$ can be attributed to random errors (Aitchison, 1986; Renner, 1991, 1993a). Empirical studies of the logratio-residuals distribution (Renner, 1991, 1993a) suggest that too low a value of q results in skewed distributions, implying that a systematic part of the variability of the data has been included in the residuals. On the other hand, too high a value of q results in a significant increase of the kurtosis of the distributions, due to overspecification of the mixing model. The hope is that an optimum value of q can be chosen by evaluating these distributions for all values of q.

A particular choice of q may also be suggested by a comparison of the distribution of ϵ, a linear combination of *centred logratio-residuals*, to the standard normal distribution. The centred logratio residuals z_{ij} are computed from the following expression:

(28)

$$z_{ij} = \log\left(\frac{x_{ij}}{x'_{ij}}\right) - \log\left(\frac{u_i}{u'_i}\right)$$

In which u_i, the geometric mean of each row, is defined as

(29)

$$u_i = (x_{i1}\ x_{i2}\ \ldots\ x_{ij}\ \ldots\ x_{ip})^{\frac{1}{p}}$$

The centred logratios are standardized to have mean values of zero and unit standard deviation for each column, and summed rowwise to form a single residual value for each observation:

(30)

$$\epsilon_i = \sum_{j=1}^{p}\left(\frac{z_{ij} - \bar{z}_j}{d_{z_j}}\right)$$

Finally, this test statistic is also standardized to have a mean of zero and unit standard deviation:

(31)

$$\epsilon_i^* = \frac{\epsilon_i - \bar{\epsilon}_i}{d_{\epsilon_i}}$$

The goodness of fit of the distribution of ϵ^* to the standard normal distribution can be evaluated for each value of q by means of general goodness-of-fit tests, such as the χ^2 and Kolmogorov-Smirnov tests, or specialized normality tests (e.g. Rock, 1987, 1988). If the distribution of the logratio-residuals does not deviate significantly from the standard normal distribution, it may be assumed that only random variation has been discarded by reducing the rank of $\boldsymbol{X}$, as expected from the assumption that the data resulted from a mixing process involving q end members.

The use of *centred logratio-residuals*, as advocated above, has the distinct advantage of treating the residuals in a symmetric way, avoiding differences due to the choice of common divisor, as reported by Renner (1993a). However, experiments with various data sets and scaling options suggest that χ^2 values derived from the distribution of (centred) logratio-residuals tend to increase monotonically with q. The goodness of fit of these distributions is thus merely useful as an indicator of possible overspecification, and cannot be used to determine a minimum value of q. It should also be noted that markedly different goodness of fit values for a given set of data may be produced by slight changes of the scaling constants g and h in equation 13, indicating that this method of selecting the optimal value of q is far from robust.

6.2 Choosing the "best" linear representation

Although the goodness of fit measures described above provide guidelines for judging the quality of the linear representation of $\boldsymbol{X}$, there is no solid criterion for selecting a particular number of end members. In practice, the coefficients of determination provide an estimate of the minimum number of end members required to "explain" the observed variation, whereas the logratio-residuals distribution provides a reasonable maximum value of q. The choice of different scaling options (equation 13) may influence these results.

An important requirement for obtaining a satisfactory linear representation is the presence of a limited number of zero values in the raw data. There are several reasons for this:

(1) Unconstrained least squares approximation of observations with many zero values commonly produces small negative values, that must be corrected by means of the constrained projection of equations 24 and 25. This correction has a negative effect on the goodness of fit statistics (angular deviations and coefficients of determination) of the linear representation. Furthermore, any pair of original and approximated observations containing at least one zero value must be excluded from the residuals test, because such pairs cannot be transformed to logratios.

(2) Any variable that is characterized by many zero values and a limited number of positive values cannot be adequately reproduced by a linear mixing model. A series of observations in which a particular component is absent, and the other components are present in different amounts, can only be interpreted as a series of mixtures of several end members in which this component is also absent (or as a series of likely end members). If the constrained linear approximation contains many zero values, a linear mixing model cannot be constructed without considerable distortion with respect to the data.

Many petrographical and geochemical data matrices contain an appreciable number of zero elements. The number of zero values in the raw data set must be minimal in order to guarantee a satisfactory linear representation with a limited number of end members. Exclusion of variables from the analysis and amalgamation of variables are two ways of tackling this problem.

Exclusion of variables from a series of exact mixtures and recalculation of the remaining variables to a constant sum will not affect the ratios of the remaining variables. The same applies to the end-member compositions. In other words, the mixing model remains essentially the same (apart from a systematic change of the mixing proportions), provided that the number of end members is smaller than the reduced number of variables. It follows that variables which are poorly approximated by a linear model can be discarded without much loss of information.

The effects of *amalgamations* are more difficult to predict. In general, amalgamations that reduce the number of zero values in the data improve the goodness of fit of the linear representation and simultaneously reduce the compositional information in the data. A practical strategy is to amalgamate variables that are presumed to have the same (or similar) genetic significance within the mixing system being analyzed.

In view of the above considerations, an absolute minimum number of observations and variables required for a satisfactory mixing model cannot be determined. However, a reasonable minimum number of observations is suggested by the normality test of residuals, which can only be considered meaningful if the distribution to be evaluated is based on at least thirty observations. Taking into account the possible presence of outliers, and the presence of a limited number of zero values in the data matrix, fifty observations would seem to be a reasonable minimum. The minimum number of variables is equal to three, if something has to be gained by representing the data in the form of a mixing model (there is always the possibility that the data can be adequately represented by mixing of two end members). A larger number of variables is preferable for a more robust model.

Commonly, several decompositions of the dataset and calculation of goodness of fit measures are carried out, using various exclusions and amalgamations. Eventually, the "best" linear representation of $\boldsymbol{X}$ must be chosen, based on all the available information, including an assessment of the effect of sampling and/or measurement errors on the data.

The principle of *parsimony* (Imbrie, 1963) is a useful guideline to the choice of q in view of the main objective of unmixing, i.e., to "explain" the observed compositional variation with a minimum number of end members. When a reasonable minimum value of q has been determined, the value of q should only be increased if the construction of a mathematically feasible or geologically reasonable mixing model with this parameter turns out to be unsuccessful.

7. THE BILINEAR PROBLEM

7.1 Coordinate transformation

When the "best" representation $\boldsymbol{X'}$ has been chosen, the number of linearly independent end members q has been fixed. The second stage of the unmixing procedure consists of estimating the end-member compositions and the mixing proportions. This is a constrained bilinear problem, which can be solved by means of a coordinate transformation technique. Our objective is to recast the linear representation $\boldsymbol{X'}$ into the form of a perfect mixing model of equation 4. This can be accomplished if the rescaled loadings $\boldsymbol{A^*}$ and the transposed rescaled reference axes $\boldsymbol{F^*}$ can be transformed to non-negative mixing proportions $\boldsymbol{M}$ and non-negative end-member compositions $\boldsymbol{B}$, respectively.

It was shown in section 1.2 that a geologically reasonable mixing model can be generated by replacing the original frame of reference with an alternative set of reference vectors consisting of a subset of "extreme" observations. The principal difference between these two frames of reference is that the vectors of the second model, $\boldsymbol{B}$, are intercorrelated, unlike the mutually orthogonal QFL vectors. The modified representation of $\boldsymbol{X'}$ is therefore termed an *oblique model*. The oblique model corresponds to a valid mixing model if all composition vectors belonging to $\boldsymbol{X'}$ are enclosed by the oblique reference vectors, as illustrated by the geometric vector model.

The exact bilinear relationship (cf. equations 4 and 23) indicates that one of the two desired matrices can be calculated given the other one, e.g.:

$$\boldsymbol{M} = \boldsymbol{X'B^T(BB^T)^{-1}} \tag{32}$$

An exact solution to this bilinear problem requires that a set of proposed end-member compositions $\boldsymbol{B}$ is linearly independent and "fits" perfectly into the mixing space, that is defined by linear combinations of the reference vectors $\boldsymbol{F^*}$ which span the $(q\text{-}1)$ dimensional hyperplane (cf. equation 21) and obey the non-negativity constraint of equation 25. If the elements of the corresponding mixing proportions matrix calculated from equation 32 are all between zero and unity, a mathematically feasible solution to the mixing problem has been obtained. If a composition vector is not contained within the mixing polytope enclosed by the proposed end members, one or more of its mixing proportions are negative or exceed unity.

The coordinate transformation by which one model can be converted into another has been referred to as *oblique projection* (Imbrie, 1963; Imbrie & Van Andel, 1964; Miesch, 1976a, 1976b). The oblique projection is defined as:

$$\begin{aligned} [W'] &= [A_p][V^{-1}V][F_p]^T = [A_o][F_o]^T \\ [F_o] &= [F_p]\,V^T \\ [A_o] &= [A_p]\,V^{-1} \end{aligned} \tag{33}$$

The modification of the principal reference axes $\boldsymbol{F}_p$ to another set of oblique reference vectors $\boldsymbol{F}_o$ is formally described as a linear transformation $\boldsymbol{V}$. The inverse transformation defines the corresponding modification from $\boldsymbol{A}_p$ to $\boldsymbol{A}_o$. This formulation is analogous to that of oblique rotation in factor analysis (although the constraints are completely different).

The inverse scaling procedure (equations 20 to 22) is used to rescale $\boldsymbol{A}_o$ and $\boldsymbol{F}_o$ separately. Our objective is to find a transformation matrix $\boldsymbol{V}$, such that after rescaling

$$[F_o^*]_{jk} \geq 0 \qquad [A_o^*]_{ik} \geq 0 \tag{34}$$

When these non-negativity requirements are met, the oblique solution to the mixing problem (cf. equation 4) is given by:

$$X' = [A_o^*][F_o^*]^T \qquad M = [A_o^*] \qquad B = [F_o^*]^T \tag{35}$$

Factor-rotation algorithms (e.g., Varimax) have been employed for solving the bilinear problem (Imbrie, 1963, Manson & Imbrie, 1964; Miesch, 1976a, 1976b; Klovan & Miesch, 1976). Rotation of orthogonal reference vectors according to the Varimax criterion commonly produces a (nearly) non-negative $\boldsymbol{M}$, but it does not remove all of the negative values from $\boldsymbol{B}$, because the end members are constrained to be mutually orthogonal. Various modifications to the Varimax-rotated axes (so-called oblique rotations) have been proposed to ensure the non-negativity of $\boldsymbol{B}$ (Clarke, 1978; Leinen & Pisias, 1984, 1986). Unfortunately, these modifications fail to take into account non-negativity constraints on $\boldsymbol{M}$. Therefore, the "factor analytic" approach can only provide feasible solutions in two special cases: (1) if the end members are known *a priori*; (2) if feasible end members in the spectrum of compositional variation under study have been sampled.

7.2 **Theoretical end members**

In certain cases, end-member compositions for a series of mixtures may be proposed on the basis of theoretical considerations or *a priori* knowledge of the geological system, as in petrogenetic problems (Miesch, 1976a, 1976b, 1976c, 1981). Commonly, such theoretical end-member compositions do not fit perfectly into the mixing space. The "nearest" vector which does fulfill this requirement can be calculated by treating the proposed composition in the same way as the rows of $\boldsymbol{X}$. The proposed composition is first scaled (equation 13) and projected onto the eigenvectors (equation 16). The principal loadings of the proposed composition are subsequently rescaled (equation 22) and premultiplied with the rescaled reference axes (equation 23) in order to obtain the estimated composition of the proposed end member, which may have to be adjusted (equation 24) in order to obey the non-negativity constraint (equation 25).

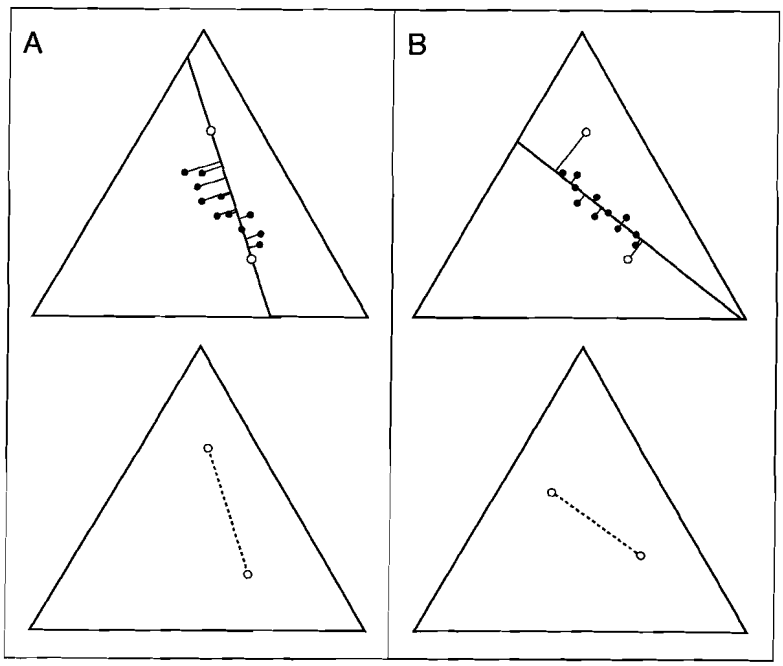

Figure 7. Difference between ordinary least squares partitioning (A) and the end-member modelling approach (B). The latter allows for errors in end-member compositions (open circles).

Any linearly independent set of theoretical end members which has been "filtered" according to the above-mentioned procedures can be used to solve equation 32 for $\boldsymbol{M}$. If the elements of $\boldsymbol{M}$ all range between 0.0 and 1.0, and if the angular deviations due to end-member "filtering" are small, the observed compositional variation has been adequately explained by mixing of the proposed end members. Note that this solution to equation 32 closely resembles the ordinary least squares solution (cf. equations 7 to 9). It is a reasonable alternative to ordinary least squares procedures, because it does not require the assumption that theoretical end-member compositions are completely free of errors. A geometrical interpretation of the differences between ordinary least squares and the end-member modelling approach is given in Fig. 7.

7.3 Selection of extreme compositions from the data set

If unmixing must be accomplished without *a priori* knowledge of end-member compositions, assumptions about feasible end members can only be based on the properties of $\boldsymbol{X'}$. The non-negativity constraint on mixing proportions, $\boldsymbol{M}$, requires that an ideal set of end-member vectors encloses all data points, as illustrated by the vector model. By definition, this set of end-member vectors is of *extreme composition* because it must contain the minimum and maximum values of all variables in the set of mixtures. An obvious possibility is that a subset of q linearly independent observations from $\boldsymbol{X'}$ fulfills this requirement, implying that feasible estimates of the "true" end members have been sampled (Miesch, 1976a, 1976b). Various strategies have been proposed for identifying such subsets in $\boldsymbol{X'}$, $\boldsymbol{W'}$, $\boldsymbol{A}^*$ or $\boldsymbol{A}$:

(1) **Column by column sorting** (Renner, 1988). The set of extreme observations selected must contain the minimum and maximum values of each column of estimated (scaled) variables or (scaled) loadings.

(2) **Construction of convex hull** (Ripley, 1990). Extreme observations must be selected from the extreme points of the convex hull or "data envelope" (e.g. Hadley, 1961).

(3) **Centroid distance-inner product selection** (Woronov, 1991b). The first extreme composition selected is the observation farthest from the centroid of the data. Subsequently, q-1 extreme points are selected on the basis of the sum of their centroid distance and their distances (inner products) to already selected extremes, which must be maximal.

(4) **Iterative oblique projection** (Imbrie, 1963; Manson & Imbrie, 1964; Klovan & Miesch, 1976). Similar to the third procedure, but requires elaborate computations and is not guaranteed to converge to a unique set of extremes.

The first two procedures commonly offer several choices of "candidate extremes", whereas the other two procedures aim at providing a unique set of extremes. If a linearly independent subset of selected data vectors is substituted in equation 32 and the calculated mixing proportions conform to the non-negativity constraint, the observed compositional variation can be adequately explained by mixing of these compositions. However, the resulting mixing model will not be valid if feasible estimates of the "true" end members have not been sampled.

If there are no true extremes among the observations, compositions "close to" a feasible set of end members cannot be identified. The absence of a set of "true" extremes implies that the number of extreme points of the convex hull of the data is larger than q (e.g., Ripley, 1990). Since the minimum number of extreme points of the convex hull equals q by definition, a set of "near" extremes can always be selected. But even if "true" extremes appear to have been identified, the validity of a mixing model with extreme observations as end members is questionable. Compositionally extreme data vectors run the greatest risk of being atypical of the mixing system under study. Solutions to the mixing problem that are based on a small subset of extreme data vectors may be seriously in error, in spite of their mathematical feasibility. A closely related drawback of such models is their lack of robustness. A general solution of the bilinear mixing problem obviously requires a different approach.

8. THE "OPTIMAL" MIXING MODEL

8.1 Additional constraints on the "optimal" solution

The bilinear mixing problem (equations 32 to 35) cannot be uniquely solved in the absence of additional constraints, because there may be an infinite number of solutions which approximately fulfill the requirements of equation 34. For example, the synthetic dat set of Table 1 can be interpreted as a set of mixtures of theoretical end members (consisting of 100% quartz, 100% feldspar, and 100% lithic grains, respectively). But this data set can also be interpreted as a series of mixtures of a different set of end members, termed arkosic arenite, quartz-arenite, and lithic arenite, respectively (see Table 2). As discussed in section 1.2, the second solution is preferred to the first, because it employs *realistic end members*,

i.e., extreme compositions actually sampled. But we can also imagine a third model, which is generated from the second by replacing the quartz-rich end member by the pure quartz arenite of the first model. It has been observed that pure quartz arenites can be formed in a humid tropical climate by prolonged chemical weathering of detrital materials (e.g. Johnsson et al., 1988), implying that the third model could also reflect a physical mixing process. Could this new model be superior to the second?

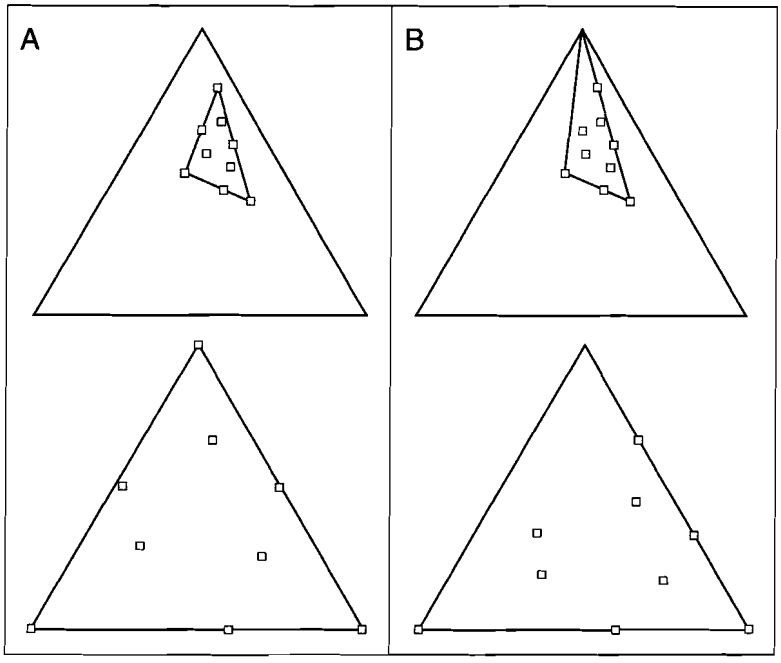

Figure 8. Two mixing models of the data set of Table 1. A: oblique projection of reference axes onto the first three data points. B: the first observation has been replaced by a theoretical end member.

The first model was judged to be inferior to the second, because it employed the most extreme set of end members possible, which cannot be considered to represent a geologically meaningful solution. The second model may be preferred over the third for similar reasons. A comparison of the second and the third model (see Fig. 8 and Table 3) readily shows that data point no. 1 is a "true extreme", which encompasses the range of observed compositional variation in conjunction with the other two extremes used in the second model. All observations are enclosed by the mixing polytope, as shown in Fig. 8A. If we choose to define a theoretical end member whose location is unnecessarily far from the data envelope (as in the third model), the contributions of this end member to each observation will be small, implying that such distant end members can only account for a relatively small part of the observed variation. A numerical comparison of both models shows that the average contribution of the theoretical end member (the pure quartz arenite) to the data is much smaller than that of its equivalent in the second model, the "extreme" observation no. 1 (see Table 3).

Table 1. Two oblique models of the data set of Table 1. The "extreme" observation in the second model has been replaced with a theoretical end member in the third model (see text for discussion).

SECOND MIXING MODEL				THIRD MIXING MODEL			
End-member contributions:				End-member contributions:			
Obs. no.	EM 1	EM 2	EM 3	Obs. no.	EM 1	EM 2	EM 3
1	1.00	0.00	0.00	1	0.67	0.00	0.33
2	0.00	1.00	0.00	2	0.00	1.00	0.00
3	0.00	0.00	1.00	3	0.00	0.00	1.00
4	0.51	0.47	0.02	4	0.34	0.47	0.19
5	0.50	0.00	0.50	5	0.33	0.00	0.67
6	0.29	0.53	0.18	6	0.20	0.53	0.28
7	0.26	0.17	0.57	7	0.17	0.17	0.66
8	0.00	0.40	0.60	8	0.00	0.40	0.60
9	0.67	0.11	0.21	9	0.45	0.11	0.44
Mean	0.36	0.30	0.34	Mean	0.24	0.30	0.46
End-member compositions:				End-member compositions:			
Label	Q (%)	F (%)	L (%)	Label	Q (%)	F (%)	L (%)
Obs. 1	80.0	5.0	15.0	Pure Q	100.0	0.0	0.0
Obs. 2	50.0	30.0	20.0	Obs. 2	50.0	30.0	20.0
Obs. 3	40.0	15.0	45.0	Obs. 3	40.0	15.0	45.0

The extreme composition of the theoretical end member induces another effect, which is clearly visible in Fig. 8B. The distribution of mixtures within the mixing polytope of the third model indicates that the upper left triangular area of the mixing polytope does not contain any observations. The composition of this distant end member is thus more extreme than needed for a mathematically valid model. Less extreme end members, i.e., end members that are located closer to the "data envelope", are more easily interpretable in terms of "mixtures of extreme composition", as shown in the first model (Fig. 2 and Table 2). In conclusion, there are several reasons for avoiding the construction of such distant end members in the absence of *a priori* knowledge of the mixing process under investigation. Conservative end-member estimates ensure the geological reasonableness of a mixing model.

In the hypothetical case of an ideal mixing model (e.g. Full et al., 1981, 1982; Williams et al., 1988; Renner, 1988; Renner et al., 1989), the average contribution of each end member to the data is roughly equal, and the data points are multivariate uniformly distributed within the mixing polytope enclosed by the end-member vectors. Unfortunately, the theoretical concept of an ideal configuration cannot be put to any practical use, because this desired configuration cannot be obtained by any premeditated sampling scheme if nothing is known about the nature of the physical mixing process by which the compositional

variation was presumably generated. In general, the mixing proportions $\boldsymbol{M}$ are unknown stochastic functions of the spatial sampling coordinates (x,y,z), and the nature of the spatial mixing pattern is related to the cumulative effects of physical transport. Sampling of a mixture under investigation (e.g., a three-dimensional sediment body) according to a random uniform spatial scheme fails to guarantee a multivariate uniform distribution of observations within the mixing polytope. *A priori* knowledge of the spatial mixing pattern, which could serve as a guideline for choosing a particular sampling strategy, is generally absent, because the spatial mixing pattern is precisely what we are trying to reconstruct by inverse modelling.

If the observed compositional variation is largely attributable to mixing, it is implicitly assumed that the end-member contributions display a sufficiently wide range of variation to enable a reconstruction of the end-member compositions. In practice, it cannot be safely assumed that all errors have been completely "filtered" from the modelled compositional variation of $\boldsymbol{X'}$, which is reflected in the multidimensional geometry of $\boldsymbol{M}$. This implies that trivial errors in $\boldsymbol{M}$ are to be expected in any realistic mixing model. Similarly, it cannot be assumed that all outliers have been removed, implying that a small proportion of the data points should be allowed to remain outside the mixing polytope. In other words, a robust end-member estimation procedure is required, in order to ensure that data points which are far removed from the centre of mass of the data have a minimal effect on the solution. An interesting detail is that such data points generally correspond to the so-called "true extremes" selected by the procedures discussed in section 7.3. A robust estimation procedure should employ the collective properties of the data set and aim at the construction of "geologically reasonable" (i.e., conservative) end members.

The above conclusions can be summarized by the following rule: *the optimal solution to the bilinear mixing problem consists of a set of end members that encloses as many of the data points as "tightly" as possible* (Full et al., 1981, 1982; Renner, 1988; Ripley, 1990). In fact, this rule turns out to be the only additional criterion for assessing the validity of a set of end members in the absence of *a priori* knowledge of the geological system. With the help of this rule, we can select the "best" mixing model from a set of available models, as discussed above. But more importantly, this rule enables us to estimate the "optimal" set of end-member compositions from which the observed variation could have been generated.

8.2 Iterative strategies and robust initial end-member estimates

The preferred strategy for solving the bilinear mixing problem is an iterative estimation procedure, which does not require that all of the non-negativity constraints are taken into account at the same time (Full et al., 1981; Renner, 1988; Ripley, 1990). A commonly adopted approach is to provide an initial guess of the end-member compositions, based on the properties of $\boldsymbol{X'}$. The proposed set of initial end members must be linearly independent and entirely non-negative. If we start out with a trial matrix of end members $\boldsymbol{B}$, we can generate the corresponding $\boldsymbol{M}$ by means of oblique projection, as outlined in section 7.1. The discrepancies between an ideal $\boldsymbol{M}$ and the current $\boldsymbol{M}$ are evaluated in order to define the necessary improvements to $\boldsymbol{M}$. The end-member matrix $\boldsymbol{B}$ corresponding to this improved $\boldsymbol{M}$ is then calculated and checked for non-negativity. If required, the new set of end members is adjusted by means of a constrained projection into the mixing space, as

described in section 5.3. Improved oblique solutions can be generated until the constraints on an optimal $\boldsymbol{M}$ have been satisfied.

The LSQSEEK algorithm of Renner (1988) and the EXTENDED QMODEL algorithm of Full et al. (1981, 1982) are conceptually similar, although the former is based on an iterative optimization of equation 32, whereas the latter employs an iterative optimization of equations 33 to 35. The first procedure requires the computation of $\boldsymbol{M}$ from the estimated data $\boldsymbol{X'}$ and the inversion of a (pxp) matrix $\boldsymbol{BB^T}$ in each iteration step (cf. equation 32). The oblique projection method allows for a separate rescaling of $\boldsymbol{A_o}$ and $\boldsymbol{F_o}$ (cf. equations 20 to 22), and the inversion of a usually much smaller (qxq) transformation matrix $\boldsymbol{V}$ (cf. equation 33). The latter procedure is preferred for reasons of computational efficiency. Both algorithms enlarge the mixing polytope in each iteration cycle, in order to enclose data points which are located outside the polytope generated in the previous iteration cycle. Polytope-enlargement continues until all data points have been enclosed, or until the polytope vertices "touch" the edge of the non-negative mixing space defined by equation 25.

Full et al. (1981) and Renner (1988) suggested that a set of "near extremes" could be used for initialising an iterative search for feasible end members according to the strategy described above. However, the constraints on an "optimal" mixing model discussed in the previous section indicate that a set of "near extremes" is not necessarily the best starting point for algorithms which eliminate negative mixing proportions by increasing the size of the mixing polytope in each iteration cycle. A successful approach along these lines obviously requires that the risk of inadvertently selecting one or more atypical observations is minimized, because a wrong choice of initial end-member estimates cannot be corrected by these algorithms, which can only attempt to modify the initial compositions to a set of even more extreme "feasible" compositions. A better way of estimating initial end-member compositions is by making use of the limitations of the iterative algorithms: we can start within the convex hull of the data, because the mixing polytope can only be enlarged at each iteration step. Provided that we have developed a robust strategy for improving the model in each iteration cycle, this should minimize the risk of forcing the model to include atypical data points located on the edge of the convex hull.

A robust estimation of initial end-member compositions can be achieved by *Q-mode cluster analysis*. When q "families" of observations have been identified (and possibly a number of aberrant observations, which do not belong to these clusters), one observation can be selected from each cluster, as suggested by Preisendorfer (1988) and Renner (1988). A more sophisticated variation on this theme is the use of *fuzzy clustering* (Full et al., 1982; Bezdek et al., 1984). The fuzzy-clustering algorithm defines the location of q cluster centres (which represent centres of mass of the estimated data) by an iterative procedure. The compositions represented by the cluster centres are projected into the mixing space as described in section 7.2, in order to provide a robust starting point for iterative procedures aimed at locating a set of "optimal" end members in the mixing space.

9. ITERATIVE CONSTRUCTION OF "OPTIMAL" END MEMBERS

9.1 A new bilinear unmixing algorithm

The new iterative procedure aimed at reconstructing the "optimal" end members follows the general approach outlined in the previous section. The "optimal" end members calculated by the algorithm are based on the collective properties of the data set, in order to minimize the effects of possible outliers. This is accomplished by a robust method used for defining improvements to the end-member compositions matrix $\boldsymbol{B}$ in each iteration cycle. The method is based on the simple notion that each column of the mixing proportions matrix $\boldsymbol{M}$ defines two subspaces in the mixing space: one subspace contains the observations for which column values are non-negative, the other subspace contains the observations for which column values are negative. The negative column values correspond to observations that are located outside the mixing polytope in the subspace farthest from the end member being evaluated. Such observations can be included in an enlarged mixing polytope, if one or more of the other end members is moved into the subspace, i.e., "away" from the end member corresponding to the column being evaluated.

The size of the mixing polytope can be kept as small as possible by moving only one end member for the purpose of eliminating negative values from each column of $\boldsymbol{M}$. The "centre of mass" of each cluster of points characterized by negative contributions of a particular end member, termed the *correction vector* $\boldsymbol{Y}$, is calculated to determine which end member must be moved. Subsequently, the end-member vertex closest to each "centre of mass" is displaced outward, over a distance determined by (1) the proportion of data points in the subspace being evaluated, and (2) the average negative contribution of these data points to the end member being evaluated. After evaluation of each of the columns of $\boldsymbol{M}$, a *matrix of oblique coordinates*, $\boldsymbol{T}$, is constructed, which contains the proposed set of new end members expressed as linear combinations of the current end members. Details of this numerical procedure are given in Appendices II and III.

The improvements of this new algorithm over those of Full et al. (1981, 1982) can be summarized as follows:

(1) The lack of explicit non-negativity constraints on the proposed end-member compositions in EXTENDED QMODEL often results in unrealistic mixing models with negative end-member components. Full et al. (1981) suggested that such unrealistic end-member compositions could be "adjusted" by setting negative end-member components to zero, and reimposing the constant-sum constraint. However, compositions which have been "adjusted" according to this procedure do not fit into the mixing space. Consequently, negative components commonly reappear in such "adjusted" end members after the unconstrained projection into the mixing space employed by the EXTENDED QMODEL algorithm. This problem has been solved by applying the constrained least squares projection described in equations 24 and 25 (see Appendix II).

(2) The EXTENDED QMODEL polytope is enlarged in each iteration cycle by moving its edges outward, parallel to the current polytope edges, until all mixing proportions are non-negative. This approach, in conjunction with the far from robust procedure

by which the correction vector is constructed (discussed under (3) below), results in an overestimation of the size of the mixing polytope, implying that the estimated compositions of the end members are more extreme than required for a feasible solution. The solutions provided by EXTENDED QMODEL are therefore not "optimal" according to the criteria of section 8.1. This procedure has been replaced by a more conservative polytope adjustment scheme. In each iteration cycle, a matrix of new oblique coordinates, $\boldsymbol{T}$, is formed by moving only the end-member closest to each correction vector $\boldsymbol{Y}$ outward. Negative mixing proportions in $\boldsymbol{M}$ will eventually be eliminated by these iterative corrections to $\boldsymbol{B}$ (for details of this procedure, see Appendix III).

(3) The EXTENDED QMODEL criterion for estimating the amount of polytope enlargement is based on the largest negative mixing proportion for each end member. This procedure relies on the position of a single data point with respect to the current oblique model, and is therefore extremely sensitive to outliers. It has been replaced by a more robust polytope enlargement scheme based on a correction vector $\boldsymbol{Y}$, calculated separately for each end member. The correction vector represents the "centre of mass" of the observations outside the current mixing polytope in the subspace defined by negative contributions of the end member being evaluated. A full account of this polytope enlargement scheme has been included in Appendix III.

9.2 Convergence criteria

Ideally, the iterative procedure outlined in Appendices II and III will converge towards a mixing model that is subject to the constraints listed in section 1, and is optimal in the sense of section 8.1. In practice, it is not always possible to conform to the rigid mathematical constraints on a perfect mixing model, due to finite precision of computing equipment, and the presence of measurement errors and/or outliers in the data. Convergence is monitored by two parameters, termed *convexity error* and *projection error*, respectively. In order to add flexibility to the modelling process and ensure rapid convergence, cutoff values can be specified for these parameters. Other constants are used to delimit the number of iteration steps, and indicate a fatal error condition, respectively.

These four parameters and their cutoff-values (constants c_1 to c_4) define four *exit codes* of the iterative algorithm (see Appendix II), which are briefly discussed below, together with some suggestions for tuning the algorithm to fit the needs of a given data set:

1. The **convexity error** measures the discrepancy between the current oblique model and an ideal model that would enclose all of the data points. The convexity error is determined by evaluating the location of data points external to the mixing polytope. It incorporates two measures of misfit: the proportion of data points external to the polytope (***PROP***), and their mean squared distance to the edge of the current mixing polytope (***DIST***). The convexity error is defined as follows:

$$\log (PROP) + \log (DIST) \tag{36}$$

For example, when 10% of the observations is not enclosed by the mixing polytope and is characterized by an average end-member "contribution" of -10%, the convexity error equals -3. **cutoff 1** represents a negligible convexity error, e.g. -6. **Exit code 1** indicates that the iterative algorithm has converged to a stable configuration with a negligible convexity error, i.e., a satisfactory approximation of an optimal mixing model.

2. The **projection error** measures the difference between two successive oblique solutions, i.e., the extent to which the previous model has been changed by the end-member adjustment procedure. It is defined as follows:

(37) $$\frac{1}{q^2} \sum_{k=1}^{q} \sum_{j=1}^{q} (v_{jk}^{(i)} - v_{jk}^{(i-1)})^2 \cdot$$

Cutoff 2 represents the logarithm of a negligible projection error (e.g. -12). **Exit code 2** also indicates convergence of the iterative algorithm, but the unstable configuration does not necessarily imply that the final oblique model approximates an optimal mixing model. In certain cases, models with smaller convexity errors can be produced by choosing a smaller value of cutoff 2. In other cases, a large convexity error associated with the final model indicates that the end members cannot be displaced so as to enclose more observations without introducing unrealistic end-member compositions (i.e., negative values in $\boldsymbol{B}$). Although displacement of the current end members is required by the data configuration (step 3 in Appendix II), the new end members are projected back onto their previous positions on the edge of the mixing space (step 4 in Appendix II). In the latter case, a stable configuration can be reached by increasing the negligible convexity error (cutoff 1), allowing for mixing models with larger convexity errors to be produced. If the model fit is poor (i.e., many negative mixing proportions), the data set may not have been generated by mixing of linearly independent end members.

3. The **number of iterations** is used to delimit the amount of computer time. **cutoff 3** represents the maximum number of iterations (e.g. 100). **Exit code 3** indicates that the maximum number of iterations has been exceeded. The invalid final configuration indicates that a meaningful mixing model cannot be obtained with the current cutoff values. In order to judge whether an approximate mixing model could have been constructed by increasing cutoff values 1 and/or 2, the oblique model with the smallest convexity error is reproduced, together with the smallest projection error encountered during the iterations.

4. The **condition number** of the transformation matrix $\boldsymbol{V}$ measures the degree of linear independence among the end members. **cutoff 4** represents the non-singularity treshold, below which linear independence among rows of $\boldsymbol{V}$ (and consequently, $\boldsymbol{B}$) is taken to be absent. Depending on the matrix inversion algorithm used, it can be defined as the logarithm of the minimum ratio of the q-th to the 1-st singular value of $\boldsymbol{V}$, or the logarithm of the minimum value of the determinant of $\boldsymbol{V}$ (e.g. -10). **Exit code 4** indicates that a fatal error has occurred, because the non-singularity treshold has been crossed. The oblique model "collapses" in cases where there is (near) linear

dependence among the end members. This error may result from an inappropriate choice of initial end members (cf. Harvey & Lovell, 1992).

The algorithm is guaranteed to converge if compositional variation in the estimated data reflects mixing of q linearly independent end members, because each mixing polytope encloses that of the previous iteration. In such cases, the convexity error and projection error are smaller for each successive iteration step. The simultaneous decrease of errors is produced by a scaling factor, that determines the distance over which an end member is allowed to move. The scaling factor is defined as:

(38) $$[\overline{m}_k]\ [prop_k]^{c_5}$$

The proportion of data points outside the current mixing polytope, ***prop***, and the mean negative mixing proportion, m, are determined for each end member separately. c_5 is a weighing constant which influences the properties of the final mixing model in the following way: If c_5 is equal to 0.0, no weighing is performed (i.e., the proportion of observations enclosed by the mixing polytope is not taken into account). Non-negativity constraints on $\boldsymbol{M}$ are emphasized if c_5 ranges from 0.0 to 1.0. Values greater than 1.0 result in more conservative (less extreme) end-member estimates, which allow for negative values in $\boldsymbol{M}$. The standard case of linear weighing corresponds to $C_5 = 1.0$.

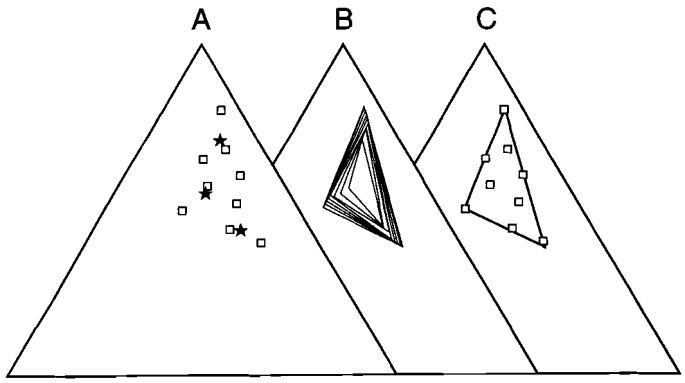

Figure 9. Construction of approximate mixing model for data set of Table 1. A: initialisation with three fuzzy cluster centres (shown as stars). B: a series of iteration steps. C: the final mixing model.

In order to test if the algorithm is capable of reconstructing the correct mixing structure of the synthetic data set of Table 1, an iterative search was initialised with three "fuzzy cluster centres" (Fig. 9A), and allowed to run until improvements to the mixing proportions matrix had become negligible, assuming that the data are free of errors ($p = q$). Constants c_1 to c_5 used in this experiment were specified as follows: -18, -12, 100, -12, 0.5. A series of iteration steps is reproduced in Fig. 9B (steps 0 to 5, 7, 10 and 20) The end-member compositions are almost perfectly reproduced, as shown in Fig. 9C.

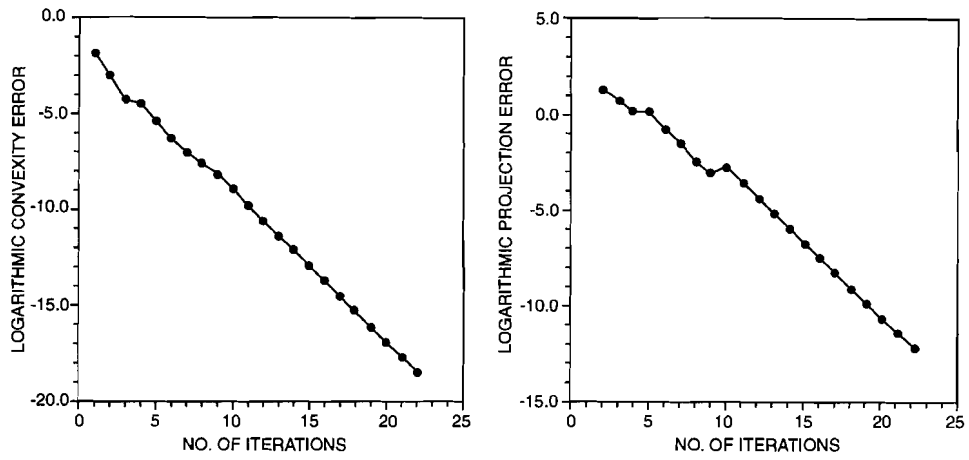

Figure 10. Convexity and projection errors for successive iteration steps decrease nearly monotonically, until convergence is reached at step 22 (see also Fig. 9).

Fig. 10 shows the monotonically decreasing convexity and projection errors associated with the iterative construction of the mixing model. This simple exercise demonstrates that the algorithm is robust, because it converges smoothly, given the limited number of observations. Algorithmic stability is illustrated by the fact that the mixing polytope has not expanded beyond the actual end members (Fig. 9C).

9.3 The final mixing model

Assuming that convergence has been reached, a mathematically satisfactory (approximate) mixing model of the data set under investigation has been obtained. The final (optional) step to be taken is the elimination of negative mixing proportions, by setting the remaining (trivial) negative values of $\boldsymbol{M}$ to zero. This final adjustment should minimize the distortion of $\boldsymbol{X'}$ and conform to the weighted least squares criterion.

A non-negative mixing proportions matrix $\boldsymbol{M}$ fulfilling these criteria can be obtained by means of a *non-negative least squares approximation* (e.g., Lawson & Hanson, 1974) of the scaled oblique loadings of each estimated observation. In formal terms, this problem is defined as:

(39) $$[F_o]\,[a_o]^T \approx [w']^T$$

subject to

(40) $$[a_o]^T \geq 0$$

After this final correction has been made and the matrices have been rescaled to the original units of measurement, the mixing model obeys all non-negativity constraints listed in section 1.

If the convexity error of the final model is small, the correction will have no measurable effect on the estimated data. However, if the convexity error of the final model exceeds a negligible error, the goodness of fit measures should be recalculated to judge whether the fit of the approximation has deteriorated appreciably. Assuming that this is not the case, the resulting mixing model is satisfactory from all of the mathematical points of view discussed above. It can only be judged by the modeller if the solution is also geologically feasible.

The validity of the mixing model obviously depends on the "geological reasonableness" of the end-member compositions. But the ultimate test of the model is the construction of contour maps of the mixing proportions (cf. Imbrie & Van Andel, 1964). Such maps should display spatially coherent patterns of end-member contributions. The presence of such spatial and/or temporal trends indicates that neighbouring and/or successive observations are not independent, as expected under the assumption of physical mixing. Independent observations would produce random spatial patterns, indicating that the hypothesis of a physical mixing process involving the modelled end members is untenable.

Acknowledgements

Thoughtful comments on a draft version of this chapter were provided by J.A. van Dam, G. Frapporti, W. Spakman, S.P. Vriend, and G.J. van der Zwaan. The final version was reviewed by J.C. Davis and P.G.M. van der Heijden, whose positive suggestions are gratefully acknowledged.

APPENDIX I: **Algebraic symbols used**

Upper case: matrices and vectors
Lower case: matrix elements and scalars

$\boldsymbol{A}$	=	(nxq) matrix of principal or oblique loadings
$\boldsymbol{B}$	=	(qxp) end-member compositions matrix
c	=	constant rowsum of compositional data
$\boldsymbol{D}$	=	various ($px1$) vectors of standard deviations
$\boldsymbol{E}$	=	(nxp) matrix of additive errors
$\boldsymbol{F}$	=	(pxq) matrix of principal or oblique reference axes
$\boldsymbol{G}$	=	($px1$) vector of maximum scaling constants
$\boldsymbol{H}$	=	($px1$) vector of minimum scaling constants
i	=	subscript: observation index ($1 \leq i \leq n$)
j	=	subscript: variable index ($1 \leq j \leq p$)
k	=	subscript: end-member index ($1 \leq k \leq q$)
$\boldsymbol{L}$	=	(pxp) diagonal eigenvalues matrix
$\boldsymbol{M}$	=	(nxq) mixing proportions matrix
n	=	number of observations
p	=	number of variables
q	=	number of end members
$\boldsymbol{R}$	=	($px1$) vector of correlation coefficients
$\boldsymbol{S}$	=	($qx1$) vector of scale factors
$\boldsymbol{T}$	=	(qxq) oblique coordinates matrix
$\boldsymbol{U}$	=	($nx1$) vector of geometric row-means
$\boldsymbol{V}$	=	(qxq) oblique transformation matrix
$\boldsymbol{W}$	=	(nxp) scaled data matrix
$\boldsymbol{X}$	=	(nxp) raw data matrix
$\boldsymbol{Y}$	=	($qx1$) correction vector
$\boldsymbol{Z}$	=	(nxp) matrix of logratio residuals
ϵ	=	univariate centred logratio residual
χ	=	goodness of fit statistic
Θ	=	angle (in degrees) between two vectors

Superscript: matrix operators

$\boldsymbol{T}$	=	transpose
$\boldsymbol{-1}$	=	inverse
$'$	=	least squares estimate
$*$	=	rescaled least squares estimate
$\boldsymbol{(i)}$	=	index of iteration cycle

APPENDIX II: **The end-member modelling algorithm**

0. Start: Set iteration counter and exit code to 0. Provide sensible initial end-member compositions which have been projected into mixing space (cf. sections 8.2 and 7.2, respectively). Form rows of initial transformation matrix V from principal loadings of "filtered" initial end-member estimates (cf. equations 13 and 16).

1. Update iteration counter. Invert transformation matrix V and calculate condition number.
If near linear dependence among end members is suspected (i.e., condition number of V is less than cutoff 4), stop.
Fatal error: near singularity (exit code = 4).

2. Perform oblique projection (cf. section 7.1). Compute convexity error of M.
If convexity error is negligible (i.e., less than cutoff 1), stop.
Convergence: stable configuration (exit code = 1).

3. Save current V if convexity error is smaller than that of previous iterations. Calculate T matrix: oblique coordinates of new end members with respect to the previous end members *(see Appendix III).*

4. Perform matrix multiplication in order to obtain the compositions of the new end members B':

$$B'^{(i)} = T^{(i)} B^{(i-1)}$$

Impose non-negativity constraints on the new end members by projecting the rows of B' into the mixing space (cf. equations 24 and 25).

5. Calculate principal loadings of non-negative end-member compositions to form updated transformation matrix V (cf. equations 13 and 16). Calculate projection error of new V with respect to previous V. Save projection error if it is smaller than that of previous iterations.
If projection error is negligible (i.e., less than cutoff 2), stop.
Convergence: unstable configuration (exit code = 2).

6. If maximum number of iterations (cutoff 3) has been reached, replace current V with V corresponding to minimum convexity error, and stop.
No convergence: invalid configuration (exit code = 3).

7. Return to step (1) for another iteration cycle.

APPENDIX III: **Calculation of polytope enlargement**

The distances over which the current end members should be moved "outward" in order to improve the oblique model are obtained at step 3 of the iterative algorithm discussed in Appendix II. The oblique coordinates of the new set of end members $\boldsymbol{T}$ are calculated as follows:

1. Initialise $\boldsymbol{T}$ as an identity matrix, representing the oblique coordinates of the current set of end members.

2. For every end member k ($1 \leq k \leq q$):

2a. Set all elements of the correction vector $\boldsymbol{Y}$ to 0.0

2b. Scan the k-th column of $\boldsymbol{M}$ for negative values. Each row of $\boldsymbol{M}$ in which the k-th value is negative represents an observation outside the mixing polytope spanned by the current end members, located in a segment of the mixing space opposite to the k-th end member. Add the values of such rows of $\boldsymbol{M}$ to the corresponding elements of $\boldsymbol{Y}$.

2c. After the k-th column of $\boldsymbol{M}$ has been scanned, each element of $\boldsymbol{Y}$ is divided by the number of negative values encountered in that column. The correction vector $\boldsymbol{Y}$ now represents the average location (centre of mass) of external data points opposite to the k-th end member.

2d. Determine the maximum value of $\boldsymbol{Y}$. The index number corresponding to this value will be termed i. The i-th end member is closest to the centre of mass of the external data points, represented by $\boldsymbol{Y}$.

2e. Displace the i-th end member over a distance proportional to the k-th element of $\boldsymbol{Y}$, using the scaling factor of equation 38, i.e., replace the zero value of $\boldsymbol{T}(i,k)$ by a "weighted" value of $\boldsymbol{Y}(k)$.

3. If k is less than q, return to (2) for relocation of another end member.

4. The absolute values of the elements of $\boldsymbol{T}$ are summed row-wise. Each rowsum replaces the corresponding diagonal element of $\boldsymbol{T}$, so that the new rowsums of $\boldsymbol{T}$ equal 1.0. The rows of $\boldsymbol{T}$ now represent the oblique coordinates of a new set of end members, expressed as linear combinations of the current set of end members.

CHAPTER 4

UNRAVELLING MIXED PROVENANCE OF COASTAL SANDS: THE PO DELTA AND ADJACENT BEACHES OF THE NORTHERN ADRIATIC SEA AS A TEST CASE

Abstract

Many (if not all) sedimentary basin fills are mixtures of sediments supplied by different sources. A fundamental problem in sedimentary provenance studies is that compositional variation within or among sandstone suites is considered to reflect mixing, but the exact nature of the mixing process is unknown. Observed compositional variation can be cast into the form of a linear mixing model by means of inverse modelling techniques. A new algorithm developed for this purpose is briefly discussed. The inverse modelling approach can help to (1) increase the resolution of provenance models; (2) reduce the problematic effects of varying sampling scales; (3) reduce the extent of a priori knowledge required for successful model predictions. The modelling experiment illustrates how spatial patterns of compositional heterogeneity can be used to predict dispersal patterns of sands and the location of source areas.

The Po-delta front and adjacent beaches of the Northern Adriatic Sea are an ideal natural laboratory for this experiment. The present situation and late Holocene evolution of this area are well-documented, enabling a rigorous testing of model predictions. Compositions of coastal sands, which serve as input for the model, indicate a "recycled orogen" or "mixed" provenance (cf. Dickinson, 1985). The test results show that the performance of the end-member modelling algorithm is quite satisfactory. Three out of four modelled end members closely approximate the compositions of sediments supplied by fluvial drainage basins in the area. A fourth end member, that is poorly represented in the material studied, displays a clear affinity to its "actual" source composition. The modelled alongshore variation of beach sands, expressed as proportional end-member contributions, is in general agreement with present dispersal patterns and historical records of the area. An overall southwest to southward dispersal suggested by the modelling results is attributable to shifting of Po distributaries during the late Holocene. Recycling of these ancient Po sediments is related to the present anthropogenically induced decrease of fluvial sediment supply, and the ensuing widespread coastal retreat in the area studied.

1. Introduction

The production of sediments and the modification of sediment composition along the pathway between source area and final site of deposition is influenced by a large number of physical, chemical, and biological factors. The sediment-forming process is still not quite understood (Ibbeken & Schleyer, 1991), although considerable advancements in the understanding of sand(stone) provenance have been made in the past decades. Parent lithology, climate and relief are the principal determinants of sand(stone) framework composition (e.g., Dickinson, 1985, 1988; Dutta, 1992). On the scale of global dispersal systems, parent lithology and relief are functions of plate-tectonic setting. The validity of large-scale empirical provenance models, which relate ternary subcompositions of sands and sandstones to plate-tectonic environments (Dickinson, 1985, 1988; Valloni, 1985), has been

convincingly demonstrated. However, the provenance discrimination models developed by the "Dickinson school" are useful for classifying means (i.e., mixtures) of sandstone suites only on the largest scale. Erroneous interpretations may result if "local" provenance signals in the data have not been suppressed by temporal and spatial "averaging" of sandstone compositions (e.g. Ingersoll, 1990; Ingersoll et al., 1993). This averaging approach has the distinct advantage of robustness, but implies a limited spatial and temporal resolution of current plate-tectonic provenance models. It is therefore not surprising that many sand suites plot in the "recycled orogen" and "mixed provenance" fields of the ternary provenance diagrams (Dickinson, 1985, 1988).

The analysis of compositional variation of sand(stone) suites on smaller spatial and/or temporal scales cannot rely on generally applicable provenance models. Ingersoll (1990) suggested that "small scale" provenance analysis requires a different approach, because "*..specific source-rock types, rather than tectonic setting, determine provenance [fields]...*". A large number of solutions to problems of "local" or "short term" compositional variation have been proposed. To name a few examples: (1) The compositions of sand(stone)s of known monolithologic parentage has been compared to those of "calibrated" suites, in order to estimate the combined influence of relief and climate in the source area (e.g., Basu, 1985; Grantham & Velbel, 1989; Girty, 1991; Dutta, 1992); (2) Discriminant functions based on compositions of recent sands of known parentage have been used to infer parent lithologies of fossil sands from the same basin (Ingersoll, 1990); (3) A technique which conceptually "erodes" and "mixes" known sedimentary parent lithologies has been employed to explain patterns of compositional variation in syntectonic conglomerates (Graham et al., 1986; DeCelles, 1988; Pivnik, 1990; DeCelles et al., 1991). A similar approach was used as part of a comprehensive provenance and mass-balance study of a series of drainage basins along an active margin in Calabria, Italy (Ibbeken & Schleyer, 1991). All of these solutions require a considerable amount of *a priori* knowledge of source area lithology and physiography in order to guarantee a successful application. Such detailed information is not generally available for fossil basins.

The review presented above indicates that provenance studies would greatly benefit from methodological improvements specifically designed to (1) increase the resolution of provenance models; (2) reduce the problematic effects of varying sampling scales; (3) reduce the extent of *a priori* knowledge required for successful model predictions. It will be shown that these problems are closely related, indicating that they can be tackled within the same mathematical framework. A constrained linear model is proposed for describing patterns of compositional variability within and among sand(stone) suites in natural sedimentary systems in terms of mixing of a limited number of end-member assemblages. This model offers a concise description of the system under study, and helps to overcome many of the current problems in sedimentary provenance studies.

2. Patterns of compositional variation

The observed compositional variation among and within sand(stone) suites in sedimentary systems can be attributed to a variety of processes. The compositional and textural properties of sediments are affected by selection, mixing, and mechanical breakage of grains during transport, and chemical-mineralogical transformations during chemical weathering. All of these modifications are selective: the extent to which selection occurs depends on the

range of physical and chemical properties of the the grain population under investigation (i.e., durability, chemical stability, size, shape, and specific gravity). During transport, each grain behaves differently, depending on its size, shape, and specific gravity. Transport of sediments is therefore strongly non-linear with respect to the bulk properties of sediments. It is well-known that grain-size distributions are affected by selective transport and deposition (e.g., Komar, 1977; Bardsley, 1978; Dacey & Krumbein, 1979; McLaren, 1981; McLaren & Bowles, 1985; Paola et al., 1992). The same applies to the other bulk physical properties, such as shape and density distributions. In a sedimentary system, mean transport rates will be different for each size/shape/density class within a grain population. In the hypothetical case of an ideal fluvial system with no tributaries that is fed by a single source, all of the observed spatial variation of bulk physical and textural properties can be attributed to selective transport if no mechanical or chemical weathering occurred in the system being studied, and if the initial characteristics of the sediment supplied to this ideal system did not vary. In this case, all of the observed variation of size, shape, and density distributions must reflect varying proportional contributions of each size/shape/density class to the sediment. Consequently, the chemical and petrographical composition within each size/shape/density class must be the same at every location. In other words, selective transport alone does not affect the ratios of grain types belonging to a single size/shape/density class.

The concept of framework composition employed by the "Gazzi-Dickinson school" (Gazzi, 1966; Dickinson, 1970; Ingersoll et al., 1984) is based on ratios of classes of principal framework grains, i.e., grains with similar shape and specific gravity (quartzose grains, feldspars, and polymineralic grains). Effects of shape and density selection are minimized by discarding certain classes of grains with deviating properties, such as platy micaceous grains and accessory "heavy" minerals. In addition, the definition of framework composition generally applies to ratios of principal framework elements within a narrow range of grain sizes. All of these restrictions aim at minimizing effects of size, shape and density selection, which may have taken place during transport of the sediment. The analysis of compositional modification can be simplified to a considerable extent if it is accepted that compositional variations attributable to size, shape, and density selection can be eliminated by quantifying framework compositions of sand-sized sediments according to the criteria defined above. This proposition is not unreasonable, as shown by Ingersoll et al. (1984) and Zuffa (1985), who demonstrated that framework compositions of different grain-size classes of the same sediments, determined according to the Gazzi-Dickinson conventions, form tight clusters in QFL-space. It may be expected that framework compositions determined according to the Gazzi-Dickinson conventions are equally robust with respect to small variations of shape and specific gravity.

The elimination of selective transport and deposition from our observations leaves three possible mechanisms of compositional variation: mechanical weathering (breakage of grains without chemical-mineralogical modification), chemical weathering (chemical-mineralogical transformation and dissolution), and physical mixing of sediments from various sources. If none of these mechanisms contributes to the spatial heterogeneity of bulk sediment properties, its principal framework composition as defined above does not show any spatial variation, and the sediment shed by this source can be represented by a single data point in a ternary diagram (QFL-space). Within this frame of reference, variations of framework composition can be classified in terms of selective and non-selective modifications.

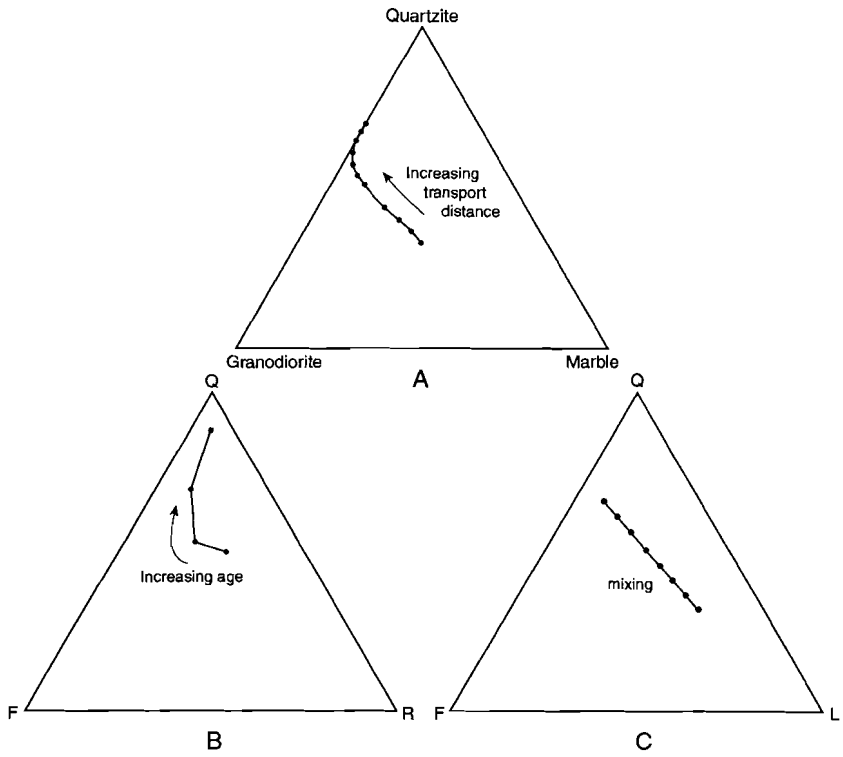

Figure 1. A: Abrasion of conglomerate-clast assemblage (Abbott & Peterson, 1978). B: Weathering chronosequence of fluvial sands in point bar (Johnsson & Meade, 1990). C: Mixing of two "source compositions".

A. Selective modifications: weathering

The class of principal framework grains can be subdivided into various types of minerals and polymineralic lithic fragments. Each grain type is characterized by its own chemical and mechanical stability, that will determine the rate at which it will dissolve, decompose, or disaggregate under given environmental conditions. Selective modifications, such as chemical and mechanical weathering, treat each type of framework grain differently, and will cause changes to the ratios of framework elements. On account of their selective nature, mechanical and chemical weathering are intrinsically non-linear functions of the compositional variables. They can be identified under (natural) laboratory conditions as distinctly curved trends in compositional space. Compositional patterns attributable to chemical weathering can be recognized in sediments which have undergone *in situ* modifications. They are most pronounced in sediments of monolithologic parentage (e.g., soils and saproliths in first-order fluvial drainage basins). However, similar effects may be observed in more distal parts of sedimentary systems, where sediments from various sources have been sufficiently homogenized by mixing, prior to being subjected to *in situ* modification. Two examples of curved compositional trends resulting from

progressive non-linear modifications by mechanical weathering (Abbott & Peterson, 1978) and chemical weathering (Johnsson & Meade, 1990) are depicted in the ternary diagrams of Fig. 1A and 1B, respectively.

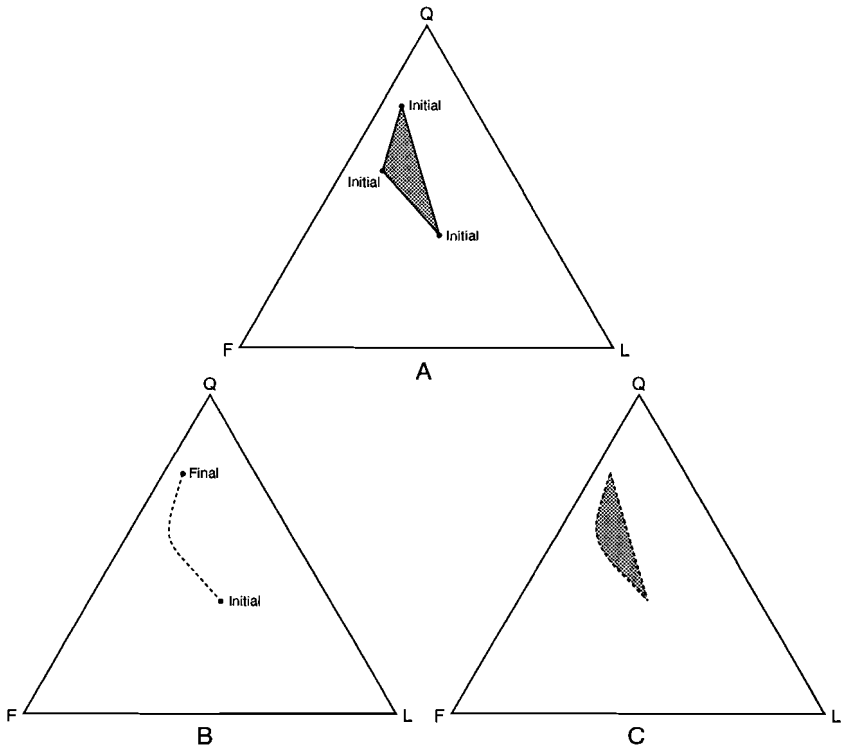

Figure 2. A: Mixing of three "source compositions". B: Pattern of compositional variation in soil profile (weathering chronosequence). C: New pattern of sediment compositions after transport and mixing.

B. Non-selective modifications: mixing

Physical mixing of sediments from compositionally distinct sources induces strictly linear trends in compositional space, because all principal framework grains of similar size, shape, and density are treated in the same way during the transport process. For example, all possible mixtures of two compositions can be represented by a straight line segment in a three dimensional QFL-space (Fig. 1C), whereas mixing of sediments from three distinct sources produces a triangular field in QFL-space that is enclosed by the "source compositions" (Fig. 2A). Linear mixing in sedimentary systems is a primary cause of compositional variation on widely different scales. On the smallest scale, compositional variation of detrital sediments carried by first-order streams reflects contributions of different parent rocks. On a larger scale, compositional variation of sands in large fluvial systems reflects the mixing of sediments delivered by its "second-order" tributary streams. Patterns of

compositional variation in the shallow marine environment can be attributed to mixing and dispersal of sediments from various river systems ("third order"). A considerable proportion of the observed compositional variation in sandstone suites is thus determined by hierarchical tributary structures, that can be recognized from the uplands in which sediments are produced to the ocean basins in which they are eventually deposited. Examples of this "mixing hierarchy" are presented by DeCelles & Hertel (1989), Johnsson (1990), and Ingersoll et al. (1993).

The points raised above imply that the perceived effects of a modification process depend to a large extent on the range of physical properties displayed by the grain population under study. This has important consequences for the analysis and modelling of compositional modifications. Certain modifications, which behave in a non-linear way with respect to the bulk properties of sediments can be regarded as linear if we restrict our observations to framework-grain populations with similar physical properties (size/shape/density).

In a sedimentary system, selective and non-selective modifications usually go together, as illustrated with the following example. The principal framework compositions of a series of observations arranged along a vertical profile through a soil and saprolith into an unweathered polymineralic parent rock are expected to show a non-linear compositional trend attributable to *in situ* weathering, represented by the curved line segment in Fig. 2B. As soon as this weathering residue is eroded from the bedrock surface, and enters the sedimentary (fluvial) system, its spatial pattern of compositional variation will change due to physical mixing of materials derived from various levels in the original soil profile. The new pattern of compositional variation displayed after transport will consist of a roughly triangular area delimited by the original trend and the straight line between the two extreme compositions (Fig. 2C). In this particular case, the resulting pattern of compositional variation is virtually indistinguishable from that of the ternary mixing system depicted in Fig. 2A. Based on these considerations, one might argued that compositional variation in many natural sedimentary systems can be adequately *described* by a linear mixing model. However, additional requirements for assessing the plausibility of physical mixing must be provided by a coherent spatial distribution of "mixing proportions" in the area under investigation, and by the geological reasonableness of the "source compositions" (Imbrie & Van Andel, 1964; Weltje, 1994).

3. The linear mixing model

A general expression of linear mixing can be formulated as follows (Jöreskog et al., 1976; Menke, 1984; Renner, 1988): Compositional data are generally cast into the form of a matrix $\boldsymbol{X}$, with n rows representing observations, and p columns representing variables. By definition, all compositional variables are non-negative, and each row of the data matrix sums to a constant $\boldsymbol{c}$, usually 1, 100, or 10^6 (for measurements recorded as proportions, percentages, or parts per million, respectively).

$$\textbf{(1)} \qquad \sum_{j=1}^{p} x_{ij} = c \qquad\qquad x_{ij} \geq 0$$

If compositional variation among a series of measured specimens results from physical mixing, each row of the matrix of compositional data $\boldsymbol{X}$ is a non-negative linear

combination $\boldsymbol{M}$ of a fixed number (q) of end-member compositions, represented by the rows of $\boldsymbol{B}$.

In matrix notation, this perfect mixing can be expressed as

$$\boldsymbol{X} = \boldsymbol{MB} \tag{2}$$

subject to the following non-negativity and constant-sum constraints:

$$\begin{aligned} \sum_{k=1}^{q} m_{ik} &= 1 \qquad & m_{ik} &\geq 0 \\ \sum_{j=1}^{p} b_{kj} &= c \qquad & b_{kj} &\geq 0 \end{aligned} \tag{3}$$

Although this representation is acceptable from an algebraic point of view, it does not account for the fact that perfect mixing cannot be demonstrated in practice, due to "errors" in $\boldsymbol{X}$. Therefore, the assumption is made that the data matrix $\boldsymbol{X}$ is made up of a systematic part $\boldsymbol{X'}$, attributable to perfect mixing, and a matrix of "error terms" $\boldsymbol{E}$, representing non-systematic contributions to $\boldsymbol{X}$, i.e., sampling and measurement errors, and natural heterogeneity of the materials analyzed. In other words, the observed compositional variation is made up of "signal" and "noise". We will assume that these errors are relatively small and $\boldsymbol{X'}$ "closely" resembles $\boldsymbol{X}$. By definition, the rows of $\boldsymbol{X'}$, the estimated matrix of perfect mixtures, must consist of non-negative contributions $\boldsymbol{M}$ of q end-member compositions $\boldsymbol{B}$:

$$\begin{aligned} \boldsymbol{X'} &= \boldsymbol{X} - \boldsymbol{E} \\ \boldsymbol{X'} &= \boldsymbol{MB} \end{aligned} \tag{4}$$

The range of each variable in $\boldsymbol{X'}$ cannot exceed that of the corresponding variable in the end members $\boldsymbol{B}$, due to the non-negativity constraint on $\boldsymbol{M}$. In other words, the end-member matrix contains the extreme values of each variable. By definition, the rows of $\boldsymbol{X'}$ are also compositions, and therefore

$$\begin{aligned} \sum_{j=1}^{p} x'_{ij} &= c \qquad & x'_{ij} &\geq 0 \\ \sum_{j=1}^{p} e_{ij} &= 0 \end{aligned} \tag{5}$$

The above considerations lead to the following mathematical formulation of the mixing model (subject to the constraints listed above):

$$\mathbf{X} = \mathbf{MB} + \mathbf{E} \quad (6)$$

In terms of mathematical modelling, equation 6 is the *forward model*. If a set of end members has been specified, the composition of any mixture can be produced by simple matrix multiplication, as shown by Graham et al. (1986) and Ibbeken & Schleyer (1991). However, the fundamental problem in sedimentary provenance studies is the opposite: observed compositional variation is considered to reflect mixing, but the exact nature of the mixing process is unknown. In such cases, our objective is to estimate the mixing parameters from the data by means of *inverse modelling* techniques. Inverse modelling of parent lithologies can provide important constraints on the nature of the source area, information presently regarded as indispensible for successful forward modelling. For instance, each "third-order" composition (*sensu* Ingersoll, 1990) that is considered suitable for plotting in one of the ternary plate-tectonic provenance diagrams is derived from a data set whose pattern of compositional variation contains a wealth of information about its lower-order parentage. Many of the current problems with respect to model resolution and sampling scale can be reduced significantly, if such information is extracted from the compositional variability displayed by sandstone suites.

4. Inverse modelling strategy

Fitting a mixing model to compositional data is a hazardous task if no *a priori* information about the number of end members and/or their compositions is available. In such cases, the mixing problem is stated in explicit form, indicating that all of the parameters of the mixing process must be estimated from the data:

- $\mathbf{X'}$ (the "perfect mixture" compositions)
- $\mathbf{E}$ (the non-systematic contributions to the data)
- q (the number of end members)
- $\mathbf{B}$ (the end-member compositions)
- $\mathbf{M}$ (the end-member contributions to each "perfect mixture")

A fundamental assumption is that the set of end members from which the observed variability has been generated is *linearly independent*, i.e., that none of the end members can be generated by mixing of other end members (otherwise, the problem cannot be solved). This requirement can be demonstrated by referring to Figs. 1C and 2A. Fields in compositional space enclosed by the end-member compositions represent *mixing spaces*. If the end members are linearly independent, the number of dimensions of the mixing space reflects the number of end members, q. In other words, the number of linearly independent "sources", q, is equal to the number of dimensions occupied by the data. This concept of dimensionality is used in the first modelling stage, in order to partition the data matrix into "perfect mixtures" (signal), and "non-systematic contributions" (noise), following equation 4. A matrix of "perfect mixtures" can be generated for every value of q ($2 \leq q \leq p$), using fundamental concepts of linear algebra (*singular value decomposition* and *constrained*

weighted least squares approximation). Each approximated matrix conforms to the non-negativity constraint of equation 5.

A strategy aimed at constructing an *optimal solution* to the mixing problem should take into account that the model must be as *simple* as possible. This implies that the number of end members, q, is determined by the minimum number of dimensions required for a satisfactory approximation of $\boldsymbol{X}$. The number of end members in the mixing model is thus equal to the "approximate dimensionality" of the data, which can be estimated without knowledge of the end-member compositions. If desired, the columns of the data matrix can be scaled to equal "weights" prior to the partitioning into signal and noise, so that each variable is equally important in determining the approximate dimensionality of the data. Without scaling, the weight of each variable largely depends on its standard deviation (Miesch, 1980).

If q has been estimated, a mathematically and geologically feasible mixing model must be constructed which adequately describes the "filtered" compositional variation. In other words, a matrix of non-negative end-member contributions, $\boldsymbol{M}$, and a matrix of q realistic end-member compositions, $\boldsymbol{B}$, must be found, which will yield the approximated data $\boldsymbol{X'}$ after matrix multiplication (cf. equation 6). This is a difficult problem, *to which no unique solution exists*. There may be an infinite number of mixing models that fit a given set of data within tolerable error, and the particular combination of mixing parameters which actually produced the data cannot be reconstructed.

5. The "optimal" mixing model

A unique "unmixing" solution can be provided if additional constraints on the model parameters are introduced. A practical way of doing this is by specifying constraints which will ensure the geological reasonableness of the model. Therefore, additional constraints on $\boldsymbol{M}$ and $\boldsymbol{B}$ are specified as follows. Of primary concern is that the modelled end members enclose the smallest possible mixing space, so that each end member contributes significantly to the observed compositional variation, and its composition can be easily interpreted in geological terms. However, negative values of "end-member contributions" are not allowed in the model, and a good fit of the model to the approximated data requires that the number and magnitude of "negative contributions" are as small as possible. In a geometrical sense, the set of end members must enclose as many of the observations as possible, because any observation not enclosed by the end members is distorted in the modelled representation of the data. The apparent contradiction of these two requirements enables the optimal solution for a given (minimal) value of q to be defined as *the smallest possible mixing space which encloses a sufficiently large proportion of the data points.*

It is also highly desirable that any strategy for estimating the end-member compositions is *robust*, i.e., that adding or removing a limited number of observations has a minimal effect on the solution. Because the "actual" mixing parameters are unknown and cannot be reconstructed from the data alone, it is ultimately up to the modeller to determine which estimates are reasonable under given conditions. The required trade-off between a fully non-negative mixing-proportions matrix on the one hand, and the desire for "conservative" end-member estimates on the other hand, must also be built in to the algorithm. Therefore, the

end-member estimation procedure must be flexible. The simplest way to implement all of the above-mentioned constraints and requirements is by making use of iterative algorithms, which construct an optimal solution from a sensible initial guess of the model parameters.

In the past decades, various strategies for solving the mixing problem have been proposed by Imbrie (1963), Imbrie & Van Andel (1964), Jöreskog et al. (1976), Miesch (1976a, 1980, 1981), Clarke (1978), Full et al. (1981, 1982), Dymond (1981), Dymond et al. (1984), Menke (1984), Leinen & Pisias (1984), Renner (1988), Renner et al. (1989), and Ripley (1990). Although some of these methods may provide a satisfactory answer to the mixing problem, none completely fulfills the general requirements formulated above (i.e., simplicity, mathematical and geological reasonableness, robustness, and flexibility). An inversion scheme which takes into account all of the above-mentioned properties has been developed by the author. A full account of the algebraic details is published elsewhere (Weltje, 1994).

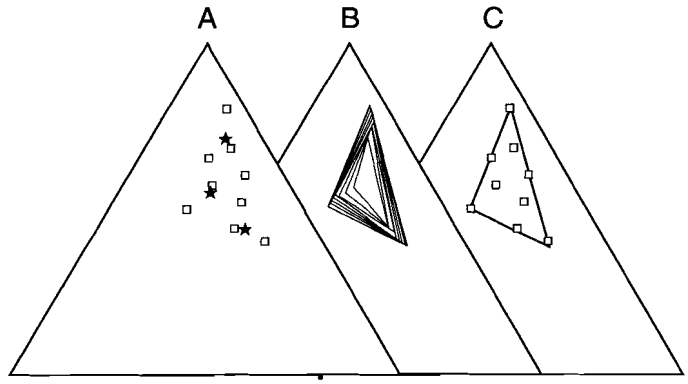

Figure 3. Iterative construction of approximate mixing model with three end members. A: initialisation with fuzzy cluster centres, shown as stars. B: a series of iteration steps. C: the final mixing model.

A practical application of the inversion algorithm, shown in Fig. 3, will serve to illustrate the basic concept of the iterative construction of "optimal" end-member compositions. The data in the ternary diagram of Fig. 3A consist of three "source compositions" and six mixtures. The number of end members is thus known *a priori*. Fig. 3A also shows the locations of three "centres of gravity" of the data set, that have been calculated using a Q-mode cluster algorithm (Full et al., 1982; Bezdek et al., 1984). These centres of gravity are the robust initial end-member estimates employed by the iterative procedure. Because a set of end members has been specified, the matrix of mixing proportions corresponding to these end members can be calculated, for example from the exact bilinear relationship of equation 4. This matrix of mixing proportions is evaluated in order to define improvements to the end members, which aim at reducing the number and magnitude of negative mixing proportions. In the next iteration cycle, the updated matrix of end-member compositions is used to generate a new mixing proportions matrix. In a geometrical sense, the mixing space "grows" in each iteration cycle, until the specified constraints on an optimal mixing model have been satisfied (Fig. 3B). Modifications to the end-member matrix are based on the

collective properties of the data set, in order to ensure that possible outliers have a minimal effect on the locations of the end members. In this example, it was assumed that the data were free of error, and the iterative procedure was allowed to run until improvements to the mixing proportions matrix became negligible. Fig. 3C shows that all of the data points are enclosed by the final mixing space, and that the original "source compositions" are accurately identified.

6. Application to Northern Adriatic coastal sands

The current modelling experiment is intended to provide an analog for the worst case in provenance studies: unravelling the provenance of a fossil basin fill, for which no additional information about hinterland and sediment dispersal is available. In this case, the only input of the inverse model consists of the compositions of modern beach sands. The experiment aims at predicting the locations and compositional signatures of fluvial input. The Po-delta front and neighbouring beaches of the Northern Adriatic Sea (Fig. 4) form an ideal natural laboratory for evaluating the performance of the model, because the present dispersal pattern, the composition of fluvial sands, and the late Holocene evolution of the northern Adriatic coastal plain and Po delta are well documented. This provides an opportunity to assess the usefulness of the inverse modelling approach for the analysis of provenance and sediment dispersal in fossil basins.

There are a number of local peculiarities (as in every case history), which may blur the attempted provenance reconstruction. Beach sands of the northern Adriatic Sea are derived from a few large rivers (such as the Po and Adige), and numerous smaller streams, which drain a lithologically diverse Alpine-Apenninic hinterland composed of siliciclastic sediments, carbonates, igneous rocks, metamorphites, and volcanites (Pigorini, 1968; Nelson, 1970; Gazzi et al., 1973). The predominance of sedimentary rocks in the source areas indicates that most of the detritus delivered to the present Adriatic coast must have been recycled. Zuffa (1987) showed that the averaged (third-order) composition of these river sands is consistent with a "recycled orogen" provenance *sensu* Dickinson (1985, 1988). Furthermore, beach sands along this wave-dominated coast contain high proportions of mechanically and chemically unstable framework components (limeclasts), that are highly susceptible to selective destruction by wave action (cf. Mack, 1978; Suttner et al., 1981; Sedimentation Seminar, 1988). Another factor which may be expected to obscure the provenance signal is the presently widespread coastal retreat in this area, which re-introduces ancient sands into the modern system (Brambati et al., 1978; Bondesan et al., 1978; Dal Cin, 1983).

The inversion algorithm was applied to a data set collected and analysed by Gazzi et al. (1973). The data set consists of 53 samples of modern beach sands (grain-size range: 1 to 5 ϕ) from the northern Adriatic coast between Trieste and Pesaro (Italy). The petrographic composition of each sample was estimated by counting 500 points in thin section according to the Gazzi-Dickinson conventions (Gazzi, 1966; Dickinson, 1970; Ingersoll et al., 1984). Sampling stations are depicted in Fig. 4. The average inter-sample distance (±6 km) and the size of the sampling area (300 km) are comparable with that of many provenance studies in fossil basins. The raw data set was slightly modified for input into the modelling programs. A numerical value of 0.1% was assigned to certain grain types that were reported as occurring in "trace" amounts. This value represents the precision of point-counts of 500

Table 1. Pre-processing of input data (from Gazzi et al., 1973) for the end-member modelling experiment.

Original variables:	New variables:	Labels:
Quartz	Quartz	Q
K-feldspar Albite Plagioclase	Feldspar	F
Acidic volcanites Basic volcanites	Volcanic lithics	Lv
"Serpentine" Serpentine schist Phyllite	Metamorphic lithics	Lm
Shale Calcareous siltstone Non-calcareous siltstone	Siliciclastic lithics	Ls
Sparite	Sparite	Sp
Micrite	Micrite	Mi
Bioclasts	Bioclasts	Bi
Dolostone	Dolostone	Do
Chert	Chert	Ch
Micas & "other"	(excluded)	-

grains. Gazzi et al. (1973) distinguished 19 compositional classes of grains. Two classes were excluded from the data, on account of their deviating shape ("micas"), or their lack of genetic significance ("others"). Other grain types that are absent in many samples, and present in small amounts in a limited number of samples cannot be adequately represented by the linear mixing model. Such grain types were combined with others on the basis of textural and compositional criteria. A reduction of the number of compositional classes to 10 was considered satisfactory. These modifications are summarized in Table 1. Eventually, the (53x10) array of beach sands was recalculated to a constant sum of 100% for subsequent modelling.

A series of approximations to the data was generated, one for each value of q. The minimum number of dimensions (end members) required for a satisfactory approximation of the data was estimated by calculating the *coefficients of determination* (Fig. 5a). The coefficients of determination represent the proportions of the column variances that can be reproduced by the approximated data. This proportion is equal to the squared correlation coefficient of the input variables and their approximated values (Miesch, 1976, 1980). As shown in Fig. 5A, only four variables (quartz, micrite, feldspar, and sparite) can be adequately reproduced by a two end-member model. The goodness of fit of the other six variables increases gradually as the number of end members is increased, indicating that the

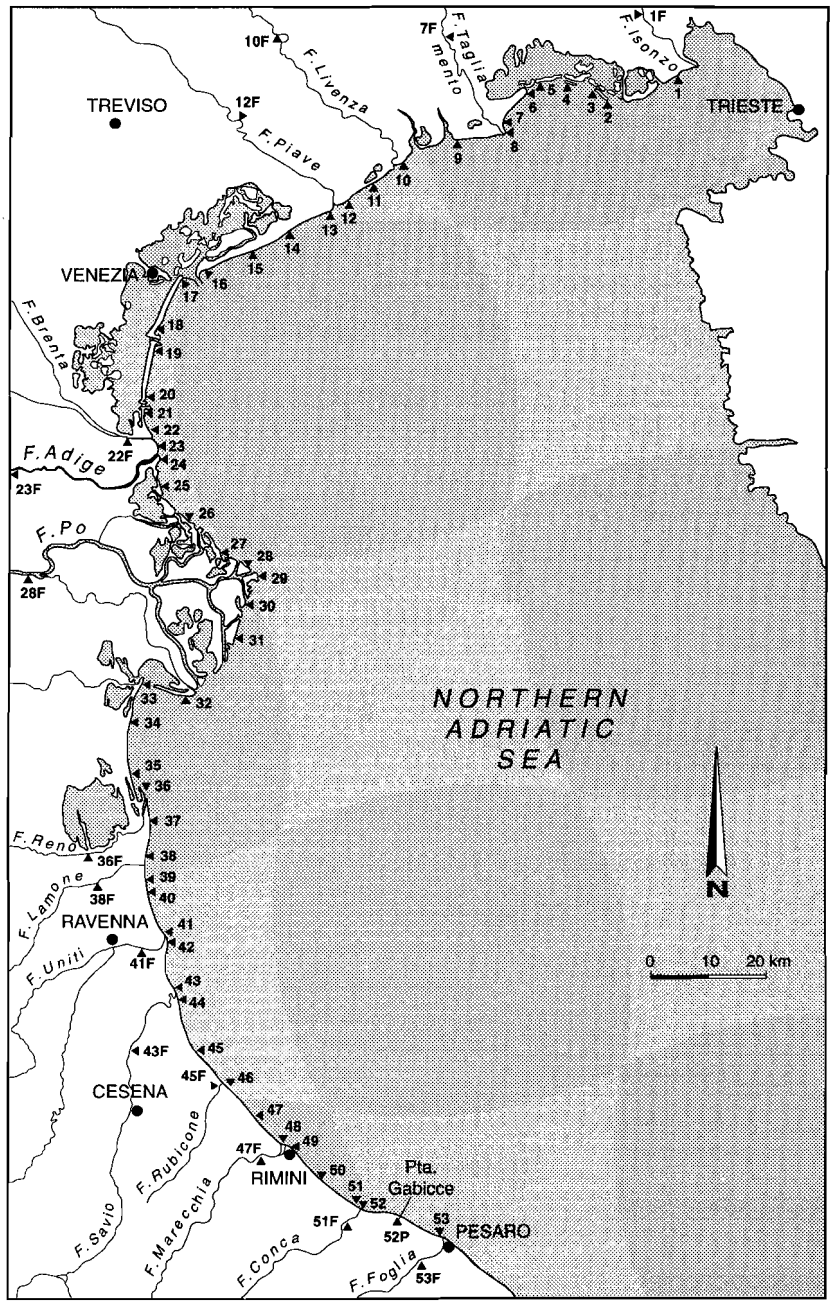

Figure 4. Simplified map of the northern Adriatic Sea, showing coastal and fluvial sampling stations (after Gazzi et al., 1973).

mixing system is quite "noisy". All of the variables (except for "chert") can be reasonably well reproduced by a four end-member model, as indicated by their coefficients of determination which exceed 0.5 (i.e., 50% of the variance is reproduced, equivalent to a

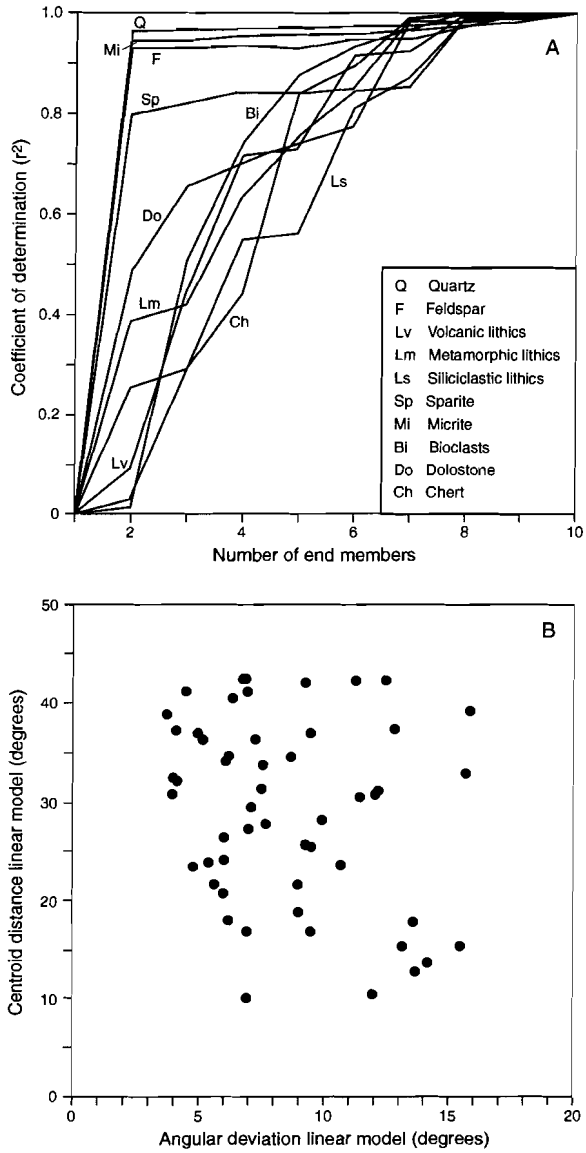

Figure 5. A: coefficients of determination suggest that the minimum number of end members equals four. B: a four-dimensional approximation of the input data does not show any outliers.

correlation coefficient of 0.7). Increasing the number of end members to five would only improve the goodness of fit of chert to a considerable extent, whereas the number of end members would have to be increased to six in order to reach a high-precision approximation. A mixing model with four end members seems to be a reasonable choice in view of the "noise" in the mixing system, and the desire for a sparse description of the basin fill under study.

In order to investigate if the observations can be adequately represented in four dimensions, the "angular deviation" and "centroid distance" of each observation vector were computed, using the "coefficient of proportional similarity" of Imbrie & Purdy (1962). The "angular deviation" is defined as the angle between each observation and its predicted composition according to the model. The "centroid distance" of an observation is defined as the angle between the average composition of the approximated data set and the approximated composition vector. Scatter graphs of angular deviations vs. centroid distance can be used to identify observations for which both values are relatively large (Fig. 5B). Such observations are potential outliers, that could influence the modelling results. The scatter graph of Fig. 5B shows a random pattern, which indicates that no outliers are present in the four-dimensional approximation of the data.

Table 2. Goodness of fit statistics for linear model with four end members and final mixing model. Fit of model to input data decreases slightly by imposing non-negativity constraints on mixing proportions.

Coefficients of determination:	Linear model	Mixing model
Quartz	0.97	0.97
Feldspar	0.94	0.94
Volcanic lithics	0.72	0.66
Metamorphic lithics	0.64	0.59
Siliciclastic lithics	0.55	0.48
Sparite	0.84	0.84
Micrite	0.96	0.95
Bioclasts	0.74	0.66
Dolostone	0.71	0.68
Chert	0.44	0.37
Mean coefficient of determination	0.75	0.71
Mean angular deviation	8.45^0	8.95^0
Goodness of fit of mixing model residuals:		
Number of logratio-residuals calculated		36
Chi-square value of distribution (df=2)		4.28
Associated significance probability		0.88

Four end-member compositions were constructed by means of the iterative procedure described above. A stable solution was obtained after 146 iterations, when improvements to the mixing proportions matrix had become negligible. As expected from the "noisiness" of the data, negative mixing proportions could not be fully eliminated by the iterative algorithm. Because the average magnitude of negative contributions was small, the goodness of fit of the final mixing model was only slightly reduced by imposing non-negativity constraints on the mixing proportions matrix (see Table 2). An *a posteriori* goodness of fit test indicated that the distribution of *centred logratio-residuals* (cf.

Aitchison, 1986) does not deviate significantly from a multivariate normal distribution, suggesting that only random variation has been discarded by assuming that the data set was generated by mixing of four end members (Renner, 1991; Weltje, 1994). A comparison of the observed and modelled longshore variation for each grain type is depicted in Fig. 6. The major trends of longshore variation in the beach sands are well reproduced, indicating that a four end-member representation adequately captures the overall pattern of variation. Extreme values of poorly approximated variables have been smoothed, due to the smaller variance of the model. Systematic deviations from the observed grain content are limited to variables that are poorly reproduced by the model, such as volcanic lithics. Fig. 6 shows that the high peak of volcanic lithics observed between sampling stations 21 and 25 is strongly underestimated in the modelled representation.

7. Interpretation of modelling results

The modelling results can be interpreted by plotting the end-member contributions as a function of the spatial sampling coordinates. The spatial pattern of end-member contributions to the Adriatic beach sands is coherent and easily interpretable (Fig. 7). End member 1 contributes a large proportion of material to beach sands in the northern part of the area (stations 1 to 20), whereas its contributions to the other beach sands are very small. End member 2 contributes a large proportion of material to the beaches located between stations 21 and 25. Contributions of end member 3 are virtually absent in the northern part of the area, but they increase dramatically on the beaches between stations 26 and 39. The contribution of end member 3 can be traced to station 43, where it diminishes rapidly towards the south. End member 4 contributes a large proportion of material to the beaches between stations 44 and 53. The compositions of beach sands between stations 40 and 44 can be largely attributed to mixing of end members 3 and 4. The longshore variation can be conveniently summarized in terms of four "sedimentary petrological provinces" (*sensu* Edelman, 1933). For future reference, these provinces are labelled A, B, C, and D (from northwest to southeast). The skewed patterns of contributions from end members 2 and 3 could reflect a predominantly southeastward longshore dispersal, although the gradual transition from province C to province D could also indicate a northward dispersal of sands in province D.

The alongshore contributions of end members 1 and 4 show a second, subsidiary mode, suggesting that a small proportion of beach sands in widely separated areas has been derived from parent lithologies with similar characteristics. If the end members are to be interpreted as geographically distinct fluvial source assemblages, these subsidiary modes would have to be regarded as "noise" or artifacts of the modelling procedure. However, a more flexible interpretation can be made by taking into account that the end members can only be modelled under the assumption of linear independence. End members whose compositions can be expressed as mixtures of other end members cannot be reconstructed from the data. Following this view, the subsidiary modes of end members 1 and 4 can be interpreted as contributions of minor sediment sources, whose compositions can be expressed as non-negative mixtures of the modelled end members. Increasing the number of end members does not necessarily resolve the contributions of such sources, unless their linear dependence is an artifact induced by the reduction of the dimensionality of the input data. True linear dependence (colinearity) in compositional space is a fundamental problem that cannot be resolved by inverse methods (see also Harvey & Lovell, 1992).

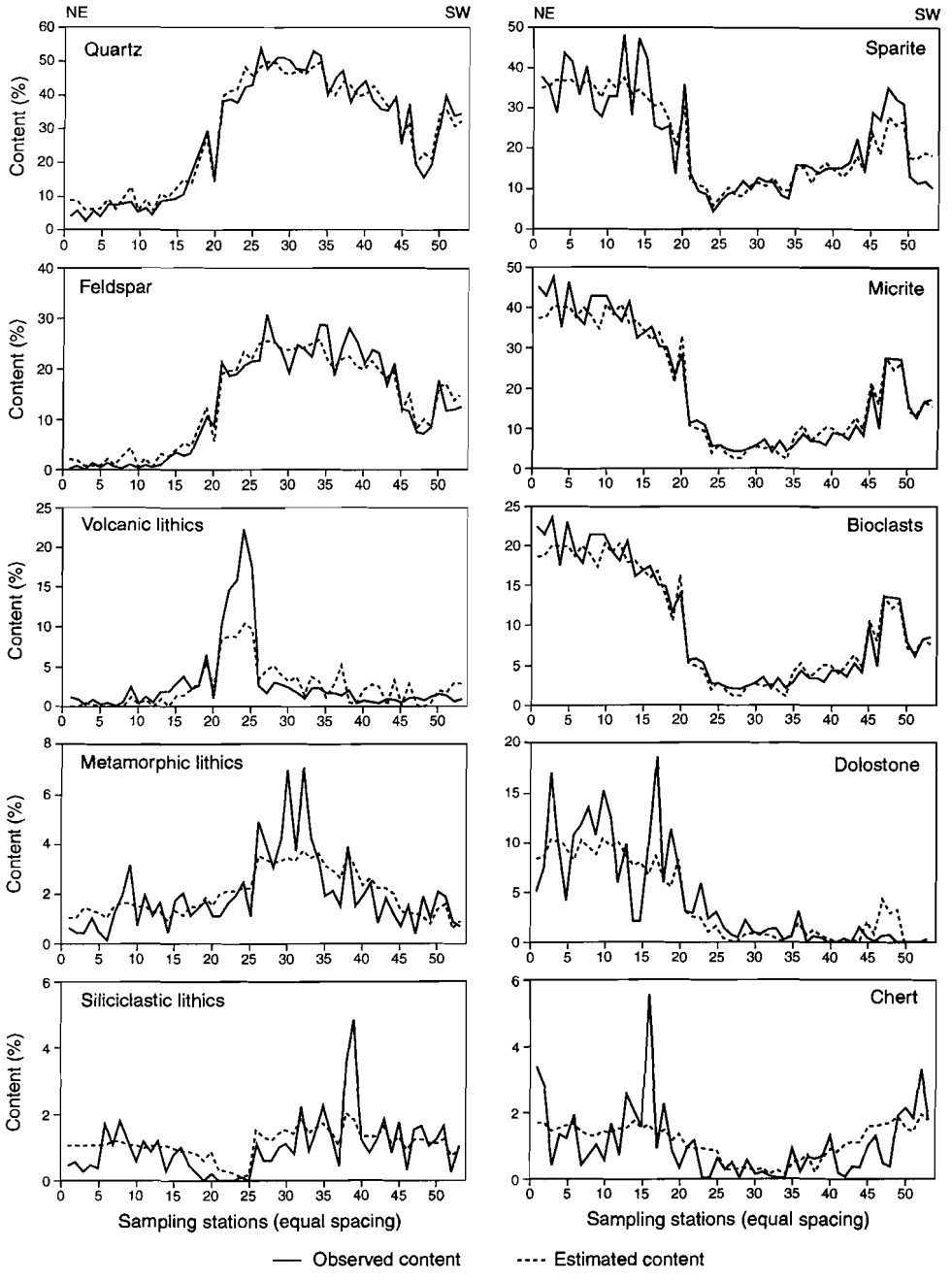

Figure 6. Comparison of observed and estimated longshore variation of the ten grain types. Note smoothing effect due to smaller variance of the mixing model.

If the geographical pattern of end-member contributions to the beach sands is interpreted in terms of "sedimentary petrological provinces", the end-member compositions must

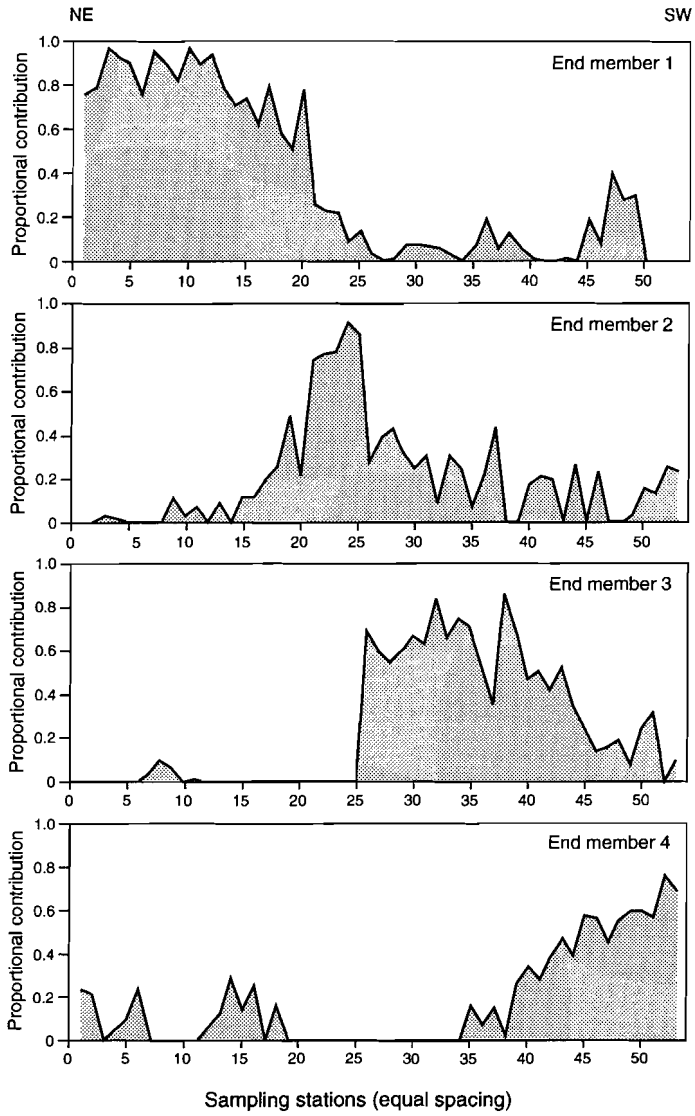

Figure 7. Estimated longshore contributions of the modelled end members to the northern Adriatic beaches.

represent sediments derived from four major drainage basins or source areas. The lithologic characteristics of these hypothetical source areas can be inferred from the end-member compositions depicted in Fig. 8 and Table 3. End member 1 consists predominantly of carbonate (micritic, sparitic, and dolomitic grains), and contains minor amounts of quartzose grains. Such sediments can only be derived from a source area which consists almost exclusively of carbonate rocks. End member 2 contains a large amount of quartz, feldspar, and volcanic lithics. Small amounts of carbonate lithics point to the presence of sedimentary rocks in the source area. An unknown, but presumably small proportion of the other grain

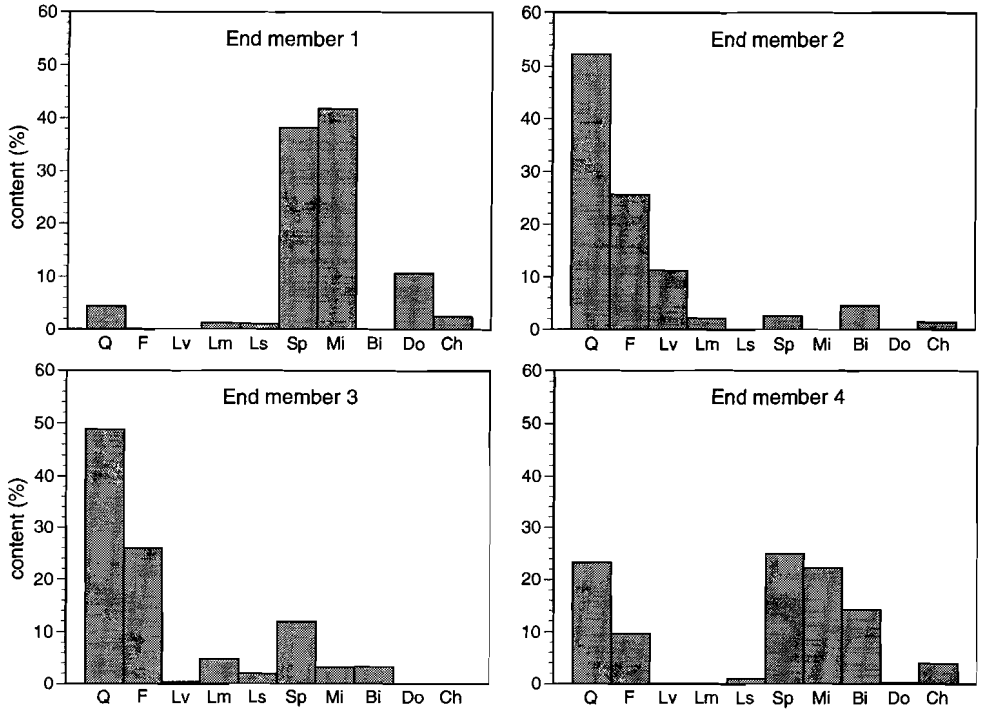

Figure 8. Modelled end members of northern Adriatic beach sands (see also Table 3).

types could have been reworked from these sedimentary rocks, but igneous, metamorphic and volcanic rocks are expected to be the dominant lithologies in the source area. End member 3 appears to be derived from a mixed source area in which sedimentary, igneous and metamorphic rocks are present. The source area of end member 4 consists of various sedimentary parent lithologies; carbonates and siliciclastic rocks are expected to be the dominant lithologies in this area, whereas volcanites and metamorphites appear to be absent.

Table 3. Modelled end members of northern Adriatic beach sands (see also Fig. 8).

Grain types	EM 1 (%)	EM 2 (%)	EM 3 (%)	EM 4 (%)
Quartz	4.3	52.3	49.1	23.4
Feldspar	0.0	25.6	26.1	9.7
Volcanic lithics	0.0	11.3	0.4	0.0
Metamorphic lithics	1.3	2.3	4.1	0.0
Siliciclastic lithics	1.1	0.0	2.1	1.0
Sparite	38.2	2.6	11.8	25.0
Micrite	41.8	0.0	3.1	22.3
Bioclasts	0.0	4.5	3.3	14.4
Dolostone	10.7	0.0	0.0	0.2
Chert	2.5	1.4	0.0	4.0

8. Validation of modelling results

The mixing model would represent the final result of this study, if the sediments had been sampled in a fossil basin fill for which no additional information was available. In practice, even a limited amount of additional information can provide a considerable refinement of model interpretations. For instance, the spatial pattern of end-member contributions can be compared to isopach-maps, palaeocurrent measurements, and sedimentary facies associations, in order to judge whether the palaeogeographic locations of sediment sources predicted by the model conform to other lines of evidence. If the composition of the sand-sized portion of a basin fill accurately reflects its parent lithologies, the interpretation of end-member compositions can be strengthened by comparing the end members to synthetic mixtures of rocks from the hinterland, which may be present in the basin fill in the form of conglomerate clasts. If the data set consists of point-counting results, as in this case, compositions of possible source rocks could be quantified by point-counting of crushed conglomerate clasts. Ideally, synthetic mixtures of parent lithologies closely approximate the end-member compositions, allowing to estimate the contributions of each parent lithology to the size fraction studied.

For the Po-delta plain and adjacent coastal zones, a wealth of additional information is available for testing the model predictions. The results of three tests will be presented, each of which requires a higher level of *a priori* knowledge.

9. The first test: matching of possible source compositions

The modelling results can be examined in more detail by comparing the end members to the sediments supplied by the rivers debouching in this area. Gazzi et al. (1973) analyzed the compositions of possible source sediments, in order to unravel the dispersal pattern along the Adriatic shoreline. This second data set consists of 15 fluvial samples and 1 sample from the Miocene Marnoso-Arenacea Formation exposed along the Adriatic coast. An (16x10) array of "possible source compositions" was obtained by the same pre-processing steps used for the beach sands (Table 1). The sampling stations of these possible source compositions are depicted in Fig. 4 (samples marked by a suffix "F" or "P"). Unfortunately, only one sample is available from each possible source. It has been observed that fluvial sediments in this area display a considerable compositional variation (Jobstraibizer & Malesani, 1973; Gazzi et al., 1973), indicating that the source compositions are also subject to errors of sampling, measurement, and natural heterogeneity.

The model predictions were tested by expressing the possible source compositions in terms of non-negative mixtures of the end members calculated from the beach sands. In order to account for errors in all of the compositions used for this test, the end-member compositions were appended to the data set of source compositions. Subsequently, a second mixing model was constructed in which all source compositions were expressed as non-negative mixtures of the four modelled end members. The mixing proportions associated with each source composition express the similarity of each source assemblage to the modelled end members. Sources which display the strongest similarity to the modelled end members can be regarded as the most likely suppliers of sediment to beaches in which the modelled contributions of these end members is largest. The calculated similarities have been plotted against the approximate river-mouth locations in Fig. 9.

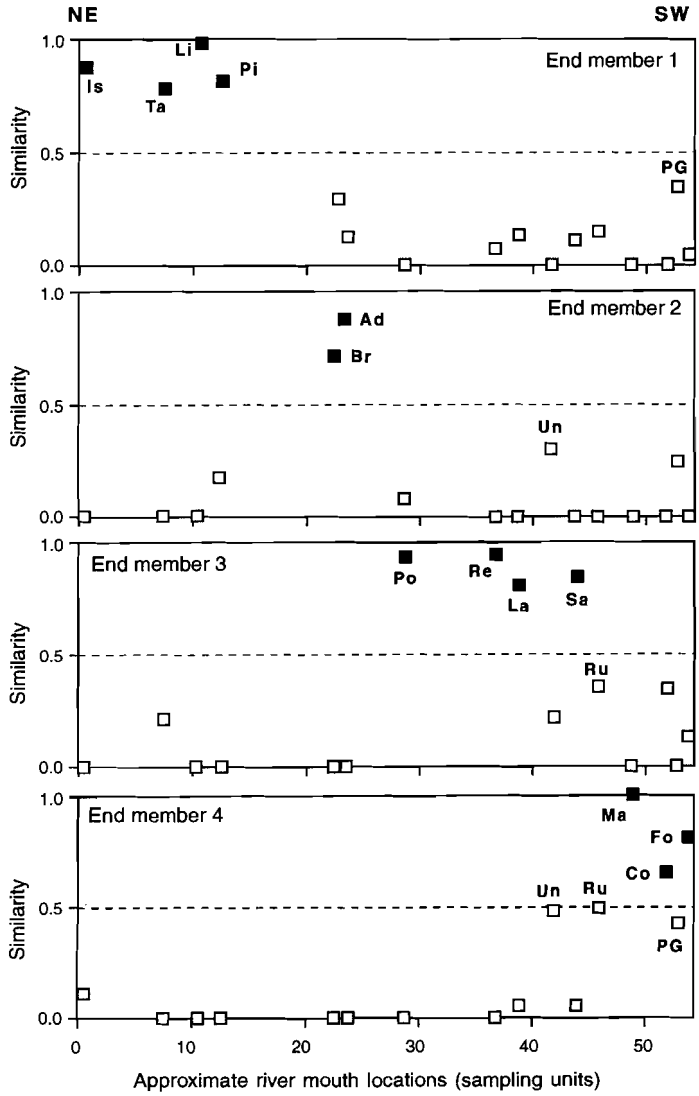

Figure 9. Similarity of candidate "source assemblages" to modelled end members. PG = Punta Gabicce; abbreviations of fluvial systems are given in Table 4.

Fig. 9 shows that end member 1 is most similar to sediments of the Isonzo, Tagliamento, Livenza, and Piave rivers, which debouch in the northeastern part of the study area (province A). End member 2 closely resembles sediments of the Brenta and Adige rivers. Coastal province B coincides with the locations of the river mouths. End member 3 displays a strong affinity with sediments supplied by the Po, Reno, Lamone, and Savio rivers. The geographical extent of province C also corresponds to the locations of these river mouths. End member 4 closely resembles sediments of the Marecchia, Conca and Foglia rivers, which contribute sediments to beaches of province D.

A number of sediment sources in the transitional area between provinces C and D are more difficult to classify in terms of compositional similarity to a particular end member. These are the Uniti and Rubicone rivers, and the sandstone cliffs of Punta Gabicce, in which the Marnoso-Arenacea Formation is exposed. Sediments supplied by these sources can be interpreted as mixtures of end members 3 and 4, with smaller amounts of end members 1 and/or 2. Contributions of sediments from these sources could at least partly explain the complicated pattern of mixing observed in the transition zone of provinces C and D.

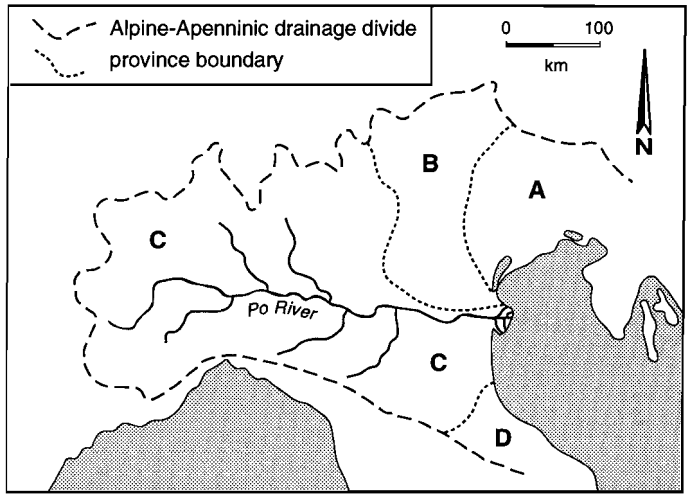

Figure 10. The four "sedimentary-petrological provinces" (cf. Edelman, 1933) recognized on the basis of the modelling results.

The overall spatial coherence of probable sediment sources and their corresponding sedimentary petrological provinces convincingly demonstrates the general validity of the model predictions. The beach sands closely resemble the compositions of their fluvial sources, indicating that compositional modifications due to physical and chemical processes (i.e., selective transport, mechanical and chemical weathering) are of minor importance. Furthermore, longshore dispersal of beach sands appears to be of limited extent, in view of the lack of offset between locations of river mouths and their corresponding sedimentary petrological provinces. The only clear evidence of net longshore dispersal is provided by the sediments of province A, which extend far southwestward of their nearest likely source. The drainage basins which provided the beach sands of the four sedimentary-petrological provinces are displayed in Fig. 10.

10. The second test: matching of predicted fluvial input

A compilation of physiographic data on the fluvial drainage systems is presented in Table 4. The Po river is by far the largest river in terms of drainage basin area, discharge, and sediment load. Second largest (but an order of magnitude smaller than the Po) is the Adige river. Together, these two rivers account for one third of the total freshwater input into the Adriatic Sea (Pettine et al., 1985). The other rivers are far less important in terms of liquid discharge and sediment load. They supply comparable amounts of sediment to the Adriatic

Table 4. Physiographic characteristics of fluvial systems, based on various sources.

Fluvial systems	(Abbr.)	Basin area (10^3 km^2)	Mean annual discharge (m^3 s^{-1})	Solid load (10^6t yr^{-1})
Isonzo	Is			
Tagliamento	Ta			
Livenza	Li	1.0 - 2.0 (*)	80 - 100 (*)	< 1.0 (*)
Piave	Pi			
Brenta	Br			
Adige	Ad	12.2	220	1.0
Po	Po	63.6	1500	14.0
Reno	Re	3.8	80 (?)	2.0 (?)
Lamone	La			
Uniti	Un			
Savio	Sa			
Rubicone	Ru	0.5 - 1.5 (*)	50 - 80 (*)	< 1.0 (*)
Marecchia	Ma			
Conca	Co			
Foglia	Fo			

(*) estimated mean for rivers in this group
(?) values based on single reference only

References: Nelson, 1970; CNR, 1976; Hendershott & Rizzoli, 1976; Brambati et al., 1977; Bondesan et al., 1978; Catani et al., 1978; Dal Cin, 1983; Bortoluzzi et al., 1984; Pettine et al., 1985; Milliman & Syvitsky, 1992.

beaches, except for the Reno river (Milliman & Syvitsky, 1992), which carries an unusually large solid load with respect to the other smaller rivers in this area. The physiographic data in Table 4 have been combined with the results of the first matching exercise, in order to predict a "weighted average" composition of sediment supplied by each source area to its corresponding province. This test is much more straightforward than the first, because the source assemblages are not forced to conform to a predefined set of compositions, such as the modelled end members. Instead, fluvial source assemblages and physiographic data are combined to arrive at an independent prediction of sediment composition. Proportional contributions of individual rivers of each province were estimated on the basis of drainage area, discharge, and solid load. These estimates are based on averaged parameter values reported by various authors, and reflect the present conditions of rivers debouching in this area. Three source assemblages were excluded from this test on account of their lack of affinity to a particular end member (Uniti and Rubicone rivers, and the sandstone cliffs of Punta Gabicce). The estimated weights (mixing proportions) and the compositions of the synthetic river mixtures are depicted in Table 5 and Fig. 11, respectively.

Fig. 11 shows that end member 1 is reasonably well approximated by a synthetic mixture of fluvial sands from province A, although the former contains more sparite and less chert than the latter. End members 3 and 4 are very well approximated by synthetic mixtures of sands from provinces C and D, respectively. In view of possible errors in the source

Table 5. Estimated synthetic mixtures of fluvial sands delivered to the northern Adriatic coast. Weights based on physiographic data of Table 4.

Fluvial systems	Mixture 1	Mixture 2	Mixture 3	Mixture 4	Mixture 2A
Isonzo	0.25				
Tagliamento	0.25				
Livenza	0.25				
Piave	0.25				
Brenta		0.25			0.25
Adige		0.75			0.50
Po			0.65		0.25
Reno			0.15		
Lamone			0.10		
Savio			0.10		
Marecchia				0.33	
Conca				0.33	
Foglia				0.33	

compositions, it is concluded that end members 1, 3, and 4 accurately reflect the compositions of sands supplied by the Dolomites, the Po river basin, and the Northern Apennines, respectively.

End member 2 is poorly approximated by a synthetic mixture of Adige and Brenta sands. The lack of fit of end member 2 to the synthetic Adige-Brenta mixture points to a discrepancy between model predictions and the "actual" situation. Fig. 6 shows that the modelled volcanic lithics content of beach sands between stations 21 and 25 is systematically lower than the observed content in province B. This strongly suggests that beach sand compositions in province B are not well approximated by the mixing model. Furthermore, the angular deviations of beach sands in province B are systematically larger in the final model than in the original four-dimensional approximation of the data. A synthetic mixture to which Po sand has been added shows a much better resemblance to end member 2, indicating that end member 2 can be loosely interpreted as a mixture of sands supplied by the Brenta-Adige rivers and the Po river basin. The modelled composition of end member 2 is not sufficiently extreme for an adequate approximation of the volcanic lithics content in beach sands of province B, implying that compositional differences between Po-type sediments (similar to end member 3) and Adige-Brenta-type sediments (similar to end member 2) have been underestimated by the model.

The lack of fit of end member 2 can be attributed to the fact that Adige-Brenta input is well represented in only 5 out of 53 observations. The iterative algorithm, which produces conservative end-member estimates based on the collective properties of the data set, did not increase the size of the mixing space sufficiently to construct an end-member composition that encloses all of the observations from province B. This implies that the "true" contributions of Adige-Brenta sands to the coastal sands in the other provinces are lower than the modelled contributions of end member 2. The lack of fit of end member 2 illustrates a possible disadvantage of the robust estimation procedure employed by the end-member modelling algorithm. However, the conservative estimation procedure guarantees

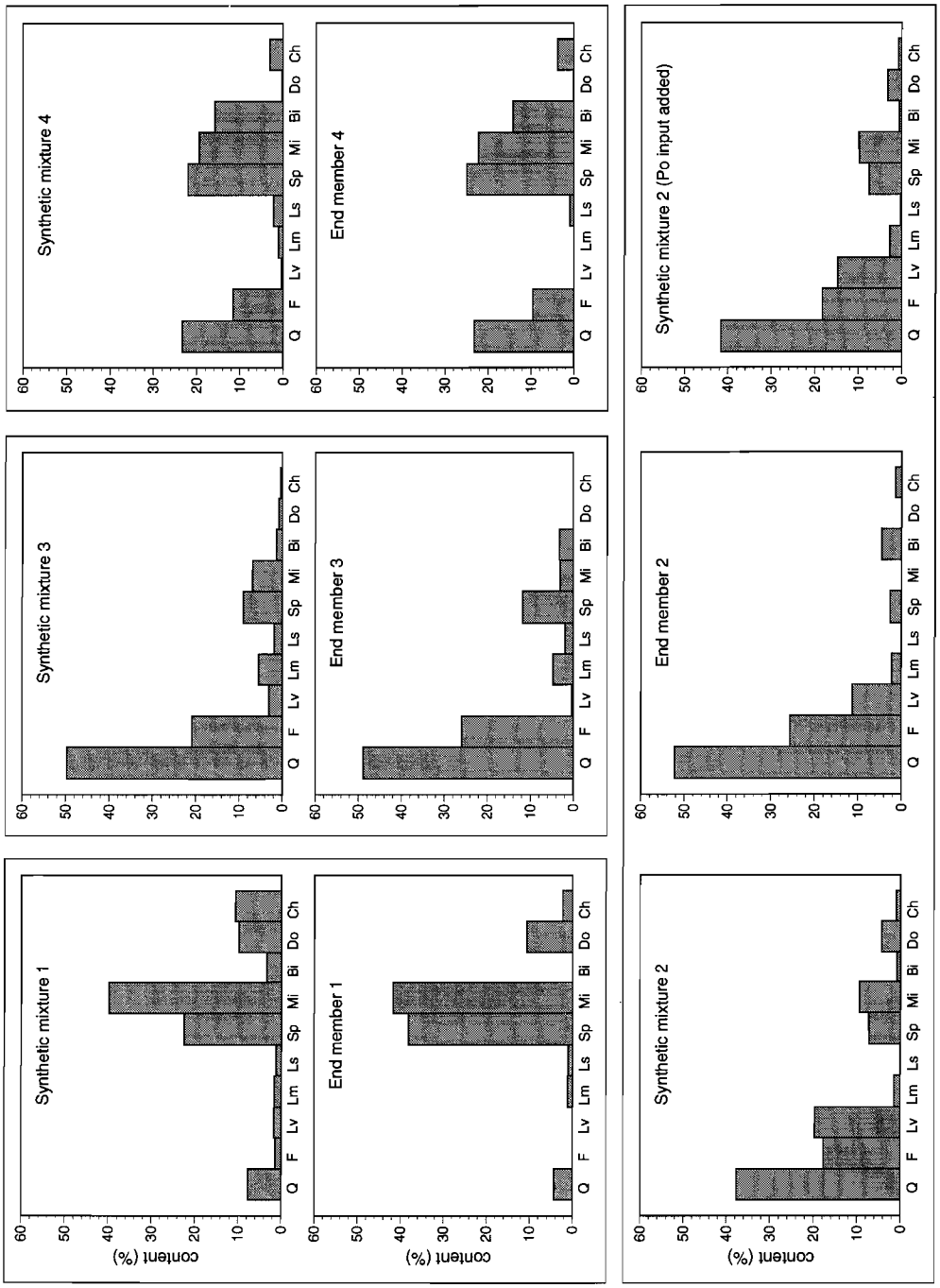

Figure 11. Synthetic "weighted mean" compositions of sediments supplied by each of the provinces to the northern Adriatic coast (lack of fit of end member 2 is discussed in text).

the geological reasonableness of hypothetical end member compositions, as shown above. In the absence of *a priori* knowledge of the area under study, conservative estimates are preferred over more extreme end-member estimates. Extreme end-member estimates improve the overall fit of the model to the data, but may not be interpretable in geological terms.

11. Late Holocene evolution and present situation

Spatial mixing patterns of sands along wave-dominated coasts are the result of multiple cycles of erosion, transport, and deposition. The modelled mixing patterns thus represents the cumulative effects of long-term sediment transport. In comparison to the time scale of these processes, present physiographic characteristics of drainage basins, locations of river mouths, fluvial sediment compositions, and recent littoral drift patterns can be regarded as "snap shots". Discrepancies between long-term dispersal patterns and "snap shots" of the present situation in the study area could be due to recent anthropogenically induced environmental changes in this densely populated region.

The Holocene evolution of the Po basin has been reconstructed in great detail (Pigorini, 1968; Nelson, 1970; Van Straaten, 1970; Rizzini, 1974; Colantoni et al., 1979; Gandolfi et al., 1982; Dal Cin, 1983), enabling a comparison of modelling results with the past 3000 years of coastal evolution. The late Holocene evolution of the Po basin is characterized by progradation of the shoreline, which started around 3000 yr BP and has continued up to recent times (Fig. 12). The presently widespread erosion of Northern Adriatic beaches is ascribed to a profound anthropogenically induced decrease of fluvial bedload (CNR, 1976; Bondesan et al., 1978; Brambati et al., 1978; Dal Cin, 1983). Widespread coastal retreat confirms the idea that model predictions could partly reflect ancient compositional signals, due to reworking of older deposits. Historical records of coastal plain evolution and present sedimentological research shed more light on the origin of deposits currently subject to reworking along the Northern Adriatic coast.

From the Roman age to 1200 AD, the most important branches of the Po were located south of the present delta. The Po of Ferrara consisted of two main distributaries: the Po di Volano and the Po di Primaro (the present Reno river), which built cuspate deltas (Fig. 12; Nelson, 1970; Gandolfi et al., 1982). In the same period, the mouth of the Adige river shifted southward to its present position. Detailed petrographical studies have shown that southward dispersal of Adige and Po sands was much more extensive than it is at present (Rizzini, 1974; Gandolfi et al., 1982). Around 1200 AD, a natural diversion occurred at Ficarolo, which resulted in an abrupt northward shift of the Po mainstem. Discharge of the southerly Po di Ferrara branches decreased, and a new cuspate delta developed just north of the present Po delta, close to the mouth of the Adige river (Nelson, 1970; Gandolfi et al., 1982). This delta was built by two distributaries: the Po di Tramontana and Po di Levante (Fig. 12). It also received sediment from minor distributaries of the Adige River (Dal Cin, 1983). Around 1600 AD, the rapid growth of this delta threatened to block the ports of the Venetian Republic with silt, and a diversionary canal was dug at Porto Viro to correct this situation. From this time onward, the evolution of the Po delta has been largely controlled by human activity. In the second half of the 18th century, the largely inactive Po di Primaro branch was connected with the drainage basin of the Reno River (Bondesan et al., 1978). The rapid advancement of the modern lobate Po delta in the past 400 years is

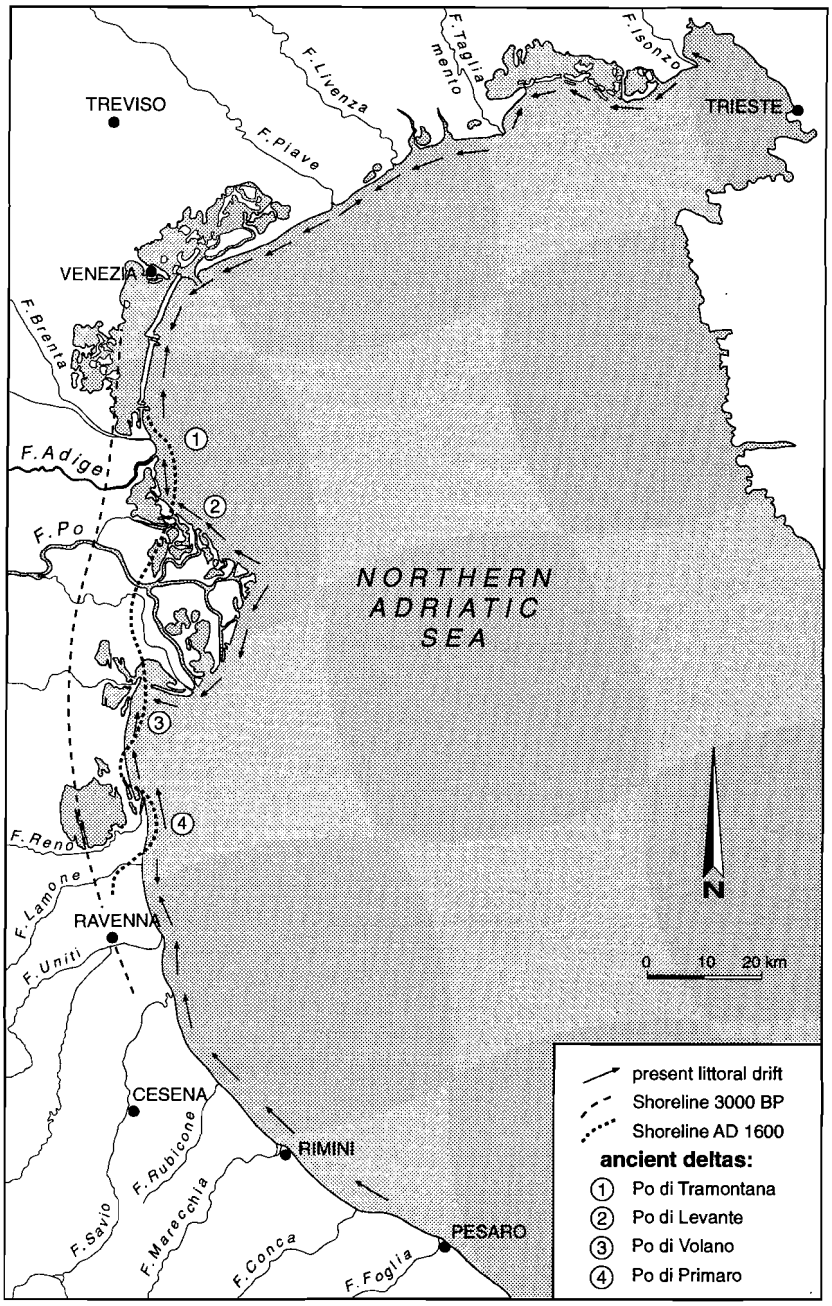

Figure 12. Present littoral drift (after Bondesan et al., 1978; Brambati et al., 1978; Dal Cin, 1983), and historical data (after Nelson, 1970; Colantoni et al., 1979; Gandolfi et al., 1982).

attributable to deforestation of the drainage basin, the construction of artificial levees, and the confinement of its deposits to a small area (Nelson, 1970; Dal Cin, 1983).

The present situation of the Northern Adriatic coastal zone can be summarized as follows. In the northern part of the area, erosion balances accretion, and longshore dispersal of sands is mainly to the west-southwest (Brambati, 1970; Brambati et al., 1977, 1978; Gandolfi et al., 1978a). The beaches near the Brenta and Adige rivers, just north of the Po delta, are presently subject to erosion (CNR, 1976). Beach sands in the area between the Po delta and the mouth of the Adige River are derived from reworked ancient sediments, and do not reflect recent input of the Adige River (Dal Cin, 1983). The pronounced seaward extension of the modern lobate delta effectively precludes southward dispersal of sediments from province B (Gandolfi et al., 1982). The Po delta, which has prograded rapidly in the past four hundred years due to human intervention, is currently retreating in many areas, and regaining its original cuspate morphology. Sands are dispersed from the main river mouth towards the northwest and southwest by divergent longshore transport (Dal Cin, 1983). The area south of the Po delta is characterized by northward littoral drift. Erosion prevails over accretion (Gazzi et al., 1973; Rizzini, 1974; Dal Cin, 1983). Detailed studies in this area indicate that coastal erosion is especially prominent in the area around the river mouths of the Reno and Savio rivers. Beach accretion occurs in the area just south of the present Po delta, due to the northward dispersal of reworked sands of the Reno mouth (Bondesan et al., 1978). The present regional dispersal patterns converge in the areas directly north and south of the Po delta (Fig. 12; Gazzi et al., 1973).

12. The third test: historical evolution and present conditions

How do the historical evolution and recent dispersal patterns fit the modelling results? This is most conveniently discussed for each end member (and its corresponding province) separately.

End member 1 can be reasonably well approximated by a synthetic mixture of fluvial sediments supplied by the hinterland of province A. This province extends beyond the lagoon of Venice up to the Brenta river mouth, indicating that west-southwestward dispersal prevails in this area. The predicted longshore dispersal is confirmed by sedimentological observations (Brambati, 1970; Brambati et al., 1977, 1978; Catani et al., 1978; Gandolfi et al., 1978a). Local contributions of end member 4 to beaches in province A reflects the compositional similarity of certain fluvial sources (Tagliamento and Piave rivers) to sediments derived from the Northern Apennines, which cannot be resolved on this scale. In conclusion, there are no discrepancies between model predictions and other lines of argument.

The second validation test showed that end member 2 cannot be satisfactorily approximated by a synthetic mixture of Brenta and Adige sands. The addition of Po sands improves the goodness of fit to a considerable extent, indicating that modelled composition of end member 2 is not sufficiently extreme to provide an accurate approximation of Adige-Brenta input. Consequently, the contribution of end member 2 to beach sands of provinces C and D, which suggests a southward dispersal of Adige-Brenta sands, must be regarded as a modelling artifact. Sedimentological data indicate a northward littoral drift in the northern part of province B, whereas bidirectional transport characterizes the southern part of this province (CNR, 1976; Dal Cin, 1983). Beach sands in the southern part of province B are inferred to have been derived from reworking of the ancient Po di Tramontana delta (Dal Cin, 1983). Because this delta was fed by the Po and Adige rivers, the composition of

beach sands in the southern part of province B cannot be considered as conclusive evidence for southeastward dispersal of Adige sands, as suggested by Gazzi et al. (1973) and Gandolfi et al. (1978b).

End member 3 can be well approximated by a synthetic mixture of Po sands and minor amounts of Reno, Lamone, and Savio sands. There is little doubt that the sands of the present Po-delta, which forms the northern part of province C, have been supplied by the Po. In fact, it can be assumed that virtually all of the sand carried by the Po branches in the past 400 years has contributed to the construction of the modern lobate delta (Gazzi et al., 1973; Dal Cin, 1983). A northward littoral drift is present in the area south of the Po delta (Rizzini, 1974; Bondesan et al., 1978; Dal Cin, 1983), implying that the Po river is an unlikely source of beach sands in this area. The origin of Po-type sands in the southern part of province C must be largely attributed to reworking of ancient Po di Primaro deposits. The ancient Po di Primaro delta corresponds to the present Reno river mouth, which is presently subject to erosion (Bondesan et al., 1978). Coastal progradation in the area of the former Po di Volano delta, further to the north (Fig. 12), reflects the northward littoral drift of these reworked Po deposits (Bondesan et al., 1978). It seems likely that the beaches in the southern part of province C have also been fed by sands of the Lamone and Savio rivers, that are compositionally similar to end member 3. A contribution of reworked Savio sands to the beaches of province C is strongly suggested by sedimentological and historical data, which indicate erosion in front of the river mouth (Bondesan et al., 1978). In conclusion, there is no evidence for a southward dispersal of sediments in province C, as suggested by the modelling results. The alongshore variations of end member contributions in the southern part of province C merely reflects the reworking of ancient Po-type sands.

End member 4 closely fits the synthetic mixture of Marecchia, Conca, and Foglia sands, indicating that beach sands of province D have been supplied by recycling of sedimentary rocks of the Northern Apennines. The beach sands near Rimini (stations 47 to 49) show a distinct affinity with end member 1 (Fig. 7). This affinity has been attributed to a local supply of sands from the Marecchia river, which contain a large proportion of carbonate (Gazzi et al., 1973). Detailed heavy-mineral studies of Holocene beaches located between stations 47 and 51 (Rizzini, 1974) strongly suggest that a considerable proportion of sands in this area is derived from reworking of relict shelf sands, which were transported towards the shoreline during the Holocene sea-level rise. These relict shelf sands were supplied by the Po River during the previous Pleistocene lowstand, when the entire Northern Adriatic shelf had become an extensive alluvial plain (Pigorini, 1968; Van Straaten, 1970; Colantoni et al., 1979). The Po-signature does not clearly show up in the modelling results, although contributions of end member 3 to the beaches between stations 50 and 51 indeed show a small peak (Fig. 7). Northward longshore dispersal is of limited extent in the southern part of province D. Model predictions closely match the actual situation.

13. Comparison with plate-tectonic provenance models

In order to compare the results of the provenance modelling experiment with the plate-tectonic provenance models developed by Dickinson and co-workers (summarized by Dickinson, 1985, 1988), the four end-member compositions and the mean composition of the Adriatic beach sands have been plotted in the QtFL and QmFLt diagrams of Dickinson (1985). In the terminology of Ingersoll (1990), the end-member compositions and the

averaged composition would have to be regarded as "second-order" and "third-order" compositions, respectively. The grain types used in the modelling experiment were amalgamated to provide a reduced set of variables in agreement with the Dickinson (1985) conventions (see Table 6). The proportions of monocrystalline and polycrystalline quartz have not been recorded separately by Gazzi et al. (1973). For lack of a better alternative, all quartz has been classified as monocrystalline. The Adriatic beach sands contain an appreciable proportion of extrabasinal carbonate grains (detrital limeclasts), which are commonly ignored on account of their susceptibility to weathering and diagenesis (Dickinson, 1985). However, Mack (1984) and Zuffa (1980, 1987) have shown that such extrabasinal grains may help to clarify provenance relationships in certain cases.

The "third-order" provenance fields of Dickinson (1985) are shown in Fig. 13. The compositions obtained by excluding the extrabasinal carbonate grains from the modelling results are depicted on the left-hand side of Fig. 13. The total lithic population has been employed for the construction of provenance diagrams on the right-hand side of this figure. The actual plate-tectonic provenance types (*sensu* Dickinson, 1985) and source-area characteristics of the four end-member assemblages have been summarized in Table 7. This Table also shows the extent to which the ternary provenance diagrams of Dickinson (1985) are capable of recognizing the plate-tectonic setting of the four end-member assemblages.

Table 6. Simplification of modelled end-member compositions for display in ternary provenance diagrams of Dickinson (1985).

Amalgamation of variables for plate-tectonic provenance classification		
Original variables:	New variables:	Labels:
Extrabasinal limeclasts	Sp + Mi + Bi + Do	Lc
Total non-quartzose lithics	Lv + Lm + Ls	L
Total non-carbonate lithics	Lv + Lm + Ls + Ch	Lt
"Monocrystalline" quartz	Q	Qm
Total quartzose grains	Q + Ch	Qt

The QtFL diagram correctly identifies the "recycled orogen" provenance of end members 1, 2, and 3. End member 4 contains too few non-quartzose lithics (L) to be classified correctly: the sedimentary parentage of Northern Apenninic input is not recognized (although the location of end member 4 is very close to the "recycled orogenic" field). Adding the carbonate lithics (Lc) to non-quartzose lithics (L) produces a catastrophic misinterpretation of end members 1 and 4, and the "third-order" composition. The QtFL diagram is unable to cope with extrabasinal limeclasts, due to the fact that all lithic sands containing small proportions of quartz and feldspar are classified as "magmatic arc" sediments. In this case, the use of QmFLt diagrams requires the assumption that all quartz is monocrystalline; the locations of data points in the QmFLt diagram are therefore not very reliable. Apart from end member 2 and the mean composition of the data set, none of the other compositions are correctly classified in this diagram. In view of the high abundance of carbonate lithics, possible errors resulting from the assumption that all quartz is

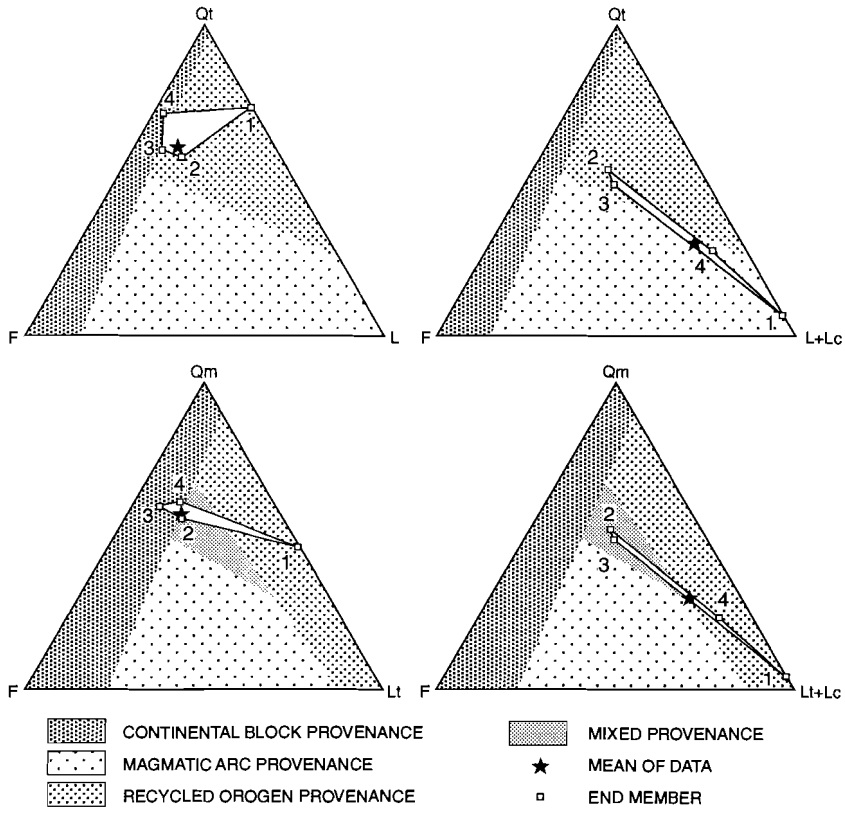

Figure 13. Ternary provenance diagrams (cf. Dickinson, 1985), showing predictive region of second-order provenance types for Adriatic beach sands. See text for discussion.

monocrystalline are of minor importance for the location of data points in the QmFLt+Lc diagram. The second-order parentage of all end members is correctly identified by the QmFLt+Lc diagram. The mean composition of the Northern Adriatic beach sands is also satisfactorily classified.

Predictive regions of compositional variation have been constructed by connecting the end members plotted in the ternary diagrams by a set of lines (Fig. 13). This predictive region represents the projection of the three dimensional mixing space (a tetrahedron in compositional space) onto the constant sum plane of the ternary diagram. The average composition of any sand suite from one of the second-order drainage basins or the local beaches in the study area should plot in this predictive region, provided that the lower-order parentage has been accurately reconstructed. This approach potentially eliminates the scale problem in current provenance models and simultaneously improves the resolution of the model, by enabling a comparison of "second-order" and "third-order" provenance. Furthermore, the predictive region constructed from the inverse modelling results is superior to the polygonal field of "dispersion" or "variation" commonly employed in sedimentary provenance studies, whose physical and statistical meaning is obscure (Philip et al., 1987).

Table 7. Summary of actual source-area characteristics and empirical classification of provenance types according to the ternary provenance diagrams of Dickinson (1985).

End member (province)	1 (A)	2 (B)	3 (C)	4 (D)	mean
Source area	S. Alps	S. Alps E. Alps	E. Alps W. Alps N. Apennines	N. Apennines	Alps Apennines
Dominant parent lithologies	sedimentary (carbonate)	sedimentary igneous metamorphic	sedimentary igneous metamorphic	sedimentary (siliciclastic)	sedimentary igneous metamorphic
Provenance type (Dickinson, 1985)	recycled (lithic)	recycled or mixed	recycled or mixed	recycled (transitional)	recycled or mixed
QtFL	+	+	+/-	-	+
QtFL+Lc	-	+	+	-	-
QmFLt	+/-	+	-	+/-	+/-
QmFLt+Lc	+	+	+	+	+

End-member classification according to ternary plate-tectonic provenance diagrams of Dickinson (1985):

+ = correct; - = incorrect; +/- = "nearly" correct.

14. Discussion and conclusions

The comparison of model predictions and the "actual" situation indicates that the performance of the end-member modelling algorithm is quite satisfactory. Three out of four modelled end members closely approximate the compositions of sediments shed by the major source areas of the beaches studied. A fourth end member displays a clear affinity to its "actual" source composition. The compositional signature of this end member appears to have been underestimated by the robust estimation procedure, on account of its small overall contribution to the data set. In spite of the lack of fit, its composition is geologically reasonable. On the scale of this regional survey, small colinear sediment sources can be detected (e.g., the Marecchia River in province D), but their contributions cannot be resolved. The modelled alongshore variation of beach sands, expressed as proportional end-member contributions, is in general agreement with present dispersal patterns and historical records of the area. A detailed analysis of historical records and present littoral drift shows that the overall southwest to southward dispersal suggested by the modelling results must be attributed to shifting of Po distributaries in historical times. Recycling of these ancient Po sediments is related to the present decrease of fluvial sediment supply, and the widespread coastal retreat in the area studied.

The results of the validation tests demonstrate that compositional variation of the Northern Adriatic beach sands can be adequately represented by a linear mixing model, in spite of the fact that sands along this wave-dominated coast consist predominantly of chemically and mechanically unstable grains, that are highly susceptible to selective destruction.

Mechanical destruction and/or chemical weathering of coastal sands have not noticably affected the modelling results. A reason for the apparent lack of compositional modification is the high rate of sediment supply which prevailed during the late Holocene in this area. The generally high rate of Holocene coastal progradation indicates that the average sand grain spends only a brief interval of time in transport before it is deposited and buried. However, these conditions have changed drastically in the recent past, as a result of human activity.

The present beach sand compositions provide a time-averaged signal of late Holocene sediment dispersal, because ancient sands are being eroded and re-introduced into the dispersal system. The temporal resolution appears to be of the order of hundreds to thousands of years, reflecting the balance between overall coastal progradation and retrogradation. This balance, in turn, is determined by the interplay of local sediment supply and baselevel variations. Dispersal patterns can only be studied because the temporal resolution of provenance signals is (at least) an order of magnitude lower. Highest recorded frequencies of provenance signals in fossil sands are of the order of 20 to 25 kyr (Weltje & De Boer, 1993). On average, compositional signatures of fluvial sediments supplied by "first" and "second" order drainage basins are inferred to be stable over much longer intervals (Velbel & Saad, 1991).

Many (if not all) sedimentary basin fills are mixtures of sediments supplied by different sources. This applies to spatial variation within a given time-slice, but it can also apply to temporal compositional variation of sediments supplied by a single source area. A method for apportioning mixtures to their respective sources is a prerequisite for the unravelling of complex patterns of provenance and dispersal. A simple graphical representation of the mixing model in the plate-tectonic provenance diagrams clearly demonstrates the usefulness of this approach to the analysis of compositional variation. The general solution to the mixing problem in sedimentary provenance studies provides a major step forward towards successful mass-balancing and three-dimensional forward modelling of sedimentary basin fills (e.g., Leeder, 1991). Although the inversion algorithm is a powerful tool for unravelling complex patterns of compositional variation, it cannot provide an "explanation" of the observed patterns of compositional heterogeneity. The mixing model merely represents the output of a complicated data manipulation procedure. It can only be judged by the modeller if the estimated mixing parameters are also geologically feasible.

Acknowledgements

Critical reviews and positive suggestions by P.L. de Boer, S.B. Kroonenberg, N. Molenaar and G. Postma are gratefully acknowledged.

Basin Research (1992) **4**, 37–68

Oligocene to Early Miocene sedimentation and tectonics in the southern part of the Calabrian-Peloritan Arc (Aspromonte, southern Italy): a record of mixed-mode piggy-back basin evolution

GertJan Weltje

Comparative Sedimentology Division, Institute of Earth Sciences, University of Utrecht, PO Box 80021, NL 3508 TA Utrecht, The Netherlands

ABSTRACT

The Calabrian–Peloritan Arc (southern Italy) represents a fragment of the European margin, thrusted onto the Apennines and Maghrebides during the Europe–Apulia collision in the late Early Miocene. A reconstruction of the pre-Middle Miocene tectono-sedimentary evolution of the southern part of the Calabrian–Peloritan Arc (CPA) is presented, based on a detailed analysis of the Stilo–Capo d'Orlando Formation (SCO Fm). Deposition of the SCO Fm occurred in a series of mixed-mode piggy-back basins. Basin evolution was controlled by two intersecting fault systems. A NW–SE oriented system delimited a series of sub-basins and fixed the position of feeder channels and submarine canyons, whereas a NE–SW oriented system controlled the axial dispersal of coarse-grained sediments within each of the sub-basins. From base to top, sedimentary environments change from terrestrial and lagoonal to upper bathyal over a timespan of approximately 12 Myr (late Early Oligocene–late Early Miocene). During this interval, extensional tectonic activity alternated with oblique backthrusting events, related to dextral transpression along the NW–SE oriented faults. This produced a characteristic pulsating pattern of basin evolution.

Oligocene–Early Miocene evolution of the W. Mediterranean basin was dominated by 'roll back' of the Neotethyan oceanic lithosphere. Considerable extension in the overriding European Plate gave rise to the formation of a back arc-thrust system. The initial stages of Calabrian Basin evolution are remarkably similar to the evolution of rift basins in the back arc (Sardinia). The Calabrian basins, which are inferred to have originated as thin-skinned pull-apart basins, were subsequently incorporated into the Apennines–Maghrebides accretionary wedge by out-of-sequence thrusting, and became decoupled from the back arc. Periodic restabilization of the accretionary wedge, resulting in an alternation of backthrusting and listric normal faulting, provides an explanation for the structural evolution of these mixed-mode basins. The basins of the southern part of the CPA may be termed 'spanner' or 'looper' basins, in view of their characteristic pulsating structural evolution, superimposed upon their migration toward the foreland. This new term adequately accounts for the occurrence of tectonic inversions in long-lived piggy-back basins, as expected in the light of the dynamics of accretionary wedges.

1 INTRODUCTION

The Calabrian–Peloritan Arc (CPA) is a curved segment of the W. Mediterranean composite orogenic system, which includes the Italian mainland (Apennines) and northern Africa (Maghrebides). The CPA forms the highest tectonic element of this composite system and overlies Apenninic and Maghrebide units along two NW–SE trending oblique thrust zones: the Taormina Line in the SW, and the Pollino Line in the NE (Amodio-Morelli *et al.* 1976; Colella, 1988; Van Dijk & Okkes 1991; Fig. 1). The basement nappes of the CPA, consisting of Palaeozoic continental plutonic and metamorphic rocks, represent a fragment of the European–Iberian continental margin (Ogniben 1973; Bouillin 1984; Knott 1987) which has moved SE-ward to its present position as a result of NW-ward subduction of oceanic (Neotethyan) and continental (Apulian) lithosphere below the Iberian–European Plate.

The Calabrian basement units are quite distinct from the Apenninic and Maghrebide thrust sheets, which consist of ophiolites and Meso-Cenozoic sedimentary rocks, derived from the descending African plate. The Calabrian

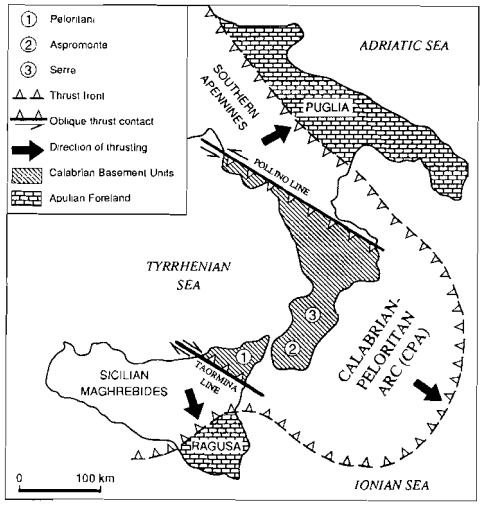

Fig. 1 The Apennines–Maghrebides thrust belts and the Calabrian–Peloritan Arc (CPA). The CPA overlies the Southern Apennines and Sicilian Maghrebides along two oblique thrust zones, the Pollino and Taormina Lines, respectively (modified after Amodio-Morelli *et al.* 1976; Colella 1988; Van Dijk & Okkes 1991).

basement complex was accreted to the Apennines–Maghrebides orogenic system during the Late Early Miocene, when the closure of Neo-Tethys had been completed, and continental collision with the African (Apulian) margin took place (Knott 1987; Roure *et al.* 1990, 1991; Wezel 1974). Two stages can be distinguished in the Cenozoic history of the CPA: The first, pre-Middle Miocene stage is related to the subduction of Neotethyan oceanic lithosphere and opening of the Ligurian–Provencal back arc basin (Rehault *et al.* 1985; Dercourt *et al.* 1986; Knott 1987). The second, post-Early Miocene stage is related to Neogene subduction of Apulian continental lithosphere in the Apennines and Maghrebides, and opening of the Tyrrhenian back arc basin (Rehault, Moussat & Fabbri 1987; Kastens *et al.* 1988; Roure *et al.* 1990, 1991).

2 PURPOSE OF THIS STUDY

The post-Early Miocene tectonic and sedimentary evolution of the CPA have been relatively well studied (e.g. Ghisetti & Vezzani 1981, 1982; Barrier 1986; Moussat *et al.* 1986; Meulenkamp, Hilgen & Voogt 1986; Van Dijk 1991; Van Dijk & Okkes 1991), but there are still many open questions regarding the Early Cenozoic geological history. For this reason, the pre-Middle Miocene record of the CPA has, as yet, not contributed much to existing kinematic and/or geodynamic reconstructions of the early stages of Apenninic–Maghrebide evolution. In an attempt to bridge this gap, a detailed study of the Stilo–Capo d'Orlando Formation of the southern part of the CPA was undertaken. The main results of this study are given here for three purposes: The first is to depict the pre-Middle Miocene 'mixed-mode' piggy-back basin evolution in the southern part of the CPA, based on sedimentological, stratigraphical, and structural data, collected between 1985 and 1989 in the Aspromonte area, and supplemented with palynological analyses. The second is to discuss the tectonic and sedimentary history of the southern part of the CPA in the light of current ideas on the evolution of the W. Mediterranean back arc-thrust system. The third is to propose a new concept of piggy-back basin evolution within the framework of the dynamics of accretionary wedges.

3 PRE-MIDDLE MIOCENE PALAEOGEOGRAPHICAL FRAMEWORK

Up to the Late Early Oligocene (Fig. 2a) Calabria was part of the European–Iberian continental margin, together with the present Sardinian and Corsican 'blocks' (Boccaletti *et al.*, 1990; Bouillin 1984; Bouillin, Durand-Delga & Oliver 1986; Courme & Mascle 1988; Dercourt *et al.* 1986; Dewey *et al.* 1989; Rehault, Mascle & Boillot 1984; Rehault, Boillot & Mauffret 1985). Along the SE margin of the European–Iberian Plate, an accretionary wedge had been active from the Late Cretaceous onward. It was formed by the NW-ward subduction of Neotethyan oceanic lithosphere below the European–Iberian Plate (Bouillin 1984; Knott 1987; Dewey *et al.* 1989).

Rifting and formation of the Ligurian–Provencal basin started around 30 Ma, in the Late Early Oligocene (Cherchi & Montadert 1982a,b; Rehault *et al.* 1985). Numerous Oligo-Miocene NE–SW oriented rift basins have been described from S. France, the Balearic Islands and Sardinia (Rehault *et al.* 1985, and references therein). The history of one of these basins, the Sardinian Rift, has been well documented on the basis of sedimentological and biostratigraphical studies, and radiometric datings of intercalated volcanites (Pecorino & Pomesano Cherchi 1969; Cherchi 1974; Cherchi & Montadert 1982a,b; Cherchi & Trémolières 1984; Fig. 27). Formation of oceanic crust in the Ligurian–Provencal back arc basin took place between 23 Ma and 19 Ma (Burrus 1984). It involved an about 30° counterclockwise rotation of the Sardinia–Corsica–Calabria 'block', between 20.5 Ma and 19 Ma (Montigny *et al.* 1981). This rotation was accompanied by dextral strike-slip along a series of NW–SE oriented faults in the Ligurian–Provencal Basin (Rehault *et al.* 1985; Fig. 2b).

The rate of Africa–Eurasia convergence was approximately 1 cm yr^{-1} in the Oligocene–Early Miocene interval, whereas the rate of oceanic spreading in the Ligurian–Provencal Basin, which must have been approximately equal to the rate of outward migration of the Apennines–Maghrebides orogenic front, is estimated to have been 4–5 cm yr^{-1} (Dercourt *et al.* 1986). At least half of the effective convergence (i.e. the local rate of subduction in

front of the CPA) can be attributed to extension in the overriding European–Iberian Plate (De Jonge & Wortel 1990). The difference between the local rate of subduction in the Apennines–Maghrebides foredeep, and the rate of convergence of the African and European plates points to the importance of 'roll back', i.e. the downward motion of the subducted lithospheric slab due to gravitational forces, leading to an oceanward migration of the trench (Dewey 1980; Le Pichon & Alvarez 1984; Wortel & Cloetingh 1986). 'Roll back' of the Apulian lithosphere explains the coupling of extension in the back arc area with compression along the leading edge of the Sardinia–Corsica–Calabria 'block', where the Apennines–Maghrebides thrust system was formed (Fig. 2b).

4 PRE-MIDDLE MIOCENE DEFORMATION ON NORTHEASTERN SICILY

The basin, that was located between the overriding European–Iberian Plate and the subducting African Plate, was made up of three distinct paleogeographical domains: The European ('Internal') continental domain, which includes the present CPA, the Neotethyan ('Sicilide') oceanic domain, and the African ('External') continental domain (Giunta 1985; Roure *et al.* 1990, 1991). These domains were probably separated by old transform faults, inferred to have been active intermittently from the Mesozoic onward (Channell, Catalano & d'Argenio 1980; Giunta 1985; Montanari 1987). Remnants of these domains have been recognized in the thrust belts of the CPA, the Maghrebides and the S. Apennines (Ogniben 1960, 1973; Wezel 1974; Giunta 1985; Roure *et al.* 1990, 1991). The discontinuous migration of the Apennines–Maghrebides thrust system towards the African foreland has been reconstructed on the basis of analyses of Eocene–Early Miocene sediments incorporated within the European and Neotethyan units (Ogniben 1960; Wezel 1974; Giunta 1985; Puglisi 1987; Montanari 1986, 1987; Fig. 3).

In the European domain, deposition of siliciclastic sediments started in Late Eocene times. The first influx of lithic arenitic detritus derived from the European margin is attributed to a Late Cretaceous–Eocene thrusting phase, which caused a rejuvenation of the source area (Puglisi 1987). In the Late Eocene–Early Oligocene, turbidites of the Frazzanò Formation were deposited in the northern part of the European domain (Ogniben 1960; Coltro 1967). The coeval Piedimonte Formation, consisting of sandstones, conglomerates and calcareous mudstones (Truillet 1962; Neumann & Truillet 1963; Ferrara 1974; Carmisciano, Lentini & Puglisi 1981b) was deposited in the southern part of the European domain. The Frazzanò Formation was incorporated within the Calabrian nappes by S- to SE-ward thrusting in the Early–Late Oligocene (Ogniben 1960; Wezel 1974; Puglisi 1987).

In Late Oligocene–Early Miocene times, the Stilo–Capo d'Orlando Formation (SCO Fm) was deposited in the

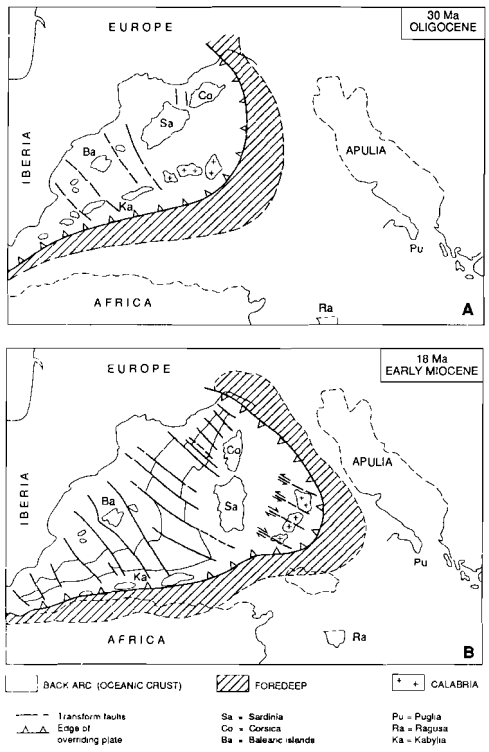

Fig. 2 Palaeogeographical evolution of the Western Mediterranean between the late Early Oligocene (A) and the late Early Miocene (B). The counterclockwise rotation of Sardinia–Corsica and the opening of the Ligurian–Provencal back arc basin were coeval with the SE-ward migration of Calabria and thrusting in the Apennines-Maghrebides (modified after Rehault *et al.* 1984; Dercourt *et al.* 1986; Boccaletti *et al.* 1990).

European domain (Guerrera & Wezel 1974; Bonardi *et al.* 1980; Courme & Mascle 1988). The SCO Fm sealed the tectonic contacts between the units of the European domain (Ogniben 1973; Amodio-Morelli *et al.* 1976; Bonardi *et al.* 1980; Giunta 1985), which had been piled up during the Early to Late Oligocene. However, the SCO Fm conformably overlies the Piedimonte Formation in the southernmost part of the European domain (Carmisciano *et al.* 1981b), indicating that the Oligocene shortening phase was limited to the northernmost European units (Puglisi 1987; Fig. 3). A similar configuration is present in the Neotethyan domain: the Late Oligocene–Early Miocene Reitano Formation (Loiacono & Puglisi 1983; Guerrera & Wezel 1974) unconformably overlies the northernmost Neotethyan units, which implies that they had also been involved in thrusting prior to the Late Oligocene. In the southern part of the Neotethyan domain, the Reitano Formation conformably overlies Eo-Oligocene deposits (Lentini & Vezzani 1978; Wezel 1973; Guerrera & Wezel 1974).

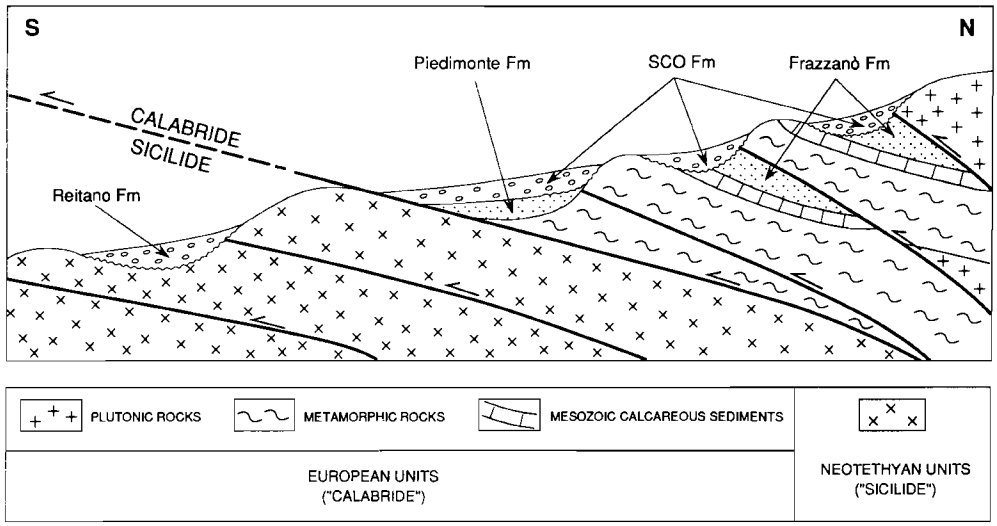

Fig. 3 Tectono-stratigraphic relationships on northeastern Sicily (modified after Lentini & Vezzani 1978; Giunta 1985; Montanari 1986, 1987; Puglisi 1987). The Frazzanò Formation was overthrusted by European ('Calabride') units in the Early Oligocene. Shortening also affected the northernmost Neotethyan ('Sicilide') units. In the Late Oligocene–Early Miocene, these deformed units were unconformably covered by the Stilo–Capo d'Orlando Formation (SCO Fm) and the Reitano Formation. The conformable contact between the Piedimonte Formation and the SCO Fm in the southernmost 'Calabride' units indicate that these units had not been affected by internal deformation. Similar tectono-stratigraphic relationships exist in the Neotethyan domain (see text). Accretion of thrust sheets to the Calabrian–Maghrebide accretionary wedge during the Neogene was accompanied by movements of the older thrusts.

The Neo-Tethys Ocean was closed in the Early Miocene, when the Calabrian basement complex was thrusted further onto the 'Sicilide' Maghrebide units (Wezel 1974; Giunta 1985; Montanari 1986, 1987). Closure was accompanied by emplacement of a tectono-sedimentary complex, the 'Varicoloured Clays' or 'Argille Scagliose', on top of the Calabrian units in Late Burdigalian–Early Langhian times (Wezel 1974; Carmisciano *et al.* 1981a; Meulenkamp *et al.* 1986; Courme & Mascle 1988). This locally well-stratified, and in other places chaotic allochthonous complex was formerly interpreted as an olistostrome (Görler 1978), but now it is generally regarded as a tectonic mélange, that was backthrusted onto the Calabrian units (Wezel 1974; Montanari 1987), and outlines decollement levels in the external parts of the Apennines-Maghrebides thrust belts (Roure *et al.*, 1990, 1991). The Early Miocene shortening phase marked the end of rotation of the Corsica–Sardinia–Calabria 'block' and the end of oceanic accretion in the Ligurian–Provencal back arc basin (Cherchi & Montadert 1982a,b).

5 NEOGENE HISTORY OF THE CALABRIAN–PELORITAN ARC

The Neogene history of the CPA is characterized by progressive thrusting activity and formation of piggy-back basins in the external Apennines–Maghrebides, synchronous with the opening of the Tyrrhenian back arc basin (Malinverno & Ryan 1986; Rehault *et al.* 1987; Roure *et al.* 1990, 1991). Recently acquired geological and geophysical data (ODP Leg 107; Kastens *et al.* 1988; Wang *et al.* 1989) support the view that the Tyrrhenian back arc basin opened by detachment of a formerly continuous lithosphere along a SE-ward facing low-angle normal fault, which merges subhorizontally into the lower crust. This detachment of the CPA from Sardinia is presumably driven by 'roll back' of the Ionian subduction zone (Dewey 1980; Kastens *et al.* 1988; Wang *et al.* 1989). The Ionian Sea is interpreted as a remnant of Neo-Tethys, where subduction 'roll back' is still active (Finetti 1985, and references therein).

The CPA was subject to a complex interaction of strike-slip, extensional and compressional tectonics from the Middle Miocene onward (Ghisetti & Vezzani 1981; Boccaletti, Nicolich & Tortorici 1984; Meulenkamp *et al.* 1986; Barrier & Montenat 1987; Van Dijk & Okkes 1991). On the basis of its Neogene tectono-sedimentary evolution, the CPA can be divided into a number of large segments, bounded by NW–SE trending strike-slip faults, i.e. parallel to the Taormina and Pollino Lines (Meulenkamp *et al.* 1986; Moussat *et al.* 1986; Van Dijk & Okkes 1991). In the northern part of the CPA, sinistral strike-slip displacement occurred during the Neogene, whereas the southernmost

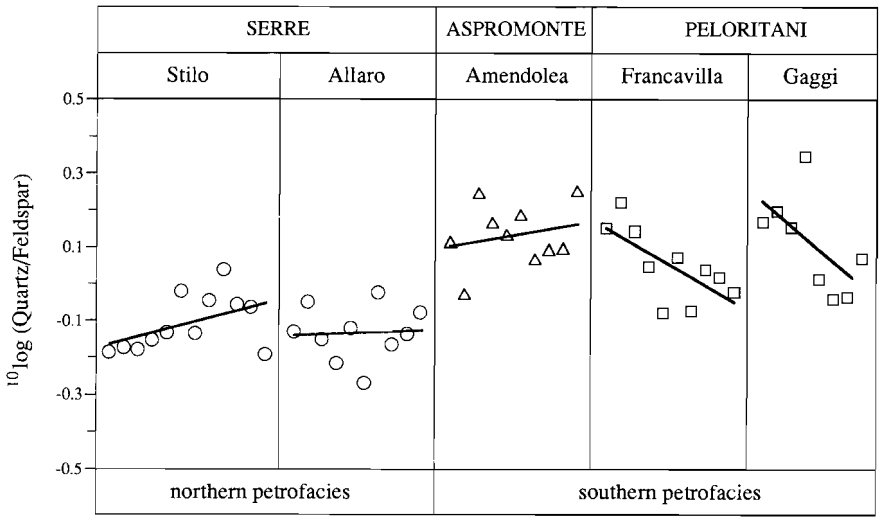

Fig. 4 An illustration of the 'segmented' source–basin relationships in the southern part of the Calabrian–Peloritan Arc during deposition of the Stilo–Capo d'Orlando Formation (data from Cavazza 1989). Sections are arranged according to geographic position from NE (Stilo), to SW (Gaggi). Samples of each section are arranged in stratigraphic order from left to right. Vertical compositional trends in each section are approximated by first-order polynomial regression. The three major segments of the southern Calabrian–Peloritan Arc (Fig. 1) can be distinguished on the basis of a combination of different mean Quartz/Feldspar ratios (the northern and southern petrofacies of Cavazza 1989) and vertical compositional trends (a slight or negligible upward increase of Quartz/Feldspar ratios in Serre and Aspromonte, versus a considerable upward decrease of Quartz/Feldspar ratios in the Peloritani mountains).

part of the CPA was affected by dextral strike-slip (Fig. 2b). Neogene dextral strike–slip between Serre and Aspromonte along a major NW–SE oriented fault is reported by Moussat *et al.* (1986) and Meulenkamp *et al.* (1986). Some of these Neogene shear zones coincide with lateral discontinuities of the Calabrian basement units, suggesting that Neogene strike–slip deformation occurred along reactivated fracture zones.

6 THE CALABRIAN BASEMENT UNITS

The Calabrian basement units of Aspromonte (Fig. 5) consist of granitoid plutonites and an assemblage of Palaeozoic greenschist-amphibolite grade metasedimentary rocks (phyllites, schists and gneisses). They are characterized by a complex history of Hercynian and Alpine metamorphism (Atzori *et al.* 1984; Bonardi *et al.* 1979, 1984, 1987; Platt & Compagnoni 1990), and their geometrical relationships are poorly known. In the central part of the area, the Aspromonte Unit crops out, whereas lower units are locally exposed in tectonic windows (Bonardi *et al.* 1979). Recent (micro-)structural and petrological research in the NE Aspromonte area has shown that two stages of Alpine deformation can be recognized in the Aspromonte Unit (Platt & Compagnoni 1990). The first of these deformation stages (pre-Late Oligocene) may have been associated with crustal thickening and brittle thrusting. The second Alpine deformation phase occurred in Late Oligocene times (25–30 Ma; Bonardi *et al.* 1987). This retrograde metamorphic event, which is widespread in the Aspromonte Unit, was interpreted as the result of uplift and extension (Platt & Compagnoni 1990).

Klippen of the Stilo Unit, the highest tectonic element of the southern part of the CPA, are present in SE Aspromonte (Bonardi *et al.* 1984), overlying the Aspromonte Unit. These klippen include remnants of the sedimentary cover of the Stilo Unit, which consists mainly of Upper Jurassic carbonates. In Aspromonte, their presence is limited to a narrow zone between the villages of Samo and Bova Marina (Afchain 1968; Bonardi *et al.* 1984; see Fig. 5). The youngest sediments on top of the Stilo Unit are exposed in one small outcrop near the village of Palizzi (Bouillin *et al.* 1985). Here, karstified Upper Jurassic carbonates and carbonate breccias are overlain by a bauxitic-lateritic paleosol of unknown post-Jurassic age. This paleosol is, in turn, covered by the Palizzi Formation, a mixed siliciclastic-carbonate sequence of Early Oligocene age. Faunal and floral content of the Palizzi Formation indicate the evolution from a lagoonal to a shallow open marine environment (Bouillin *et al.* 1985). The interpretations of Bouillin *et al.* (1985) are confirmed by the results of palynological analyses (N.M.M. Janssen, tables 2,3), which indicate that the Palizzi Formation can be assigned to the lowermost Oligocene (Lower Rupelian; NP21). The

Palizzi Formation has been overthrusted by gneissic rocks of the Aspromonte Unit which are, in turn, covered by the SCO Fm.

7 THE STILO–CAPO D'ORLANDO FORMATION

The Stilo–Capo d'Orlando Formation (SCO Fm; Bonardi *et al.* 1980) unconformably overlies the Calabrian basement complex. It crops out in the Peloritani Mountains of Sicily, and along the Ionian coast of S. Calabria (Fig. 5). Conglomerates, breccias and coarse-grained sandstones predominate in the lower part of the SCO Fm, passing upwards and laterally into fine-grained sandstones, siltstones and mudstones. Breccias at the base of the SCO Fm consist almost exclusively of clasts derived from phyllites and Jurassic carbonates of the Stilo Unit (Bonardi *et al.* 1984). Conglomerates are mostly polymict, containing clasts derived from the Calabrian substrate (dominant clast types: low to high-grade metamorphics and granitoid plutonics; Bonardi *et al.* 1980). The origin of porphyric clasts, locally abundant in conglomerates of the SCO Fm, cannot be traced to basement rocks presently outcropping in the southern part of the CPA (Ferla & Alaimo 1976). The geometry and tectonic controls of the basins in which the SCO Fm was deposited, are poorly known. Ideas proposed include an extensional basin consisting of numerous blocks, bounded by NE–SW and NW–SE trending faults (Meulenkamp *et al.* 1986), and a series of piggy-back or satellite basins (Puglisi 1987).

Detailed investigation of the SCO Fm in SE Aspromonte (1985–1986) resulted in a new working hypothesis for pre-Middle Miocene basin evolution (Weltje 1988a,b). It can be summarized as follows: Deposition of the SCO Fm occurred in a series of NE–SW oriented basins, which were carried piggy-back on top of the Calabrian basement nappes. The basins were delimited by NW–SE trending transverse fault zones, which also determined the locations of the main feeder systems. Each basin of the SCO Fm was therefore fed by its own, tectonically defined segment of the Calabrian hinterland. During an Oligocene extensional phase, mainly coarse-grained clastics were deposited. Their axial dispersal pattern resulted from lateral confinement by NE–SW trending syn- and antithetic normal faults. A subsequent tectonic inversion is marked by a shift in the depositional style to a transverse (SE-ward) dispersal of mainly fine-grained sediments. Slumping and sliding of sediments, related to tilting and the formation of backthrusts, occurred during the peak of this compressional phase, in the Late Early Miocene. The 'segmented' source–basin relationships of the Calabrian basins are confirmed by the data of Cavazza (1989). Each major segment of the southern part of the CPA (Peloritani, Aspromonte and Serre) is characterized by a distinctive compositional evolution pattern, when the vertical compositional trends within the SCO Fm are taken into account (Fig. 4).

8 AGE OF THE STILO–CAPO D'ORLANDO FORMATION

The age of the SCO Fm., as determined on the basis of coccoliths and planktonic foraminifera is controversial: Bonardi *et al.* (1980) carried out the first systematic study and considered the upper fine-grained part of the SCO Fm to be of Early to Middle Miocene age (Aquitanian–Langhian; NN1–NN5), confirming the results obtained by earlier biostratigraphic analyses (Bonardi *et al.* 1971; Guerrera & Wezel 1974). In the lowermost coarse-grained units of the SCO Fm, no calcareous microfossils were found. This view is not supported by planktonic microfossil datings of other authors, who concluded that the major part of the SCO Fm was deposited in Late Oligocene times: Meulenkamp *et al.* (1986), Barrier *et al.* (1987) and Courme & Mascle (1988) considered the SCO Fm to be of Late Oligocene to Early Miocene age (Chattian–Burdigalian; NP24–NN2). Benthic foraminiferal assemblages in the upper fine-grained deposits of the SCO Fm in the S. Serre area (Agnana–Antonimina; Nicotera 1963) also suggest an Oligocene age.

Datings based on other fossil groups support an Oligocene age of the lower part of the SCO Fm: Assemblages of larger foraminifera in calcarenites, occurring near the base of the SCO Fm at several localities in the Serre, were dated as Early to Late Oligocene (Nicotera 1963; Afchain 1966). *Lepidocyclina* (*N.*) *praemarginata* assemblages from Placanica and M. Tronato (two localities in the N. and S. Serre, respectively), which were studied morphometrically (Den Hartog Jager 1985), provide an accurate dating of the base of the SCO Fm. According to the revision (Laagland 1990) of a larger foraminiferal zonation proposed by Drooger & Laagland (1987), the base of the SCO Fm should be assigned to the 'praemarginata zone' of the Upper Lower Oligocene (Upper Rupelian; top NP23). A Late Early to Early Late Oligocene age (Upper Suevian–Lower Arvenian; NP23–24?) was established for vertebrate remains from the lignite-bearing deposits at the base of the SCO Fm in the Agnana area (Esu & Kotsakis 1983; Kotsakis 1984).

Biostratigraphic datings carried out for this study, using dinoflagellate cysts (Table 2), combined with the results of previous datings on the basis of coccoliths (Gelderloos & Schaafsma 1984; Van Haeringen 1985), indicate that the SCO Fm comprises the Upper Rupelian–Lower Burdigalian interval (NP23–NN2). In view of datings based on other fossil groups, such as in situ larger foraminifera and the dinoflagellates, it is unlikely that the presence of all Palaeogene microfossils in the SCO Fm can be attributed to redeposition of older sediments, as stated by Bonardi *et al.* (1980). Redeposited Cretaceous and Upper Paleocene–Lower Eocene palynomorphs were observed in a few samples of the SCO Fm, as well as palynomorphs from the lowermost Oligocene (NP21), but most of the Oligocene assemblages show no sign of mixing or reworking (N.M.M. Janssen, pers. comm.).

The presence of a bedded chert ('silexite') in the upper

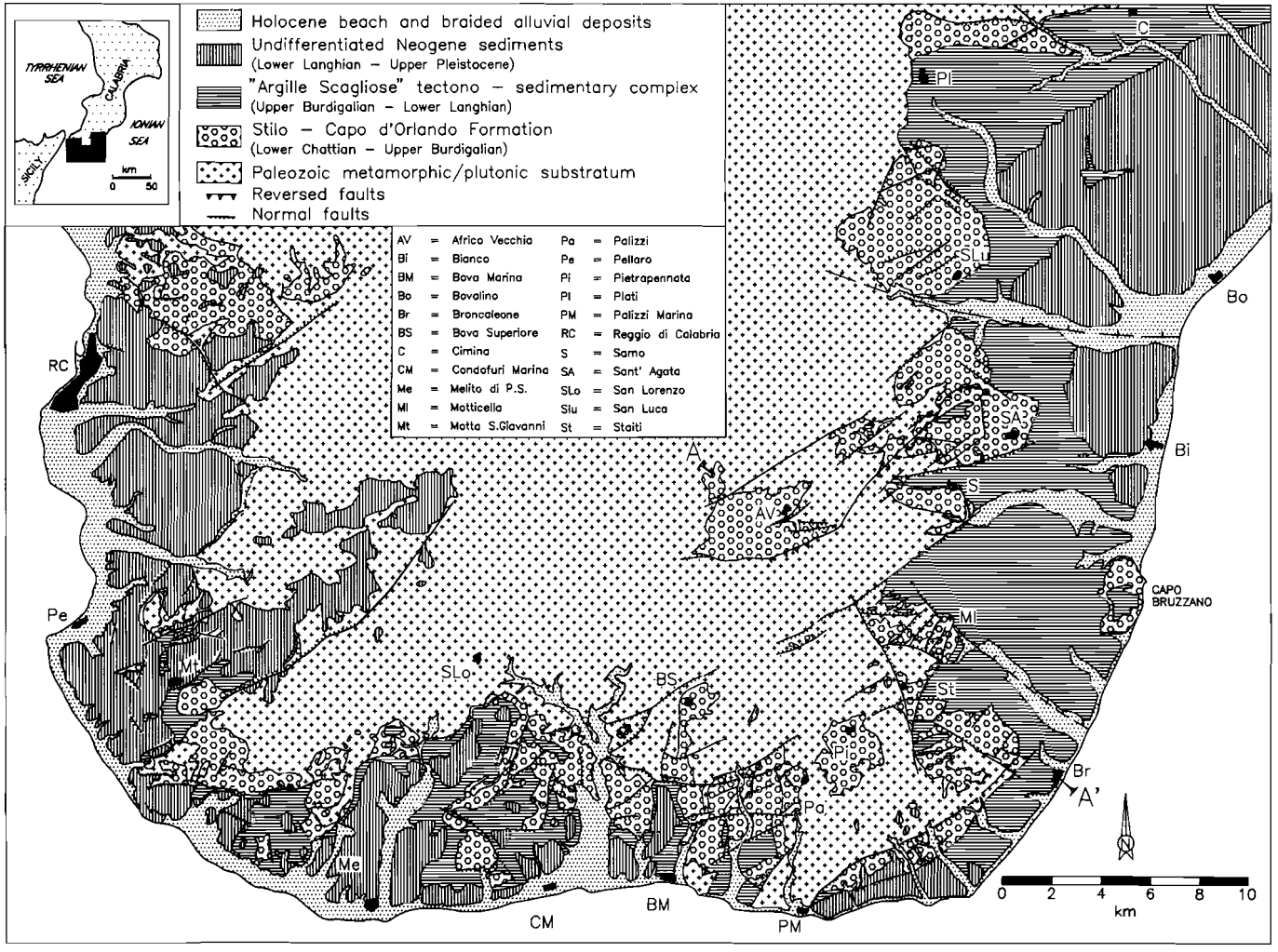

Fig. 5 Simplified geological map of Aspromonte, based on unpublished 1:25,000 maps made by students of the Institute of Earth Sciences, University of Utrecht (1981–1986). See Fig. 6 for a NW–SE profile through the southeastern part of the area (A–A').

Table 1. Summary of lithofacies descriptions and interpretations.

Facies	Description	Interpretation
A	Mono- to oligomict breccia; locally red colouration, laterally discontinuous	Subaerial scree or scarp breccia
B	Poorly sorted, disorganized conglomerate, showing occasional grading, red colouration and sandy interbeds	Subaerial to subaqueous debris flows (alluvial fan ?)
C	Graded, stratified, clast- to matrix-supported conglomerate; loading and "floating" clasts common; interbeds of structureless or parallel laminated sandstone; backsets, water-escape pillars, high-angle foresets	Subaqueous debris flows, coarse-grained delta slope deposits (debris cones)
D	Moderately sorted sandstone with trough cross-stratification, linguoid bars, backflow ripples and traces of rootlets	Fluvio-deltaic deposits; distal braidplain
E	Poorly sorted, upward fining pebbly sandstone beds with 'armoured' mud balls, capped with green to brown parallel laminated lignite-rich siltstone; miniature Gilbert-type delta lobes	Subaqueous deltaic deposits
F	Upward fining grey to yellow pebbly sandstone beds; 'floating' clasts and asymmetric load-casts are common. Capped with grey siltstone, showing trough-cross lamination, convolute lamination and occasionally wave ripples; marine fossils	High-density turbidites, shallow to deep marine (below storm wave base); delta slope and submarine canyon
G	Thin bedded alternations of sandstone and grey mudstone; often bioturbated. Contains a variety of faunal/floral elements: from lagoonal palynomorphs to bathyal foraminifera	Lagoonal to deep marine sandy and muddy deposits
H	Finely laminated chert ('silexite'); radiolarians and planktonic foraminifera	Deep marine biogenic deposit
I	Calcareous mudstone, strongly bioturbated; doublets of bivalves	Shallow (?) marine intrabasinal ridge deposit

Table 2. Dinoflagellate assemblages and biostratigraphic datings of the Palizzi Formation [locality Sporta, 1 km S of Palizzi (Fig. 5)] and the SCO Fm of NE and SE Aspromonte [localities: Aria del Vento, 2 km N of Plati; Africo Vecchio; Chorio, 4 km WSW of Africo Vecchio; Capo Bruzzano; Motticella (Fig. 5)]. Samples from each locality are arranged in stratigraphic order from left to right. Palynological analyses carried out by N.M.M. Janssen. Dinoflagellate taxonomy after Lentin & Williams (1989). Symbols used: # = Oligocene marker species (according to unpublished range charts of the Laboratory of Palynology and Paleobotany, Utrecht); P = present; C = common; A = abundant; D = dominant; R = reworked; ? = uncertain.

LOCATIONS	Sporta			Aria d.V.			Africo V.			Chorio			Capo B.			Mott.	
SAMPLES	A	B	C	4A	8A	9A	38A	39A	41A	45A	47A	48A	58A	59A	61A	66B	66C
DINOFLAGELLATE SPECIES																	
Achomosphaera alcicornu													C				
Adnatosphaeridium reticulense				P													
Apectodinium spp.														R	R		
Areosphaeridium diktyoplokus					R												
Areosphaeridium pectiniformis					P												
Chiropteridium spp. #															C		
Cordosphaeridium cantharellum				P	C	P								C	C		P
Cordosphaeridium minimum					P									P			
Corrudinium incompositum #				R	R												
Deflandrea spp.	P		P		A	P		P			P		C	C	P		C
Diphyes colligerum				P													
Distatodinium craterum				P									P	P			
Glaphyrocysta cf. semitecta #	A		A								?		P				?
Heteraulacacysta leptalea																	?
Homotryblium floripes			C														
Homotryblium spp.				C	A	A	P		P	P	C		A	A	A	C	A
Hystrichokolpoma cinctum				C	P								C	C	P		
Hystrichokolpoma rigaudiae					C						P			C			P
Impagidinium aculeatum				P											A		
Impagidinium dispertitum				P	C												
Impagidinium velorum				P	P												
Leptodinium italicum #															C		
Lingulodinium machaerophorum		?		P										P			
aff. Lithosphaeridium sp.																	P
Operculodinium centrocarpum			P	C	C	A	P				C				C.		
Operculodinium cf. placitum			C														
Pentadinium laticinctum					P	P											P
Phtanoperidinium amoenum #											C						
Phtanoperidinium comatum #				C						?			C	?			P
Polysphaeridium subtile														C			
aff. Polysphaeridium sp.	D		D			C							C	C			D
Reticulatosphaera actinocoronata			C	C	A				P		C		P	C	C		C
Rhombodinium sp.			P														
Systematophora spp.	P	P	C	D	A	D	P	P	P	P	A	P	A	D	D	P	C
Tectatodinium minutum					P												
Thalassiphora pelagica				C										C			
Wetzeliella cf. gochtii #				P		P											P
Wetzeliella symmetrica			C			C					?						
Spiniferites/Achomosphaera group	P		C	D	D	A			P		A		D	D	D		A
peridinoid cysts	P		C														
Cretaceous cysts															R		
BIOSTRATIGRAPHIC AGE	NP21			NP24			?			NP24			NP25			NP24	

part of the SCO Fm was already mentioned by Bonardi *et al.* (1971, 1980), Lorenz (1984), and Barrier *et al.* (1987). This 'silexite', which also occurs at several locations in Aspromonte (Figs 23, 24), has been described by numerous authors working in the W. Mediterranean. Its formation is generally related to (submarine) volcanic activity. The 'silexite' provides an excellent marker bed because of its limited thickness, wide lateral extent and well constrained Early–Middle Burdigalian age (for reviews and descriptions see Didon *et al.* 1969; Wezel 1977; Lorenz 1984). Its position near or at the top of the SCO Fm indicates that the upper part of the SCO Fm can be assigned to the Middle Burdigalian (base NN3).

The SCO Fm is covered by the allochthonous 'Argille Scagliose' (Figs 5,6). Red clays in the upper fine-grained part of the SCO Fm, deposited in Aquitanian time, have been interpreted as the first influx of resedimented "Argille Scagliose" material (Caire 1961; Barrier *et al.* 1987), predating the emplacement of the bulk of this tectono-sedimentary complex. Biostratigraphic studies of the 'Argille Scagliose' of Aspromonte have shown that it consists of tectonically transported and/or resedimented Cenomanian–Upper Oligocene deposits (Afchain 1967; Luciani *et al.* in press). The transition between the SCO Fm and the 'Argille Scagliose' of Aspromonte is either gradual or abrupt. In the latter case, no reworked components from the SCO Fm are intercalated in the 'Argille Scagliose', and a basal shear plane has not been observed. The 'Argille Scagliose' is locally found directly on top of the Calabrian basement units. In the Langhian, shallow marine deposits (calcarenites, sands and clays) were deposited on top of the 'Argille Scagliose' in the S. part of the CPA (Carmisciano *et al.* 1981b; Meulenkamp *et al.* 1986; Courme & Mascle 1988).

9 SEDIMENTOLOGY OF THE STILO–CAPO D'ORLANDO FORMATION

9.1 Methods

The SCO Fm in Aspromonte is generally well exposed, but strongly fragmented by numerous post-depositional normal and oblique-slip faults. Locally, small-scale NW and SE facing post-depositional reverse faults were also observed (see Figs 5,6). As a result of this extensive deformation, sediments of neighbouring fault blocks can usually not be correlated. Therefore, a detailed description of individual sequences was not appropriate for creating a general picture valid for the whole area. Because the SCO Fm is characterized by strong lateral and vertical variability, attention was paid primarily to the description and interpretation of individual lithofacies. Brief descriptions and interpretations of the lithofacies distinguished in the field are given below, and a summary of their characteristics and environmental interpretation is presented in Table 1. A composite column was constructed for every small area where lithological units could be traced laterally, in order to summarize and analyse major lateral and vertical trends within the SCO Fm. Two characteristic sedimentological profiles are presented in Figs 23 and 24.

Palaeoflow directions were reconstructed by measuring the orientation of a number of different sedimentary structures: in coarse-grained lithofacies of the SCO Fm gravelly foresets, pebble clusters and clast imbrication were measured. In sandy/silty lithofacies, trough and planar cross-lamination were measured. Generally, palaeoflow directions had to be inferred by combining the observation of several differently oriented two-dimensional outcrops. Measurement of sedimentary structures on bedding planes was only possible in one case: an excellent exposure of the linguoid bar complex described below as lithofacies D. A summary of sedimentological observations (palaeocurrents, slump fold axes and synsedimentary faults) is presented on isopach maps of coarse- and fine-grained lithofacies (Figs 21,22).

9.2 Lithofacies descriptions and interpretations

Lithofacies A: breccia (Fig. 7)

This lithofacies is usually a few metres thick and poorly bedded. It is laterally discontinuous, especially at the base of the SCO Fm, and tends to pinch out over short distances (tens of metres). Sediment is generally clast-supported and poorly sorted; imbrication of clasts was not observed. Locally, breccias are sandy and stratified, showing alternations of moderately sorted clast- and matrix-supported layers. Main constituents are low-grade metamorphic and/or Upper Jurassic carbonate clasts, derived from the Stilo Unit. Breccias consisting chiefly of carbonate clasts are only found at the base of the SCO Fm. Outsized clasts of Jurassic carbonate are a common feature of these breccias: their size may be up to tens of metres (see also Bonardi *et al.* 1984). Many of these large blocks consist of strongly cemented clast-supported breccia, containing minor amounts of red matrix. Fig. 7 shows a breccia of granitoid clasts, which occurs only in the northern part of the area (Aria del Vento, N of Plati), and was derived from a local source.

Lithofacies A is interpreted as a scarp breccia or scree. The occurrence of lithofacies A at the base of the SCO Fm appears to be limited to areas where the sedimentary cover of the Stilo Unit is still present, testifying to its local origin. The carbonate breccia clasts within this lithofacies are polycyclic (Bouillin *et al.* 1985). Its locally conspicuous red colouration and strong cementation are the likely result of subaerial weathering and lithification.

Lithofacies B: disorganized conglomerate (Fig. 8)

This lithofacies consists of very coarse-grained, ungraded and poorly sorted beds, with exceptionally large clasts, up to several metres in diameter, locally. Characteristic features include a matrix-supported texture and the presence of sand-rich interbeds. Imbrication of clasts is rare. Composite beds are up to tens of metres thick and

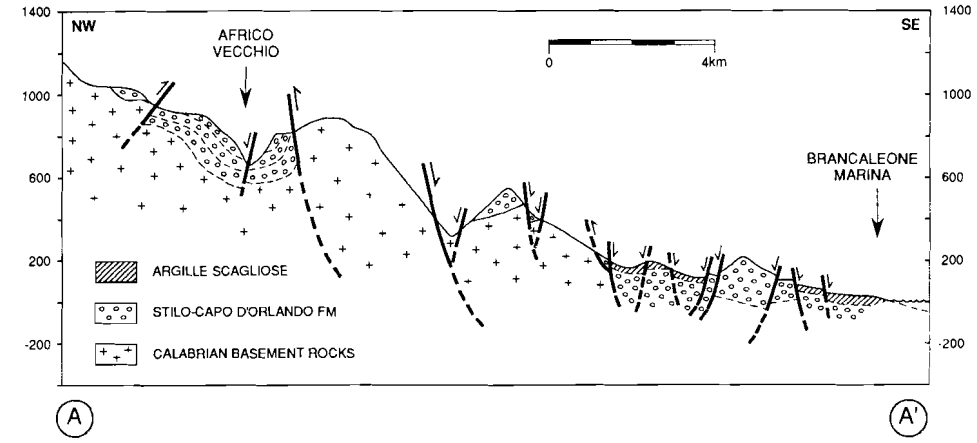

Fig. 6 Simplified NW–SE profile through the southeastern Aspromonte area (vertical exaggeration: 5 ×). See Fig. 5 for the position of line A–A'.

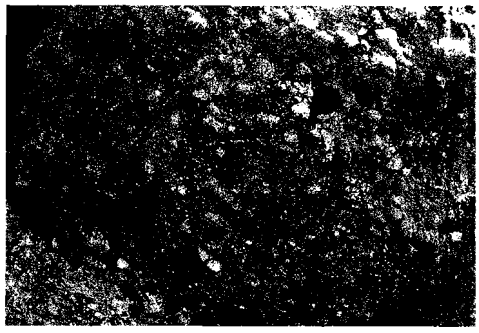

Fig. 7 Lithofacies A [Aria del Vento; 2 km N of Plati (Fig. 5)]. Inversely graded base of monomict bed, consisting of granitoid clasts. Lens cap (5 cm) for scale.

Fig. 8 Lithofacies B [Monte Palecastro; 1 km SW of Samo (Fig. 5)]. Modified debris flow deposit, showing relatively well-developed clast imbrication. Flow from right to left; Hammer (30 cm) for scale.

poorly defined. Locally, they show a conspicuous red to brown colour. In places where this unit represents the base of the SCO Fm, it is sometimes underlain by a deeply red-coloured paleosol, covering weathered rocks of the Stilo or Aspromonte Unit (e.g. Torrente Misacrifa, 3 km W of Condofuri Marina).

This lithofacies is interpreted as a subaerial to subaqueous debris flow deposit. Texture and red colouration are not necessarily indicative of subaerial deposition, but the presence of a deeply red-coloured, possibly bauxitic paleosol underlying this unit strongly suggests subaerial deposition of at least the lower part. Features indicative of subaqueous deposition (cf. Nemec & Steel 1984) have not been observed.

Lithofacies C: conglomerate–sandstone couplets (Figs 9 and 11)

Conglomerate/sandstone couplets are arranged in upward fining cycles of decimetres to several metres thick. Conglomerate beds are poorly sorted and structureless, inversely, or normally graded. Locally, stratification and imbrication are well developed (Fig. 9). Conglomerate beds tend to become sandier towards the top, corresponding to a textural change from clast- to matrix-support. The conglomerate beds are capped by discontinuous, upward-fining sandstone layers (up to one metre thick). The sandstones show a normally graded and structureless lower part with pebble strings and 'floating' clasts. In the upper part of sandstone beds, parallel laminae and/or current ripples are locally present. On top of this sandstone, a parallel laminated interval of dark brown, lignite-rich siltstone was occasionally observed. Lenticular bedding and scouring of conglomerate–sandstone couplets are a common feature of this lithofacies (Fig. 11). The upper part of the sequence described above, i.e. the matrix-supported

Fig. 9 Lithofacies C [Torrente Misacrifa; 3 km NW of Condofuri Marina (Fig. 5)]. Lenticular bedding, clast imbrication, and larger clasts protruding from the top of conglomerate beds into the overlying sandstones are clearly visible. Flow from lower right to upper left; hammer (30 cm) for scale.

conglomeratic interval and the overlying sandy interval, are locally absent.

Sedimentary structures observed in this lithofacies include asymmetric structures resembling "pebble clusters" (Dal Cin 1968) or "cluster bedforms" (Brayshaw 1984). These bedforms are well developed at certain locations (Fig. 11). Less commonly, high-angle planar gravelly foresets (height 20–50 cm) and backsets (cf. Postma 1984) are present. Liquefaction structures (water-escape 'pillars' of gravel in sand), observed at a few locations, are oriented obliquely to the bedding planes. Vertical transitions from sandstones to conglomerates are marked by loading of larger clasts. Vertical transitions from conglomerates to sandstones are marked by relatively large clasts protruding from the top of conglomerate beds into the sandstone (Fig. 9). Tightly packed gravel layers, texturally similar to pebble strings observed within sandstone beds of this lithofacies, are inferred to be the result of reworking of the tops of conglomerate beds.

This lithofacies is interpreted as a subaqueous debris flow deposit. The subaqueous nature of this deposit is suggested by the presence of water-escape structures, clasts protruding from the top of conglomerate beds into the overlying sandstone, loading of clasts at the base of conglomerate beds into the underlying sandstone, the upward transition from a clast- to a matrix-supported texture, and the massive and/or evenly laminated nature of the interbedded sands (cf. Nemec & Steel 1984; Hein 1984; Postma, Nemec & Kleinspehn 1988). High-angle foresets within this lithofacies point to the presence of transverse bars (Hein & Walker 1977), prograding over a subhorizontal depositional surface. At other locations, the presence of liquefaction structures, which are oblique to bedding planes, and backsets suggests a depositional slope (cf. Postma 1984; Colella *et al.* 1988). The "pebble clusters" or "cluster bedforms", which were described as the dominant bedform in certain braided fluvial deposits (Brayshaw 1984), appear to be equally characteristic of lithofacies C. The 'ideal' sequence of this lithofacies, as described above, may be variously modified depending on the intensity of reworking processes. Some of the resulting 'residual' or 'winnowed' subfacies strongly resemble alluvial conglomerates (cf. Nemec *et al.* 1984). In these cases, the presence of associated 'structureless' sandstone beds usually provides the necessary clues for interpretation (Hein 1984). Comparable conglomerate-sandstone couplets, inferred to have been deposited as a submarine canyon fill, were described by Clifton (1984).

Lithofacies D: sandstone (Figs 10 and 12)

This lithofacies consists of moderately sorted coarse- to medium-grained sandstones without mudstone interbeds. Beds are usually several dm to 2 m thick, and frequently amalgamated. Common sedimentary structures include trough-cross-stratification (50 cm wide) and current ripples. This lithofacies is extremely well exposed on a dipslope of the Mt. Varet (4 km NW of Sant'Agata). The surface relief consists of numerous linguoid bars with steep slipfacies (Fig. 10), showing typical out-of-phase relationships (Miall 1977). Individual bars are generally 50 cm high, 2–3 m wide and about 10 m long (Fig. 12). On a few bars, current ripples have been preserved. Some of the palaeocurrent measurements obtained from these ripples diverge markedly from the mean direction of downstream bar migration. Small-scale current ripples on bar tops are indicative of sediment transport in roughly the same direction as bar migration, whereas ripples on lower parts of the bar relief suggest local sediment transport opposite or perpendicular to bar migration (backflow ripples). In addition, numerous small, round holes, interpreted as traces of rootlets, were observed on some of the bar tops.

The linguoid bar complex of lithofacies D conforms well to the criteria formulated by Miall (1977) for sandy braided systems, and may have been deposited on a distal braidplain. The orientation of current ripples on bar sides and the presence of rootlets indicate that this complex was at least

Fig. 10 Lithofacies D [Monte Varet; 3 km NW of Sant'Agata (Fig. 5)]. Steep foresets of stacked linguoid bars; Flow from right to left (height of individual bars is *c.* 1 m).

(a)

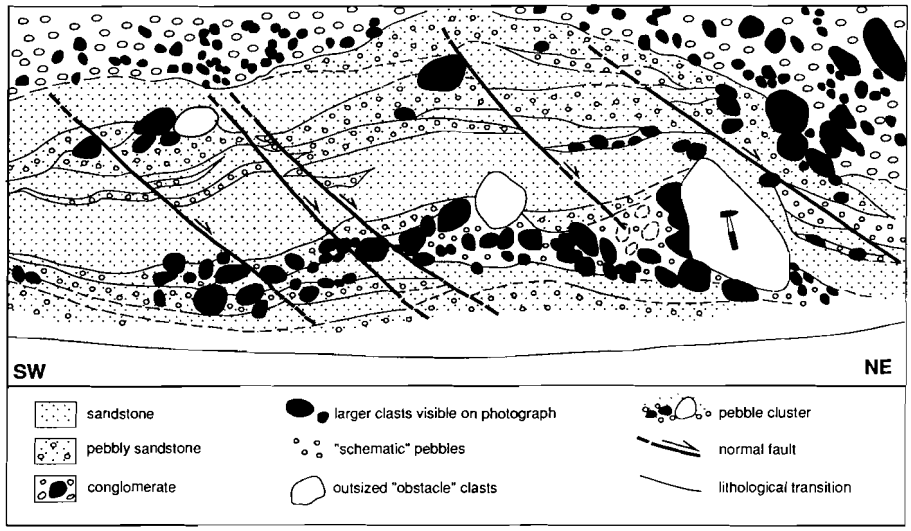

(b)

Fig. 11 Photograph (a) and line drawing (b) of lithofacies C with clearly developed 'cluster bedforms' or 'pebble clusters' [2 km SW of Pietrapennata (Fig. 5)]. Flow from left to right; hammer (30 cm) for scale.

periodically subject to partial emergence. In view of its close association with marine deposits (lithofacies F, G and H), a fluvio-deltaic setting is most likely.

Lithofacies E: pebbly sandstone (Figs 13 and 16)

This lithofacies consists of upward fining beds of several dm to 2 m thick (Fig. 13). The base of the beds is formed by a poorly sorted, normally graded and structureless pebbly sandstone, sometimes underlain by a disorganized or normally graded conglomerate layer. Sandstone colours range from yellow to red- or dark-brown. Angular clay flakes of various sizes are common in the basal portion of sandstone beds. 'Armoured' mud balls were observed on a few locations. Sandstone beds are capped by parallel laminated very fine sandstone-siltstone alternations, containing intervals of transported plant debris (lignite). The base of sandstone beds is usually sharp and flat, but large, shallow scours were also observed. Convolute lamination and water-escape structures are absent, but large intraformational 'rip-up' clasts were observed at some locations. Lateral relationships between pebbly sandstones and fine sandstone–siltstone intervals, observed in one outcrop (4 km WSW of Africo Vecchio; Fig. 16), suggest that after

Fig. 12 Lithofacies D [Monte Varet; 3 km NW of Sant'Agata (Fig. 5)]. Downstream view along the axis of a linguoid bar. Fieldwork assistant (1.75 m) for scale.

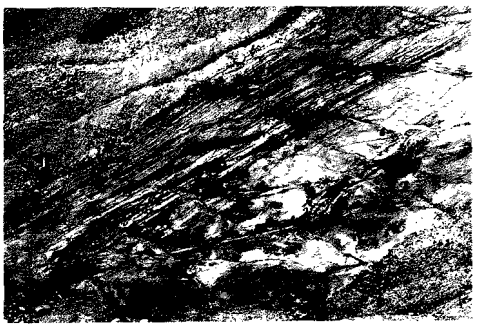

Fig. 13 Lithofacies E [4 km WSW of Africa Vecchio (Fig. 5)]. An upward fining sequence of conglomerate, structureless sandstone and parallel laminated fine sandstone–siltstone makes up one (composite) bed. Note the flat base of the overlying bed. Hammer (30 cm) for scale.

deposition and subsequent partial erosion of the fine-grained sediments, the remainder was covered by pebbly sandstones with high-angle cross-stratification. The orientation of the sandstone-siltstone intervals and the foreset bedding in the pebbly sandstone are subparallel. This indicates that the fine-grained sediments were deposited on inclined surfaces.

The absence of cross-bedding, and the occurrence of large intraformational clasts, suggest a subaqueous mass-flow depositional mechanism (cf. Lowe 1982; Hein 1984), in spite of the general absence of soft-sediment deformation structures. In the area around Africo Vecchio, lithofacies E is enveloped by lagoonal and shallow marine sediments. The lateral relationships between coarse- and fine-grained sediments of this lithofacies (Fig. 16), are interpreted as the filling of abandoned channels or depressions with fine-grained sediment. The high-angle slipfaces observed within this fill are interpretcd as foresets of transverse bars or 'miniature' Gilbert-type delta lobes. The presence of 'armoured' mud balls and abundant lignite in this lithofacies suggests deposition in a subaqueous deltaic environment.

Lithofacies F: pebbly sandstone–mudstone couplets (Figs 14 and 15)

This lithofacies consists of upward-fining sandstone-mudstone beds with a highly variable thickness (10 cm to 2 m). Sandstone beds are usually light-grey or -yellow coloured, and better sorted than those of lithofacies E. Small, usually elongated clay pebbles are abundant near the base of beds. Conglomerates occur at the base of thick beds. Thinner beds consist of normally graded and structureless pebbly sandstone. Beds are frequently amalgamated: these composite beds show internal loading and scours filled with coarser sediments (Fig. 14). 'Floating' pebbles and conglomerate strings are present in nearly all

Fig. 14 Lithofacies F [Torrente Caloiro; 2 km WSW of Sant'Agata (Fig. 5)]. Thick composite beds of this lithofacies frequently show scouring and loading on different scales. Flow from right to left; hammer (30 cm) for scale.

Fig. 15 Lithofacies F [Scilindermeno; 3 km NNE of Bova Marina (Fig. 5)]. Amalgamated and reworked thin sandstone beds, showing small-scale wave ripples, trough-cross lamination, parallel lamination and convolute lamination. Lens cap (5 cm) for scale.

of the beds. The tops of the beds consist of parallel laminated and trough cross-laminated fine sand and silt, capped by grey mudstone showing convolute lamination. Thin sandstone beds (less than 50 cm thick) of this lithofacies are locally amalgamated, which results in composite beds with an alternation of graded, parallel laminated, and cross-laminated intervals. Cross-laminated intervals include a number of different sedimentary structures: planar and trough cross-lamination (current ripples), climbing ripples, convolute lamination, and occasionally wave-ripples (Fig. 16). On locations where amalgamation of sandstone beds is less common, base-missing Bouma sequences (Tb-e; Tc-e) were observed without signs of wave-reworking. Pebbly mudstones, including large intraformational clasts, and slumps are commonly observed in this lithofacies. Systematically asymmetrical loading structures are visible in thick beds in numerous places, especially near Sant'Agata and at Capo Bruzzano. Thin (5–10 cm) intercalations of micritic limestones containing planktonic foraminifera were observed at a few locations. The trace fossil *Terebellina*, forming horizontal calcareous tubes (Fig. 18), is common in mudstones of this lithofacies.

Sediments of this lithofacies are interpreted as high-density turbidites (Lowe 1982). They were deposited in a marine environment, as indicated by the frequent presence of *Terebellina*, characteristic of "offshore muddy deposits" (Bromley 1990). The frequently found systematically asymmetric orientation of load-casts suggests that part of this lithofacies was deposited on a high-angle slope. The validity of this primary dip indicator is supported by measurements of paleocurrents and slump-fold orientations: directions of sediment transport are the same as expected on the basis of asymmetry of load-casts and *vice*

(a)

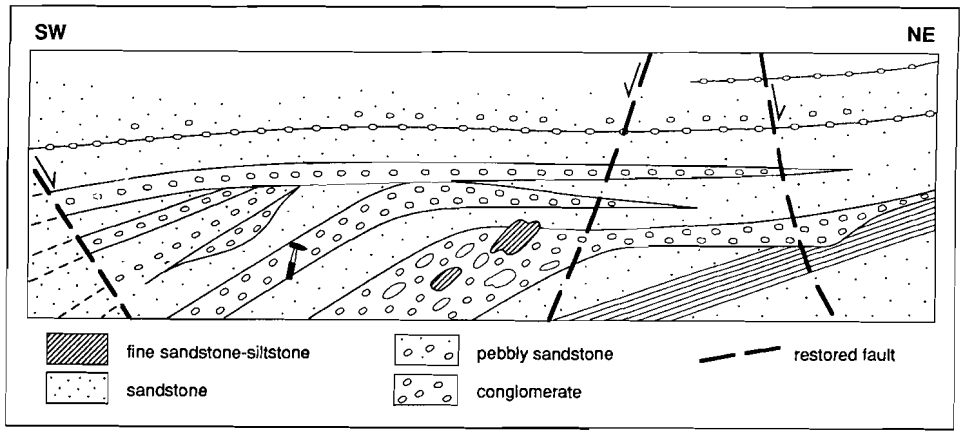

(b)

Fig. 16 Lithofacies E: photograph (A) and reconstruction (B) of relationships between conglomerate, pebbly sandstone and fine sandstone-siltstone in an exposure 4 km WSW of Africo Vecchio (Fig. 5). Alternating layers of fine sand and silt were deposited on top of an inclined surface. These deposits were partially eroded and subsequently covered by top- and foresets of transverse bars, consisting of pebbly sand. Flow from upper right to lower left; hammer (30 cm) for scale.

versa. The angle of deposition, as estimated from the axis of symmetry of these load-casts, is inferred to have been up to 20°. At certain localities, a shallow marine environment (above storm wave base) is indicated by the occurrence of partly reworked turbidites and the presence of wave ripples. At other localities, the intercalation of micritic limestones containing only planktonic foraminifera, and the absence of reworking suggest a deeper marine environment (below storm wave base).

Lithofacies G: sandstone–mudstone couplets (Fig. 17)

This lithofacies consists of mudstones alternating with thin-bedded sandstones/siltstones. Mudstones are usually brown, green, or grey coloured. Sandstones are yellow to dark-brown and poorly sorted, irregularly bedded and strongly bioturbated. Occasionally, faint parallel lamination and/or current ripples were observed. In this lithofacies, mudstones dominate over sandstones. Sandstone/mudstone ratio ranges from 1 to 50; the thickness of sandstone beds ranges from 10 cm to 20 cm in the former, and from 1 cm to 5 cm in the latter case. Trace fossils include *Terebellina* (Fig. 18) and *Paleodictyon*.

These sediments are interpreted as bioturbated offshore sandy and muddy deposits, for which *Terebellina* is a characteristic trace fossil (Bromley 1990). The depositional depth of lithofacies G varies from lagoonal and shallow marine near the base of the SCO Fm (N.M.M. Janssen, personal communication), to upper bathyal in its topmost part (Nicotera 1963; Barrier *et al.* 1987), confirmed by the presence of *Paleodictyon*. This wide paleobathymetric range was not recognized in the field.

Lithofacies H: 'Silexite' (Fig. 19)

This lithofacies, occurring in the upper part of the SCO Fm, is usually overlain by lithofacies G, and ranges in thickness from 5 m to 25 m. It consists of a thinly bedded alternation of chert and mudstone, showing parallel lamination on a millimetre to centimetre scale. The lamination consists of alternating quartz-rich and clay-rich intervals. Laminae are straight, undulous or even tightly folded. Occasionally, small scale, low-amplitude current ripples or signs of bioturbation were observed. In thin sections, recrystallized diatoms (chalcedony), radiolarians and sponge spicules are visible in clay-rich intervals. Quartz-rich intervals have been completely recrystallized, and consist entirely of micro-polycrystalline quartz. Planktonic foraminifera are present in clay-rich laminae, whereas benthic foraminifera were not observed. A detailed description of the microscopic features is given by Didon *et al.* (1969).

Lithofacies H is interpreted as a biogenic chert, on the basis of the siliceous microfossil remains visible in thin sections. The 'silexite' was deposited in a deep marine environment, as inferred from its biogenic origin and its stratigraphic position, directly underlying lithofacies G, which is inferred to have been deposited at upper bathyal

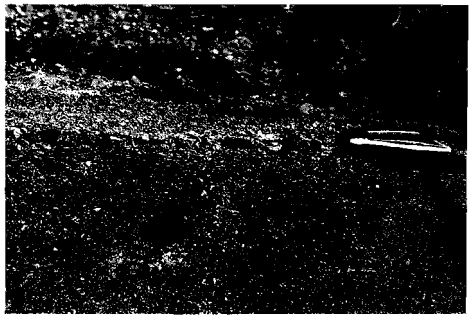

Fig. 17 Lithofacies G [Piscopi; 4 km NW of Staiti (Fig. 5)]. Usually, thin-bedded sandstones of this lithofacies have been strongly bioturbated. Lens cap (5 cm) for scale.

Fig. 18 Calcareous tubes, attributed to the trace fossil *Terebellina*, on bedding planes of lithofacies G [Fiumara Butramo; 1 km SE of Samo (Fig. 5)]. Lens cap (5 cm) for scale.

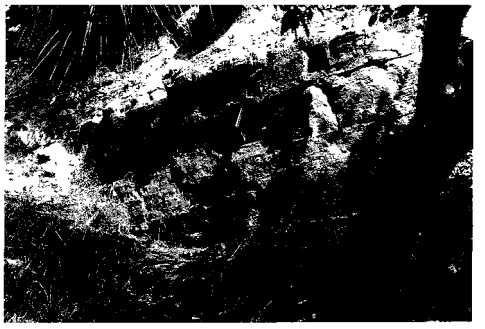

Fig. 19 Lithofacies H, the so-called 'silexite', interealated in sediments of lithofacies G [Coletta; 4 km SSE of Motta San Giovanni (Fig. 5)]. The parallel laminae, consisting of alternating quartz-rich and clay-rich intervals are clearly visible. Hammer (30 cm) for scale.

depths. The preservation of very thin laminae, and the virtual absence of benthic microfossils and bioturbation suggest oxygen depletion in deeper parts of the basin during deposition of the 'silexite'. This may indicate that formation of the 'silexite' was the result of a siliceous microfossil bloom. The exceptionally high surface water productivity may have been caused by volcanic activity. Under such circumstances, dys- or anaerobic bottom conditions can be established by the oxidation of excess organic C, transferred from the surface into deeper waters.

Lithofacies I: carbonate/calcareous mudstone

In one small outcrop, about 6 km W of Motticella, a 2 m-thick calcareous mudstone was found at the base of the SCO Fm, overlain by Early Miocene sediments of lithofacies G. Sedimentary structures and bedding have not been recognised, due to intense bioturbation and post-depositional tectonic deformation. Doublets of poorly preserved bivalves (*Linga* sp.?) were found in this lithofacies, as well as small planktonic foraminifera. The depositional environment of lithofacies I cannot be defined with any certainty. The macrofossils found in this lithofacies consist of only one (possibly two) different forms, which is a common feature of 'stressed' environments. Deposits strictly comparable to lithofacies I have not been found at the base of the SCO Fm elsewhere in Aspromonte. It can be assumed that carbonate-rich sediments were not widely distributed, because they could only be deposited in laterally confined parts of the basin which were sheltered from coarse clastic sedimentation.

10 OLIGOCENE–EARLY MIOCENE DEPOSITIONAL ENVIRONMENTS

10.1 Overall palaeo-environmental evolution

The sedimentological interpretations of individual lithofacies (Table 1), coupled with their vertical superposition (Figs 23, 24), clearly show that the occurrence of certain subenvironments is limited to the lower or upper part of the SCO Fm: lithofacies deposited in a continental setting (A, and B underlain by red paleosols) are only present at the base of the formation, whereas deep marine deposits (H and the uppermost units of G) are confined to its upper part. The SCO Fm thus represents an overall transgressive sequence, in which the transition from a terrestrial to a deep marine environment was recorded. This interpretation is consistent with the palynological analyses carried out for the present study (N.M.M. Janssen), as well as observations of other authors:

(1) In the Serre area, shallow marine deposits (FORAMOL-carbonates and sands containing larger foraminifera, marine molluscs and echinids) are present in the lower part of the SCO Fm (Principi 1940; Nicotera 1963; Afchain 1966; Meulenkamp *et al.* 1986). In the S. Serre, these shallow marine deposits are underlain by lagoonal sediments (alternations of mudstones and coarse-grained sandstones containing lignite beds, laeustrine carbonates, and brackish-water molluscs; Principi 1940; Nicotera 1963). Palynofacies analyses of samples from the lowermost part of the SCO Fm in NE Aspromonte also suggest that sedimentation started in a terrestrial to lagoonal setting, which rapidly changed to a shallow marine environment, as inferred from the abundance of land-derived organic matter (wood, cuticles), and the appearance of shallow marine dinoflagellate cysts, whereas deep marine forms are absent (Tables 2 and 3; N.M.M. Janssen, pers. comm.). No calcareous microfossils were found at these levels.

(2) Deep marine foraminiferal assemblages, consisting of planktonic and upper bathyal benthic forms (Murray 1973; Boltovskoy & Wright 1976; Wright 1978) have only been observed in the upper fine-grained part of the SCO Fm [lists of foraminiferal species from the SCO Fm can be found in Nicotera (1963), Guerrera & Wezel (1974), Barrier *et al.* (1987), and Courme & Mascle (1988)]. Palynofacies analyses of these upper levels (NP25–NN2) also indicate a deep marine environment (Table 3). The environment and age of the upper part of the SCO Fm are in accordance with previous interpretations: The SCO Fm is generally considered to represent an Early Miocene slope, canyon or proximal submarine fan association (Bonardi *et al.* 1980; Carmisciano & Puglisi 1982; Cavazza 1989).

10.2 Lateral and vertical lithofacies transitions

High rates of erosion and sediment supply may be assumed during deposition of the proximal, coarse-grained lithofacies of the SCO Fm, indicating rapid uplift of the source area. Synsedimentary tectonic activity is also indicated by the frequently abrupt lateral and unconformable vertical transitions between fine- and coarse-grained sediments, and by the rapid lateral thickness variations of individual lithofacies. Because lithofacies distribution in the SCO Fm was tectonically controlled, a reliable picture of proximal-distal relationships can only be deduced from a comparison of time-equivalent lithofacies, directly underlying the 'silexite' marker bed (lithofacies H). In NE Aspromonte (Fig. 24), the 'silexite' overlies sediments of lithofacies D (column 17), E (column 18) and G (column 16). Lithological correlation of stratigraphic columns in this area suggests that the top of lithofacies B (column 14) can be placed at the same stratigraphic level. The succession of Capo Bruzzano (7 km SE of Sant'Agata; see Fig. 5) is located in the same area. Here, the 'silexite' is intercalated in lithofacies F. In S. Aspromonte, the 'silexite' is intercalated in lithofacies G (Fig. 23). This indicates that virtually all different sub-environments were present within the basin when the 'silexite' was deposited (Early Burdigalian).

Sedimentation in Aspromonte started with local deposition of coarse-grained subacrial sediments (lithofacies

Table 3. The evolution of depositional environments in the Palizzi Formation [locality Sporta, 1 km S of Palizzi (Fig. 5)] and the SCO Fm of NE- and SE-Aspromonte [localities: Aria del Vento, 2 km N of Plati; Africo Vecchio; Chorio, 4 km WSW of Africo Vecchio; Capo Bruzzano; Mottieella; Brancaleone Superiore (Fig. 5)]. Samples from each locality are arranged in stratigraphic order from left to right. Palynological analyses carried out by N.M.M. Janssen. Classification of organic matter types after Van Bergen *et al.* (1990). Symbols used: P = present; C = common; A = abundant; D = dominant; R = reworked; ? = uncertain.

LOCATIONS	Sporta			Aria d.V			Africo V.				Chorio			Capo B.			Mott.			Br.
SAMPLES	A	B	C	4A	8A	9A	37A	38A	39A	41A	45A	47A	48A	58A	59A	61A	66B	66C	68A	88A
ACID-RESISTANT ORGANIC MATTER																				
bisaccate pollen grains	C	D	A	C	A	A	C	P	P	C	P	C	C	C	A	D	C	C		C
asaccate pollen grains	P		P								P							P		C
spores	P	P	P	P	P	P		P			P							P		C
Botryococcus sp.			P				P													
Pediastrum sp.									P											
Tasmanites sp.	P		P												P	P		P		R
dinoflagellate cysts	D	P	C	A	C	C		P	P	P	P	C	P	P	C	C	P	P		
acritarchs						P														
wood	C	A	A	A	A	C	C	A	C	A	A	A	A	C	C	A	A	C	P	A
plant tissue	D	D	D	D	D	C	C	C	P	D	D	D	D	A	C	A	D	A		D
cuticles	P	A	A	C	C	C	A	A	A	C	A	C	C	P	P	P		P		P
fungal remains	C		C			P	P	C	P		P						P	P		C
foraminifera remains															P	P		P		
animal remains							P	P			P				P					P
"woody" black-brown discrete SOM	P	A	A	C	C	C	P	A	A	A	A	A	C	D	A	D	A	A	D	C
"herbaceous" ,, ,, ,,	A	A	A	A	A	A	A	A	A	A	D	D	D	A	A	C	C	D	P	A
"woody" black ,, ,,	P	P	P	C	C	C	P	C	A	C	C	P	C	C	C	C	C	C	C	C
DEPOSITIONAL ENVIRONMENT																				
terrestrial							*													
lagoonal	*		*					*	*		*						*			*
shallow marine		*	*	*	*	*		*	*	*	*	*					*	*		
intermediate marine						*								*	*					
deep marine																*				
uncertain													*						*	
BIOSTRATIGRAPHIC AGE	NP21			NP24			?				NP24			NP25			NP24			?

A,B), presumably in the form of alluvial fans. These rapidly evolved to a lagoonal and shallow marine fan-deltaic association, dominated by sediments of lithofacies C and F. A part of the sediments of facies C was deposited on a steep subaqueous slope (backsets and oblique liquefaction structures), whereas other sediments of this lithofacies were deposited on a subhorizontal surface (high angle foresets). A similar conclusion can be drawn from the lateral variability of lithofacies F: the conspicuous asymmetry of sedimentary structures suggests that at least part of lithofacies F was deposited on a steep submarine slope. A considerable palaeobathymetric range of lithofacies F is indicated by the local presence of small-scale wave ripples (deposited above storm wave base), as opposed to the local absence of wave reworking, coupled with the presence of planktonic foraminiferal carbonate mudstones (deposited below storm wave base). These different depositional settings of lithofacies C and F can be explained by assuming that the basin was filled by debris cones, i.e. coarse-grained fan-deltaic systems with steep subaqueous slopes, dominated by mass flow deposition (cf. Postma 1990).

Relationships between lithofacies C and F within the debris cones are inferred to have been partly lateral and partly vertical. A lateral transition can be assumed in places where facies C pinches out and is transient into facies F (e.g. in the area between Staiti and Brancaleone). This can be explained by assuming that the coarse-grained lithofacies C was deposited near the base of the delta slope, and finer-grained sediments were transported further out into the basin to be deposited as lithofacies F. In the northern part of the area (e.g. between Plati and Sant'Agata), the grainsize of the sediments supplied by the source decreased considerably during deposition of the upper part of the SCO Fm. In such cases, facies C was covered by facies F, which is interpreted as the submarine, distal equivalent of the fluvio-deltaic facies D and E. Comparable lateral and vertical transitions can be assumed for facies F and G in the upper part of the SCO Fm. Between Bova Marina and

Fig. 20 Slumps, pebbly mudstones and intraformational 'rip-up' clasts occur frequently in the upper part of the SCO Fm [Lithofacies F; 1 km S of Bova Superiore (Fig. 5)]. Horizontal scale is approximately 10 m.

Bova Superiore, a rapid lateral transition from facies F to G is present. On the other hand, facies F is gradually succeeded by facies G in relatively distal parts of the basin (e.g. at Capo Bruzzano), indicating a general deepening towards the top of the SCO Fm.

Two distinct coarse-grained fan-deltaic depositional systems are present in S. and E. Aspromonte, which can therefore be divided into two sub-basins. These systems are distinguished on the basis of different sedimentary sequences (the composite columns in Figs 23 and 24), palaeoflow directions (Figs 21, 22) and conglomerate clast compositions. Sediments of the SCO Fm in W. Aspromonte, E and NE of Reggio di Calabria (Gelderloos & Schaafsma 1984; see Fig. 5) are interprcted as a third fan-deltaic system, characterized by SW-ward sediment dispersal. The latter was not studied in detail.

11 THE COARSE-GRAINED DELTAIC SYSTEMS

11.1 The southern deltaic system

The southern deltaic system is present in the SE Aspromonte area, and is characterized by a NE- to SE-ward sediment dispersal, one single 'fining upward' sedimentary cycle, and the presence of Jurassic carbonate clasts in coarse-grained units (Figs 21, 23). The SCO Fm in SW Aspromonte (the area NW of Melito di Porto Salvo) is inferred to belong to this system as well, because it can be easily correlated with sedimentary sequences further E, and shows a comparable direction of sediment dispersal. But there are also two important differences between the SCO Fm of SW and SE Aspromonte: (i) Jurassic carbonate

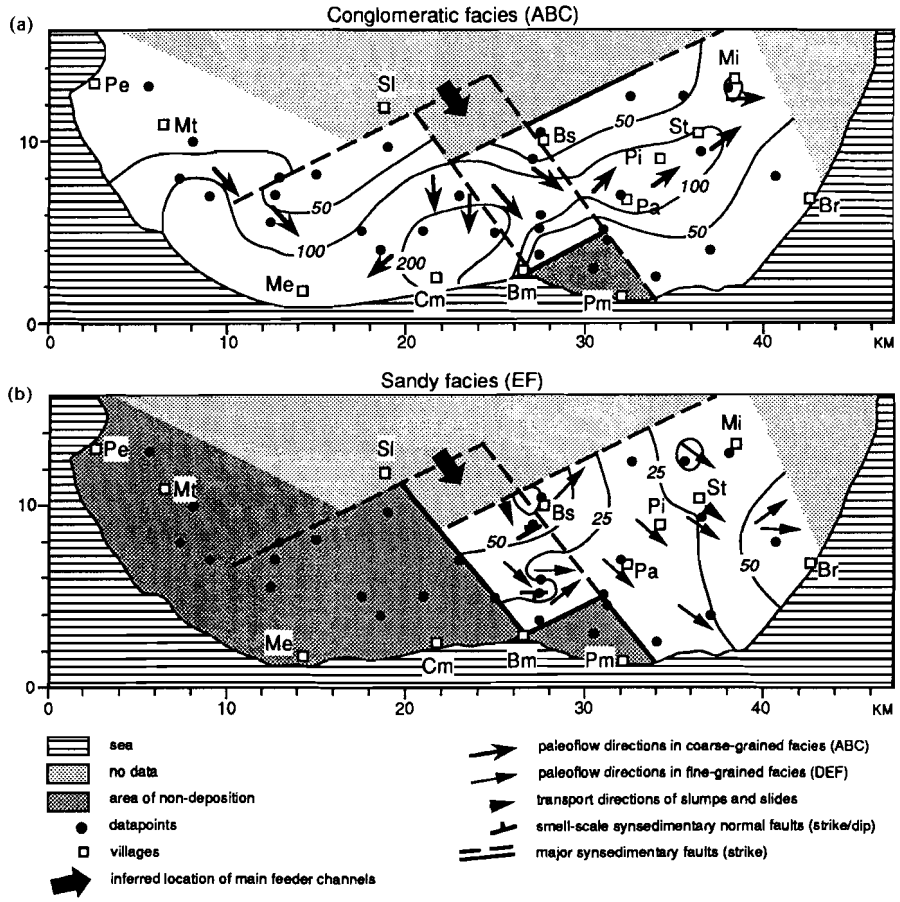

Fig. 21 Isopachs, palaeoflow pattern and synsedimentary deformation in the southern part of Aspromonte. (a) Conglomerate/breccia (lithofacies A–C); (b) Sandstones (lithofacies E, F).

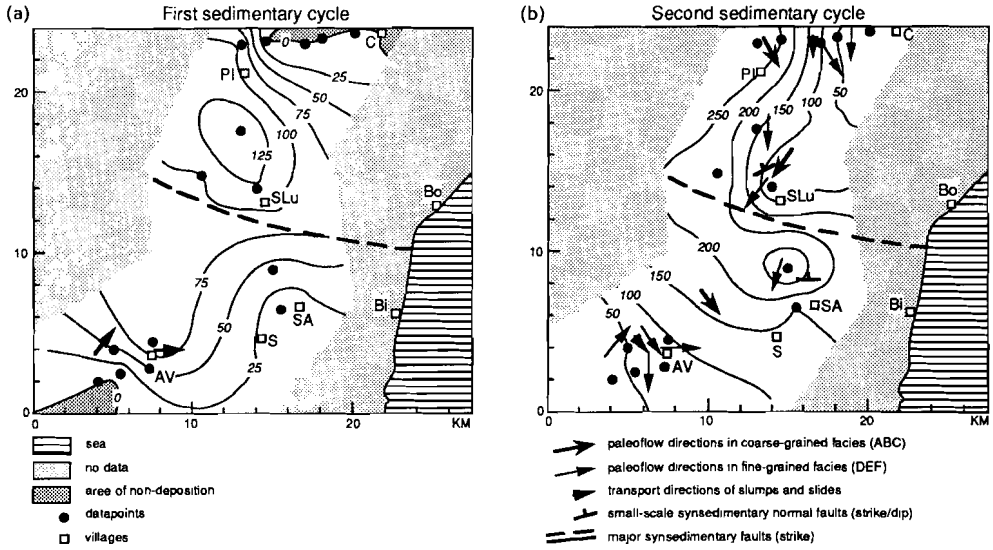

Fig. 22 Isopachs, palaeoflow pattern and synsedimentary deformation in the northeastern part of Aspromonte. (a) First sedimentary cycle (lithofacies A–G); (b) Second sedimentary cycle (lithofacies A–F).

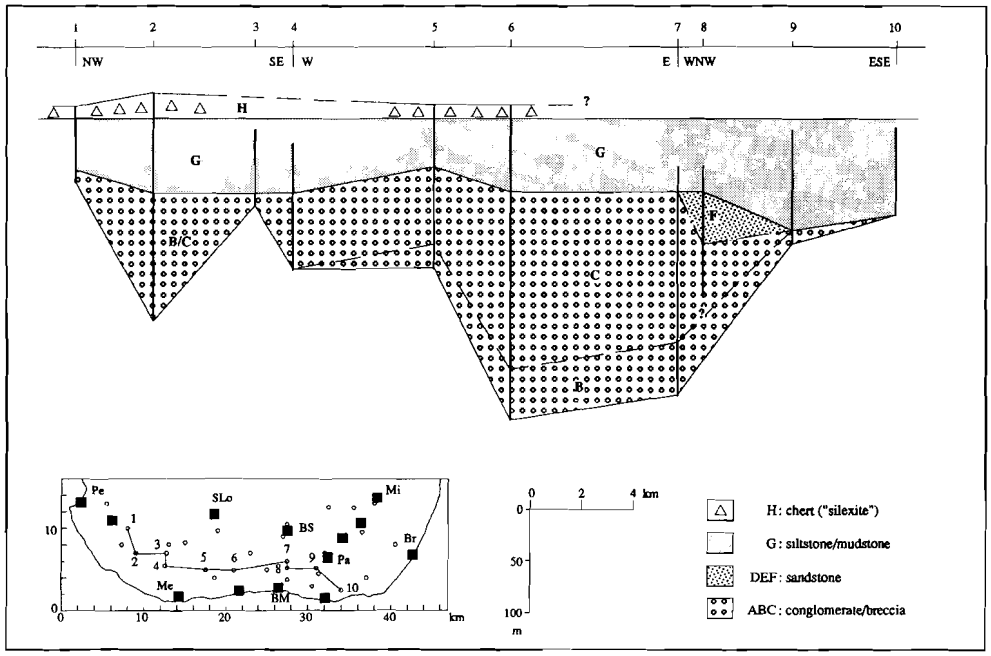

Fig. 23 Sedimentological profile through the southern part of Aspromonte.

clasts, a distinctive feature of this system in SE Aspromonte, have not been observed W of the Amendolea River; (ii) In SW Aspromonte, the abrupt transition from coarse- to fine-grained sediments (C–G) is often unconformable and marked by an erosional surface, whereas a conformable and gradual transition via sandy facies (E and/or F) is present in SE Aspromonte. Major feeder channels of the southern deltaic system were located near the village of San Lorenzo and possibly also to the W of Aspromonte, e.g. near the present Messina Strait (Fig. 21).

In the S. Aspromonte area (Fig. 23), the lowermost part of the SCO Fm consists of subaerial debris flow deposits, scarp breccias and lignite-rich sands, locally underlain by a deeply red-coloured paleosol, indicating a continental or lagoonal setting (lithofacies A, B and ?E). After rapid drowning of the basin and simultaneous uplift of the source area, the S. coarse-grained deltaic system developed (lithofacies B, C, D, E and F). Its initial progradation can be observed 3 km S of Bova Superiore, where a coarsening-upward sequence is exposed. However, on many locations, the coarse-grained subaqueous deposits form the base of the sequence. The coarse-grained base of the SCO Fm in SW Aspromonte (lithofacies B in the area N of Melito) is inferred to have been deposited in a subaerial environment, and is tentatively attributed to an initial phase of alluvial fan sedimentation. On top of the coarse-grained deltaic sequence, fine-grained clastics were deposited, containing a foraminiferal fauna indicating upper bathyal depths (lithofacies G), and an intercalation of 'silexite' (lithofacies H). The latter two lithofacies clearly indicate a deepening phase. In areas of previous non-deposition or erosion, they are found also directly on top of the basement together with local carbonate accumulations (lithofacies I). In the SW part of Aspromonte, 50–60 m of facies G was deposited on top of the coarse-grained deltaic sediments, before the 'silexite' was deposited (Fig. 23). Biostratigraphic datings of the fine-grained sediments indicate that the deposition of coarse-grained sediments had ceased by latest Oligocene time (NP25).

11.2 The northern deltaic system

The northern deltaic system is present in the NE part of Aspromonte, and is characterized by a SW- to SE-ward sediment dispersal, and the absence of Jurassic carbonate clasts in coarse-grained units (Fig. 22). Two distinct upward fining sedimentary cycles can be distinguished within the northern deltaic system, although the lower one is generally incomplete. This is especially the case in the area around Africo Vecchio, which represents the distal part of this system (Fig. 24). The major feeder channel of the northern deltaic system was located NW of Plati.

The lowermost cycle starts with coarse-grained sediments (lithofacies B, C). The first intercalation of fine-grained sediments (lithofacies G), forming the topmost part of the lower upward fining cycle, contains no calcareous microfossils. Palynological analyses suggest that these sediments were deposited in a shallow marine or lagoonal setting. The transition from the lower to the upper cycle is abrupt, except in the distal part of the northern deltaic system. Near Africo Vecchio, a progradational trend is

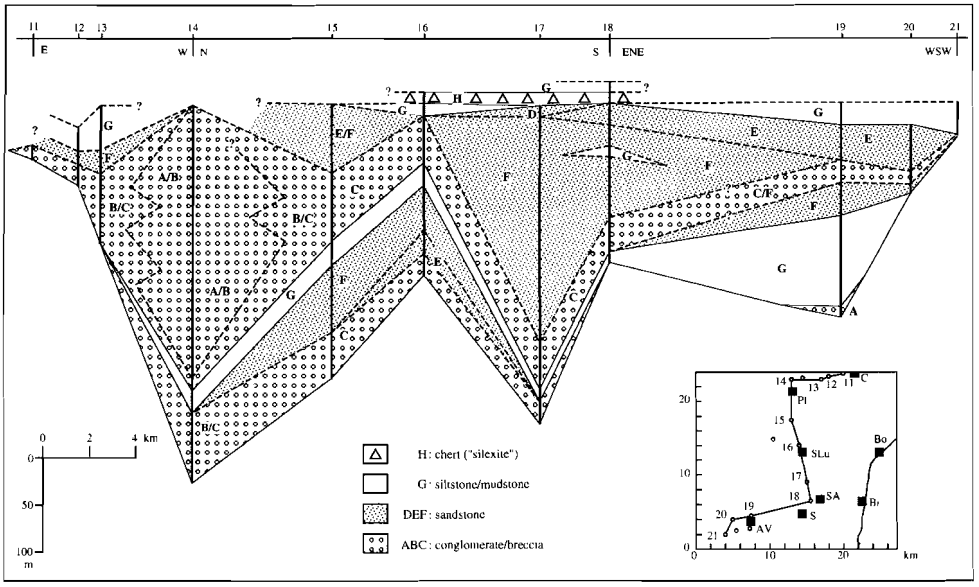

Fig. 24 Sedimentological profile through the northeastern part of Aspromonte.

present at the transition from the lower to the upper sedimentary cycle: coarse-grained deltaic sediments (lithofacies C, F and E) overlie fine-grained shallow marine (lagoonal) sediments (lithofacies G). Near Sant'Agata, facies F is covered by facies E or D, corresponding to a shift from a delta slope to a fluvio-deltaic environment. The coarse-grained sediments of the upper sedimentary cycle are also covered by sediments of lithofacies G. This second intercalation of lithofacies G points to a considerable deepening, and locally contains the 'silexite' marker bed (lithofacies H). In the northern sedimentary system, the 'silexite' was deposited almost directly on top of coarse-grained sediments of the second cycle (Fig. 24), suggesting that deposition of coarse-grained sediment continued up to the Early Miocene (NN2).

12 SYNSEDIMENTARY TECTONICS

12.1 Fault systems and tectono-sedimentary cycles

The lateral variability observed within the SCO Fm points to a strong influence of intrabasinal faults on the sedimentation pattern (Figs 21–24), especially in the coarse-grained units B and C that show abrupt thickness changes over and along present-day faults, inferred to have been active also during deposition of the SCO Fm. Two main synsedimentary fault systems were recognized (Meulenkamp *et al.* 1986; Weltje 1988b; Van Dijk & Okkes 1991). The first is a NE–SW trending system, roughly parallel to the overthrusts of the external Calabrian accretionary wedge (Finetti 1985). This fault system is referred to as the longitudinal system. The second is a NW–SE to WNW–ESE trending fault system, termed the transverse system. The transverse fault system partly corresponds with the strike-slip faults which separated different segments of the CPA during the Neogene (Meulenkamp *et al.* 1986; Moussat *et al.* 1986; Van Dijk & Okkes 1991). At present, normal faulting prevails along both systems (Ghisetti & Vezzani 1981, 1982; Figs 5, 6). Most of the faults in the CPA have been reactivated several times in different tectonic regimes. Repeated tectonic inversions are well documented for the Neogene, during which extension and compression (transpression) alternated (e.g. Boccaletti *et al.* 1984; Ghisetti & Vezzani 1981; Meulenkamp *et al.* 1986; Van Dijk 1991; Moussat *et al.* 1986). During deposition of the SCO Fm, a similar alternation of extension and compression gave rise to a characteristic pulsating pattern of basin evolution.

Two tectono-sedimentary cycles can be recognized in the sub-basins of the S. Serre and Aspromonte areas. At present, there are insufficient biostratigraphic data available for an accurate dating of the cycles, but preliminary results suggest that the first cycle spans the Late Oligocene interval, and the second cycle ean be attributed to the Early Miocene interval. The southern depositional system was active during the first cycle, whereas the northern coarse-grained depositional system was active during both cycles. Each cycle corresponds to an upward fining sequence of the SCO Fm. A cycle starts with a phase of uplift and extension, in which mainly coarse-grained sediments are produced. In the course of the cycle, the coarse clastic supply diminishes, and a tectonic inversion occurs. The end of each cycle is characterized by oblique backthrusting events ('push ups'), which are ascribed to transpression. In the SE Aspromonte area, the first cycle is clearly marked by changes in paleoflow patterns, accompanying the activity of the principal faults. A schematic picture of fault activity during a tectono-sedimentary cycle is presented in Fig. 25. Structural models of 'mixed-mode' basins (Gibbs 1984, 1987), which exploit the geometric analogy between thin skinned thrusting and listric extensional faulting, emphasize that faults are commonly rooted in sub-horizontal detachment zones. The 'roll on–roll off' pattern, which marked the tectono-sedimentary evolution of the Aspromonte basin, was produced by episodic re-utilization of the thrust- or detachment-zones of the Calabrian basement units.

12.2 The first tectono-sedimentary cycle (Late Oligocene)

The start of the first tectono-sedimentary cycle (NP24) coincided with the uplift and subsequent extension of the Aspromonte basement between 30 Ma and 25 Ma (Platt & Compagnoni 1990; Bonardi *et al.* 1987; Table 2). Synsedimentary extensional faulting is clearly documented in the SE part of Aspromonte, where thick coarse-grained units (lithofacies A, B, C) are confined to a narrow elongated area, delimited by NE–SW trending longitudinal faults (Fig. 21a). The coarse-grained units show a rapid stepwise thinning to the NW and SE. In the SW part of Aspromonte (between Motta San Giovanni and Condofuri Marina), a repetitive pattern of comparable lateral thinning and thickening trends was observed in the coarse-grained units. The palaeocurrents (Fig. 21a) indicate that dispersal of coarse-grained sediment was mainly parallel to the NE–

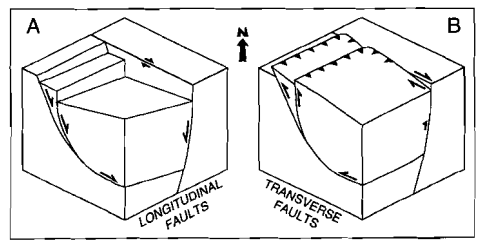

Fig. 25 The 'roll-on–roll-off' activity of the longitudinal and transverse faults during a tectono-sedimentary cycle: (A) Oblique extensional faulting during phases of uplift and extension; (B) During compressional phases, oblique backthrusts or 'push ups' were formed, and dextral strike–slip occurred along the major transverse faults (see text).

SW trending longitudinal faults. The coarse-grained sediments of the SCO Fm were laterally confined by dominantly NE–SW oriented syn- and antithetic longitudinal faults, which delimited a series of narrow grabens.

The influence of the transverse fault system on sediment distribution in the southern depositional system is less conspicuous, but can also be inferred from a combination of palaeocurrents and lateral changes in thickness. The thickness of coarse-grained facies reaches a maximum between the villages of Condofuri Marina and Bova Marina (Figs 21a, 23), on the SW side of the major transverse fault in this area. The radial palaeoflow pattern suggests sediment input from a point source which must have been located near the village of San Lorenzo, in the upper reaches of the present Amendolea river. The same point source is inferred for the sandy–silty lithofacies (E, F), which were deposited on top of the coarse-grained units in the SE Aspromonte area. The location of this inferred point-source corresponds to the position of the 'Condofuri Zone' of Meulenkamp *et al.* (1986), a fault zone which was recognized on the basis of stratigraphic analyses of Neogene sediments.

Tectonic inversion occurred during or after the deposition of lithofacies E and F, as demonstrated by the reactivation of this major transverse fault. The block which bordered the faultzone to the SW was uplifted and affected by erosion during or after deposition of lithofacies E and F, whereas it previously formed a local depocentre for the coarse-grained sediments (Fig. 21b). This conspicuous change of the sediment dispersal pattern can be explained by a N- to NW-ward backthrusting of the fault block, which caused its tilting towards the S and pushed up its N tip. Additional evidence for this inversion can be found in the sediments of lithofacies E and F to the NE of the transverse fault zone. They are characterized by a general SE-ward dispersal pattern, which was apparently unaffected by the NE–SW oriented longitudinal faults (Fig. 21b). Local deviations from the general SE-ward dispersal (e.g. near Bova Marina and Brancaleone) are mainly caused by wave reworking. A true exception is found in the area around Bova Superiore, where NE-ward dispersal was parallel to the NE–SW oriented faultzone delimiting the conglomeratic facies to the NW. The proximity of this faultzone can also be inferred from the frequent intercalations of large intraformational clasts, pebbly mudstones and southward directed slumps in this part of the area (Fig. 20). On the other side of this fault, between the villages of Bova Superiore and Samo, a small outcrop of calcareous mudstones with bivalves is present (lithofacies I). Carbonate accumulation is inferred to have taken place on an intrabasinal ridge, which separated the southern from the northern sub-basin.

A detailed reconstruction of the first tectono-sedimentary cycle in the northern sub-basin was not possible. S- to SW-ward thinning of coarse-grained facies and thickening of fine-grained facies in the same direction suggests the presence of a point source NW of Plati, coinciding with the transverse fault which separates Serre and Aspromonte (Bonardi *et al.* 1984; Messina *et al.* 1988; Figs 22, 24). At the end of the first cycle, the sediments of the northern depositional system were backthrusted towards the N–NW (at Aria del Vento, N of Plati). Their present subvertical position is inferred to be the result of two successive backthrusting events. The second backthrusting event also affected the coarse-grained sediments of the second cycle (presently characterized by a S- to SE-ward dip of 45°).

12.3 The second tectono-sedimentary cycle (Early Miocene)

Deposition of coarse-grained clastics during the second tectono-sedimentary cycle was limited to the northern deltaic system. In the southern system, only fine-grained lithofacies (G) were deposited. In the NE part of Aspromonte, lateral confinement of coarse-grained clastics by longitudinal normal faults is less well documented, except for the area between Plati and Cimina, where a stepwise, fault-controlled lateral thinning of coarse clastics in an E-ward direction was observed (Figs 22b, 24). Contemporaneous activity of the longitudinal and transverse fault systems is inferred on the basis of lateral thinning of coarse clastics in both E- and SW-ward directions. The wedge shape of the coarse-grained sediments in this area suggests that deposition took place on a tilted footwall block or half-graben (cf. Leeder & Gawthorpe 1987). The extensional origin of this wedge-shaped pattern is also suggested by numerous E–W to NE–SW oriented small scale normal faults in deposits of the second cycle (Fig. 22b). In spite of the fact that the northern depositional system is characterized by S-ward directed palaeocurrents, its sediments were not supplied from the N (the S. Serre area). The northern depositional system must have been fed from the W or NW, because Jurassic carbonates of the Stilo Unit, which are an important constituent of the Calabrian basement in the area around the village of Antonimina in the S. Serre, are absent in the coarse-grained sediments of the northern depositional system. This indicates that Serre and Aspromonte were effectively separated by activity of the transverse fault system.

The shift from extension to compression at the end of the second tectono-sedimentary cycle, coeval with the continental collision on Sicily, is well documented in the southern depositional system. The Lower-Middle Burdigalian 'silexite' marker bed, intercalated in the upper part of the SCO Fm, is locally absent, whereas the SCO Fm is conformably overlain by the Late Burdigalian–Early Langhian 'Argille Scagliose', in which no reworked components of the SCO Fm have been observed. This leads to the conclusion that the upper part of the SCO Fm, including the 'silexite', was removed in the Middle-Late Burdigalian interval, prior to the emplacement of the 'Argille Scagliose'. The presence of tightly folded, slumped 'silexite' beds, observed south of the village of Motta San Giovanni, suggests that submarine sliding was responsible for this removal. The inversion of intrabasinal listric normal faults, and related tilting of the fault blocks towards the S, provides a mechanism for the submarine sliding of

the 'silexite' beds, triggering the downslope movement of unconsolidated piles of sediments (Fig. 25). The S-ward tilting of fault blocks is also suggested by the frequent occurrence of pebbly mudstones and S-ward directed slumps in the uppermost part of the SCO Fm all over Aspromonte (Figs 21b, 22b). This tilting is attributed to a second phase of oblique N- to NW-ward backthrusting in the N part of Aspromonte, as observed at Aria del Vento (N of Plati).

13 THE BOUNDARY BETWEEN BOTH SUB-BASINS: THE BACKTHRUST OF SAMO

The Same block, consisting of Calabrian basement rocks covered by sediments of the southern depositional system, was thrusted onto sediments of the northern depositional system (Figs 5, 6) along a NE–SW oriented fault, traceable from Campolico (3 km NW of Samo) to Monte Lesti (2 km S of Africo Vecchio). The backthrusted Samo block is bounded at its NE side by a NW–SE oriented subvertical fault, cross-cutting the thrust plane. At the other side of this fault, the backthrust can be traced in a NE-ward direction up to Mt. Varet (4 km N of Samo, see Fig. 5). In this part of the area, basement rocks were not involved in thrusting, and the sediments of the SCO Fm are virtually undeformed, indicating that shortening at this side of the NW–SE oriented fault was limited. N- to NW-ward tectonic transport of the Samo block can be assumed on the basis of NE–SW to E–W trending fold axes in sediments of the footwall, observed in the area W of Sant'Agata, and the area S of Africo Vecchio. The minimum amount of horizontal displacement of the Samo block is inferred to be one km, as indicated by the presence of overthrusted sediments in the area between Monte Jofri and Portella d'Orgaro (about 4 km WNW of Samo, see Fig. 5). The original location of the Samo block is inferred to have been NE of Motticella. The N- to NW-ward direction of backthrusting indicates that the NW–SE oriented bounding fault was a transpressional dextral strike-slip or oblique-slip fault (oblique backthrust).

Biostratigraphic analyses of the footwall sediments exposed at Portella d'Orgaro, 3 km WNW of Samo (Van Haeringen 1985) indicate the presence of Upper Aquitanian–Lower Burdigalian (NN2) coccolith assemblages, thus excluding a Palaeogene age of this backthrusting event as suggested by Minzoni (in press). The presence of 'Argille Scagliose' in the footwall indicates that the backthrusting occurred after the Middle Burdigalian, i.e., during or after the second tectono-sedimentary cycle, which coincided with the emplacement of the 'Argille Scagliose'. The position of the oblique backthrust of Samo corresponds to the boundary of the northern and southern depositional systems. Thus, a N- to NW-ward displacement of (at least part of) the southern sub-basin with respect to the N sub-basin should be incorporated into a reconstruction of the pre-Middle Miocene Aspromonte Basin. A more precise reconstruction of relationships between the two depositional systems of the SCO Fm can be made by taking into account the sedimentological observations:

(1) A convergent paleoflow pattern of coarse-grained sediments is present in the N-most part of the southern sub-basin: palaeoflow of the SCO Fm upon the Samo block is consistently towards the SE; Near Staiti and Motticella, paleoflow is towards the NE and E, respectively (Fig. 21a). During the second tectono-sedimentary cycle, transport of coarse clastics in the northern sub-basin (Sant'Agata block) was to the S–SE (Fig. 22b). The presence of a NW–SE oriented synsedimentary transverse fault, which separated the northern from the southern sub-basin, would explain the apparent deflection of palaeoflow directions towards the SE. Sediments derived from both deltaic systems would have been transported along this faultzone into deeper parts of the basin, i.e. in the direction of Capo Bruzzano.

(2) At Capo Bruzzano (7 km SE of Sant'Agata, see Fig. 5), the base of the SCO Fm is not exposed. The lowest levels show NE- to SE-ward sediment transport and contain Jurassic carbonate clasts. On higher levels, only S to SE directed palaeocurrents are present, and Jurassic carbonate clasts are absent. This may indicate that the base of the sequence, deposited during the first cycle, was largely derived from the southern sub-basin, and the upper part of the sequence, deposited during the second cycle, was largely derived from the northern sub-basin. The sediments of Capo Bruzzano, consisting of lithofacies F, are therefore thought to represent the fill of a submarine canyon, which was fed by both depositional systems. The inferred transverse fault located between both sub-basins of Aspromonte apparently formed a topographic 'low' (cf. Gawthorpe & Colella 1990), and therefore fixed the position of this canyon.

The Aspromonte basin thus provided temporary storage for clastics derived from the European (Sardinian) hinterland, because a large part of the detritus was transported out of the basin via submarine canyons (Fig. 26). Some of this material eventually reached the foredeep: Oligo-Miocene submarine fan systems like the Reitano Formation (Loiacono & Puglisi 1983), that were deposited on top of Neotethyan oceanic crust, consist of metamorphic and plutonic detritus derived from the basement rocks of the S. part of the CPA (Puglisi 1987). This type of dispersal and temporary storage is termed 'cascade feeding' (Got *et al.* 1981).

14 STRUCTURAL EVOLUTION OF SOUTHERN CALABRIA

14.1 Late Early Oligocene reactivation of faults

The simultaneous activity of the longitudinal and transverse faults, inferred on the basis of the combined structural-

sedimentological analysis of the SCO Fm (Figs 21–24), was initiated during uplift and subsequent extension of the Aspromonte area in the Late Oligocene (Platt & Compagnoni 1990). Several observations suggest that both fault systems already existed, and were reactivated as oblique-slip faults (Fig. 25a) when deposition of the SCO Fm started:

(1) The WNW–ESE oriented transverse fault which forms the tectonic contact between the Calabrian basement units of Serre and Aspromonte (the Antonimina–Molochio Line; Messina *et al.*, 1988) is reported to have been sealed by sediments of the SCO Fm (Bonardi *et al.* 1984), indicating that this fault had been active prior to deposition of the SCO Fm. Another transverse fault in the same area, 2–3 km to the S, was reactivated during deposition of the SCO Fm (see Fig. 5), and delimited the northern sub-basin of Aspromonte to the NE. Sedimentary facies and sequences of the SCO Fm in the S-most part of the Serre near Antonimina and Cimina (Nicotera, 1963), are distinctly different from those in the N-most part of Aspromonte at Aria del Vento (near Plati), and cannot be correlated. Furthermore, the absence of Jurassic carbonate clasts from the Stilo Unit in sediments of the northern depositional system of Aspromonte indicates that these sediments were not derived from the S. Serre, but may have been supplied from the NW by a feeder channel which was fixed by the active transverse fault (see Fig. 26). This 'segmented' source–basin relationship is also supported by lateral and vertical compositional trends of the SCO Fm (Fig. 4).

(2) A reactivation of the longitudinal faults is most likely from the fact that the S. part of the CPA had been subject to S- to SE-ward thrusting during the Early Oligocene shortening phase, which preceded deposition of the SCO Fm. This phase is clearly documented on NE-Sicily, where the Frazzanò Formation was incorporated into the pile of European and Neotethyan nappes, which were unconformably covered by the SCO Fm and the Reitano Formation (Ogniben 1960; Lentini & Vezzani 1978; Puglisi 1987; Fig. 3). The pre-Late Oligocene deformation phase observed in the Aspromonte Unit, inferred to have been associated with crustal thickening and brittle thrusting prior to uplift and exhumation of the Aspromonte Unit (Platt & Compagnoni 1990), can also be attributed to this Early Oligocene shortening phase. Overthrusting of the lowermost Oligocene Palizzi Formation (Bouillin

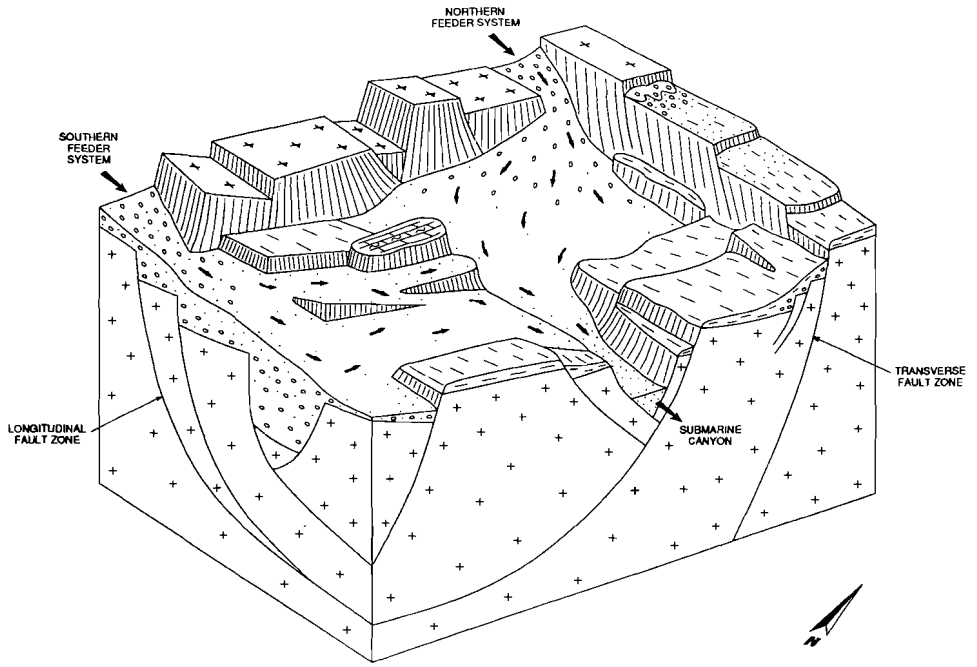

Fig. 26 Reconstruction of the relationship between fault pattern and dispersal of coarse-grained sediments in the Aspromonte Basin. NW–SE to WNW–ESE oriented transverse faults fixed the location of feeder channels and submarine canyons, and determined the boundaries between different sub-basins. The NE–SW oriented longitudinal faults delimited a series of elongated fault blocks parallel to the basin margin, and controlled sediment dispersal within each of the sub-basins. The southern system was active during the first tectono-sedimentary cycle, whereas the main activity of the northern system occurred during the second cycle. Dispersal paths of both systems ('cascade feeding') are depicted by arrows.

et al. 1985; N.M.M. Janssen, tables 2 and 3) by rocks of the Aspromonte Unit may have occurred in the same time interval (corresponding to biozones NP21–NP23).

14.2 Oligo–Miocene strike-slip displacement

Large scale dextral strike-slip displacement along some of the transverse faults during the Oligo–Miocene interval is suggested by palaeogeographical scenarios emphasizing the oblique convergence of the European and African margins (Fig. 2). Dextral strike-slip movements along NW–SE oriented transform faults, which are necessary to account for the rotation of the Corsica–Sardinia 'block', were confirmed by geophysical studies of the W. Mediterranean back arc basins (Montigny *et al.* 1981; Burrus 1984; Rehault *et al.* 1984, 1985; Dewey *et al.* 1989; Boccaletti *et al.* 1990). Field observations in Aspromonte do not confirm large-scale dextral displacement between the different sub-basins during deposition of the SCO Fm, but rather suggest that the Aspromonte basin formed a single segment of this inferred strike-slip belt. Minor dextral strike-slip displacements along the transverse faults within this segment, resulting from N–S to NW–SE compression, adequately explain the oblique backthrusting and S-ward tilting ('push-up') of individual fault blocks (Fig. 25b). Strike-slip displacement during Oligocene–Early Miocene extensional phases has not been documented, and may be difficult to prove in the absence of conclusive evidence (see review by Gawthorpe & Colella 1990). The apparent contradiction of regional palaeogeographic models and field observations leads to the conclusion that two types of transverse faults were present in the S. part of the CPA:

(1) Major transverse faults or fault zones, which have been intermittently active as dextral strike-slip faults, at least from the Neogene onward (Boccaletti *et al.* 1984; Meulenkamp *et al.* 1986; Moussat *et al.* 1986). They are represented by the present day Taormina Line (Amodio-Morelli *et al.* 1976), and possibly also by the fault zone between Serre and Aspromonte (Meulenkamp *et al.* 1986; Moussat *et al.* 1986). The spacing of these strike-slip faults, bounding the Aspromonte segment on its SW and NE side, is approximately 50 km. These faults may correspond in part to the 'tectonic lines' of Boccaletti *et al.* (1990), and the transform faults of Rehault *et al.* (1984, 1985) and Dewey *et al.* (1989). Large-scale strike-slip displacement along the major transverse faults seems reasonable, because these faults also coincide with lateral discontinuities within the Calabrian basement complex (Bonardi *et al.* 1984; Messina *et al.* 1988).

(2) Minor transverse faults include those that bounded tilted fault blocks and fixed the entry points of coarse clastics within the Oligo–Miocene Aspromonte basin. These minor faults may be termed transfer faults (Gibbs 1984; Leeder & Gawthorpe 1987), because they separated basinal compartments characterized by different fault geometries, and by different amounts of stretching or shortening during deposition of the SCO Fm. Displacement during sedimentation of the SCO Fm is inferred to have been predominantly oblique, reflecting the number and geometry of structural elements in different sub-basins on both sides of the fault. Some of these transfer faults were reactivated during the Neogene as strike-slip faults (Meulenkamp *et al.* 1986; Moussat *et al.* 1986). The NW–SE oriented 'Condofuri Line' (Meulenkamp *et al.* 1986), that fixed the position of the point source of the southern depositional system, should be regarded as one of these minor faults. There is no evidence to suggest a tectonic superposition of the NE-Aspromonte area upon the SW-Aspromonte area along the 'Condofuri Line', as postulated by Van Dijk & Okkes (1991).

14.3 Calabrian Basin formation

Calabria is inferred to have formed a part of the Corsica–Sardinia 'block' up to the Late Miocene, at the start of rifting on the upper Sardinian margin and the formation of the Tyrrhenian back arc basin (Kastens *et al.* 1988). The position of Calabria is generally assumed to have been somewhere E or SE of Sardinia (Fig. 2), i.e. on the N. margin of Neo-Tethys (Bouillin 1984; Knott 1987). The Oligocene evolution of the Sardinian Rift, a back arc basin of the Apennines–Maghrebides orogenic system (Cherchi & Montadert 1982a, b) is remarkably similar to that of the Aspromonte basin (Fig. 27). Close similarities with regard to timing of basin formation [Late Early Oligocene (NP23/24), approximately 30 Ma], tectonic style, and sedimentary facies in both areas suggest that the structural evolution of the Calabrian basement complex was initially coupled with that of the back arc area of the SE-ward migrating orogenic system.

The combination of the inferred dextral strike-slip along the major transverse fault zones, the extensional mode of basin formation, and the thrust belt geometry of the CPA that was inherited from pre-Late Oligocene shortening events, suggest that the Calabrian basins originated as a series of thin-skinned pull-apart basins (cf. Royden 1985). The geometry of the Calabrian basins was determined by the longitudinal and transverse faults, which had probably formed during (or before) the Early Oligocene thrusting phase. In the Late Oligocene–Early Miocene, the basins were subsequently carried 'piggy-back' towards the SE on top of the Calabrian basement nappes, and became incorporated into the Calabrian–Maghrebide accretionary wedge.

15 LARGE-SCALE CONTROLS ON BASIN EVOLUTION

15.1 Growth of the Maghrebide accretionary wedge

The pulsating evolution of the Aspromonte basin can be regarded as a response to episodic N–S to NW–SE oriented

compression, that induced progressive S- to SE-ward thrusting of Calabrian basement units onto Neotethyan oceanic units, as recorded on Sicily (Fig. 3). The tectono-stratigraphic relationships of the Eocene–Early Miocene sediments on NE Sicily can be used to make some inferences about the pre-Middle Miocene sequence of thrusting: The first thrusting phase, tentatively placed in the Late Cretaceous–Eocene, involved only European basement units (in the Sardinian hinterland?). In addition, the Early–Late Oligocene thrusting phase involved the N-most Neotethyan units (unconformably covered by Late Oligocene sediments). During the thrusting phase in the Early Miocene, continental collision occurred on Sicily. Accretion of new thrust sheets was accompanied by movements of the older thrusts ('out-of-sequence' thrusts), and backthrusting of the 'Argille Scagliose'. The internal shortening of the Calabrian units by N- to NW-ward oblique backthrusting during deposition of the SCO Fm, as observed in Aspromonte, is interpreted as a response to this 'out-of-sequence' thrusting. Between periods of shortening, the Aspromonte basin was subject to extension. The characteristic pulsating basin evolution of Aspromonte, which resulted from this alternation of compression and extension (Fig. 25), can be linked to the growth pattern of the Calabrian–Maghrebide accretionary wedge (cf. Platt 1986).

During its evolution, an accretionary wedge will deform internally until it has reached a stable configuration, and will then try to maintain an equilibrium profile (Platt, 1986). Extension and compression may therefore occur in the rear part of accretionary wedges, depending on the prevailing type of accretion. Following Platt (1986), the late thrusting and backthrusting events in the rear of the Calabrian–Maghrebide accretionary wedge should be related to phases of 'in-sequence' thrust propagation, i.e. frontal accretion, which lengthened the wedge and induced internal shortening (Fig. 28a). The extension can be related to sediment underplating or duplex formation, which thickened the rear part of the wedge, and caused it to extend in order to maintain a 'critical taper' (Fig. 28b). Growth of the Calabrian–Maghrebide orogenic wedge seems to have occurred primarily by underplating or duplex formation, in view of the dominantly extensional setting of the Calabrian basins. The occurrence of large-scale underplating may reflect the importance of 'roll back' in this interval.

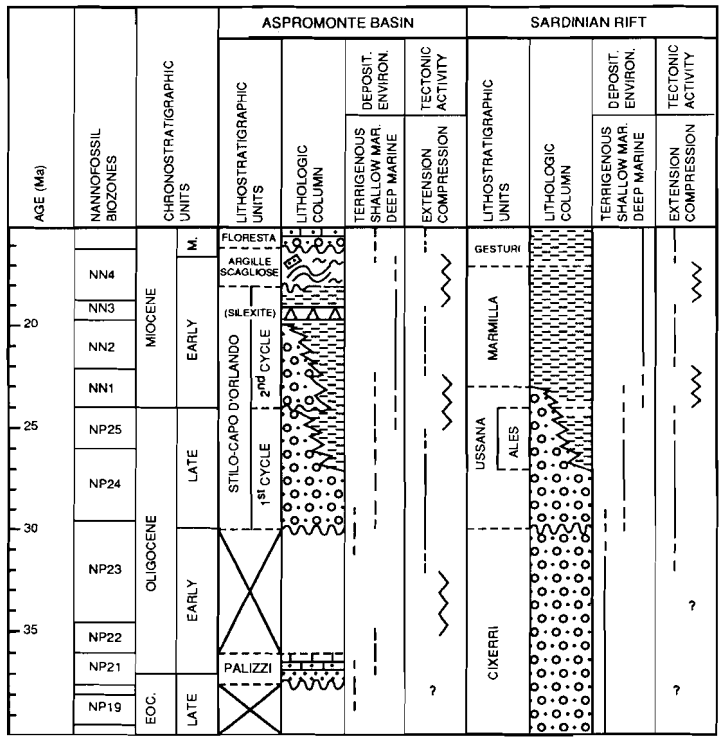

Fig. 27 Late Eocene to Middle Miocene tectono-sedimentary evolution of the southern part of the Calabrian–Peloritan Arc (this paper) and western Sardinia (Cherchi & Montadert 1982a, b; Cherchi & Trémolières 1984).

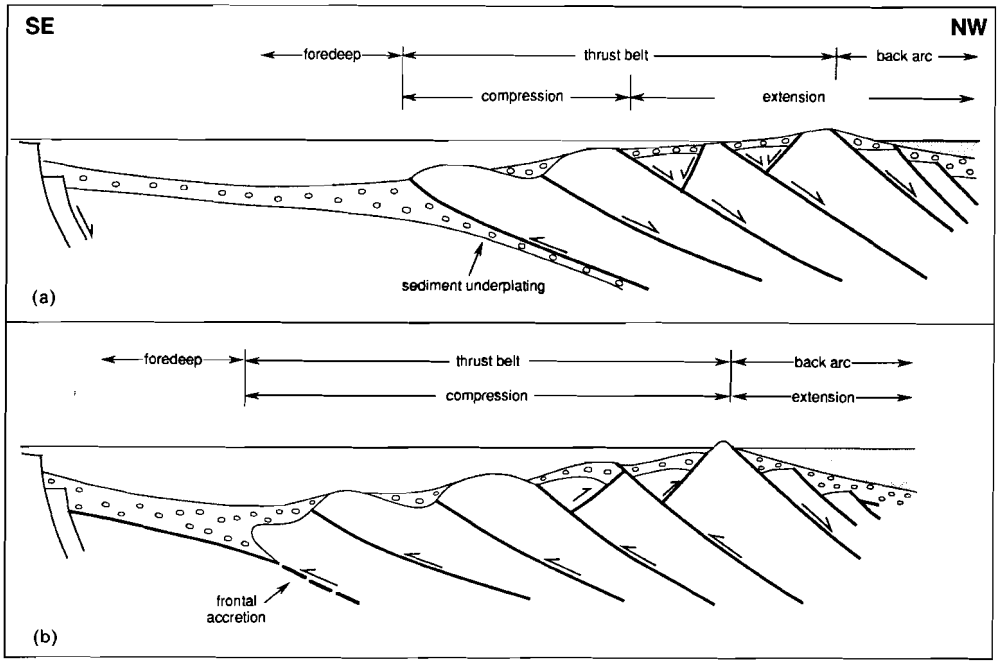

Fig. 28 Mixed-mode piggy-back basins (modified after Platt 1986): (a) Extension caused by large-scale sediment underplating or duplex formation below the rear part of the wedge; (b) Backthrusting and 'out-of-sequence' thrusting accompanied in-sequence thrust propagation or 'frontal accretion'.

15.2 Migration of the Calabrian–Peloritan Arc

The 'arc migration model' (Malinverno & Ryan 1986) attempts to explain the Neogene tectonic evolution of the CPA on a much larger scale, i.e. that of the entire back arc-thrust system. It centres around the fact that opening of the Tyrrhenian back arc basin and thrusting in the Apennines-Maghrebides occurred simultaneously. According to this model, which has been refined by others (e.g. Kastens *et al.* 1988; Wang *et al.* 1989), the SE-ward migration of the CPA is accomplished by a SE dipping low-angle detachment of the upper lithosphere in the Tyrrhenian back arc basin. The downward 'roll back' force, acting on the leading edge of the overriding plate, is considered to be the driving force of this gravitational arc migration. In other versions of the 'arc migration model', mantle doming in the back arc area, contributing to the formation of core complexes, has also been postulated (Van Dijk & Okkes 1991; Carmigniani & Kligfield 1990). A comparable model was proposed for the Neogene basin evolution in the E. Mediterranean Hellenic arc (Meulenkamp *et al.* 1988). Episodic 'roll-back'-induced southward transport of the Hellenic supracrustal slab over a low-angle S-ward dipping detachment fault in the back arc area (Lister *et al.* 1984) may account for the coupling of extension in its rear part (the Aegean Sea), with thrusting in its frontal part (Crete). The Neogene evolution of basins on Crete can be explained by assuming that extension and gravitational collapse of the overthickened wedge occurred between phases of tectonic transport.

The 'arc migration model' can also be used as a working hypothesis for the pre-Middle Miocene evolution of the CPA, because it satisfactorily explains the following facts: (1) 'Roll back' operated in the Late Oligocene–Early Miocene interval (Dercourt *et al.* 1986; De Jonge & Wortel 1990); (2) extension in the Ligurian–Provencal basin was coeval with rotation of the Sardinian–Corsican–Calabrian 'block' and thrusting in the Apennines–Maghrebides (e.g. Burrus 1984; Bouillin 1984; Rehault *et al.* 1985; Cherchi & Montadert 1982a, b; Wezel 1974); (3) Pre-Middle Miocene and Neogene basin evolution in the CPA were very similar (This paper and Van Dijk 1991, respectively), and also share many characteristics with basin evolution in comparable settings, e.g. the Hellenic arc (Meulenkamp *et al.* 1988; Postma *et al.* in press).

The growth pattern of the Calabrian–Maghrebide accretionary wedge and the 'arc migration model' both provide an explanation of basin evolution in the CPA, albeit on different scales. They emphasize back arc and thrust belt evolution respectively, and are probably not mutually exclusive. It appears that in back arc-thrust systems like the Apennines–Maghrebides, the evolution of

basins in the inner part of the thrust belt is closely related to episodic tectonic movements driven by 'roll back'. Unfortunately, the early history of the Apennines–Maghrebides system is not (yet) sufficiently known to justify any speculations on the link between pre-Middle Miocene back arc and thrust belt evolution in the CPA.

16 'SPANNER' OR 'LOOPER' BASINS: A DYNAMIC VIEW

The Oligocene–Early Miocene basins of the S. part of the CPA were carried on top of the progressively SE-ward migrating Calabrian basement units, and acted as temporary sediment reservoirs for the Apennines–Maghrebides foredeep. They share these characteristics with the so-called 'piggy-back' or 'satellite' basins of the N. Apennines (Ori & Friend 1984; Ricci Lucchi 1986). But there are also important differences between the basins of Aspromonte and these classical piggy-back basins: The structural evolution of the Aspromonte basins is associated with episodic 'out-of-sequence' thrusting and backthrusting, strike-slip deformation, and extensional tectonics, whereas the evolution of typical piggy-back basins is (implicitly) related to in-sequence thrust propagation (Ori & Friend 1984; Ricci Lucchi 1986). In view of their origin as extensional or pull-apart basins and subsequent pulsating tectono-sedimentary evolution, the Aspromonte basins may be considered typical examples of 'mixed-mode' basins (*sensu* Gibbs 1987).

The synchronous occurrence of compression and extension in the Apennines has led some authors to distinguish different types of basins within the chain: Roure *et al.* (1990; 1991) use the term 'distensional piggy back basins' to characterize basins which formed above the flats of thrusts, that were reactivated as detachment faults in the inner part of the chain. Boccaletti *et al.* (1990) distinguish 'piggy-back' basins (compressional) and 'intra-deep' or 'back' basins (extensional), and relate their position within the chain and their structural evolution to the migration of the thrust front (in time and space). These distinctions between extensional and compressional piggy back basins seem arbitrary in the light of the dynamics of accretionary wedges: shifts from extension to compression and *vice versa* are to be expected during growth of the wedge, especially in its rear part (Fig. 28). Many long-lived piggy back basins are therefore likely to become subject to episodic tectonic inversions (as illustrated by Van Dijk 1991; Postma *et al.*, in press; and this paper). If it is accepted that tectonic inversions in long-lived piggy-back basins are the rule, rather than the exception, a new terminology is needed: basins which originate and travel piggy-back on top of a thrust belt, and are episodically subject to tectonic inversions, may be termed 'spanner' or 'looper' basins. This new term accurately describes the pulsating kinematic evolution of such basins, that is superimposed upon their net displacement toward the foreland (Fig. 28). According to this view, the 'classical' piggy-back basin on the one hand, and the thin-skinned extensional or pull-apart basin on the other, are reinterpreted as end member stages of 'mixed mode' basin evolution in back arc-thrust systems.

ACKNOWLEDGEMENTS

This paper is the result of a series of field campaigns carried out by the author during the summers of 1985, 1986 and 1989. I thank P. L. De Boer for his indispensable sedimentological advice in the field, and his critical comment on (many) draft versions of this paper. I would also like to thank N. M. M. Janssen (Laboratory of Palynology and Palaeobotany, University of Utrecht), who carried out the palynological analyses. The simplified geological map of Aspromonte (Fig. 5) is largely based on 1:25,000 maps made between 1981 and 1986 by J. Gelderloos, A. van Haeringen, F. J. Hilgen, R. Mulder, R. H. van Rijckevorsel van Kessel, Chr. E. Schaafsma and J. P. de Visser (Institute of Earth Sciences, University of Utrecht). The use of their maps is gratefully acknowledged. Critical reviews by G. Postma, E. Barrier, and F. Roure, as well as constructive suggestions by M. J. R. Wortel, W. Nijman, J. P. Van Dijk, J. E. Meulenkamp and R. L. M. Vissers were very helpful.

CHAPTER 6

END-MEMBER MODELLING AS A TOOL FOR TRACING PALEOGENE THRUST-WEDGE EVOLUTION IN THE SOUTHERN PART OF THE CALABRIAN-PELORITAN ARC (SICILY, ITALY)

1. Introduction

Fossil basin fills along active margins contain sand-sized detritus shed by structural units of the folded and thrusted hinterland in response to paleotectonic activity. Some of these rocks have been completely removed by erosion in the course of the orogenic evolution, and they cannot be examined directly. For this reason, the analysis of secular variations of sandstone framework composition has turned out to be particularly useful for tracing the evolution of orogenic source areas (e.g., Dickinson & Rich, 1972; Schwab, 1981; Ingersoll, 1983; Valloni & Zuffa, 1984; Dickinson et al., 1985; Dorsey, 1988; Lundberg, 1991; Marsaglia & Ingersoll, 1992).

In the previous chapter (Weltje, 1992), a reconstruction of Oligocene to Early Miocene sedimentation and tectonics in the southern part of the Calabrian-Peloritan Arc (CPA) was presented, based on a detailed analysis of the Stilo-Capo d'Orlando Formation (SCOFm). A model of "mixed-mode" piggy-back basin evolution was proposed, resulting from an alternation of oblique backthrusting and transtension along preexisting fault zones in the Calabride-Maghrebide thrust belt. This model of pulsating basin evolution was compared to mechanical models of thrust-wedge evolution (cf. Platt, 1986), which predict "out of sequence" thrusting and backthrusting in the internal part of the orogenic wedge in response to piggy-back thrusting, and extension in response to sediment underplating or duplex formation at the base of the wedge.

The brief summary of pre-Middle Miocene thrust-belt evolution on northeastern Sicily presented by Weltje (1992) strongly suggested that Paleogene thrusts in the inner part of the Calabride-Maghrebide wedge were reactivated several times during subsequent deformation events. Unfortunately, the structural and stratigraphic data available at the time did not fully allow to demonstrate the importance of "out of sequence" thrusting in the CPA, as inferred on the basis of the reconstructed Oligocene to Early Miocene basin evolution. In this chapter, it is attempted to reconstruct the Paleogene thrust-belt evolution in the southern part of the CPA in more detail, by taking into account recently published revisions of structural and stratigraphic relations on northeastern Sicily.

The current review summarizes "generally" accepted and/or well documented structural relations and biostratigraphic ages in the most internal part of the orogen, i.e., the former European (Calabride) and Neotethyan (Sicilide) terranes which have been thrusted in a south to southeastward direction onto the African foreland. The structural and stratigraphic relations allow to propose a scenario of pre-Middle Miocene thrust-belt evolution, that is compared to the provenance evolution of Late Eocene to Early Miocene "piggy-back" basin fills, in order to examine the validity of the basin model proposed by Weltje (1992).

2. Structural units

Timing and sequence of thrusting in the Calabride-Maghrebide orogen are still poorly known, in spite of a large number of geological studies carried out in the past decades. Any attempted review of Calabride-Maghrebide thrust-belt evolution is severely hampered by the multitude of structural and sedimentary classification schemes proposed by various authors. The widely different views are attributable to the poorly constrained biostratigraphic ages of the pre-Middle Miocene deposits, and the complex geometric relations of structural units in the internal part of the Calabrian-Maghrebide orogen. The thrust sheets of the southern part of the Calabrian-Peloritan Arc are exposed in three different areas: from northeast to southwest, these are the Serre, Aspromonte, and Peloritani (see Fig. 4 in the previous chapter). In this study, the Calabride-Maghrebide thrust belt of northeastern Sicily and southern Calabria has been subdivided according to the schemes proposed by Lentini & Vezzani (1978), Giunta (1985), and Bonardi et al. (1976, 1979, 1984, 1992). From base to top of the tectonic sequence, the principal structural units are (Table 1):

SICILIDE UNITS s.l. ("Neotethyan" oceanic paleodomain): exposed in northern and central Sicily.

> **"External" Sicilide units**: Mesozoic to Paleogene sedimentary units (Lentini & Vezzani, 1978).
> **Monte Soro units**: Mesozoic sedimentary units (Lentini & Vezzani, 1978). These units have been thrusted onto the external Sicilide units during or after the Early Miocene.

LOWER CALABRIDE UNITS ("European" continental paleodomain): exposed in northeastern Sicily (Peloritani Mountains). These units are separated from the "Neotethyan" units by the "Taormina Line", an oblique thrust zone which delimits the CPA to the southwest (see Fig. 4 in the previous chapter).

> **Longi-Taormina units**: Low-grade Paleozoic metasedimentary basement with a Mesozoic-Paleogene sedimentary cover (Coltro, 1967; Lentini & Vezzani, 1975; Lentini, 1975; Bonardi et al., 1976; Arnone et al., 1979; Montanari, 1987, 1989; Nigro, 1992). A complicated thrust sequence accompanied by the formation of numerous duplexes developed in at least two stages: the first shortening event probably occurred in the Early Oligocene, the second in the Late Early Miocene (Nigro, 1992).
> **Fondachelli Unit**: low-grade Paleozoic metasedimentary rocks (Bonardi et al., 1976).
> **Mandanici Unit**: low-grade Paleozoic metasedimentary basement with Mesozoic-Paleogene (?) sedimentary cover. Alpine greenschist facies metamorphism has been recognized in the Mesozoic sediments (Atzori et al., 1975; Bonardi et al., 1976; Zuppetta & Sava, 1987). This unit has also been recognized in a small tectonic window in the Aspromonte area (Bonardi et al., 1984).

UPPER CALABRIDE UNITS ("European" continental paleodomain): exposed in northeastern Sicily (Peloritani area) and in southern Calabria (Aspromonte and Serre area).

Aspromonte Unit: medium to high-grade Paleozoic metamorphic basement intruded by granitoid plutonites and affected by Late Oligocene greenschist facies metamorphism (Bonardi et al., 1976, 1979, 1987, 1992). The Late Oligocene metamorphic event is attributed to uplift and extension; it was preceded by an Alpine event related to crustal thickening and brittle thrusting (Platt & Compagnoni, 1989). Internal shortening of the Aspromonte Unit is attributed to transpression during the Early Oligocene and Late Early Miocene (Weltje, 1992). This unit has not been recognized in the Serre area.

Stilo Unit: plutonic and low-grade Paleozoic metamorphic basement with a Mesozoic-Paleogene (?) sedimentary cover (Bonardi et al., 1979, 1984). This unit has not been recognized in the Peloritani area.

Table 1. Lithology of principal Calabride-Maghrebide structural units and related Paleogene sediments.

Structural units		Pre-Late Eocene substratum			Paleogene sediments	
Group	Unit	Assembl. A	Assembl. B	Assembl. C	Eocene to Oligocene	Oligocene to Miocene
Upper Calabride	Stilo	+	+	+	PaFm	SCOFm
	Aspromonte	+	+	-	-	SCOFm
Lower Calabride	Mandanici	-	+	+	cgl. (?)	SCOFm
	Fondachelli	-	+	-	-	SCOFm
	Longi-Taormina	-	+	+ Mi	FrFm	SCOFm
Sicilide s.l.	Monte Soro	-	-	+ MP	PiFm/iRFm	SCOFm
	"external" Sicilide	-	-	+ Po	eRFm	-

Pre-Late Eocene rocks: + = present; - = absent

Assemblage A: Medium to high-grade metasedimentary rocks and plutonic rocks
Assemblage B: Low to medium-grade metasedimentary rocks
Assemblage C: Mesozoic and pre-Late Eocene calcareous rocks
(Mi = Militello Fm.; MP = Monte Pomiere Fm.; Po = Polizzi Fm.)

Paleogene siliciclastics: PaFm = Palizzi Fm.; cgl. (?) = conglomerate (exact age unknown);
FrFm = Frazzanò Fm.; PiFm = Piedimonte Fm.;
iRFm = "internal" Reitano Fm.; eRFm = "external" Reitano Fm.;
SCOFm = Stilo-Capo d'Orlando Fm.

3. Paleogene detrital deposits

The Paleogene detrital deposits which have been deposited on top of the Calabride-Maghrebide structural units (see Table 1) are briefly discussed below.

The **Palizzi Formation** (PaFm) is a lagoonal to shallow marine deposit which unconformably covers karstified Jurassic carbonates attributable to the Stilo Unit. Its presence is limited to a small outcrop in the Aspromonte area (Bouillin et al., 1985). Its age corresponds to that of the Upper Eocene to Lower Oligocene nannofossil biozone NP21 (Weltje, 1992). The Palizzi Fm. has been overthrusted by high-grade metamorphic rocks of the Aspromonte Unit.

The **Frazzanò Formation** (FrFm) has been tentatively attributed to the Late Eocene-Early Oligocene (Coltro, 1967; Duée, 1969; Nigro, 1992). It is in (conformable?) stratigraphic contact with sediments of the underlying Longi-Taormina Unit (Militello Formation). The top of the Militello Fm., which is considered to be of an Early to Middle Eocene age, contains "megabreccias" of Jurassic carbonate clasts, low-grade metamorphic clasts, and resedimented Eocene faunal elements (Fig. 1). The Frazzanò Fm. has been overthrusted by low-grade metamorphic rocks as a result of internal deformation of the Longi-Taormina units (Duée, 1969; Lentini & Vezzani, 1975; Lentini, 1975; Bonardi et al., 1976; Arnone et al., 1979; Nigro, 1992).

The **Piedimonte Formation** (PiFm) is attributed to the Late Eocene-Early Oligocene (Truillet, 1962; Neumann & Truillet, 1963; Puglisi, 1992). The Piedimonte Fm. unconformably covers the Monte Soro Units (Caire & Truillet, 1967), and is in (para)conformable stratigraphic contact with the overlying SCOFm (Fig. 1; Puglisi, 1992). The transition from Piedimonte Fm. to SCOFm is characterized by an interval with slumps and carbonate "megabreccias" (Fig. 1; Truillet, 1962; Carmisciano et al., 1981b; Cassola et al., 1990).

The **Reitano Formation** has been subdivided into an "internal" and "external" facies on the basis of tectono-stratigraphic and compositional differences (Loiacono & Puglisi, 1983; Puglisi, 1992; Cassola et al., 1992). The **"internal" Reitano Formation** (iRFm) unconformably covers the Monte Soro units. Carbonate breccias of the Monte Pomiere Formation locally form its base (Fig. 1; Puglisi, 1992). The **"external" Reitano Formation** (eRFm) of the Sicilide units conformably overlies the Polizzi Formation (Fig. 1). Both Reitano facies are of Early Oligocene age (NP21-NP23: Courme & Mascle, 1988; Cassola et al., 1992; Costa et al., 1992).

The **Stilo-Capo d'Orlando Formation** (SCOFm) unconformably covers the thrust sheets of the southern part of the CPA, i.e., the upper and lower Calabride units and the Monte Soro units (Fig. 1; Bonardi et al., 1980; Cassola et al., 1990; Puglisi, 1992). According to Weltje (1992), the age of the SCOFm ranges from Late Early Oligocene (NP23/24) to Late Early Miocene (NN3). This age assignment has recently been confirmed by biostratigraphic data of Minzoni et al. (1992), Minzoni (1993), and Luciani et al. (in press). These authors claim to have identified three lithostratigraphic units within the SCOFm: their lowermost unit can be correlated with the lower tectono-sedimentary cycle of the SCOFm (NP23/24 to NP25; Weltje, 1992); the other two units (which have not been clearly differentiated) seem to correspond to the upper tectono-sedimentary cycle of the SCOFm (NN1 to NN3; Weltje, 1992).

Lagoonal to shallow marine calcareous lithofacies have been deposited in the Late Early Oligocene (NP23) throughout the southern part of the CPA, especially in the Serre area

(Nicotera, 1963; Afchain, 1966; Meulenkamp et al., 1986). They are commonly included in the SCOFm (Bonardi et al., 1980; Weltje, 1992). Other characteristic lithofacies at the base of the SCOFm are red-coloured breccias in which phyllite, quartz, and Jurassic carbonate clasts predominate (Truillet, 1961; Atzori et al., 1977). The "megabreccias" and "red conglomerates" in Aspromonte and Peloritani contain large olistoliths of Jurassic carbonates derived from the sedimentary cover of the Stilo Unit (Bonardi et al., 1982, 1984). The SCOFm is unconformably covered by the allochtonous "Argille Scagliose Varicolori", a tectono-sedimentary complex backthrusted onto the Calabrian basement units in the Late Early Miocene (Fig. 1; Carmisciano et al., 1981b; Meulenkamp et al., 1986; Courme & Mascle, 1988; Weltje, 1992).

4. Paleogene tectono-sedimentary evolution

The following sequence of deformation events in the Calabride-Maghrebide thrust belt has been reconstructed on the basis of structural and stratigraphic data summarized in Fig. 1:

The first clearly recognizable deformation of the Calabride-Maghrebide units occurred in the Middle to Late Eocene. This phase is marked by megabreccias within the pelagic Militello Formation, by thrusting of the Longi-Taormina units onto the Monte Soro units, and by deposition of the breccias of the Monte Pomiere Formation on the Monte Soro units. This thrusting phase was followed by the first influx of siliciclastic material of the Frazzanò Fm., Piedimonte Fm., and "internal" Reitano Fm., which were deposited on top of the deformed Longi-Taormina and Monte Soro units in the Late Eocene to Early Oligocene. The coeval Palizzi Fm. of the Aspromonte area was deposited on top of brecciated and karstified Jurassic carbonates of the Stilo Unit, suggesting that emplacement of the Stilo Unit also occurred prior to the Late Eocene.

The youngest sediments incorporated in the Longi-Taormina units, the Frazzanò Fm., indicate that further shortening within the Calabrian thrust belt occurred after the Early Oligocene. In the Peloritani Mountains, remobilisation of the Aspromonte Unit is indicated by overthrusting and greenschist-facies metamorphism of the Aspromonte and Mandanici units. This metamorphism also affected the overthrusted Mesozoic-(?)Paleogene sedimentary cover of the Mandanici Unit. It can be correlated with the first phase of Alpine deformation recognized in the Aspromonte area, that is attributed to crustal thickening and brittle thrusting (cf. Bonardi et al., 1987, 1992; Zuppetta & Sava, 1987; Platt & Compagnoni, 1989; Messina et al., 1990). An upper age limit for this thrusting event is provided by a second metamorphic event, attributed to uplift and extension, which was dated radiometrically as Late Oligocene (Bonardi et al., 1987). In the Aspromonte area, the Aspromonte Unit also overthrusted Jurassic carbonates of the Stilo Unit with their Early Oligocene cover (Bouillin et al., 1985; Weltje, 1992).

The SCOFm unconformably covers the tectonic contacts between the Calabride thrust sheets throughout the southern part of the CPA (Bonardi et al., 1980), as well as tectonic contacts between the Longi-Taormina units and the Monte Soro units (Duée & Truillet, 1967; Cassola et al., 1990). A stratigraphic contact has been observed between the Piedimonte Fm. and the SCOFm, marked by slumps and megabreccias at the top of the Piedimonte Fm. (NP23?). Shallow marine carbonates (NP23) and megabreccias of subaerial origin, made up of Jurassic carbonates, phyllite, and quartz pebbles, largely derived from the sedimentary

cover of the Stilo Unit, are widespread at the base of the SCOFm in the southern part of the CPA. They represent the first unconformable sediments deposited on top of the Calabride units after the shortening event. The lower and upper age limits indicate that this second thrusting phase must have occurred within the time interval spanned by nannofossil biozone NP23, i.e., the Late Early Oligocene.

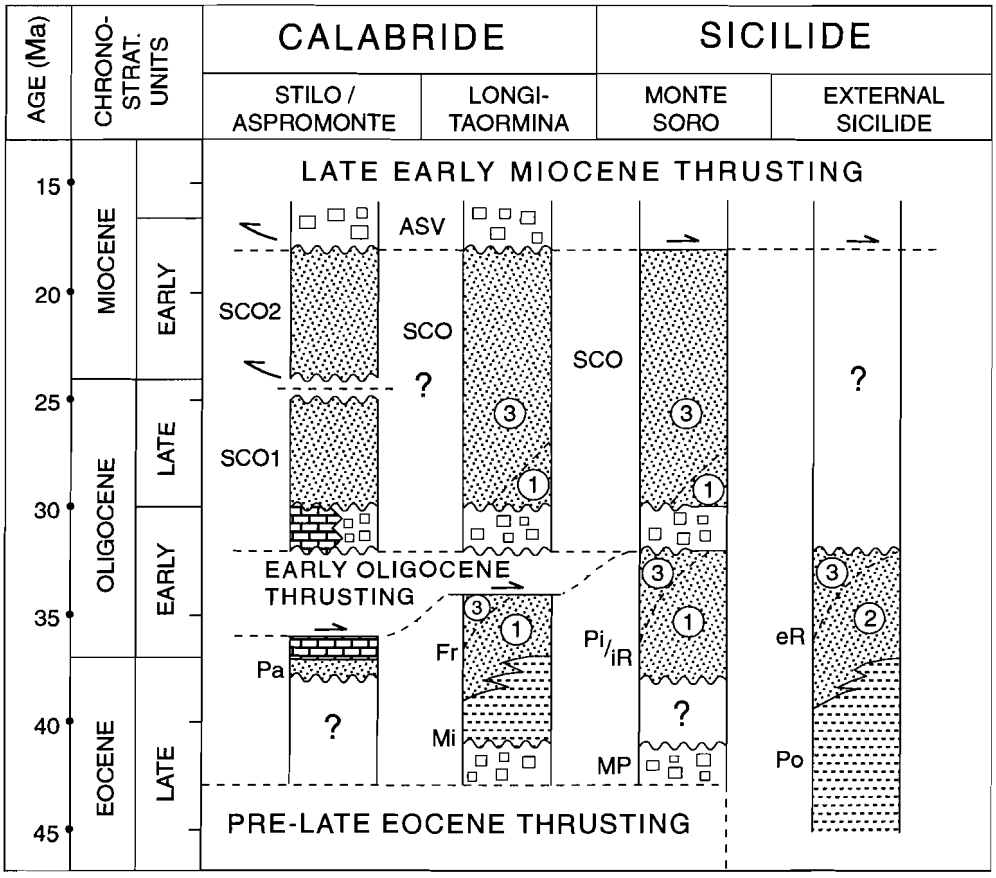

Figure 1. Synthesis of structural and stratigraphic data (Lithologic units are defined in Table 1; ASV = Argille Scagliose Varicolori; numbers 1 to 3 refer to modelled end members, see text).

Late Oligocene uplift and exhumation of the Aspromonte Unit (Bonardi et al., 1987; Platt & Compagnoni, 1989) gave rise to extensional basin formation during the first tectono-sedimentary cycle of the SCOFm (NP24-NP25; Weltje, 1992). Rapid subsidence during the first tectono-sedimentary cycle is documented by lithofacies assemblages showing an evolution from lagoonal and shallow-marine to deep-marine environments. The end of the first tectono-sedimentary cycle is marked by oblique backthrusting of the Aspromonte Unit and the SCOFm, in the Late Oligocene-Early Miocene (NP25-NN1; Weltje, 1992). This transpressional event was followed by a second tectono-sedimentary cycle recognized within the SCOFm (NN1-NN3), which ends with a Late Early Miocene shortening phase widely

recognized throughout the Maghrebides and Apennines (e.g., Meulenkamp et al., 1986; Courme & Mascle, 1988; Roure et al., 1990; Weltje, 1992).

This third major deformation phase in the Late Early Miocene marked the continental collision on Sicily. Progressive deformation is indicated by the influx of detritus derived from the Calabrian basement units in the external Sicilide domain where the Late Oligocene to Early Miocene "Numidian Flysch" was deposited (Guerrera et al., 1986, 1987; Grasso et al., 1987; Carmisciano et al., 1987). The "Numidian Flysch" forms a thick turbidite sequence consisting of quartzarenitic detritus, dispersed in an east or southeastward direction from a deltaic source on the African foreland (Wezel, 1974; Benomran et al., 1988; Guerrera et al., 1992). Deformed Cretaceous to Paleogene pelagic sequences referred to as "Argille Scagliose Varicolori", which incorporate olistoliths of the "Numidian Flysch", were backthrusted onto the internal units of the Calabride-Maghrebide thrust belt during the collision. Widespread slumping of the topmost part of the SCOFm in the Early Miocene (NN3; Weltje, 1992), and the influx of resedimented "Argille Scagliose Varicolori" material in the Aspromonte area mark the start of this deformation event. The Early Middle Miocene Floresta Formation, which unconformably covers the "Argille Scagliose Varicolori" in the Aspromonte and Peloritani areas (Carmisciano et al., 1981b; Meulenkamp et al., 1986; Courme & Mascle, 1988) provides an upper age limit for its emplacement.

Other events, for which no upper age limit is available, may also be attributed to the Late Early Miocene phase of deformation: "Out of sequence" thrusting is documented in the Peloritani, where the uppermost Longi-Taormina subunit has overthrusted the Monte Soro units, as well as the lower Longi-Taormina subunits which incorporate the upper part of the SCOFm (Nigro, 1992). In Aspromonte, north to northeastward backthrusting of the Aspromonte Unit onto the SCOFm and the "Argille Scagliose Varicolori" has been observed (Weltje, 1992). Deformation of the external Sicilide domain occurred during or after this phase: lower and upper time limits are provided by the presence of Early Miocene sediments within these units, and the oldest unconformable sediments on top of the deformed units, which have been dated as Early Late Miocene. The more external units of the African foreland were accreted to the Sicilian wedge between Late Miocene and present times (Bianchi et al., 1987; Lentini et al., 1990; Roure et al., 1990); backthrusts attributable to Late Miocene-Early Pliocene deformation are well developed along the eastern side of the Aspromonte Mountains.

5. Compositional evolution of Eocene to Miocene basin fills

The Paleogene compositional evolution of the Calabride-Maghrebide basin fills of northeastern Siciliy has been investigated in a series of petrographic studies (Carmisciano & Puglisi, 1978a, 1978b, 1982; Puglisi, 1979; Carmisciano et al., 1981b; Loiacono & Puglisi, 1983). The results of these studies, which have been carried out following uniform criteria (essentially those of Gazzi, 1966; Dickinson, 1970; Gazzi et al., 1973) were discussed in two review papers by Puglisi (1987a, 1987b). The compositional database is summarized in Table 2.

Puglisi (1987a) interpreted the compositional evolution of framework components in terms of the provenance types of Dickinson (1985). The Late Eocene to Early Miocene framework compositions of the Frazzanò Fm., Piedimonte Fm., and "internal" Reitano Fm. are

Table 2. Late Eocene to Early Miocene provenance record. Framework mineralogy and accessory minerals were analysed by Puglisi (1987a, 1987b). Rock fragments are modelled in this chapter.

PETROGRAPHIC DATA BASE NORTHEASTERN SICILY (number of analyses)					
Lithostrat. units	Biostrat. age	Data source	Framework mineralogy	Rock fragments	Accessory minerals
Frazzanò (FrFm)	L. Eoc. - E. Olig.	Carmisciano & Puglisi (1978b)	20	20	20
Piedimonte (PiFm)	L. Eoc. - E. Olig.	Carmisciano et al. (1981b)	18	18	15
int. Reitano (iRFm)	L. Eoc. - E. Olig.	Puglisi (1979)	18	18	18
ext. Reitano (eRFm)	L. Eoc. - E. Olig.	Puglisi (1979)	25	25	25
		Loiacono & Puglisi (1983)	10	10	-
Stilo-Capo d'Orlando (SCOFm)	L. Olig. - E. Mioc.	Carmisciano & Puglisi (1978a)	24	24	24
		Carmisciano et al. (1981b)	2	2	2
		Carmisciano & Puglisi (1982)	10	10	10

characterized by the evolution from "recycled orogen" or "mixed" provenance to "basement uplift" provenance, whereas the SCOFm shows an exclusive "basement uplift" provenance. The accessory mineralogy of the Frazzanò Fm., Piedimonte Fm., "internal" Reitano Fm., and SCOFm (Puglisi, 1987b) displays an analogous compositional evolution from associations dominated by ultrastable minerals (zircon, tourmaline, rutile, anatase, brookite) to associations dominated by metastable minerals (garnet, monazite, xenotime). The "external" Reitano Fm. shows an evolution from "magmatic arc" to "basement uplift" provenance, whereas its accessory mineral assemblage evolves from an unstable association (titanite, epidote, staurolite, chloritoid, clinopyroxenes, amphiboles) to the metastable assemblage mentioned above (Puglisi, 1987b).

Puglisi (1987a, 1987b) attributed these compositional trends to the start of thrusting in the Calabride paleogeographic realm and the ensuing rejuvenation of the source area. More information about provenance was provided by analysis of quartz-grain populations (Puglisi, 1991), which allowed to identify three groups of parent-rock assemblages (cf. Basu, 1985b). Quartz-grain assemblages of the Frazzanò Fm., Piedimonte Fm., and "internal" Reitano Fm. indicate a low to medium-grade metamorphic parentage, those of the "external" Reitano Fm. a medium to high-grade metamorphic parentage, and those of the SCOFm a high-grade metamorphic to plutonic parentage. Puglisi (1991) concluded that the petrographic evolution of these Formations indicates a peak of thrusting activity in the Oligocene, i.e., during or after deposition of the Frazzanò Fm. and Piedimonte Fm., and before deposition of the SCOFm. So far, the rock-fragment analyses listed in Table 2 have not been investigated in detail.

6. End-member modelling of rock-fragment assemblages

The analysis of rock-fragment assemblages by means of end-member modelling should enable a straightforward interpretation of compositional variation in terms of parent lithologies. In the ideal case, associations of rock-types subject to erosion during evolution of the Calabride-Maghrebide thrust belt should allow to trace the deformation or emplacement of specific structural units. The end-member modelling technique has been discussed in detail in chapters 3 and 4. The raw data set used for this end-member modelling experiment consists of 127 observations (Table 2) arranged in a series of (composite) stratigraphic sections. The compositions of rock-fragment assemblages were estimated by point-counting of 100 grains in thin sections of medium to coarse-grained sandstones. In the original petrographic studies listed in Table 2, up to 14 different classes of rock fragments were distinguished on the basis of textural and compositional criteria (described by Carmisciano & Puglisi, 1978b; Puglisi, 1979). The raw data set was modified for input into the modelling programs by amalgamating several types of rock fragments present in a limited number of observations into five genetically meaningful classes (Table 3).

Table 3. Description and interpretation of rock-fragment classes used as input data for the end-member model.

LABEL	BRIEF DESCRIPTION	INTERPRETATION
GRANITE-GNEIS	Phaneritic rock fragments (crystal size > 0.03 mm), consisting of quartz, K-feldspar, plagioclase, and micas. With or without tectonite fabric.	Plutonic and high-grade metamorphic rocks
MICA-SCHIST	Phaneritic rock fragments (crystal size > 0.03 mm) with tectonite fabric, consisting chiefly of micas and quartz.	Medium to high-grade metamorphic rocks
PHYLLITE	Aphanitic rock fragments (crystal size < 0.03 mm) with tectonite fabric, made up of quartz and micas.	Low to medium-grade metamorphic rocks
SEDIMENTS	Extrabasinal limeclasts (micrite, sparite, calcarenite, calcilutite, and dolomite) and siliciclastic sedimentary rocks (arenites, wackes, siltites, and chert).	Sedimentary rocks
VOLCANITES	Various types of basic and acidic volcanic grains, with or without zoned plagioclase phenocrysts in a micro or crypto-crystalline groundmass (porphyric texture).	Contemporaneous volcanic activity

The resulting (127x5) matrix was scaled columnwise to assign equal "weights" to each of the classes. In order to estimate the minimum number of end members, a series of constrained least squares approximations was generated to assess the goodness of fit of linear representations of the data in two to five dimensions, following procedures outlined in chapter 3. Fig. 2 shows that the coefficients of determination of granite-gneis and volcanites strongly increase for models up to three end members, and hardly improve by increasing the number of end members beyond three. Mica-schist and Phyllite provide little information about the optimum number of end members: their fit improves gradually as the number of end members is increased. Increasing the number of end members beyond three improves the goodness of fit of sediments to a considerable extent, but the coefficients of determination show that modelling precision would not improve greatly for any of the other

rock-types. It is concluded that mixing of three end members provides the simplest reasonable explanation of compositional variation in the data.

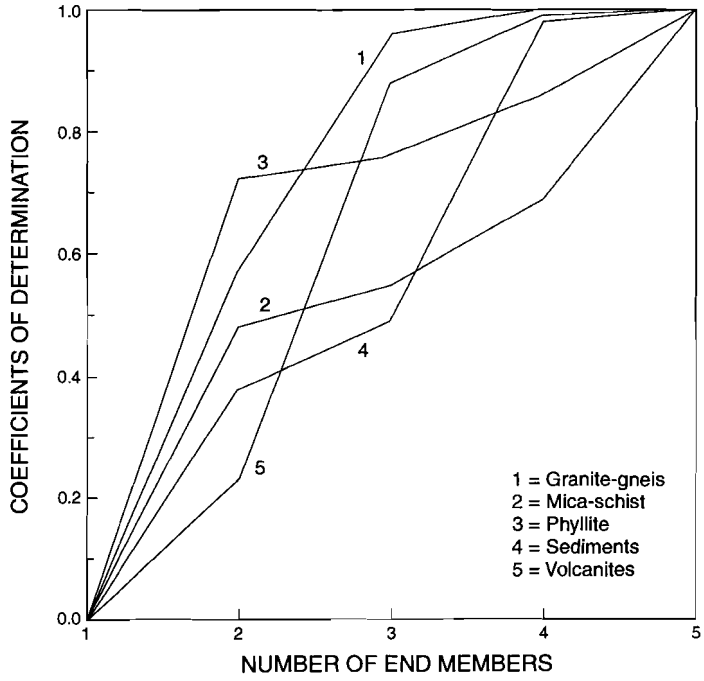

Figure 2. Coefficients of determination for various numbers of end members. All rock fragments (apart from sediments) are reasonably well approximated by mixing of three end members.

Table 4. Goodness of fit statistics for model with three end members. Fit decreases slightly as a result of imposing non-negativity constraints on the mixing-proportions matrix.

Coefficients of determination:	Linear model:	Mixing model:
Granite-gneis	0.96	0.95
Mica-schist	0.55	0.52
Phyllite	0.76	0.77
Sediments	0.49	0.45
Volcanites	0.88	0.88
Mean coefficient of determination	0.73	0.71
Mean angular deviation	12.4^0	12.7^0

Goodness of fit of mixing model residuals:	
Number of logratio residuals	54
Chi-square value of distribution (df=2)	5.07
Associated significance probability	0.92

Subsequently, a ternary mixing model was constructed following the procedures discussed in chapter 3. The iterative end-member estimation procedure converged rapidly to a mixing model with a small convexity error. An *a posteriori* goodness of fit test of logratio residuals indicated that the differences between modelled and observed data can be attributed to random errors, confirming the choice of three end members. The goodness of fit of the final mixing model is summarized in Table 4.

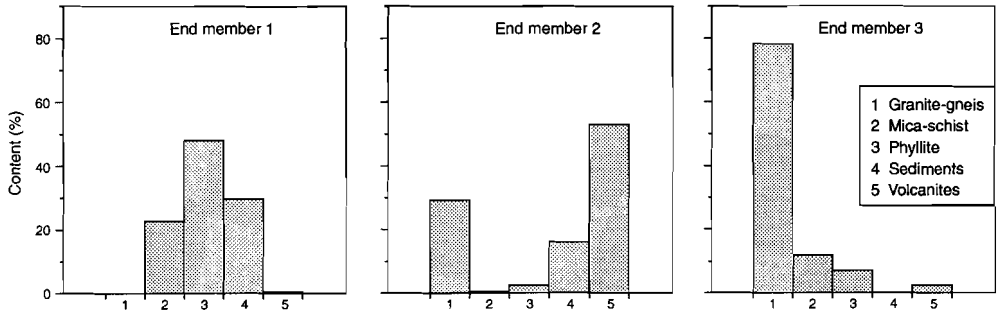

Figure 3. Modelled end members of rock-fragment assemblages. Numbers 1 to 5 refer to rock-fragment types listed in Fig. 2. See Table 5 for interpretation.

Table 5. Modelled end members of rock-fragment assemblages and their inferred provenance in terms of parent lithologies and structural units.

GRAIN TYPES:	ENDMEMBER 1:	ENDMEMBER 2:	ENDMEMBER 3:
Granite-gneis	0.0	29.1	78.5
Mica-schist	22.0	0.6	11.6
Phyllite	47.8	1.9	7.5
Sediments	29.9	15.8	0.0
Volcanites	0.3	52.6	2.4
INFERRED PARENT-ROCK ASSEMBLAGE	Low to medium-grade metamorphic + sedimentary	Volcanic + medium to high-grade metamorphic + sedimentary	Medium to high-grade metamorphic + plutonic
CORRESPONDING STRUCTURAL UNITS	Lower Calabride Units + cover of upper Calabride Units	Contemporaneous volcaniclastic input + upper Calabride Units	Upper Calabride Units

7. Interpretation of modelling results

The modelled end members of the rock-fragment assemblages are interpreted as follows (Fig. 3 and Table 5): End member 1 consists of sedimentary rocks and low to medium-grade metamorphic rocks. This association corresponds to rocks of the lower Calabride units (Longi-Taormina, Fondachelli and Mandanici) and the topmost part of the upper Calabride units (sedimentary and low-grade metamorphic rocks of the Stilo Unit). End member 2 is a mixture of volcanic rocks and high-grade metamorphic to plutonic rocks, with a small contribution of sedimentary rocks, which largely reflects contemporaneous volcanic input, mixed with rocks derived from the upper Calabride units (Aspromonte and Stilo). End

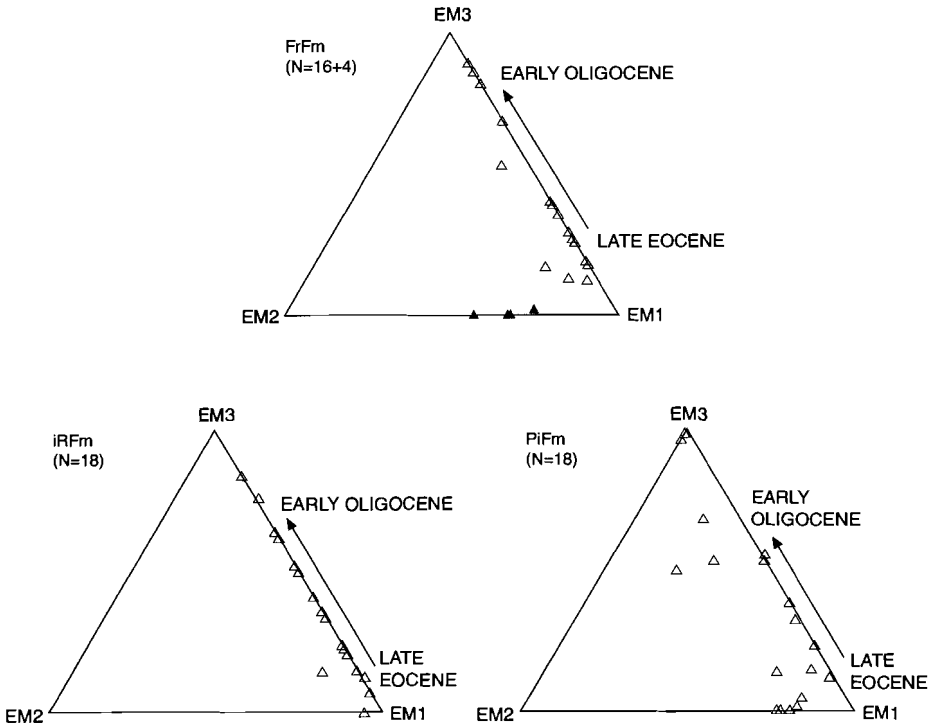

Figure 4. Compositional evolution of Late Eocene to Early Oligocene basin fills: FrFm = Frazzanò Fm., showing four outliers marked in black; iRFm = "internal" Reitano Fm.; PiFm = Piedimonte Fm. (see text).

member 3 consists of medium to high-grade metamorphic and plutonic rocks, reflecting the exclusive input of material derived from the upper Calabride units (Aspromonte and Stilo).

The mixing model shows that compositional trends within each formation allow to distinguish three types of basin fills. The Late Eocene to Early Oligocene Frazzanò Fm., Piedimonte Fm., and "internal" Reitano Fm. display identical patterns: dominant input of end member 1 at the base, with a sudden increase of end member 3 input in their topmost parts (Fig. 4). The conspicuous similarity of compositional evolution within the Frazzanò Fm., Piedimonte Fm., and "internal" Reitano Fm. indicates that these formations have been fed from the same source area. It also confirms their inferred common biostratigraphic age, ranging from the Late Eocene to the Early Oligocene. The compositional evolution of the three formations has been summarized by a single diagram in Fig. 5, which also illustrates the provenance evolution of the SCOFm and the "external" Reitano Fm. Four samples of the Frazzanò Fm. are outliers, characterized by gross angular deviations of up to 40^0 (they have been plotted as black triangles in Fig. 4, and have not been plotted in Fig. 5).

The Late Eocene to Early Oligocene compositional evolution trend of the Frazzanò Fm., Piedimonte Fm., and "internal" Reitano Fm. continues in the Late Oligocene to Early Miocene SCOFm (Fig. 5): significant contributions of end member 1 are only present in

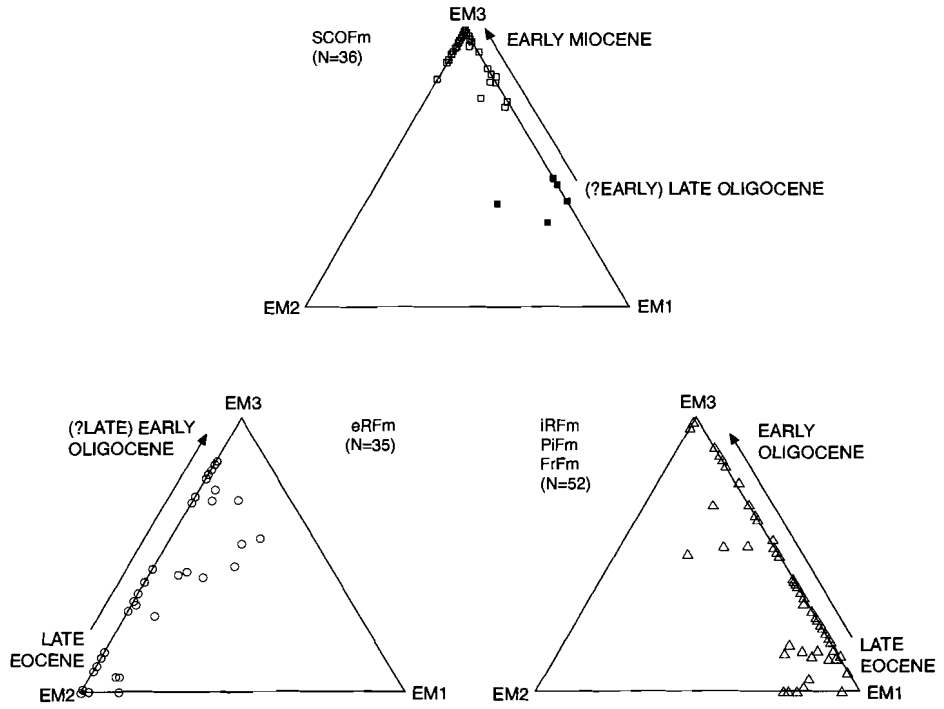

Figure 5. Compositional evolution of Late Eocene to Early Miocene basin fills: SCOFm = Stilo-Capo d'Orlando Fm. (five samples from base marked in black); eRFm = "external" Reitano Fm.; see also Fig. 4.

the lowermost part of the SCOFm. Five samples from the base of the SCOFm, whose composition clearly differs from that of the rest of the samples, have been plotted as black squares in Fig. 5. The middle and upper part of the SCOFm show a nearly exclusive input of end member 3. The overall Late Eocene to Early Miocene compositional evolution of the Calabride basin fills displays a shift from a sedimentary and low-grade metamorphic assemblage (end member 1) to a high-grade metamorphic and plutonic assemblage (end member 3). The provenance evolution of the Calabride basin fills (Frazzanò Fm., Piedimonte Fm., "internal" Reitano Fm., and SCOFm) shows that parent rocks which originated at successively deeper crustal levels were eroded in the course of the Oligocene, confirming inferences made on the basis of "conventional" methods of provenance analysis (Puglisi, 1987a, 1987b, 1991).

The Late Eocene to Early Oligocene "external" Reitano Fm. shows a completely different pattern: a gradual shift from a dominant contribution of end member 2 input in the lower part to a dominant input of end member 3 in the upper part (Fig. 5). The initial predominance of volcanic input (end member 2) and the lack of low to medium-grade metamorphic detritus in the "external" Reitano Fm. indicates that the detritus shed by the Calabrian basement units did not extend into the basinal domain occupied by the Sicilide units in the Late Eocene. This situation changed drastically in the course of the Oligocene,

as demonstrated by the distinct compositional affinity of the upper part of the "external" Reitano Fm. with the high-grade metamorphic and plutonic detritus (end member 3) shed by the upper Calabride units from the Late (Early) Oligocene onward.

The principal compositional shifts occurring within the lithostratigraphic units have been included in the tectono-stratigraphic scheme of Fig. 1. A summary of the modelled compositional evolution from Late Eocene to Early Miocene is presented in Fig. 6.

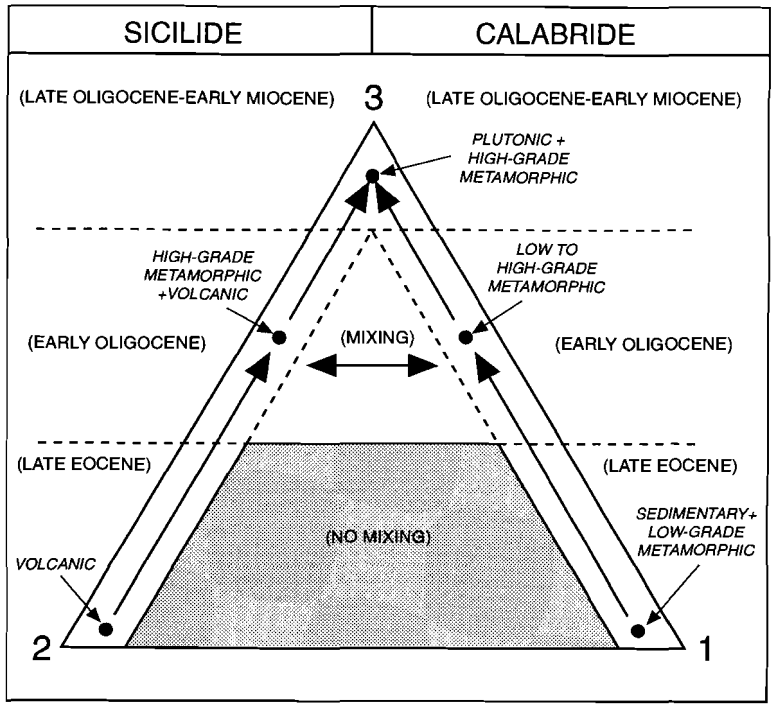

Figure 6. Schematic representation of temporal and spatial compositional trends in the Calabride-Maghrebide basin fills. Numbers 1 to 3 refer to modelled end-member assemblages.

8. Discussion and conclusions

The synthesis of structural and sedimentary data shows that shortening in the internal part of the Calabride-Maghrebide thrust belt occurred in at least three major phases, as shown in Fig. 1: (1) Middle to Late Eocene; (2) Late Early Oligocene; (3) Late Early Miocene. The oblique backthrusting event at the Oligo-Miocene boundary, recognized in Aspromonte (Meulenkamp et al., 1986; Weltje, 1992; Minzoni et al., 1992; Minzoni, 1993; Luciani et al., in press), has not been documented in the Peloritani, where detailed information about the SCOFm is lacking. The Calabrian-Sicilian record suggests that shortening of the European margin began in Eocene times. The Calabride thrust sheets were already piled up in the Late Eocene (Fig. 7A), and were remobilized several times by successive Paleogene and Neogene deformation events (Fig. 7B).

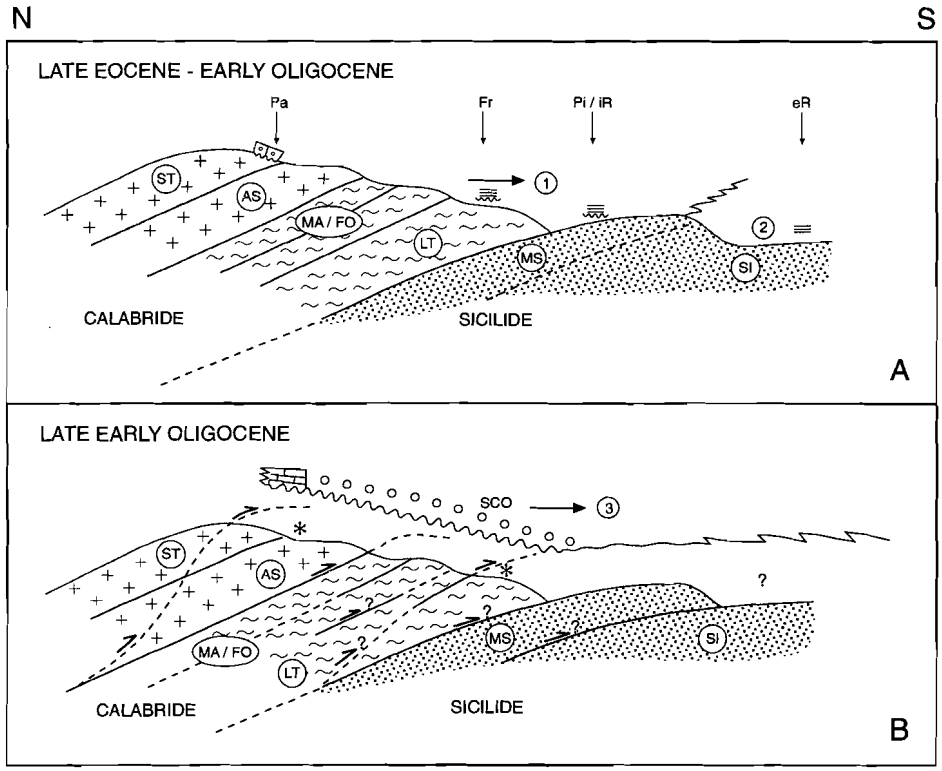

Figure 7. Reconstructed thrust-belt evolution in the southern part of the CPA.

Lithostratigraphic units: Pa = Palizzi Fm., Fr = Frazzanò Fm., Pi = Piedimonte Fm., iR = "internal" Reitano Fm., eR = "external" Reitano Fm, SCO = Stilo-Capo d'Orlando Fm., ? = hiatus, * = overthrusted formations (Pa and Fr). Structural units: ST = Stilo and Aspromonte Units (upper Calabride), MA/FO = Mandanici and Fondachelli Units (lower Calabride), LT = Longi-Taormina Units (lower Calabride), MS = Monte Soro Units, SI = "external" Sicilide Units. Symbols 1, 2 and 3 refer to detrital endmember assemblages shed by the Calabride thrust belt.

A: Late Eocene to Early Oligocene situation, after the first shortening phase. The PaFm, FrFm, PiFm and iRFm were deposited on deformed structural units, whereas the eRFm, which is characterized by a volcaniclastic provenance, was deposited on top of the not yet deformed Sicilide units. In the Late Eocene, depositional realms of the eRFm and the other formations were separated; in the course of the Early Oligocene, detritus shed by the upper Calabride units reached the site of deposition of the eRFm. B: Late Early Oligocene thrusting remobilized the Calabride units. This thrusting phase was followed by deposition of the SCOFm, which is largely made up of material derived from the upper Calabride units. Episodic backthrusting of these units continued during and after deposition of the SCOFm.

The Late Early Oligocene deformation phase reactivated virtually all of the Calabride units, i.e., the Longi-Taormina, Mandanici, Aspromonte, and Stilo units (Fig. 7B). This phase of shortening is clearly visible in the modelled Late Eocene to Early Miocene unroofing record, which displays a Late Early Oligocene shift from dominantly sedimentary and low-grade metamorphic to dominantly high-grade metamorphic and plutonic provenance. The compositional shift indicates that the uppermost Calabride units, i.e., the Aspromonte and Stilo units, became the dominant source of sediment from the Late Early Oligocene onward. This compositional evolution pattern, which is a textbook example of an unroofing sequence, confirms the late thrusting of the upper Calabride units (Aspromonte and Stilo units) onto the already deformed lower Calabride and Monte Soro units, suggested by the structural and stratigraphic data. Moreover, the contemporaneous shift from volcaniclastic to high-grade metamorphic and plutonic provenance in the external Sicilide units suggests that mixing of volcaniclastic and high-grade metamorphic input coincided with a S-ward progradation of the deformation front towards the African foreland in this interval (Fig. 7B). A second remobilisation of the Longi-Taormina units occurred in the Late Early Miocene (Nigro, 1992), providing additional evidence for "out of sequence" thrusting.

End-member modelling of rock-fragment assemblages allows to explain compositional evolutionary patterns in fossil basin fills in terms of erosion of specific structural units. The modelling results confirm inferences made by Puglisi (1987a, 1987b, 1991) and, in addition, allow for a more refined interpretation of parent lithologies than conventional methods employed in sedimentary provenance studies. In conclusion, the tectono-sedimentary reconstruction indicates that the overall Paleogene deformation record does not fit into the scheme of a simple "piggy-back thrust sequence". Instead, the Paleogene evolution of the Calabride-Maghrebide thrust belt appears to have been governed by late thrusting events, providing additional support for the Late Oligocene to Early Miocene basin-evolution scheme proposed in chapter 5 (Weltje, 1992). The example presented above shows that end-member modelling of piggy-back basin fills can provide constraints on thrust-belt evolution, even in cases where a considerable part of the thrust sheets and piggy-back basin fills has been removed by erosion. The sequence of thrust activation is generally difficult to determine in the absence of high-quality (subsurface) data, as discussed by Zoetemeijer et al. (1993). In such difficult cases, end-member modelling can be a valuable tool for the reconstruction of thrust-belt evolution.

CHAPTER 7

HIGH-FREQUENCY DETRITAL SIGNALS IN EOCENE FAN-DELTA SANDSTONES OF MIXED PARENTAGE (SOUTH-CENTRAL PYRENEES, SPAIN): A RECONSTRUCTION OF CHEMICAL WEATHERING IN TRANSIT

G.J. Weltje, S.O.K.J. van Ansenwoude & P.L. de Boer

Comparative Sedimentology Division, Institute of Earth Sciences,
P.O. Box 80.021, 3508 TA Utrecht, The Netherlands

1. Introduction

Sandstone composition is a sensitive recorder of climatic-physiographic variations in source areas (Basu, 1985a; Suttner & Dutta, 1986; Grantham & Velbel, 1988; Johnsson & Stallard, 1989; Girty, 1991; Weltje & De Boer, 1993). The extent of chemical weathering of sand-sized detritus is determined by the rate of weathering, and by the amount of time during which detritus is exposed to the weathering environment (cf. Grantham & Velbel, 1988). The rate of weathering is related to climatic factors, such as precipitation and temperature. The time during which weathering can occur is a function of tectonic relief. The extent of weathering is also strongly influenced by the presence of a vegetation cover, whose development is governed by a complex system of feedback mechanisms linked with the "independent" variables mentioned above (cf. Bull, 1991).

In a fan-delta succession in the Eocene of the southern Pyrenees, De Boer et al. (1991) described more or less regular vertical alternations of sandy conglomerates and calcareous mudstones ("parasequences") with thicknesses of the order of several metres, which extend laterally over a palaeocoastline. The fixation of the palaeocoastline over a timespan corresponding to several of these parasequences, and the lateral continuity of the fine and coarse-grained intervals from the fluvial into the marine domain, exclude the possibilities that the parasequences were produced by lateral shifting of alluvial channels or by changes of relative sea level. De Boer et al. (1991) therefore suggested that the parasequences reflect variations of sediment supply, which were attributed to more or less regular climate fluctuations, to intermittent tectonic activity, or to a combination of both. These inferences were supported by numerical modelling experiments, which suggested that the observed small-scale grain-size variations could have been produced by varying erosion rates due to climatic fluctuations, or alternatively, by intrabasinal thrusting. The latter could have caused the episodic trapping of detritus behind intrabasinal thrusts (cf. Belt & Lyons, 1989), or the episodic shedding of material previously stored upon blind thrusts (cf. Peper & De Boer, 1994).

If climatic and/or physiographic variations in the source area have indeed contributed to the observed vertical grain-size variations, they are likely to be recognized in the petrographic

composition of the coarse-grained sediments, in view of the inferred humid tropical to seasonal subtropical palaeoclimatic conditions in the southern Pyrenees during the Eocene (Haseldonckx, 1973). Under such climatic conditions rapid chemical weathering of silicate rocks occurs (cf. Johnsson et al., 1988). Furthermore, the generally high rates of sediment supply and subsidence in foreland basins are favourable for preserving subtle climatic-physiographic signals, due to limited reworking in depositional systems subject to rapid burial (cf. Heller et al., 1992). If the observed grain-size variations actually reflect the intermittent storage and release of sand-sized detritus (cf. Peper & De Boer, 1994), the base of coarse-grained intervals should show a higher proportion of chemically resistant grains than the top, because the coarse-grained material initially supplied to the basin after a period of mudstone accumulation would have been subjected to prolonged weathering.

The principal objective of this study is to examine the petrographic signature of the "parasequences" reported by De Boer et al. (1991). A detailed study of compositional variation within the coarse-grained units was undertaken. A statistical analysis of sandstone compositions was performed, and end-member assemblages were modelled following the methods described in chapter 3.

2. Geological setting of the southern Pyrenees

The Pyrenees have developed as the result of the collision between the Iberian and Eurasian plates, which took place between Late Cretaceous and Miocene times. The geometry of the Pyrenees is known in great detail, due to numerous field studies and on account of a deep seismic survey across the entire orogen which permitted the construction of a crustal balanced cross section (Fig. 1; ECORS Pyrenees Team, 1988; Roure et al., 1989; Muñoz, 1992). The central part of the Pyrenees consists of the Axial Zone antiformal stack of Hercynian basement thrust sheets, bounded to the north by the North Pyrenean Fault Zone. The North Pyrenean thrust sheets, which involve basement and cover rocks, are exposed north of this fault zone. The South Pyrenean thrust sheets, which together form the South Pyrenean Central Unit (SPCU), consist largely of Paleogene and Mesozoic platform carbonates and calcareous mudstones. The SPCU is bounded to the north by the Morreres backthrust, a passive roof thrust related to the piling up of Hercynian basement thrust sheets of the Axial Zone antiformal stack.

The SPCU is a classical example of a thin-skinned thrust belt, which developed mainly by southward piggy-back thrusting over an autochtonous Paleogene and a reduced Mesozoic series which directly overlies the basement (Williams & Fischer, 1984; Williams, 1985; Cámara & Klimowitz, 1985; Ori & Friend, 1984; Farrell et al., 1987; Vergés & Muñoz, 1990). The largely Miocene Ebro foreland basin deposits represent the last stage of basin filling. Basin fills corresponding to earlier stages occur as piggy-back basins on top of the South Pyrenean cover thrust sheets (Serres Marginals, Montsec, and Boixols thrust sheets; Fig. 1). The architecture of the piggy-back basin fills allows to distinguish several stages of basin evolution, which are closely related to the South Pyrenean thrust sequence (Mutti et al., 1985, 1988; Puigdefàbregas & Souquet, 1986; Puigdefàbregas et al., 1989, 1992; Nijman, 1993).

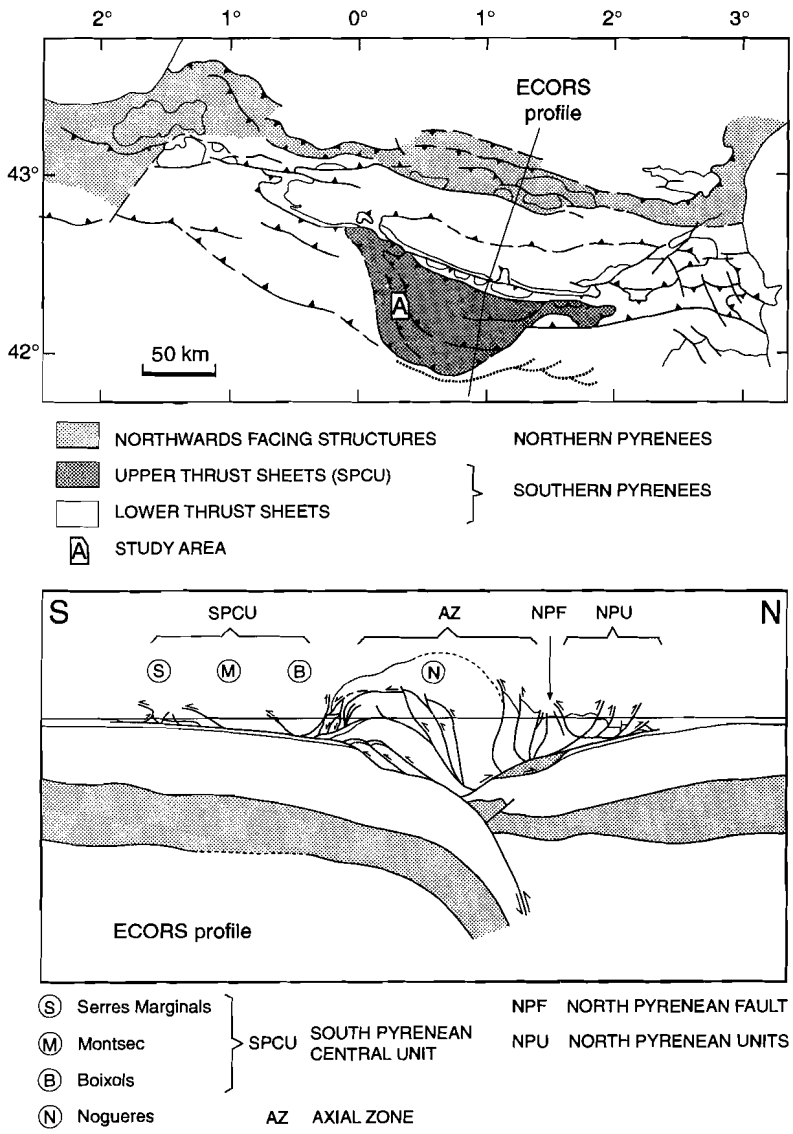

Figure 1. Simplified map view of the Pyrenees, showing the location of the study area (see Fig. 2) and the ECORS profile (crustal balanced cross-section after Muñoz, 1992).

3. The Eocene Montañana Group

The Early to Middle Eocene fluvio-deltaic sediments of the Montañana Group were deposited on top of the moving SPCU (Seguret, 1972; Nijman & Nio, 1975; Ori & Friend, 1984), and thus represent the fill of a piggy-back or thrust-sheet-top basin. The fundamental basin fill pattern of the Montañana Group is characterized by south-southwestward prograding alluvial fans, drained by a west-northwestward flowing axial fluvial system (Nijman & Nio, 1975; Cuevas et al., 1985). A break-in-slope of this system was fixed by the western lateral ramp of the SPCU (Figs. 1 and 2). Contemporaneous turbidite systems of the Hecho Group developed in the western deep marine part of the South Pyrenean Foreland Basin across the lateral ramp (Mutti et al., 1985, 1988; Nijman & Puigdefàbregas, 1989; Puigdefàbregas et al., 1992). Several "megasequences" or "allogroups" have been distinguished within the Montañana Group, based on onlap-offlap geometries and unconformities along the basin margins (Mutti et al., 1988; Nijman & Puigdefàbregas, 1989; Nijman, 1993).

Tectonic control of sedimentation within the Montañana Group was inferred from repeated shifts of the basin axis, which is defined by the location of the axial fluvial system (Nijman & Puigdefàbregas, 1989; Nijman, 1993). Northward shifts of the basin axis were, according to these authors, caused by stacking of thrust sheets in the Axial Zone and/or the southward propagation of the South Pyrenean thrust sheets. Subsequently, the tectonic relief created by stacking of thrust sheets below the Morreres backthrust resulted in increased hinterland erosion rates and a southward progradation of the alluvial fans occurred in response to an increased sediment supply. This would have caused a subsequent southward shift of the basin axis. Such tectonically induced shifts of the basin axis, in conjunction with (eustatic) base-level changes which did not affect the location of the basin axis, are considered the main controls on depositional style and long-term sequence development in the Eocene basin fill (Nijman & Puigdefàbregas, 1989; Nijman, 1993).

4. Controls on small-scale basin-fill architecture

Controls on small-scale vertical facies variations in the Upper Montañana Group were investigated by De Boer et al. (1991). In this study attention was paid to the fixation of facies boundaries by synsedimentary folding of the SPCU. A hypothetical model was presented, based on the investigation of "parasequences" within alluvial-fan and fan-delta successions of the Campanúe Formation (cf. Nijman & Nio, 1975), corresponding to tecto-sedimentary cycle 9/TE/5 of Puigdefàbregas & Souquet (1986) and the Santa Liestra sequence 2 of Crumeyrolle & Mutti (1986), Crumeyrolle (1987) and Mutti et al. (1988). The parasequences (with thicknesses of the order of ten metres) consist of alternations of sandy-conglomeratic units and calcareous mudstones. Coarse and fine-grained intervals can be correlated from the subaerial alluvial environment to the shallow marine realm near the "Castillo de Fantova" (approximately ten kilometres northeast of the village of Graus, Fig. 2). In this locality, the position of the coastline, which can be deduced from the presence of marine fossils on the one side, and the occurrence of mottled palaeosols on the other (Fig. 4), remained fixed over a timespan of the order of 100 kyr (estimated time interval based on average accumulation rates for the entire basin fill according to De Boer et al., 1991).

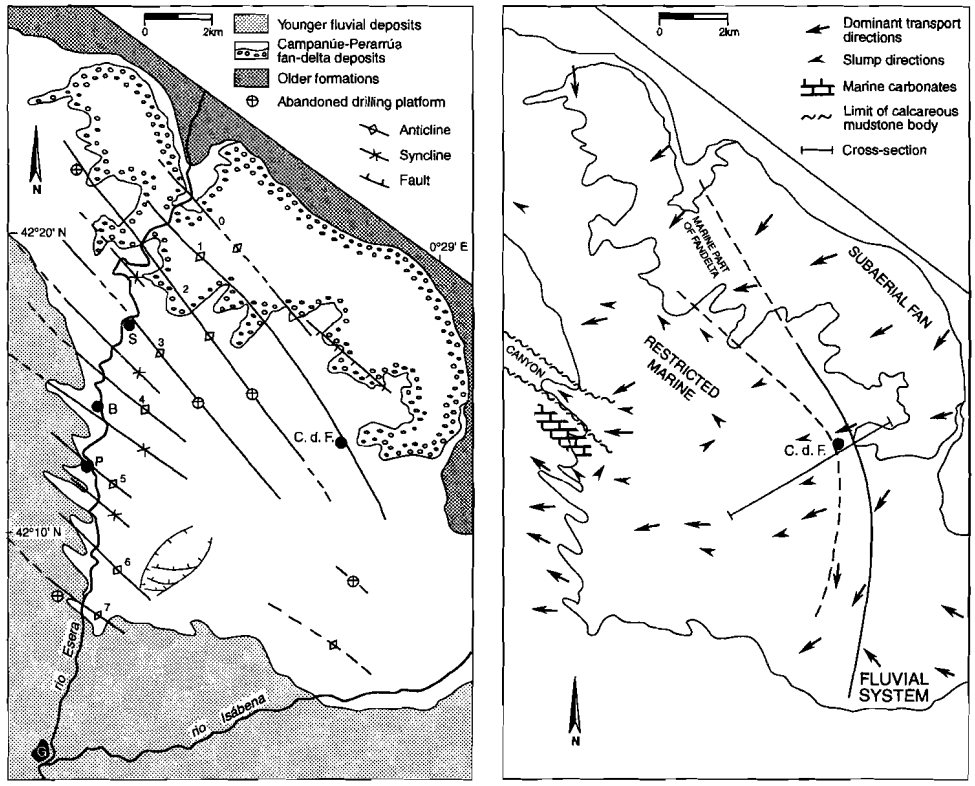

Figure 2. Left: geological map of study area (for location see Fig. 1), showing growth folds. Right: palaeogeography, showing sediment dispersal paths and profile of Fig. 3 (C.d.F. = Castillo de Fantova).

De Boer et al. (1991) reported on synsedimentary intrabasinal deformation, which locally affected sediment dispersal paths and facies distributions. A series of northwest-southeast trending growth folds was described, which may represent a system of "en echelon" folds (incipient synthetic Riedel shears) related to synsedimentary dextral strike-slip movements along the north-south trending western lateral ramp of the SPCU (Fig. 2). These intrabasinal folds were only recognized after detailed facies maps and thickness measurements had been compiled from a large number of sections and local observations in the basin. The effects of this intrabasinal folding are most clearly expressed in localities where a delicate equilibrium between rates of intrabasinal deformation, regional subsidence, and local sediment supply led to the vertical stacking of facies boundaries (De Boer et al., 1991). The fixation of the coastline near the "Castillo de Fantova" was ascribed to the synsedimentary activity of one of these anticlines, which prevented small-scale baselevel variations from influencing the non-marine facies on its northeastern flank, where a record of varying sediment supply was preserved in a fully terrestrial sequence. The terrestrial sequence is bounded by a fully marine sequence at the southwestern flank of this fold. The alternations of coarse-grained and fine-grained units at either side of the growth fold can be well correlated (Figs. 3 and 4).

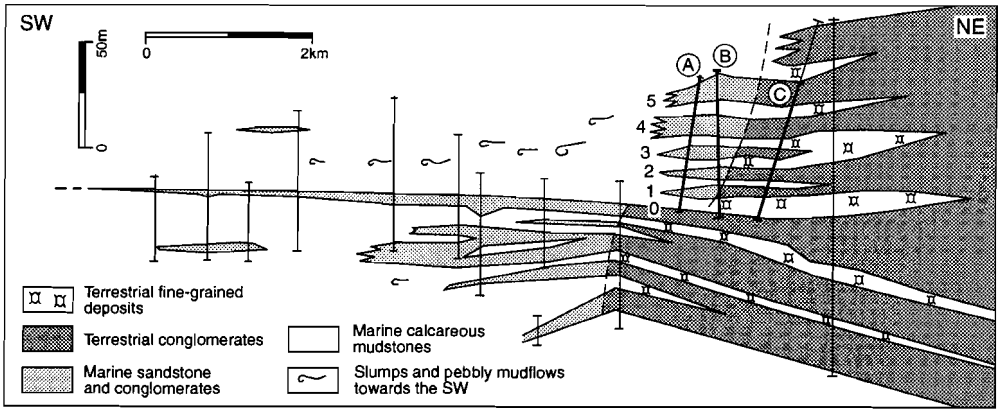

Figure 3. Sedimentological profile near the "Castillo de Fantova" (see Fig. 3 for location). Sections labelled A to C; coarse-grained intervals numbered from 0 to 5 (see Fig. 4 for details).

De Boer et al. (1991) discussed the possible intrabasinal and/or extrabasinal controls on these parasequences in detail. In their opinion, the deposition of alternating coarse and fine-grained sediments cannot be attributed to a system of laterally shifting channels and associated fine-grained interchannel deposits, because individual coarse-grained beds display a sheet-like geometry, and can occasionally be correlated over a distance of several kilometres (Fig. 3). Consequently, the observed grain-size variations must have been generated by more or less regular variations of sediment supply. Several mechanisms were discussed which may have produced these variations. As explained above, small-scale baselevel changes were ruled out as a plausible mechanism, in view of the lack of transgressive and regressive trends accompanying the observed vertical grain-size variations. De Boer et al. (1991) suggested that the parasequences could have been generated in response to short-term palaeoclimatic fluctuations (10 to 100 kyr). They did not favour the possibility of varying erosion rates in the orogenic hinterland due to episodic tectonic activity, which would have required a delicate balance between growth-fold activity, subsidence and sediment accumulation. In their opinion, deformation of the SPCU underlying the Eocene deposits in response to synsedimentary thrusting is unlikely to have sustained such delicately balanced conditions over a considerable timespan. Nevertheless, a tectonic control on long-term sedimentation patterns within the Montañana Group is undeniable. This logically follows from the large-scale tectonic setting of the Tremp-Graus Basin and the observed synsedimentary folding of the SPCU.

5. Materials, methods and results

Sandstones from base and top of five successive coarse clastic intervals were sampled in three sections of the Campanúe fan delta near the "Castillo de Fantova" (ten kilometres northeast of the village of Graus, see Fig. 2 to 4) previously described by De Boer et al. (1991). The stratigraphic positions of the samples are shown in Fig. 4. Multiple samples from the same stratigraphic level were obtained in order to reduce possible effects of lateral compositional inhomogeneity due to grain-size variations. A total of thirty-eight standard thin-sections was made. The apparent diameter of 100 quartz grains was measured in each thin section in order to obtain an estimate of the modal grain size of each sample. Twenty-eight samples with mean apparent grain sizes ranging from 0.5 to 1.5 ϕ were selected for

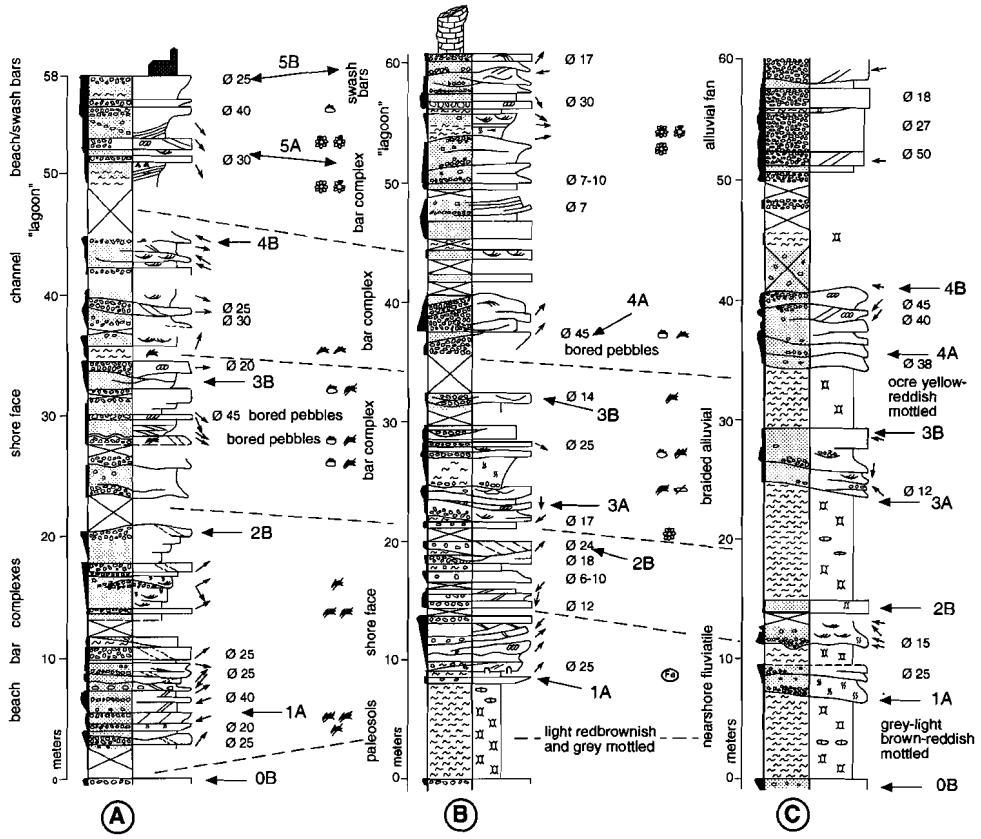

Figure 4. Sedimentological logs A to C and stratigraphic positions of sandstone samples (see Figs. 1 to 3 for location). Suffixes A and B indicate base and top samples, respectively.

point-counting analysis, fourteen from the base and fourteen from the top of the coarse-grained intervals. The petrographic composition of each sample was estimated by counting 400 points in thin-section according to the Gazzi-Dickinson conventions (Gazzi, 1966; Dickinson, 1970; Ingersoll et al., 1984). Point-counting categories are summarized in Table 1. The point-counting results are shown in Fig. 5. The compositional variation displayed by the Campanúe sandstones corresponds well to that of other lower to middle Eocene sandstones in the South Pyrenean Foreland Basin, as determined in previous petrographic studies (Valloni et al., 1984; Nagtegaal & De Weerd, 1985; Fontana et al., 1989).

Quartz (Qt), feldspar (F) and extrabasinal limeclasts (Lc) are the principal framework elements of the Campanúe sandstones. Quartz occurs mainly as monocrystalline grains, some of which show an undulose extinction. Polycrystalline quartz includes microcrystalline grains without a clear tectonite fabric. Rare cryptocrystalline quartzose grains (chert) have also been included in this category. Feldspars (K-feldspar, microcline, and plagioclase) display a wide range of alteration phenomena: some grains are virtually fresh, whereas others have been largely replaced by clay minerals, calcite, and haematite. Great care was taken in reconstructing the original feldspar content. The irregular distribution of clayey

Table 1. Point-counting categories used in this study (according to Gazzi-Dickinson conventions).

GRAIN TYPES	GROUP	LABEL
Quartz	**Qt**	
Monocrystalline quartz		Qm
Polycrystalline quartz		Qp
Feldspar	**F**	
Limeclasts	**Lc**	
Argillite/micrite grains		Lca
Micritic grains		Lcm
Bioclastic grains		Lcb
Sparitic grains		Lcs
Excluded	-	
Micas		M
Dense (incl. opaque)		D
Other		O
Unidentified		U

patches in oversized pores, the presence of vermicular kaolinite and small relict feldspar domains within these oversized pores point to the origin of the clay as an *in situ* alteration product of detrital feldspars (clayey pseudomatrix). The absence of soft-sediment deformation structures within the limeclasts indicates that they were already lithified during deposition, which points to their extrabasinal origin. Bioclasts comprise a small proportion of the total amount of limeclasts. They have been classified as extrabasinal, because they are present in subequal amounts in the marine as well as the terrestrial samples, indicating that only a minor proportion of bioclasts is of intrabasinal origin. The classes of grains which have been excluded from the "principal framework composition" (i.e., QtFLc%) comprise, on average, 5% of the total number of points counted. The class of grains labelled "other" (Table 1) includes rare accessory grains, such as volcanic lithics, Fe-(hydr)oxides, phosphate, and glauconite. The class labelled "unidentified" includes grains which have been altered beyond recognition.

6. Parent lithologies and location of source areas

The point-counting results confirm previous studies of conglomerate-clast populations and palaeoflow patterns, which indicate that the sediments of the Campanúe fan-delta were derived from a mixed sedimentary-plutonic source to the north-northeast (De Boer, 1976; Crumeyrolle, 1987; De Boer et al., 1991). A large part (>65%) of the conglomerate clasts of the Campanúe fan-delta deposits was derived from Cretaceous and Paleocene carbonate rocks, i.e., the pre-Eocene sedimentary rocks of the SPCU (Fig. 6). In the uppermost part of the fan-delta sequence, a predominance of clasts derived from the Late Cretaceous Arén Formation and from the *Alveolina*-bearing Paleocene carbonates of the Ager Formation has been observed. The stratigraphic succession of conglomerate-clast populations represents an "inverted unroofing sequence" (De Loos, 1988), which points to erosion of the northern

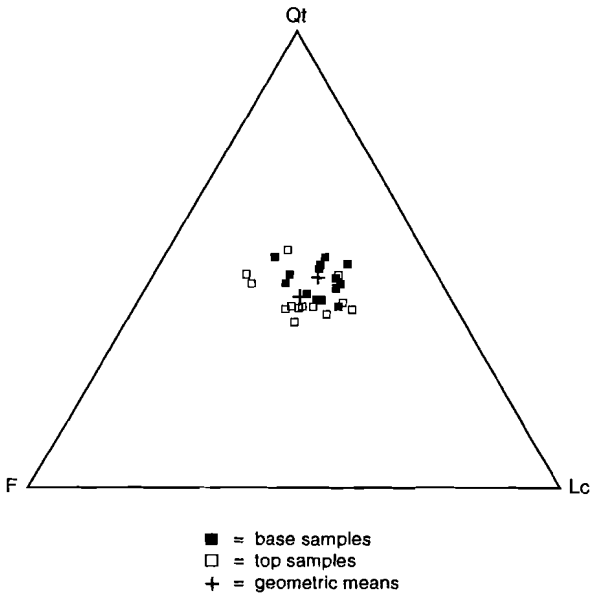

Figure 5. Principal framework compositions (QtFLc%) plotted in ternary diagram, together with geometric means of base and top samples. For symbols see Table 1.

part of the SPCU during deposition of the Campanúe conglomerate. This, in turn, indicates activity of the passive Morreres backthrust, bounding the SPCU on the northern side, due to stacking of basement thrust sheets in the embryonic Axial Zone. The Cretaceous-Paleocene successions are presently exposed in the hanging wall of the Morreres backthrust, a few kilometres to the north of the Eocene depositional site. The extrabasinal carbonate grains, which can be traced to the same parent rocks, thus were transported over a limited distance (of the order of ten kilometres), as indicated by the partially restored balanced cross section of Puigdefàbregas et al. (1992), shown in Fig. 6.

Nagtegaal & De Weerd (1985) suggested that the high content of feldspar and quartz grains in the lower Eocene sandstones of the South-Central Pyrenean Basin reflects a considerable input of detritus from the Late Carboniferous granodiorites and the metamorphic complexes in the central part of the Axial Zone. They performed cathodoluminescence studies of the quartz-grain population, which revealed a high content of blue-luminescing grains, inferred to be characteristic of igneous sources (Zinkernagel, 1978). However, the Campanúe conglomerates contain only a minor proportion (<5%) of granite/granodiorite clasts. The conspicuous near-lack of granite pebbles in the Campanúe conglomerates indicates that most of the granite clasts disintegrated in the hinterland, and reached the basin as sand-sized quartz and feldspar grains. This conclusion is supported by the results of palynological analyses (Haseldonckx, 1973), which indicate that seasonal subtropical climatic conditions prevailed in this area during the Early to Middle Eocene. Granite weathers rapidly in moist microclimates, due to the expansion of biotite, which promotes mechanical weathering (Bull, 1991). The mechanical disaggregation greatly increases the surface area of a given volume of rock, which, in turn, enhances chemical weathering of feldspars into clay

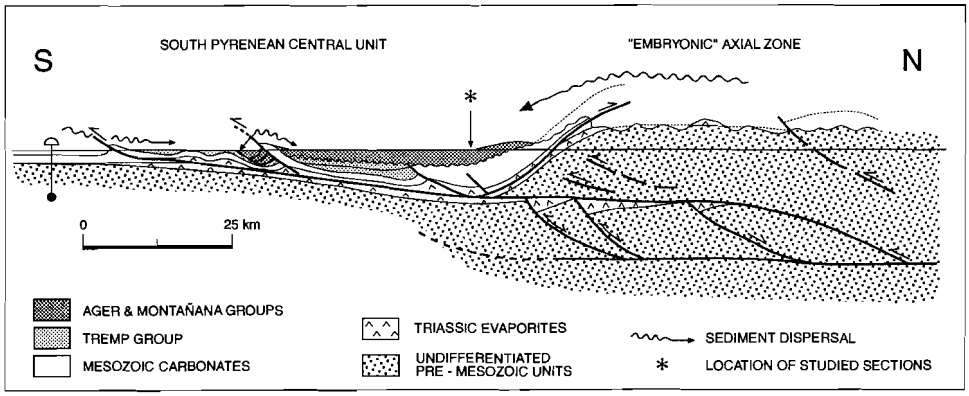

Figure 6. Partially restored balanced cross-section showing the Paleocene to Eocene geography, and the location of inferred source areas (after Puigdefàbregas et al., 1992).

minerals. This phenomenon is responsible for the observed petrographic compositional difference between sand-sized granite detritus produced in (semi)arid and (sub)humid climates (cf. Basu, 1985a; Suttner & Dutta, 1986; Girty, 1991). The inferred distance between the granodioritic complexes of the "embryonic" Axial Zone and the Eocene site of deposition was several tens of kilometres at the most, as indicated by the partially restored balanced cross section of Puigdefàbregas et al. (1992), shown in Fig. 6. Approximately 30% of the conglomerate clasts of the Campanúe Formation could not be unambiguously identified with any of the pre-Eocene lithostratigraphic units outcropping in the South-Central Pyrenees.

7. Statistical comparison of base and top samples

In a series of papers, Aitchison (1986, 1989) presented a methodology for rigorous statistical analysis of compositional data. The benchmark of this method is the transformation of raw compositional data (consisting of variables that sum to a constant) to logratios. The logratios are unconstrained variables of the form $\ln(x/y)$, where x and y represent two components of the same composition. This simple transformation removes the constant-sum and non-negativity constraints on compositional data, and enables the definition of a unique covariance structure, so that the whole range of standard multivariate statistical methods is made available for compositional data analysis. In order to investigate if statistically significant compositional differences are present between samples from the base and the top of the coarse-grained intervals, the following data-processing steps were carried out:

1. Raw compositional data were transformed to logratios. The arithmetic means and sample standard deviations of each logratio in each of the two inferred subpopulations was calculated. Fig. 5 shows the arithmetic mean logratios of the inferred subpopulations retransformed to the original units of measurement (cf. Aitchison, 1989). The arithmetic mean of logratios corresponds to the geometric mean of untransformed compositional variables, recalculated to 100%, the constant row-sum in original units of measurement.

2. It was assumed that the logratios follow an approximately Normal distribution with approximately equal standard deviations, allowing for pairwise comparisons of logratio means with a Student's t-test. Visual inspection of the logratio-distributions showed that these assumptions are reasonable (cf. Fig. 7). Student's t-tests were performed for each logratio (Table 2).

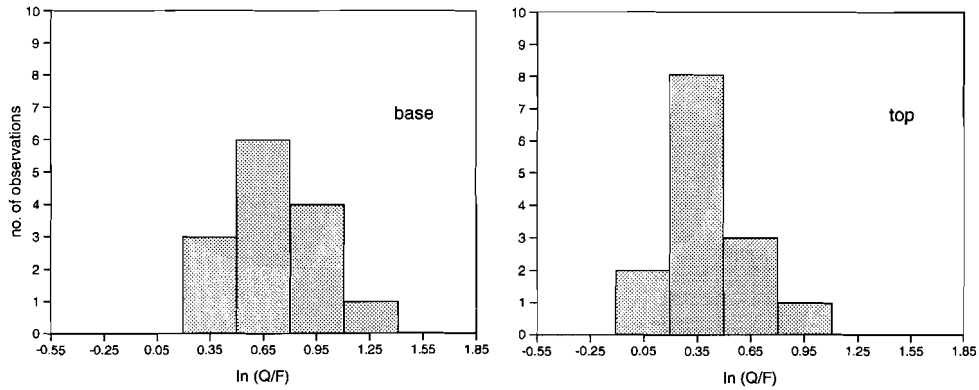

Figure 7. ln(Qt/F) of base and top samples follow an approximately Normal distribution.

Table 2. Statistics of the two-group t-tests. Difference in mean quartz/feldspar ratio of top and base samples is significant at 99% confidence level.

Compositional variables		ln (Qt/F)	ln (Qt/Lc)	ln (Lc/F)
TOP	Mean	0.4012	0.3247	0.0766
	Variance	0.0553	0.1021	0.1813
	Number	14	14	14
BASE	Mean	0.6831	0.3688	0.3144
	Variance	0.0459	0.0493	0.1027
	Number	14	14	14
t-value (df=26)		3.3156	0.4242	1.6695
Significance probability		**0.99**	0.75	0.85

The results of the t-tests (Table 2) indicate that the ln(Qt/F) means of the two subpopulations differ significantly at the 99% level, pointing to a systematic difference of quartz/feldspar ratios between base and top of the coarse-grained intervals. There is no reason to distinguish two subpopulations on the basis of distributions of ln(Qt/Lc) or ln(Lc/F). However, the standard deviations of ln(Qt/Lc) and ln(Lc/F) are larger than those of ln(Qt/F), suggesting that the observed compositional variation is largely due to to random mixing of carbonate and granite detritus. The results of the statistical analysis thus support the hypothesis of De Boer et al. (1991), who attributed the alternation of coarse and fine-grained intervals to variations of sediment supply, instead of laterally switching channels

and interchannel deposits. The systematic trend from base to top within the coarse-grained intervals indicates weathering of detritus in the hinterland during times of temporary storage, which coincided with intervals of mudstone deposition in the basin.

8. A mixing model of Campanúe sandstones

End-member modelling is a method for describing complex patterns of compositional variation in terms of mixing. A detailed account of the mathematical background and application of the method has been presented in chapters 3 and 4 of this thesis. Following the procedures set out in chapter 3, a mixing model was established in two steps.

The first step is to estimate the number of end members. In this particular case, the number of end members can be easily inferred from the nature of the data: The pattern of compositional variation cannot be described by mixing of two end members, because the datapoints do not cluster about a line on the ternary diagram of Fig. 5. An adequate description of the data requires that the number of end members is increased to three, which also happens to be the maximum number that can be distinguished (equal to the number of variables). A three end-member solution was calculated by running the end-member modelling programs with the raw QtFLc% data shown in Fig. 5. This model is presented in Fig. 8.

Table 3. Modelled end members of Campanúe sandstones and their interpretation.

Grain types	End member 1	End member 2	End member 3
Quartzose grains (Qt)	51.7	28.1	51.1
Feldspars (F)	39.8	27.9	11.7
Extrabasinal limeclasts (Lc)	8.5	44.0	37.2
Interpretation	fresh granite	carbonate + fresh granite	carbonate + weathered granite

The end-member compositions are interpreted as follows (Table 3): End member 1 consists of subequal amounts of quartz and feldspar (with a small amount of carbonate), suggesting that it represents fresh granite detritus. End member 2 can be regarded as a mixture of compositionally similar fresh granite detritus and carbonate detritus. End member 3 is interpreted as a mixture of weathered granite detritus and carbonate detritus, on account of its high quartz/feldspar ratio.

The distribution of samples within the mixing space defined by the end members clearly indicates that mixing of end members 1 and 3 prevailed in the basal parts of the coarse-grained units, whereas compositional variation in their upper parts reflects the mixing of end members 1 and 2 (Fig. 8). The mixing proportions of base and top samples thus strongly suggest the existence of two superimposed patterns of binary mixing, instead of a single pattern attributable to random ternary mixing. Contributions of end member 1 appear to be present in subequal proportions throughout the coarse-grained intervals. The spatial (temporal) relation between base and top samples indicates that the end members 2 and 3 cannot be simply regarded as two coeval source areas located in different parts of the

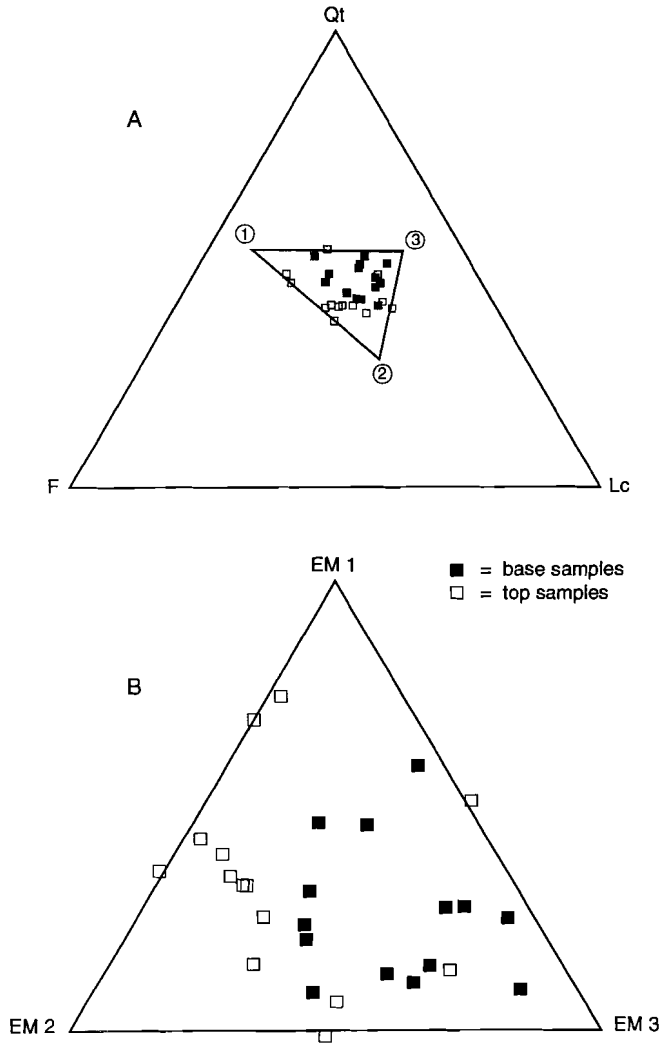

Figure 8. Mixing model of Campanúe sandstones. A: mixing polytope depicted in conventional ternary diagram. B: mixing model, showing two superimposed patterns of binary mixing (see text for discussion).

orogenic hinterland. The more plausible explanation for the temporal mixing pattern is that end members 2 and 3 represent fresh and weathered detritus shed by the same source area at different times. Carbonates were the principal parent rocks exposed in this second source area, whose detritus was mixed with granite detritus derived from the first source.

This interpretation of the modelling results is consistent with palaeogeographic and palaeotectonic reconstructions, and allows to describe the framework composition of the Campanúe sandstones in terms of proportional contributions of two distinct parent-rock assemblages, which were part of different structural units (cf. Muñoz, 1992). The first

source, located at a distance of several tens of kilometres from the basin, consisted of granodioritic rocks of the Nogueres Unit, the uppermost unit of the Axial Zone antiformal stack. The second source, which was located at a distance of about ten kilometres from the site of deposition, consisted of carbonate rocks of the South Central Pyrenean cover thrust sheets. The second source area was located along the pathway between the granitic source in the embryonic Axial Zone and the Eocene basin. The granite detritus which passed through this transitional source area shows clear signs of compositional variation attributable to chemical weathering. The quartz/feldspar ratio of the granite detritus varied between that of end members 2 and 3, depending on the rate of weathering and on the storage time in the transitional source area, which can be regarded as a subaerial sediment reservoir.

9. Spatial constraints on chemical weathering

A significant compositional trend was recognized within the coarse-grained units: granite detritus from the base has been affected by chemical weathering, whereas detritus from the upper part of the coarse-grained units is essentially fresh. From the viewpoint of linear end-member modelling of the sand fraction, chemical weathering of monomineralic rocks is indistinguishable from effects of linear mixing. Therefore, compositional shifts attributable to chemical weathering of carbonate detritus in the transitional source area cannot be recognized by the petrographic analysis of sand-sized sediments alone, but require a comparison of clay-sized carbonate weathering residues with Eocene mudstones in the Tremp-Graus Basin. Such data are presently unavailable. However, the proportional contribution of carbonate clasts to the sediment provides additional constraints on the nature of chemical weathering in the Eocene Tremp-Graus Basin.

The results of the statistical analysis indicate that compositional variation within the sandstone population was largely determined by physical mixing: granite detritus produced in the Axial Zone was mixed with carbonate detritus produced in the second source area before entering the basin, as shown in Fig. 6. Carbonate clasts are highly susceptible to chemical weathering. If random mixing of carbonate detritus and granite detritus would have taken place before the sediment was subjected to chemical weathering, the decomposition and alteration of feldspar grains would have been accompanied by extensive dissolution of carbonate. However, the statistical analysis shows that quartz/carbonate and feldspar/carbonate ratios of base and top samples are not significantly different, indicating that the proportional contribution of carbonate detritus supplied to the basin varied independently of the extent of chemical weathering of granite detritus. This implies that mixing of the two types of detritus must have occurred during or after chemical weathering of the granitic material, and excludes the possibility of chemical weathering at the site of deposition. Weathering thus preceded mixing, or mixing and weathering occurred simultaneously.

Weathering of granite detritus between its ultimate source and the basin of deposition could have taken place in the embryonic Axial Zone, i.e., before mixing with carbonate detritus, or at the site where mixing took place. The geotectonic setting of the Pyrenees leaves little doubt that the production of granite detritus in the Axial Zone was governed by high tectonic uplift rates, which created a high relief and imposed severe restrictions on microclimate conditions in the orogenic source area (cf. Bull, 1991; Johnsson et al., 1991;

Dutta, 1992). As a rule, the combination of steep slopes and high-altitude microclimates in actively uplifting mountainous source areas guarantees a more or less continuous production of fresh detritus through mechanical weathering. Chemical weathering of granite detritus in the mountainous source area is therefore not very likely.

We are left with the possibility that weathering occurred in the area where mixing with carbonate detritus took place. Climatic-physiographic signatures of detrital materials are generally acquired by chemical weathering in those parts of the sedimentary system where storage times of detritus are relatively long (cf. Johnsson & Meade, 1990; Johnsson et al., 1991). In case of the Southern Pyrenees, seasonal subtropical conditions inferred on the basis of pollen assemblages in the Eocene deltaic deposits (Haseldonckx, 1973) suggest that climatic conditions in drainage basins at relatively low altitudes favoured rapid chemical weathering, and that these subaerial sediment reservoirs may have been (intermittently) protected by a dense vegetation cover. Chemical weathering during temporary storage in the lower reaches of the feeder system therefore seems to be the most likely explanation of the observed compositional variation.

10. Tectonic vs. climatic control: discussion

The clearly recognized compositional variation in the coarse-grained units of the Campanúe Formation points to more or less regular changes of climatic-physiographic conditions in the source area. However, this observation alone does not provide any clue for ascribing the observed small-scale variations of sedimentary facies to tectonic or climatic causes. The extent of weathering is determined by the rate of weathering and by the residence time of detritus in the weathering environment. Therefore, the compositional shifts may have been produced by tectonic activity as well as by climate changes, which could have affected relief (residence time) and precipitation (weathering rate), respectively.

The systematic difference in composition of granite detritus reflects temporary storage of sand-sized material in the hinterland during intervals of mudstone deposition in the alluvial-fan system. In spite of the inferred continuous production of granite detritus in the hinterland, sand-sized material was not transported continuously towards the basin. The observed alternation of coarse and fine-grained sediments therefore requires a mechanism for the intermittent storage of coarse-grained sediment in the hinterland.

Numerical modelling of small-scale vertical grain-size alternations in the South-Central Pyrenean foreland basin (Peper & De Boer, 1994) suggests that the observed patterns could have been produced by episodic local intrabasinal uplift, due to thrusting between the source area and the site of deposition, which would have caused a nearly instantaneous redistribution of sediments in a thin veneer over a wide area. However, their experiments indicated that similar grain-size alternations can also be produced by a repeated change of erosion rates due to climatic fluctuations. Moreover, the reconstructed location of the studied sections on the partially restored balanced cross-section of the Tremp-Graus Basin (Fig. 6) indicates that there were two potential sediment traps along the pathway from source to basin: the northwestward continuation of the blind Boixols thrust (an intrabasinal thrust) and the Morerres backthrust which bounded the SPCU on its northern side, respectively. This allows to sketch three hypothetical scenarios to explain the observed lithological and compositional variations.

In the **first scenario**, coarse-grained sediments would have been trapped behind the blind Boixols thrust (cf. Belt & Lyons, 1989), whereas fine-grained sediments would have bypassed the upthrusted area to be deposited in the basin. Each coarse-grained interval in the basin would represent an episode of renewed erosion in the transitional storage area after blocking of the discharge of coarse-grained sediments. This scenario is similar to the erosion and instantaneous redistribution of sediments caused by intrabasinal blind thrusts, as envisaged by Peper & De Boer (1994). In both cases, the coarse-grained material supplied to the basin would consist of sediments previously stored behind and/or above the blind thrust.

While this scenario is undoubtedly attractive, especially because synsedimentary folding of the basin fill has been recognized (De Boer et al., 1991), it fails to account for the petrographic compositional trends within the coarse-grained intervals. The first scenario is thus unlikely, because it implies temporary storage and chemical weathering of sand-sized detritus in the basin, a mechanism that was excluded on the basis of the results of the statistical analysis.

The **second scenario** invokes intermittent storage of coarse-grained sediments due to activity of the Morerres passive roof backthrust, in response to episodic thrusting in the embryonic Axial Zone. Synsedimentary activity of the Morerres backthrust was inferred on the basis of the "inverted unroofing sequence" in the Campanúe conglomerates (De Loos, 1988). If episodic activity of the Morerres backthrust is invoked to explain the observed alternations, the mudstone intervals in the basin must have been deposited during periods in which sediment supply was blocked after activity on the thrust. Renewed deposition of coarse-grained sediments in the basin would have been possible after break-down of the physical barrier formed by the upthrusted carbonates of the SPCU, due to mechanical and chemical weathering, followed by erosion of the temporary sediment reservoir located in the footwall of the backthrust.

If tectonics are regarded as the exclusive control on sediment supply, the mudstones must have been exclusively derived from dissolution of the upthrusted carbonates of the SPCU, that formed the structural barrier. If it is assumed that coarse-grained sediments were protected by a vegetation cover, the mudstones could have been supplied by weathering of both carbonates and feldspar. The latter assumption is most likely, in view of the inferred subtropical climate in the Eocene of the Southern Pyrenees.

The **third scenario** is based on insights gained from the study of modern alluvial systems by Quaternary geologists and geomorphologists, which suggest that the observed lithological and mineralogical variations within the Campanúe Formation can also be interpreted as the result of short-term climate changes. The combination of high tectonic uplift rates, high relief, and high-altitude microclimatic conditions in orogenic source areas such as the Pyrenees favours a constant production of relatively fresh detritus by means of mechanical weathering. In the lower reaches of the alluvial feeder system, where gradients were lower and a presumably dense vegetation cover was present, sediment could be temporarily stored and modified by chemical weathering in subaerial reservoirs. The storage capacity of subaerial reservoirs is strongly influenced by climatic perturbations, such as changes in temperature and precipitation, which are the principal controls on vegetation density and runoff-infiltration ratios (Bull, 1991). Studies of Quaternary alluvial systems

indicate that the evolution of subaerial reservoirs is largely dictated by self-enhancing feedback mechanisms, which preclude a random alternation between stages of denudation and stages of colluvial aggradation and soil formation. The timing of climatically induced aggradation and degradation events as determined for Quaternary alluvial systems reflects climatic, lithologic, and tectonic controls of the time needed to replenish hillslope sediment reservoirs after a stripping event (Bull, 1991). The tectonic setting and climatic conditions in the Pyrenees during the Eocene permitted a large supply of detritus, and allowed for rapid chemical weathering. Under such circumstances, reservoirs were recharged rapidly, so that the system again became sensitive to climatic perturbations of sufficient strength to initiate a new stripping event.

11. Conclusions

It follows from the above discussion that the small-scale lithofacies alternations described by De Boer et al. (1991) can be most satisfactorily attributed to a combination of tectonic and climatic controls. Over longer time spans, tectonics and climate were equally important in determining the sediment flux from hinterland to basin in the Southern Pyrenees. Which of these two factors exerted a dominant influence on the observed short-term variations in the studied sections can (as yet) not be determined beyond reasonable doubt, in spite of the detailed reconstruction of hinterland palaeogeography, source-area lithologies, and chemical weathering in transit.

A scenario based on intermittent tectonic activity implies that the presumably dense subtropical vegetation cover in the lower reaches of the alluvial feeder system was unable to influence tectonically induced variations of sediment supply. This assertion is in conflict with the results of geomorphological studies of alluvial systems, in which variations of vegetation density, runoff-infiltration ratios, and soil erosion have been identified as the principal controls on short-term variations of sediment supply (e.g., Bull, 1991). Consequently, a tectonic scenario requires a "climatic background" of abundant subtropical vegetation that protected sand-sized sediments from erosion during periods of chemical weathering and mudstone accumulation in the basin.

A scenario based on short-term climatic fluctuations takes into account the presently available knowledge of Quaternary geomorphic systems, which provides an actualistic baseline for the interpretation of ancient sedimentary systems. Of particular interest is the notion that relatively small climatic perturbations can be amplified by self-enhancing feedback mechanisms operating in hill-slope reservoirs. However, a climatic scenario requires a "tectonic framework" provided by relatively high uplift rates and high-altitude microclimate conditions, in order to explain the presumably rapid mechanical weathering and recharging of hill-slope reservoirs. It can therefore not be concluded that palaeoclimate was the dominant control on short-term sedimentation patterns in the Campanúe fan-delta, but it can only be assumed that climatic fluctuations in this tectonically active area were large enough to initiate shifts from aggradation to degradation and *vice versa.*

The working hypotheses presented above can be tested by detailed palynological investigations (aimed at reconstructing the hinterland vegetation) and geochemical-mineralogical analysis of weathering residues and alluvial mudstone compositions (aimed at tracing the parentage and genetic significance of the fine-grained sediments). It is

difficult to imagine how a definite proof of palaeotectonic control could be obtained. A definite proof of palaeoclimatic control requires the identification of orbital frequencies in the detrital signal under investigation (cf. Weltje & De Boer, 1993). Unfortunately, the analysis of high-frequency detrital signals is, as yet, precluded by the absence of high-resolution time control in the Eocene basin fill.

CHAPTER 8

ASTRONOMICALLY INDUCED PALAEOCLIMATIC OSCILLATIONS REFLECTED IN PLIOCENE TURBIDITE DEPOSITS ON CORFU (GREECE): IMPLICATIONS FOR THE INTERPRETATION OF HIGHER ORDER CYCLICITY IN FOSSIL TURBIDITE SYSTEMS

G.J. Weltje & P.L. de Boer

Comparative Sedimentology Division, Institute of Earth Sciences,
P.O. Box 80.021, 3508 TA Utrecht, The Netherlands

Abstract

The growth pattern of fan lobes in the early Pliocene Corfu turbidite system (Greece) demonstrates that regional climatic fluctuations in the land-locked Mediterranean completely concealed global glacio-eustatic effects. The temporal evolution of the fan lobes studied closely matches the astronomical precession cycle in this time interval (±23 ka), strongly suggesting that regularly waxing and waning of the sediment supply to the delta-fed turbidite system were directly driven by changes of precipitation and continental runoff. The common lack of high-resolution time control in fossil turbidite systems may lead to mistaken interpretations of higher order cyclicity in fossil turbidite sequences produced by precession-induced variations of sediment supply at low palaeolatitudes.

1. Introduction

Turbidite systems are fed by gravitationally transported and redeposited sediments derived from intermittent storage areas, such as shelf edges and delta slopes, or directly from the continent (Mutti, 1985; Normark & Piper, 1991). The growth of (sub)recent turbidite systems, especially those associated with long-lived submarine fans located along passive Atlantic-type margins, has been strongly influenced by glacio-eustatic sea-level changes (Shanmugam et al., 1985; Stow et al., 1985). Many are inactive now, in response to the fast Holocene sea-level rise. However, the extreme magnitude and high frequency of the Quaternary glacio-eustatic sea-level changes are anomalous geologic features. Consequently, the growth of ancient, pre-Quaternary turbidite systems may have been controlled by other mechanisms (Foucault et al., 1987; Weltje & De Boer, 1990). An example of this proposition is provided by a high-resolution record of the early Pliocene turbidite system of Corfu (Greece). Our observations strongly suggest that the regular waxing and waning of the sediment supply to this delta-fed system were directly driven by precession-induced changes of precipitation and continental runoff.

2. Corfu turbidite system

The lower Pliocene siliciclastic sedimentary rocks of Corfu represent the distal part of a turbidite system, which was deposited in an elongate north-northwest oriented thrust-sheet-top basin of the external Ionian zone of the Hellenides (Monopolis & Bruneton, 1982; Jamet, 1982; Underhill, 1989). Palaeo-flow directions as revealed by sedimentary structures in the sandy turbidite beds indicate a consistent north-northwestward sediment transport, parallel to the closely spaced thrusts delimiting the basin (Monopolis & Bruneton, 1982; Jamet, 1982). Coeval terrestrial and shallow marine fan-delta sedimentary units, inferred to represent the proximal part of the same depositional system, are exposed on the Ionian Islands and on the Greek mainland (Epirus), 150 km toward the south-southeast (Doutsos et al., 1987; Clews, 1989).

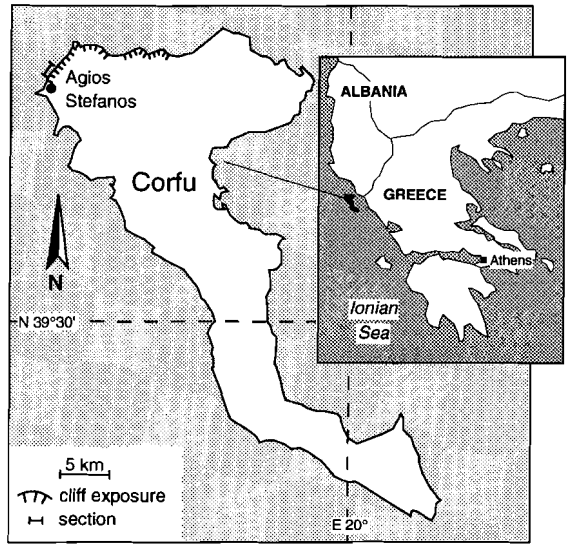

Figure 1. Northwestern Greece and location of studied section on Corfu.

The lower Pliocene turbidite sequence (*G. margaritae* biozone; Bizon, 1967; Vismara Schilling et al., 1976; Jamet, 1982) consists of a 500-m-thick series of regularly stacked depositional lobes, continuously exposed over a distance of 10 km in a series of cliffs, which make up the northwest and north coast of Corfu (Figs. 1 and 2). The section has been virtually unaffected by tectonic deformation, apart from occasional subvertical normal faults with a maximum throw of several meters. Their occurrence can be attributed to the gravitational instability of the poorly consolidated lower Pliocene sedimentary units, and to the (sub)recent uplift of the island. Units on both sides of such faults can be matched without difficulty.

3. High-resolution time control

Detailed magnetostratigraphic investigations of this lower Pliocene cliff section (Linssen, 1991; J.D.A. Zijderveld et al., unpublished data) have shown that the entire sequence spans ±500 ka and contains four geomagnetic polarity reversals. The average net sediment

accumulation rate (±1 m/ka) and the average thickness of the lobe units (20 to 25 m) indicate that each stage of lobe aggradation represents a time span of the order of 20 to 25 ka. The depositional lobes of the Corfu turbidite system can thus be classified as substages, i.e., fifth- to sixth-order sequences (cf. Mutti & Normark, 1987).

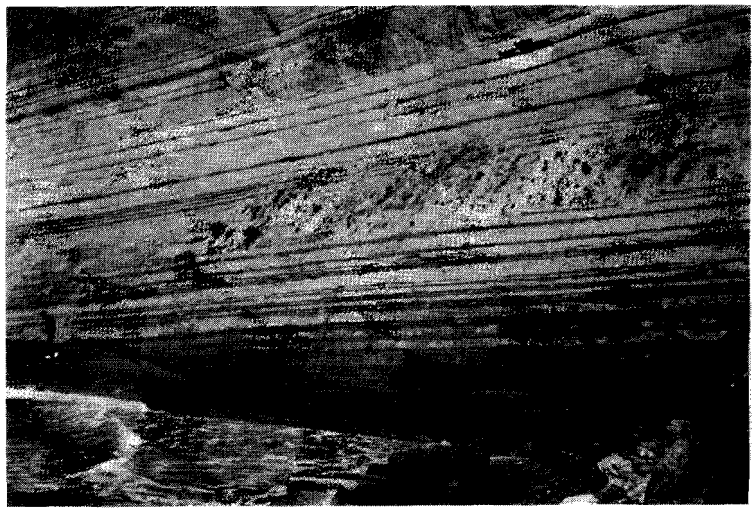

Figure 2. Detail of cliff section, showing topmost part of relatively sand-rich lobe deposit (dark layers are sandy turbidites) and overlying relatively mud-rich interlobe deposit.

An excellent coastal exposure of the three lowermost lobe units north of the village of Agios Stefanos (Fig. 1) was studied and sampled in detail, and the mineralogy of the sandstones, the magnetic susceptibility, and the floral/faunal content of the mudstones were analyzed. The total stratigraphic thickness of the section studied is 93 m. The Upper Thvera polarity reversal (4.98 Ma; Hilgen, 1991) is located 57.5 m above the base, and the subsequent Lower Sidufjall polarity reversal (4.89 Ma; Hilgen, 1991) is located 58.5 m above the top of the section investigated (Linssen, 1991; J.D.A. Zijderveld et al., unpublished data). The average net mudstone accumulation rate calculated for the three intervals between the geomagnetic reversals (Linssen, 1991) decreases from base to top.

The lithologic bed-thickness record was converted into a time series by excluding the sandy turbidite beds, representing instantaneous events, and by correcting the cumulative mudstone thicknesses by means of a linear stretching function, based on the interpolation and downward extrapolation of the upward-decreasing mudstone accumulation rate. This lithologic signal was calibrated with the Upper Thvera and Lower Sidufjall polarity reversals, which led to an age estimate of 5030 ±5 to 4945 ±5 ka for the studied interval, i.e., a timespan of 85 ±10 ka. Subsequently the lithological and mineralogical signals were resampled at 1.0 ka intervals by means of second-order polynomial interpolation. The resulting equally spaced time series were smoothed twice by a three-point moving average.

4. Temporal evolution and growth pattern of the fan lobes

The evolution of the depositional lobes is illustrated by the three signals displayed in Figure 3. The number of turbidite beds (events) per unit time interval (±1.26 ka, corresponding to

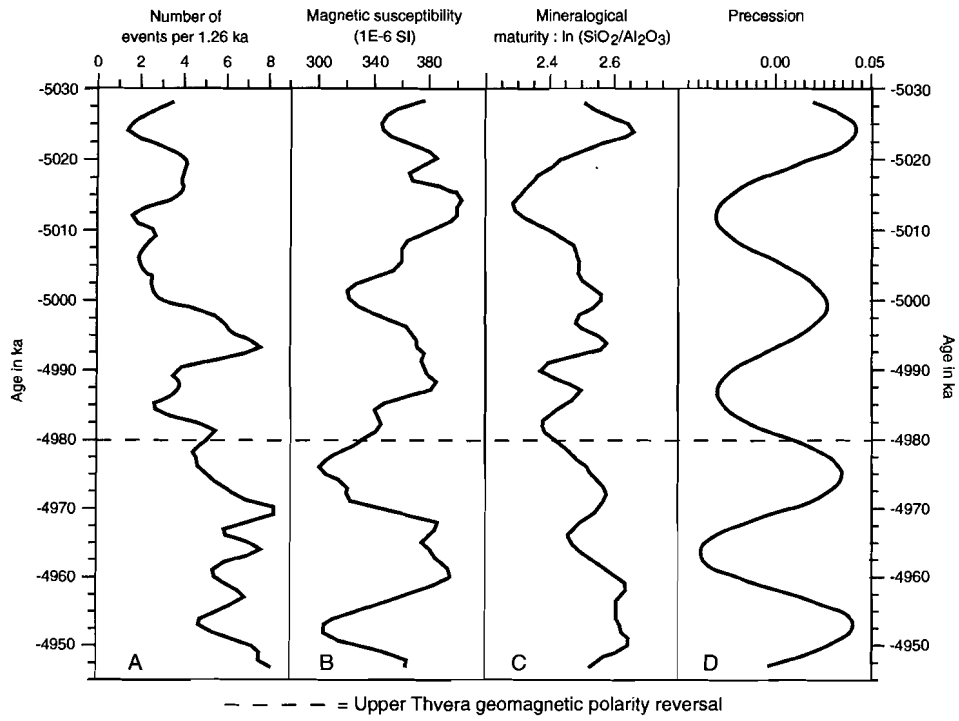

Figure 3. A: no. of events per unit time interval. B: magnetic susceptibility of mudstone. C: mineralogical maturity of sandstone. D: reconstructed precession signal (Berger & Loutre, 1991).

1.0 m of corrected mudstone thickness) shows three maxima, representing phases of accelerated growth of the lobes (Fig. 3A). The magnetic susceptibility of the mudstones shows a similar pattern (Fig. 3B). The magnetic susceptibility is inversely proportional to the $CaCO_3$ content of the mudstone and can therefore be interpreted as a dilution signal (Weedon et al., 1991). Both signals reflect a gradual and regular variation of the proportion of terrigenous sediment, which we attribute to a regular waxing and waning of sediment supply from the continent. This interpretation is confirmed by the dominance of land-derived plant fragments (lignite) in mudstones deposited during intervals of inferred maximum terrigenous supply. In mudstones deposited during periods of inferred minimum supply, the coarse-grained fraction consists almost exclusively of planktonic foraminifera.

The mineralogical maturity of the very fine sand fractions of 42 turbidites was defined on the basis of chemical analyses of their major oxide compositions. Very fine sand was selected for these analyses because this fraction is present in all turbidites and because it is composed almost exclusively of monomineralic quartz and feldspar grains, enabling a straightforward matching of chemical and mineral composition. The mineralogical maturity of the turbidite sands, expressed as $\ln[SiO_2/Al_2O_3]$ of the 63-125 μm fraction, is independent of the bed thickness of the turbidites and does not show a net trend from base to top, indicating that the character of the source area remained relatively stable. However, the mineralogical maturity signal clearly does reflect cyclic fluctuations of the intensity and/or duration of weathering of sand-sized material in the transitional source area prior to

redeposition in the turbidite system (Fig. 3C). The mineralogical maturity is negatively correlated with the sediment supply signals (Fig. 3, A and B), indicating that relatively immature sands (low Q/F ratio) were deposited during periods of maximum terrigenous supply, whereas relatively mature sands (high Q/F ratio) were deposited during periods of minimum supply.

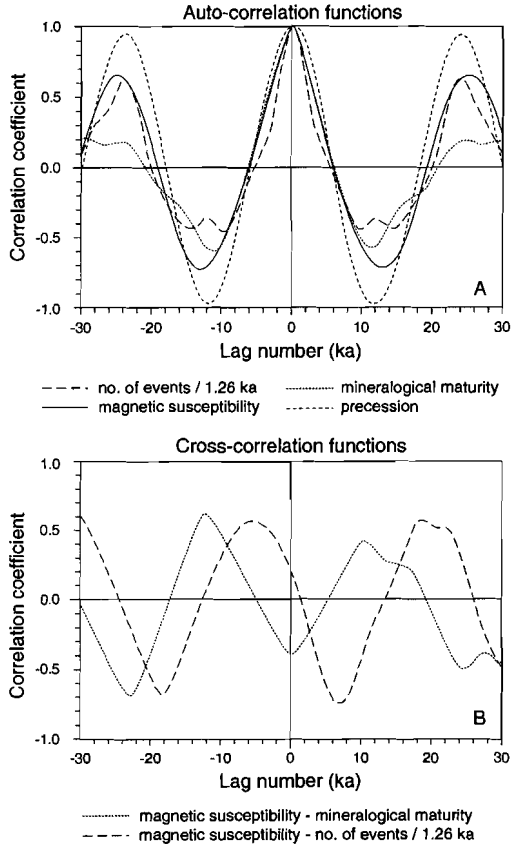

Figure 4. Autocorrelation (A) and cross-correlation (B) functions of detrended and zero-centred time series displayed in Fig. 3, showing 23-24 ka wavelength and phase relations.

5. Palaeoclimatic fluctuations

The autocorrelation functions of the signals from the Corfu sequence show a periodicity of 23-24 ka (Fig. 4A). They closely match the autocorrelation function of the precession cycle as reconstructed by Berger & Loutre (1991), which displays a period of 23 ka in this time interval (Fig. 3D). The precession cycle causes regular shifts of the caloric equator and of the low-latitude climatic belts, with a dominant period of 19-23 ka (Berger, 1978, 1988). At low latitudes, the climatic effects of the precession cycle comprise regular changes of evaporation-precipitation ratios, summer-winter contrasts, and monsoon intensity (Berger, 1978, 1988; Prell & Kutzbach, 1987; Perlmutter & Matthews, 1989; Fischer et al., 1990).

Detailed sedimentary records of precession-induced climatic and oceanographic fluctuations - inferred to reflect changes of runoff, sediment supply, and primary productivity - have been established in lower Pliocene hemipelagic sediments of the central Mediterranean (Gudjonsson, 1987; Hilgen, 1987; De Visser et al., 1989; Hilgen & Langereis, 1989; Thunell et al., 1991). The precession-induced sedimentary responses and the $\delta^{18}O$ records of the central Mediterranean lower Pliocene do not match the Atlantic $\delta^{18}O$ record, which is dominated by the 41 ka obliquity cycle and is explained in terms of glacio-eustatic effects (Joyce et al., 1990). The poor fit of the Atlantic and Mediterranean records indicates that regional climatic factors contributed significantly to the short-term palaeoclimatic and palaeoceanographic evolution of the land-locked Mediterranean basin, concealing the influence of glacio-eustatic effects.

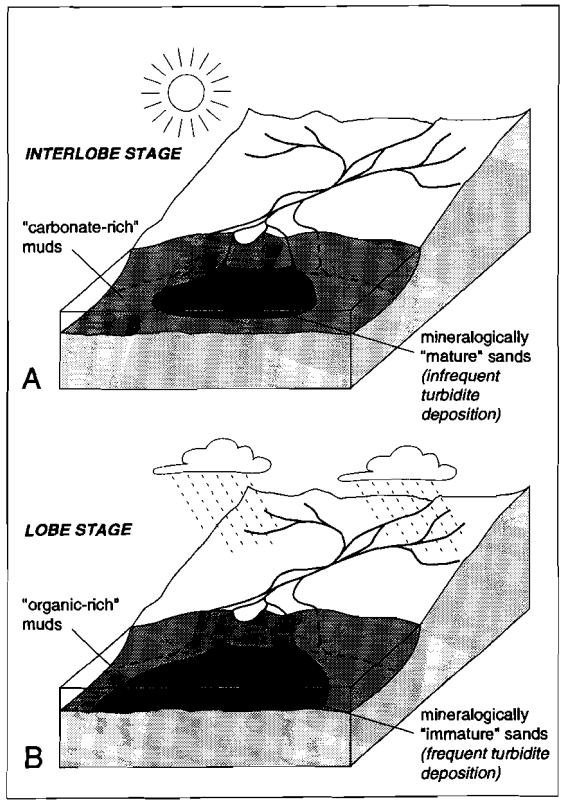

Figure 5. Fan-lobe aggradation in Corfu turbidite system. Growth stages were controlled by precession-induced alternations of relatively dry (A) and humid (B) periods.

6. Discussion and conclusions

The 23 ka wavelength of the signals recorded in the Corfu turbidites (Fig. 4A) strongly suggests that the depositional lobes developed in response to regional, precession-induced palaeoclimatic oscillations, rather than glacio-eustatic sea-level fluctuations. This interpretation is supported by (1) the apparent predominance of regional climatic effects in the Pliocene Mediterranean, as discussed above, and (2) the tectonic setting of the basin,

which precludes the presence of shelf areas, indicating that the influence of possible fluctuations of relative sea level on the sediment budget of the Corfu turbidite system was of minor or no importance.

Instead, secular fluctuations of river discharge, reflecting precipitation changes, must have caused the cyclic lobe buildup pattern observed in the delta-fed turbidite system. The link between river floods and the deposition of turbidites from hyperpycnal or underflows is well established in modern (fan-)deltaic settings (Prior & Bornhold, 1989; Normark & Piper, 1991). A periodic alternation of relatively dry and humid climatic conditions, with concomitant changes of runoff and sediment supply, provides the simplest possible explanation for the observed pattern of fan- lobe aggradation (cf. Postma et al., 1992). The phase relations between sediment supply and weathering signals support this view, as shown by the cross-correlation functions (Fig. 4B).

We propose a climatically forced aggradation pattern of the fan lobes in the Corfu turbidite system according to the following scenario: During the interlobe stages (Fig. 5A), which correspond to carbonate-rich mudstone intervals with small amounts of relatively mature sands, carbonate production in the basin was relatively high, and terrigenous input relatively low. During these dry periods, the largely immobile sands were subject to chemical weathering in the transitional source area. Acceleration of the sandy sediment supply and growth of the depositional lobes started at the transition to more humid periods. During the humid lobe stages (Fig. 5B), which correspond to organic-rich mudstone intervals with large amounts of relatively immature sands, increasingly fresh and less mature erosion products were supplied to the basin to form the major part of the lobes. Sediment supply diminished as the climate again became drier and the cycle was completed.

The exceptionally good time control of the Corfu turbidite section enables us to demonstrate that regional palaeoclimatic fluctuations may completely conceal global glacio-eustatic effects. Furthermore, the Corfu case shows that the common lack of high-resolution time control in fossil turbidite systems may lead to mistaken interpretations of higher order cyclicity in fossil turbidite systems produced by precession-induced variations of sediment supply at low palaeolatitudes.

Acknowledgements

We thank J.D.A. Zijderveld and C.G. Langereis for drawing our attention to the Corfu turbidite system; M.J. Kraus, D.J.W. Piper and G. Postma for their critical remarks and positive suggestions; T. Zalm and M. Reith for preparing the samples; F. Trappenburg for making the drawings; and attendees of the Deep-sea Clastics Workshop of the British Sedimentological Research Group, at the University of Oxford, March 1992, for their comments and suggestions.

REFERENCES

Abbott, P.L., & Peterson, G.L. (1978) Effects of abrasion durability on conglomerate clast populations: examples from Cretaceous and Eocene conglomerates of the San Diego area, California. J. Sed. Petrol., 4: 31-42.

Afchain, C. (1966) La base de la série tertiaire sur le bord de la Calabre ultérieure (note préliminaire). C. R. somm. Soc. Geol. Fr., pp. 397-398.

Afchain, C. (1967) Les argiles écailleuses versicolores et les couches à huîtres de Motticella (Reggio de Calabre, Italie méridionale). C. R. somm. Soc. Geol. Fr., pp. 366-368.

Afchain, C. (1968) Le témoin calcaire de Sideroni, près de Bova Marina (Calabre méridionale). C. R. somm. Soc. Geol. Fr., pp. 329-330.

Aitchison, J. (1986) The statistical analysis of compositional data. Chapman & Hall, London, 416 pp.

Aitchison, J. (1989) Measures of location of compositional data sets. Math. Geol., 21: 787-790.

Aitchison, J. (1990) Comment on "Measures of variability for geological data" by D.F. Watson and G.M. Philip. Math. Geol., 22: 223-226.

Aitchison, J. (1991a) Delusions of uniqueness and ineluctability. Math. Geol., 23: 275-277.

Aitchison, J. (1991b) A plea for precision in Mathematical Geology. Math. Geol., 23: 1081-1083.

Aitchison, J. (1992) On criteria for measures of compositional difference. Math. Geol., 24: 365-379.

Aitchison, J., & Shen, S.M. (1984) Measurement error in compositional data. Math. Geol., 16: 637-650.

Albarède, F., & Provost, A. (1977) Petrological and geochemical mass-balance equations: An algorithm for least-squares fitting and general error analysis. Comput. Geosci., 3: 309-326.

Amodio-Morelli, L., Bonardi, G., Colonna, V., Dietrich, D., Giunta, G., Ippolito, F., Liguori, V., Lorenzoni, S., Paglionico, A., Perrone, V., Piccaretta, G., Russo, M., Scandone, P., Zanettin-Lorenzoni, E., & Zuppetta, A. (1976) L'arco calabro-peloritano nell'orogene Apenninico-Maghrebide. Mem. Soc. Geol. It., 17: 5-60.

Arnone, G., De Rosa, P., & Mascari, A. (1979) Osservazioni geologiche nella zona di Longi (M. Peloritani occidentali). Boll. Soc. Geol. It., 98: 217-226.

Atzori, P., Carveni, P., Lentini, F., Pezzino, A., & Vezzani, L. (1977) Posizione strutturale dei lembi meso-cenozoici dell' Unità di Rocca Novara nei Monti Peloritani (Sicilia nord-orientale). Boll. Soc. Geol. It., 96: 331-338.

Atzori, P., Ferla, P., Paglionico, A., Piccarreta, G., & Rottura, A. (1984) Remnants of the Hercycnian orogen along the "Calabrian-Peloritan arc", southern Italy: a review. J. Geol. Soc., 141: 137-145.

Atzori, P., Lentini, F., Vezzani, L., Lo Giudice, A., & Pezzino, A. (1975) Natura e significato dei lembi sedimentari interposti tra la falde dell'Aspromonte e la falda di Mandanici nei Monti Peloritani (Sicilia nord-orientale). Boll. Soc. Geol. It., 94: 789-795.

Baak, J.A. (1936) Regional petrology of the southern North Sea. Ph.D. Thesis, Veenman & Zonen, Wageningen, 129 pp.

Banks, R. (1979) The use of linear programming in the analysis of petrological mixing problems. Contrib. Mineral. Petrol., 70: 237-244.

Bardsley, W.E. (1978) An extreme value model for expressing grain size and bed thickness as functions of the spatial variation of grain frequency. Math. Geol., 10: 643-655.

Barrier, P. (1986) Evolution paléogéographique du détroit de Messine au Pliocène et au Pléistocène. Giorn. Geol. (3a), 48: 7-24.

Barrier, P., Cravatte, J., Decis, R., Lanzafame, G., & Ott d'Estevou, P. (1987) Mise au point stratigraphique sur les relations entre la "couverture calabride miocène" et les "terrains post-orogéniques" dans la région du Détroit de Messine. Doc. Trav. Inst. Geol. A. de Lapparent, 11: 43-53.

Barrier, P., & Montenat, C. (1987) Essai de quantification des mouvements verticaux plio-pleistocènes dans le Détroit de Messine (Italie). TOTAL Notes et Mem., 21: 73-79.

Basu, A. (1976) Petrology of Holocene fluvial sand derived from plutonic source rocks: implications to paleoclimatic interpretation. J. Sed. Petrol., 46: 694-709.

Basu, A. (1985a) Influence of climate and relief on compositions of sands released at source areas. In: Provenance of arenites (G.G. Zuffa, ed.), Reidel Publ. Co., Dordrecht, pp. 1-18.

Basu, A. (1985b) Reading provenance from detrital quartz. In: Provenance of arenites (G.G. Zuffa, ed.), Reidel Publ. Co., Dordrecht, pp. 231-247.

Basu, A., Young, S.W., Suttner, L.J., James, W.C., & Mack, G.H. (1975) Re-evaluation of the use of undulatory extinction and polycrystallinity in detrital quartz for provenance interpretation. J. Sed. Petrol., 45: 873-882.

Belt, E.S., & Lyons, P.C. (1989) A thrust-ridge paleodepositional model for the Upper Freeport coal bed and associated clastic facies, Upper Potomac coal field, Appalachian basin, U.S.A. Int. J. Coal Geol., 12: 293-328.

Benomran, O., Nairn, A.E.M., & Schamel, S. (1987) Sources and dispersal of mid-cenozoic clastic sediments in the central Mediterranean region. Mem. Soc. Geol. It., 38: 47-68.

Berger, A. (1978) Long-term variations of caloric insolation resulting from the Earth's orbital elements. Quat. Res., 9: 139-167.

Berger, A. (1988) Milankovitch theory and climate. Rev. Geophys., 26: 624-657.

Berger, A., & Loutre, M.F. (1991) Insolation values for the climate of the last 10 million years. Quat. Sci. Rev., 10: 297-317.

Bernouilli, D., & Winkler, W. (1990) Heavy-mineral assemblages from upper Cretaceous South- and Austroalpine flysch sequences (northern Italy and southern Switzerland): source terrains and palaeotectonic implications. Eclogae Geol. Helv., 83: 287-310.

Best, T.C., & Griggs, G.B. (1991) A sediment budget for the Santa Cruz littoral cell, California. In: From shoreline to abyss: contributions in marine geology in honor of Francis Parker Shepard (R.H. Osborne, ed.), Soc. Econ. Pal. Mineral. Spec. Publ. 46, pp. 35-50.

Bezdek, J.C., Ehrlich, R., & Full, W.E. (1984) FCM: the fuzzy c-means clustering algorithm. Comput. Geosci., 10: 191-204.

Bhatia, M.R. (1983) Plate tectonics and the geochemical composition of sandstones. J. Geol., 91: 611-627.

Bianchi, F., Carbone, S., Grasso, M., Invernizzi, G., Lentini, F., Longaretti, G., Merlini, S., & Mostardini, F. (1987) Sicilia orientale: profilo geologico Nebrodi-Iblei. Mem. Soc. Geol. It., 38: 429-458.

Bizon, G. (1967) Contribution a la connaissance des foraminifères planctoniques d'Epire et les Iles Ioniennes (Grèce occidentale) depuis le Paléogène supérieur jusqu'au Pliocène. Editions Technip, Paris, 142 pp.

Blasi, A., & Manassero, M.J. (1990) The Colorado river of Argentina: source, climate, and transport as controlling factors on sand composition. J. South Am. Earth Sci., 3: 65-70.

Blatt, H. (1967) Provenance determinations and recycling of sediments. J. Sed. Petrol., 37: 1031-1044.

Blatt, H. (1978) Sediment dispersal from Vogelsberg basalt, Hessen, West Germany. Geol. Rundsch., 67: 1009-1015.

Boccaletti, M., Ciaranfi, N., Cosentino, D., Deiana, G., Gelati, R., Lentini, F., Massari, F., Moratti, G., Pescatore, T., Ricci Lucchi, F., & Tortorici, L. (1990) Palinspastic restoration and paleogeographic reconstruction of the peri-Tyrrhenian area during the Neogene. Palaeogeogr., Paleaeoclim., Palaeoecol., 77: 41-50.

Boccaletti, M., Nicolich, R. & Tortorici, L. (1984) The Calabrian Arc and the Ionian Sea in the dynamic evolution of the Central Mediterranean. Mar. Geol., 55: 219-245.

Boggs, S. Jr. (1968) Experimental study of rock fragments. J. Sed. Petrol., 38: 1326-1339.

Boltovskoy, E. & Wright, R. (1976) Recent foraminifera, Junk, The Hague, 515 pp.

Bonardi, G., Compagnoni, R., Del Moro, A., Messina, A., & Perrone, V. (1987) Reiquilibrazioni tettono-metamorfiche alpine nell'Unità dell'Aspromonte, Calabria meridionale. Rend. Soc. Italiana Mineral. Petrol., 42: 301.

Bonardi, G., Compagnoni, R., Messina, A., Perrone, V., Russo, S., De Francesco, A.M., Del Moro, A., & Platt, J.P. (1992) Sovrimpronta metamorfica alpina nell'Unità dell'Aspromonte (settore meridionale dell'Arco Calabro-Peloritano). Boll. Soc. Geol. It., 111: 81-108.

Bonardi, G., De Vivo, B., Giunta, G., & Perrone, V. (1982) I conglomerati rossi dei Monti Peloritani e considerazioni sull' Unità di Novara. Boll. Soc. Geol. It., 101: 157-172.

Bonardi, G., Giunta, G., Liguori, V., Perrone, V., Russo, M., & Zuppetta, A. (1976) Schema geologico dei Monti Peloritani. Boll. Soc. Geol. It., 95: 49-74.

Bonardi, G., Giunta, G., Perrone, V., Russo, M., Zuppetta, A., & Ciampo, G. (1980) Osservazioni sull'evoluzione dell'arco calabro-peloritano nel Miocene inferiore: la Formazione di Stilo-Capo d'Orlando. Boll. Soc. Geol. It., 99: 365-393.

Bonardi, G., Gurrieri, S., Messina, A., Perrone, V., Russo, M., & Zuppetta, A. (1979) Osservazioni geologiche e petrografiche sull'Aspromonte. Boll. Soc. Geol. It., 98: 55-73.

Bonardi, G., Messina, A., Perrone, V., Russo, S., & Zuppetta, A. (1984) l'Unità di Stilo nel settore meridionale dell'arco calabro-peloritano. Boll. Soc. Geol. It., 103: 279-309.

Bonardi, G., Pescatore, T., Scandone, P., & Torre, M. (1971) Problemi paleogeografici connessi con la successione mesozoico-terziaria di Stilo (Calabria meridionale). Boll. Soc. Natur. Napoli, 80: 147-159.

Bondesan, M., Calderoni, G., & Dal Cin, R. (1978) Il litorale delle province di Ferrara e di Ravenna (alto Adriatico): Evoluzione morfologica e distribuzione dei sedimenti. Boll. Soc. Geol. It., 97: 247-287.

Bortoluzzi, G., Frascari, F., & Ravaioli, M. (1984) Ricerche sedimentologiche in aree marine adriatiehe e tirreniche finalizzate alla comprensione dei fenomeni di inquinamento costiero. Mem. Soc. Geol. It., 27: 499-525.

Boswell, P.G.H. (1915) The stratigraphy and petrology of the lower Eocene deposits of the north-eastern part of the London Basin. Quart. J. Geol. Soc., 71: 536-588.

Boswell, P.G.H. (1916) The application of petrological and quantitative methods to stratigraphy. Geol. Mag., 53: 105-111 & 53: 163-169.

Boswell, P.G.H. (1933) On the mineralogy of sedimentary rocks. Murby & Co., London, 393 pp.

Bouillin, J.P. (1984) Nouvelle interprétation de la liaison Apennin-Maghrébides en Calabre: conséquences sur la paléogéographie téthysienne entre Gibraltar et les Alpes. Rev. Geol. Dyn. Geogr. Phys., 25: 321-338.

Bouillin, J.P., Durand-Delga, M., & Olivier, Ph. (1986) Betic-Rifian and Tyrrhenian arcs: distinctive features, genesis and development stages. In: The origin of arcs (F.C. Wezel, ed.), Elsevier Sci. Publ., Amsterdam, pp. 281-304.

Bouillin, J.P., Majeste-Menjoulas, C., Ollivier-Pierre, M.F., Tambareau, Y., & Vilatte, J. (1985) Transgression de l'Oligocène inférieur (formation de Palizzi) sur un karst à remplissage bauxitique dans les zones internes calabro-péloritaines (Italie). C. R. Acad. Sc. Paris, 301: 415-420.

Bradley, W.C. (1970) Effect of weathering on abrasion of granitic gravel, Colorado River (Texas). Geol. Soc. Am. Bull., 81: 61-80.

Brambati, A. (1970) Provenienza, trasporto e accumolo dei sedimenti recenti nelle lagune di Marano e di Grado e nei litorali tra il fiumi Isonzo e Tagliamento. Mem. Soc. Geol. It., 9: 281-329.

Brambati, A., Catani, G., & Marocco, R. (1977) Indagini sedimentologiche sulla spiaggia sottomarina dell'Adriatico settentrionale tra il fiumi Brenta e Tagliamento. Boll. Soc. Geol. It., 96: 69-86.

Brambati, A., Marocco, R., Catani, G., Carobene, L., & Lenardon, G. (1978) Stato delle conoscenze dei litorali dell'Alto Adriatico e criteri di intervento per la loro difesa. Mem. Soc. Geol. It., 19: 389-398.

Brammall, A. (1928) Dartmoor detritals: a study in provenance. Proc. Geol. Ass., 39: 27-48.

Brayshaw, A.C. (1984) Characteristics and origin of eluster bedforms in coarse-grained alluvial channels. In: Sedimentology of Gravels and Conglomerates (E.H. Koster & R.J. Steel, eds.), Can. Soc. Petrol. Geol. Mem. 10, pp. 77-85.

Breyer, J.A. (1983) Sandstone petrology: a survey for the exploration and production geologist. Mountain Geologist, 20: 15-40.

Breyer, J.A., & Bart, H.A. (1978) The composition of fluvial sands in a temperate semiarid region. J. Sed. Petrol., 48: 1311-1320.

Bromley, R. (1990) Trace fossils: biology and taphonomy. Special topics in palaeontology 3, Unwin Hyman, London, 310 pp.

Bryan, W.B., Finger, L.W., & Chayes, F. (1969) Estimating proportions in petrographic mixing equations by least squares approximation. Science, 163: 926-927.

Bull, W.B. (1991) Geomorphic responses to climatic change. Oxford University Press, New York, 326 pp.

Burrus, J. (1984) Contribution to a geodynamic synthesis of the Provencal Basin (northwestern Mediterranean). Mar. Geol., 55: 247-269.

Burt, C.L. (1937) Correlations between persons. British J. Psychol., 28: 56-96.

Butler, J.C. (1979) Effects of closure on the measures of similarity between samples. Math. Geol., 11: 431-440.

Butler, J.C. (1982) The closure problem as reflected in discriminant function analysis. Chem. Geol., 37: 367-375.

Butler, J.C., & Woronov, A. (1986) Extracting genetic information from coarse clastic modes. Comp. Geosci., 12: 643-652.

Caire, A. (1961) Note préliminaire sur les argiles varicolores des monts Péloritains et de Calabre méridionale. C. R. somm. Soc. Geol. Fr., pp. 233-234.

Caire, A., & Truillet, R. (1967) Les relations entre le domain péloritain et le flysch du Monte Soro aux environs de Roccella Valdemone, et le problème du charriage des Péloritains orientaux (Sicile). Bull. Soc. Geol. Fr. (7), IX: 255-260.

Cámara, P., & Klimowitz, J. (1985) Interpretacion geodinamica de la vertiente centro-occidental surpirenaica (cuencas de Jaca-Tremp). Estudios Geol., 41: 391-404.

Cameron, K.L., & Blatt, H. (1971) Durabilities of sand size schist and "volcanic" rock fragments during fluvial transport, Elk Creek, Black Hills, South Dakota. J. Sed. Petrol., 41: 565-576.

Carmigniani, L., & Kligfield, R. (1990) Crustal extension in the northern Apennines: the transition from compression to extension in the Alpi Apuane core complex. Tectonics, 9: 1275-1303.

Carmisciano, R., Coccioni, R., Corradini, D., D'Alessandro, A., Guerrera, F., Loiacono, F., Moretti, E., Puglisi, D., & Sabato, L. (1987) Nuovi dati sulle "successioni miste" inframioceniche dell'Algeria (Grande Kabilia) e della Sicilia (Monti Nebrodi): confronti con analoghe successioni torbiditiche nell'Arco di Gibilterra e nell'Apennino lucano. Mem. Soc. Geol. It., 38: 551-576.

Carmisciano, R., Gallo, L., Lanzafame, G., & Puglisi, D. (1981a) Le calcareniti di Floresta nella costruzione dell'Apennino calabro-peloritano (Calabria e Sicilia). Geol. Romana, 20: 171-182.

Carmisciano, R., Lentini, F., & Puglisi, D. (1981b) Caratteri petrografici ed evoluzione tettonico-sedimentaria della Formazione di Piedimonte (Sicilia nord-orientale). Rend. Soc. It. Mineral. Petrol., 37: 91-104.

Carmisciano, R., & Puglisi, D. (1978a) Caratteri petrografici delle arenarie del Flysch di Capo d'Orlando (Monti Peloritani, Sicilia nord-orientale). Rend. Soc. It. Mineral. Petrol., 34: 403-424.

Carmisciano, R., & Puglisi, D. (1978b) Il Flysch di Frazzanò (Monti Peloritani, Sicilia nord-orientale): studio composizionale. Miner. Petrogr. Acta, 22: 119-140.

Carmisciano, R., & Puglisi, D. (1982) Studio sedimentologico-petrografico del Flysch di Capo d'Orlando nei Peloritani occidentali (Sicilia). Geol. Romana, 21: 113-123.

Cassola, P., Costa, E., Loiacono, F., Moretti, E., Morlotti, E., Puglisi, D., & Villa, G. (1992) New sedimentologic, petrographic, biostratigraphic and structural data on the Reitano Flysch (Maghrebian chain, Sicily). Riv. It. Paleont. Strat., 98: 000-000 (preprint).

Cassola, P., Giammarino, S., & Puglisi, D. (1990) Elementi per l'inserimento in un quadro evolutivo paleogeografico e strutturale delle successioni torbiditiche cretaciche della Catena nebrodico-peloritana (Sicilia nord-orientale). Mem. Soc. Geol. It., 45: 503-510.

Catani, G., Marocco, R., Brambati, A., Carobene, L., & Lenardon, G. (1978) Indagini sulle cause dell'erosione nel tratto orientale del litorale di Valle Vecchia (Caorle, Adriatico settentrionale). Mem. Soc. Geol. It., 19: 399-405.

Cavazza, W. (1989) Detrital modes and provenance of the Stilo-Capo d'Orlando Formation (Miocene), southern Italy. Sedimentol., 36: 1077-1090.

Cayeux, L. (1906) Structure et origine des grès du Tertiaire parisien: études des gîtes minéraux de la France. Imprim. Nationale, Paris, 131 pp.

Cayeux, L. (1929) Les roches sédimentaire de France: roches siliceuses. Imprim. Nationale, Paris, 774 pp.

Chandler, F.W. (1988) Quartz arenites: review and interpretation. Sediment. Geol., 58: 105-126.

Channell, J.E.T., Catalano, R., & D'Argenio, B. (1980) Paleomagnetism and deformation of the Mesozoic continental margin in Sicily. Tectonophys., 61: 391-407.

Chatterjee, A., Sarkar, S.S., Nandy, S., & Saha, A.K. (1989) A quadratic programming approach for solving petrological mixing models. Indian J. Earth Sci., 16: 104-118.

Chayes, F. (1960) On correlation between variables of constant sum. J. Geophys. Res., 65: 4185-4193.

Chayes, F. (1968) A least squares approximation for estimating the amounts of petrographic partition products. Mineral. Petrogr. Acta, 14: 111-114.

Cherchi, A. (1974) Appunti biostratigrafici sul Miocene della Sardegna (Italia). 5th Congr. Neogene Medit. (Lyon, 1971), Mem. Bur. Rech. Geol. Min., 78: 433-445.

Cherchi, A., & Montadert, L. (1982b) Il sistema di rifting oligo-miocenico del mediterraneo occidentale e sue conseguenze paleogeografiche sul terziario sardo. Mem. Soc. Geol. It., 24: 387-400.

Cherchi, A., & Montadert, L. (1982a) Oligo-Miocene rift of Sardinia and the early history of the Western Mediterranean Basin. Nature, 298: 736-739.

Cherchi, A., & Trémolières, P. (1984) Nouvelles données sur l'évolution structurale au Mésozoïque et au Cénozoïque de la Sardaigne et leurs implications géodynamiques dans le cadre méditerranéen. C. R. Acad. Sc. Paris, 298: 889-894.

Clarke, T.L. (1978) An oblique factor analysis solution for the analysis of mixtures. Math. Geol., 10: 225-241.

Cleary, W.J., & Conolly, J.R. (1971) Distribution and genesis of quartz in a piedmont-coastal plain environment. Geol. Soc. Am. Bull., 82: 2755-2766.

Clemens, K.E., & Komar, P.D. (1988) Oregon beach-sand compositions produced by the mixing of sediments under a transgressing sea. J. Sed. Petrol., 58: 519-529.

Clews, J.E. (1989) Structural controls on basin evolution: Neogene to Quaternary of the Ionian zone, Western Greece. J. Geol. Soc., 146: 447-457.

Clifton, H.E. (1984) Sedimentation units in stratified resedimented conglomerate, Paleocene submarine canyon-fill, Point Lobos, California. In: Sedimentology of Gravels and Conglomerates (E.H. Koster & R.J. Steel, eds.), Can. Soc. Petrol. Geol. Mem. 10, pp. 429-441.

CNR (1976) Risultati delle ricerche fino al 1975 sul litorale alla foce dell'Adige (spiaggia modello). Gruppo di lavoro sul regime e la conservazione dei litorali, Consiglio Nazionale delle Ricerche, Padova, 36 pp. + 60 encl.

Cohen, D., & Ward, C.R. (1991) SEDNORM - A program to calculate a normative mineralogy for sedimentary rocks based on chemical analyses. Comp. & Geosci., 17: 1235-1253.

Colantoni, P., Gallignani, P., & Lenaz, R. (1979) Late Pleistocene and Holocene evolution of the North Adriatic continental shelf (Italy). Mar. Geol., 33: M41-M50.

Colella, A. (1988) Calabrian Arc (Southern Italy). In: International workshop on fan deltas (A. Colella, ed.), Excursion guidebook, University of Calabria, Cosenza, pp. 7-16.

Colella, A., De Boer, P.L., & Nio, S.D. (1981) Sedimentology of a marine intermontane Pleistocene Gilbert-type fan-delta complex in the Crati Basin, Calabria, southern Italy. Sedimentol., 34: 721-736.

Colman, S.M. (1981) Rock-weathering rates as functions of time. Quat. Res., 15: 250-264.

Colman, S.M. (1986) Levels of time information in weathering measurements, with examples from weathering rinds on volcanic clasts in the western United States. In: Rates of chemical weathering of rocks and minerals (S.M. Colman & D.P. Dethier, eds.), Academic Press Inc., Orlando, pp. 379-393.

Colman, S.M., & Dethier, D.P. (1986) An overview of rates of chemical weathering. In: Rates of chemical weathering of rocks and minerals (S.M. Colman & D.P. Dethier, eds.), Academic Press Inc., Orlando, pp. 1-18.

Coltro, R. (1967) Le formazioni cretaceo-paleogeniche della Falda di Longi nella sezione di Militello Rosmarino (Messina). Riv. It. Paleont. Strat., 73: 853-887.

Costa, E., Loiacono, F., Moretti, E., Morlotti, E., Puglisi, D., Villa, G., Cassola, P., & Sbarra, R. (1992) Stratigrafia, caratteri di facies, petrografia e caratterizzazione strutturale del Flysch di Reitano (Oligocene inferiore, Sicilia NE). Notiziario 10, suppl. Giorn. di Geol. 54(1)., pp. 1-21.

Courme, M.D. & Mascle, G. (1988) Nouvelles donnécs stratigraphiques sur les séries oligo-miocènes des unités siciliennes: conséquences paléogéographiques. Bull. Soc. geol. Fr. (8), IV: 105-118.

Crook, K.A.W. (1974) Lithogenesis and geotectonics: the significance of compositional variation in flysch arenites (graywackes). In: Modern and ancient geosynclinal sedimentation (R.H. Dott Jr. & R.H. Shaver, eds.), Soc. Econ. Pal. Mineral. Spec. Publ. 19, pp. 304-310.

Cross, W., Iddings, J.P., Pirrson, L.V., & Washington, H.S. (1902) A quantitative chemico-mineralogical classification and nomenclature of igneous rocks. J. Geol., 10: 555-690.

Crumeyrolle, P. (1987) Stratigraphie physique et sédimentologie des systèmes de dépôt de la séquence de Santa Liestra (Eocène sud-pyrénéen, Pyrénées Aragonaises, Espagne). Ph.D. Thesis, Univ. Bordeaux III, 216 pp.

Crumeyrolle, P., & Mutti, E. (1986) Stratigraphie et sédimentologie des systèmes de dépôt de plate-forme de la séquence de Santa Liestra (bassin éocène sud-pyrenéen, province de Huesca, Espagne). C. R. Acad. Sc. Paris, 303: 581-584.

Cuevas, M., Donselaar, M.E., & Nio, S.D. (1985) Eocene clastic tidal deposits in the Tremp-Graus Basin (Provs. of Lérida and Huesca). In: 6th European Regional Meeting Int. Ass. Sediment., Lleida, Spain, Excursion Guidebook, pp. 215-266.

Dacey, M.F., & Krumbein, W.C. (1979) Models of breakage and selection for particle size distributions. Math. Geol., 11: 193-222.

Dake, C.L. (1921) The problem of the St. Peter sandstone. Bull. Missouri School Mines Metall. 6 (1), 228 pp.

Dal Cin, R. (1968) "Pebble clusters": Their origin and utilization in the study of paleocurrents. Sediment. Geol., 2: 233-241.

Dal Cin, R. (1983) Il litorali del delta del Po e alle foci dell'Adige e del Brenta: caratteri tessiturali e dispersione dei sedimenti, cause dell'arretramento e previsioni sull'evoluzione futura. Boll. Soc. Geol. It., 102: 9-56.

Damuth, J.E., & Fairbridge, R.W. (1970) Equatorial Atlantic deep-sea arkosic sands and ice-age aridity in tropical South America. Geol. Soc. Am. Bull., 81: 189-206.

Darby, D.A. (1990) Evidence for the Hudson River as the dominant source of sand on the US Atlantic shelf. Nature, 346: 828-831.

Davies, D.K. (1972) Mineralogy, petrography and derivation of sands and silts of the continental slope, rise and abyssal plain of the Gulf of Mexico. J. Sed. Petrol., 42: 59-65.

Davies, D.K., & Ethridge, F.G. (1975) Sandstone composition and depositional environment. Am. Ass. Petrol. Geol. Bull., 59: 239-264.

Davies, D.K., & Moore, W.R. (1970) Dispersal of Mississippi sediment in the Gulf of Mexico. J. Sed. Petrol., 40: 339-353.

Davies, D.K., Vessell, R.K., Miles, R.C., Foley, M.G., & Bonis, S.B. (1978) Fluvial transport and downstream sediment modifications in an active volcanic region. In: Fluvial sedimentology (A.D. Miall, ed.). Can. Soc. Petrol. Geol. Mem. 5, pp. 61-84.

Davis, J.C. (1986) Statistics and data analysis in geology, second edition. Wiley & Sons, New York, 646 pp.

De Boer, P.L. (1976) Ontstaansgeschiedenis van de Eocene Campanúe Formatie. Int. Rep. Sedimentol. Dept. Leiden/Utrecht, 77 pp. (unpublished).

De Boer, P.L., Pragt, J.S.J., & Oost, A.P. (1991) Vertically persistent sedimentary facies boundaries along growth anticlines and climate-controlled sedimentation in the thrust-sheet-top South Pyrenean Tremp-Graus Foreland Basin. Basin Res., 3: 63-78.

DeCelles, P.G. (1988) Lithologic provenance modeling applied to the Late Cretaceous synorogenic Echo Canyon conglomerate, Utah: A case of multiple source areas. Geology, 16: 1039-1043.

DeCelles, P.G., Gray, M.B., Ridgway, K.D., Cole, R.B., Srivastava, P., Pequera, N., & Pivnik, D.A. (1991) Kinematic history of a foreland uplift from Paleocene synorogenic conglomerate, Beartooth Range, Wyoming and Montana. Geol. Soc. Am. Bull., 103: 1458-1475.

DeCelles, P.G., & Hertel, F. (1989) Petrology of fluvial sands from the Amazonian foreland basin, Peru and Bolivia. Geol. Soc. Am. Bull., 101: 1552-1562.

Decker, J., & Helmold, K.P. (1985) The effect of grain size on detrital modes: a test of the Gazzi-Dickinson point-counting method - Discussion. J. Sed. Petrol., 55: 618-620.

De Jonge, M.R., & Wortel, M.J.R. (1990) The thermal structure of the Mediterranean upper mantle: a forward modelling approach. Terra Nova, 2: 609-616.

De Leeuw, J., & Van der Heijden, P.G.M. (1988) The analysis of time budgets with a latent time-budget model. In: Data analysis and informatics 5 (E. Diday et al., eds.), North Holland, Amsterdam, pp. 159-166.

De Leeuw, J., Van der Heijden, P.G.M., & Verboon, P. (1990) A latent time-budget model. Statist. Neerlandica, 44: 1-22.

De Loos, W.A. (1988) Provenance of Tertiary sediments in the Tremp-Graus Basin (S. Pyrenees, Spain). In: Abstracts 9th Int. Ass. Sedimentol. Regional Meeting, Leuven (R. Swennen, ed.), p. 52.

Den Hartog Jager, D. (1985) Lepidocyclinidae van Placanica (Zuid-Calabrië). Int. Rep. Stratigraphy Dept., Inst. Earth Sci., Utrecht Univ., 50 pp. (unpublished).

Dercourt, J., Zonenshain, L.P., Ricou, L.E., Kazmin, V.G., Le Pichon, X., Knipper, A.L., Grandjacquet, C., Sborshchikov, I.M., Geyssant, J., Lepvrier, C., Pechersky, D.H., Boulin, J., Sibuet, J.C., Savostin, L.A., Sorokhtin, O., Westphal, M., Bazhenov, M.L., Lauer, J.P., & Biju-Duval, B. (1986) Geological evolution of the Tethys belt from the Atlantic to the Pamirs since the Lias. Tectonophys., 123: 241-315.

De Visser, J.P., Ebbing, J.H.J., Gudjonsson, L., Hilgen, F.J., Jorissen, F.J., Verhallen, P.J.J.M., & Zevenboom, D. (1989) The origin of rhythmic bedding in the Pliocene Trubi Formation of Sicily, Southern Italy. Palaeogeogr., Palaeoclimatol., Palaeoecol., 69: 45-66.

Dewey, J.F. (1980) Episodicity, sequence and style at convergent plate boundaries. In: The continental crust and its mineral deposits (D.W. Strangway, ed.), Spec. Pap. Geol. Soc. Can. 20, pp. 553-573.

Dewey, J.F., Helman, M.L., Turco, E., Hutton, D.H.W., & Knott, S.D. (1989) Kinematics of the western Mediterranean. In: Alpine tectonics (M.P. Coward, D. Dietrich & R.G. Park, eds.), Geol. Soc. Spec. Publ. 45, pp. 265-283.

Di Giulio, A., & Valloni, R. (1992) Analisi microscopica delle areniti terrigene: parametri petrologici e composizioni modali. Acta Natural. Ateneo Parmense, 28: 55-101.

Dickinson, W.R. (1970) Interpreting detrital modes of graywacke and arkose. J. Sed. Petrol., 40: 695-707.

Dickinson, W.R. (1985) Interpreting provenance relations from detrital modes of sandstones. In: Provenance of arenites (G.G. Zuffa, ed.), Reidel Publ. Co., Dordrecht, pp. 333-361.

Dickinson, W.R. (1988) Provenance and sediment dispersal in relation to paleotectonics and paleogeography of sedimentary basins. In: New perspectives in basin analysis (K.L. Kleinspehn & C. Paola, eds.), Springer-Verlag, New York, pp. 3-25.

Dickinson, W.R., Lawton, T.F., & Inman, K.F. (1986) Sandstone detrital modes, Central Utah foreland region: stratigraphic record of Cretaceous-Paleogene tectonic evolution. J. Sed. Petrol., 56: 276-293.

Dickinson, W.R., & Rich, E.I. (1972) Petrologic intervals and petrofacies in the Great Valley sequence, Sacramento Valley, California. Geol. Soc. Am. Bull., 83: 3007-3024.

Dickinson, W.R., & Suczek, C.A. (1979) Plate tectonics and sandstone compositions. Am. Ass. Petrol. Geol. Bull., 63: 2164-2182.

Dickinson, W.R., & Valloni, R. (1980) Plate settings and provenance of sands in modern ocean basins. Geology, 8: 82-86.

Didon, J., Fernex, F., Lorenz, C., Magne, J., & Peyre, Y. (1969) Sur un niveau remarquable de silexite dans le Néogène inferieur d'Espagne méridionale et d'Italie du Nord. Bull. Soc. geol. Fr. (7), XI: 841-853.

Dorsey, R.J. (1988) Provenance evolution and unroofing history of a modern arc-continent collision: evidence from petrography of Plio-Pleistocene sandstones, eastern Taiwan. J. Sed. Petrol., 58: 208-218.

Doutsos, T., Kontopoulos, N., & Frydas, D. (1987) Neotectonic evolution of northwestern-continental Greece. Geol. Rundsch., 76: 433-450.

Drooger, C.W., & Laagland, H. (1986) Larger foraminiferal zonation of the European-Mediterranean Oligocene. Proc. Kon. Ned. Akad. Wetensch. (B), 89: 135-148.

Duée, G. (1969) Etude géologique des Monts Nebrodi (Sicile). Ph.D. Thesis, Paris, 157 pp.

Duée, G., & Truillet, R. (1967) Les variations de faciès de l'Éocène moyen de la lame de San Fratello (nappe du flysch du Monte Soro, Sicile nord-orientale). Bull. Soc. Geol. Fr. (7), IX: 729-734.

Dutta, P.K. (1992) Climatic influence on diagenesis of fluvial sandstones. In: Diagenesis, III (K.H. Wolf & G.V. Chilingarian, eds.), Developments in sedimentology 47, Elsevier Sci. Publ., Amsterdam, pp. 191-252.

Dymond, J. (1981) Geochemistry of Nazca Plate surface sediments: An evaluation of hydrothermal, biogenic, detrital, and hydrogenous sources. In: Nazca Plate: Crustal formation and Andean convergence (L.D. Kulm, J. Dymond, E.J. Dasch & D.M. Hussong, eds.), Geol. Soc. Am. Mem. 154, pp. 133-174.

Dymond, J., Lyle, M., Finney, B., Piper, D.Z., Murphy, K., Conard, R., & Pisias, N. (1984) Ferromanganese nodules from MANOP sites H, S, and R - Control of mineralogical and chemical composition by multiple accretionary processes. Geochim. Cosmochim. Acta, 48: 931-949.

ECORS Pyrenees Team (1988) The ECORS deep reflection seismic survey across the Pyrenees. Nature, 331: 508-511.

Edelman, C.H. (1931) Over bloedverwantschap van sedimenten in verband met het zware mineralen onderzoek. Geol. Mijnb., 10: 122-124.

Edelman, C.H. (1933) Petrologische provincies in het nederlandsche Kwartair. Ph.D. Thesis, Centen's Uitg. Mij., Amsterdam, 104 pp.

Ehrlich, R., & Full, W.E. (1987) Sorting out geology - Unmixing mixtures. In: Use and abuse of statistical methods in the earth sciences (W.B. Size, ed.), Studies in mathematical geology 1, Oxford University Press, Oxford, pp. 33-46.

Eisma, D. (1968) Composition, origin and distribution of Dutch coastal sands between Hoek van Holland and the island of Vlieland. Neth. J. Sea Res., 4: 123-267.

Esu, D., & Kotsakis, T. (1983) Les vertébrés et les mollusques continentaux du tertiaire de la Sardaigne: paléobiogéographie et biostratigraphie. Geol. Romana, 22: 177-206.

Farrell, S.G., Williams, G.D., & Atkinson, C.D. (1987) Constraints on the age of movement of the Montsech and Cotiella Thrusts, south central Pyrenees, Spain. J. Geol. Soc., 144: 907-914.

Ferla, P., & Alaimo, R. (1976) I graniti e le rocce porfiriche calc-alkaline e K-andesitiche nel conglomerato trasgressivo del Miocene inferiore dei Monti Peloritani (Sicilia). Mem. Soc. Geol. It., 17: 123-133.

Ferrara, V. (1974) Stratigrafia della successione cretaceo-eocenica di Piedimonte Etneo (Catania). Riv. Miner. Sicil., 148-150: 1-23.

Field, M.E., & Pilkey, O.H. (1969) Feldspar in Atlantic continental margin sands off the southeastern United States. Geol. Soc. Am. Bull., 80: 2097-2102.

Finetti, I. (1985) Structure and evolution of the Central Mediterranean (Pelagian and Ionian Seas). In: Geological evolution of the Mediterranean Basin, (D.J. Stanley & F.C. Wezel, eds.), Springer-Verlag, New York, pp. 215-230.

Fischer, A.G., De Boer, P.L., & Premoli Silva, I. (1990) Cyclostratigraphy. In: Cretaceous resources, events and rhythms. Background and plans for research (R.N. Ginsburg & B. Beaudoin, eds.), Kluwer, Dordrecht, pp. 139-172.

Fleet, W.F. (1926) Petrological notes on the Old Red Sandstone of the West Midlands. Geol. Mag., 63: 505-516.

Flores, R.M., & Shideler, G.L. (1978) Factors controlling heavy-mineral variations on the South Texas outer continental shelf, Gulf of Mexico. J. Sed. Petrol., 48: 269-280.

Folk, R.L. (1980) Petrology of sedimentary rocks. Hemphill Publ. Co., Austin, 182 pp.

Fontana, D., Zuffa, G.G., & Garzanti, E. (1989) The interaction of eustacy and tectonism from provenance studies of the Eocene Hecho Group turbidite complex (South-Central Pyrenees, Spain). Basin Res., 2: 223-237.

Foucault, A., Powichrowski, L., & Prud'homme, A. (1987) Le contrôle astronomique de la sédimentation turbiditique: Exemple du Flysch à Helminthoïdes des Alpes Ligures. C. R. Acad. Sci. (II), 305: 1007-1011.

Franzinelli, E., & Potter, P.E. (1985) Areias recentes dos Rios da Bacia Amazônica: composições petrográfica, textural e química. Rev. Brasil. Geosci., 15: 213-220.

Franzinelli, E., & Potter, P.E. (1983) Petrology, chemistry and texture of modern river sands, Amazon river system. J. Geol., 91: 23-39.

Füchtbauer, H. (1964) Sedimentpetrographische Untersuchungen in der älteren Molasse nordlich der Alpen. Ecl. Geol. Helv., 57: 157-298.

Full, W.E., & Ehrlich, R. (1986) Comment on "An objective technique for determining end-member compositions and for partitioning sediments according to their sources". Geochim. Cosmochim. Acta, 50: 1303.

Full, W.E., Ehrlich, R., & Bezdek, J.C. (1982) FUZZY QMODEL - A new approach for linear unmixing. Math. Geol., 14: 259-270.

Full, W.E., Ehrlich, R., & Klovan, J.E. (1981) EXTENDED QMODEL - Objective definition of external end members in the analysis of mixtures. Math. Geol., 13: 331-344.

Gandolfi, G., Mordenti, A., & Paganelli, L. (1978a) Spiagge attuali e cordoni di dune nell'area del delta del Tagliamento e di Valle Vecchia. Miner. Petrogr. Acta, 22: 95-110.

Gandolfi, G., Mordenti, A., & Paganelli, L. (1978b) Caratteri composizionali del litorale alla foce dell'Adige (spiaggia modello). Miner. Petrogr. Acta, 22: 111-118.

Gandolfi, G., Mordenti, A., & Paganelli, L. (1982) Composition and longshore dispersal of sands from the Po and Adige rivers since the pre-Etruscan age. J. Sed. Petrol., 52: 797-805.

Garrels, R.M., & Mackenzie, F.T. (1971) Evolution of sedimentary rocks. W.W. Norton, New York, 397 pp.

Garzanti, E. (1991) Non-carbonate intrabasinal grains in arenites: Their recognition, significance, and relationship to eustatic cycles and tectonic setting. J. Sed. Petrol., 61: 959-975.

Gawthorpe, R.L., & Colella, A. (1990) Tectonic controls on coarse-grained delta depositional systems in rift basins. In: Coarse-Grained Deltas (A. Colella & D.B. Prior, eds.), Spec. Publ. Int. Ass. Sediment. 10, pp. 113-127.

Gazzi, P. (1966) Le arenarie del flysch sopracretaceo dell'Appennino modenese; correlazioni con il flysch di Monghidoro. Miner. Petrogr. Acta, 12: 69-97.

Gazzi, P., Zuffa, G.G., Gandolfi, G., & Paganelli, L. (1973) Provenienza e dispersione litoranea delle sabbie delle spiagge adriatiche fra le foci dell'Isonzo e del Foglia: inquadramento regionale. Mem. Soc. Geol. It., 12: 1-37.

Gelderloos, J., & Schaafsma, C.E. (1984) The Tertiary geology of the Reggio di Calabria area (Italy): New facts and consequences. Int. Rep. Stratigraphy Dept., Inst. Earth Sci., Utrecht Univ., 24 pp. (unpublished).

Gergen, L.D., & Ingersoll, R.V. (1986) Petrology and provenance of Deep Sea Drilling Project sand and sandstone from the North Pacific Ocean and the Bering Sea. Sediment. Geol., 51: 29-56.

Ghisetti, F., & Vezzani, L. (1981) Contribution of structural analysis to understanding the geodynamic evolution of the Calabrian Arc (southern Italy). J. Struct. Geol., 3: 371-381.

Ghisetti, F., & Vezzani, L. (1982) The recent deformation mechanisms of the Calabrian Arc. Earth Evol. Sci., 2: 197-206.

Gibbs, A.D. (1984) Structural evolution of extensional basin margins. J. Geol. Soc., 141: 609-620.

Gibbs, A.D. (1987) Development of extension and mixed-mode sedimentary basins. In: Continental Extensional Tectonics (M.P. Coward, J.F. Dewey & P.L. Hancock, eds.), Geol. Soc. Spec. Publ. 28, pp. 19-33.

Gilligan, A. (1919) The petrography of the Millstone grit of Yorkshire. Quart. J. Geol. Soc., 75: 251-294.

Girty, G.H. (1991) A note on the composition of plutoniclastic sand produced in different climatic belts. J. Sed. Petrol., 61: 428-433.

Giunta, G. (1985) Problematiche ed ipotesi sul Bacino Numidico nelle Maghrebidi siciliane. Boll. Soc. Geol. It., 104: 239-256.

Goldman, M.I. (1915) Petrographic evidence on the origin of the Catahoula sandstone of Texas. Am. J. Sci., 39: 261-287.

Görler, K. (1978) Neogene olistostromes in southern Italy as an indicator of contemporaneous plate-tectonics. In: Alps, Apennines, Hellenides (H. Closs, D. Roeder & K. Schmidt, eds.), Schweizerbart, Stuttgart, pp. 355-359.

Got, H., Monaco, A., Vittori, J., Brambati, A., Catani, G., Masoli, M., Pugliese, N., Zucchi-Stolfa, M., Belfiore, A., Gallo, F., Mezzadri, G., Vernia, L., Vinci, A., & Bonaduce, G. (1981) Sedimentation on the Ionian active margin (Hellenic Arc) - Provenance of sediments and mechanisms of deposition. Sediment. Geol., 28: 243-272.

Graham, S.A., Ingersoll, R.V., & Dickinson, W.R. (1976) Common provenance for lithic grains in Carboniferous sandstones from Ouachita mountains and Black Warrior basin. J. Sed. Petrol., 46: 620-632.

Graham, S.A., Tolson, R.B., DeCelles, P.G., Ingersoll, R.V., Bargar, E., Caldwell, M., Cavazza, W., Edwards, D.P., Follo, M.F., Handschy, J.F., Lemke, L., Moxon, I., Rice, R., Smith, G.A., & White, J. (1986) Provenance modelling as a technique for analysing source terrane evolution and controls on foreland sedimentation. In: Foreland basins (P.A. Allen & P. Homewood, eds.), Spec. Publ. Int. Ass. Sediment. 8, pp. 425-436.

Grantham, J.H., & Velbel, M.A. (1988) The influence of climate and topography on rock-fragment abundance in modern fluvial sands of the southern Blue Ridge mountains, North Carolina. J. Sed. Petrol., 58: 219-227.

Grasso, M., Guerrera, F., Loiacono, F., Puglisi, D., Romeo, M., Balenzano, F., Carmisciano, R., Di Pierro, M., Gonzalez-Donoso, J.M., & Martin-Algarra, A. (1987) Caratterizzatione sedimentologica, biostratigrafica e mineralogico-petrografica di "successioni miste" inframioceniche affioranti in Spagna (Catena Betica) e in Italia meridionale (M.ti Nebrodi e Apennino lucano). Boll. Soc. Geol. It., 106: 475-516.

Gray, N.H. (1973) Estimation of parameters in petrologic materials balance equations. Math. Geol., 5: 225-236.

Griffiths, J.C. (1966) A genetic model for the interpretive petrology of detrital sediments. J. Geol., 74: 655-672.

Griffiths, J.C., & Ondrick, C.W. (1969) Modelling the petrology of detrital sediments. In: Computer applications in the earth sciences: an international symposium (D.F. Merriam, ed.), Plenum Press, New York, pp. 73-97.

Groves, A.W. (1931) The unroofing of the Dartmoor granite and the distribution of its detritus in the sediments of southern England. Quart. J. Geol. Soc., 87: 62-96.

Gudjonsson, L. (1987) Local and global effects on the Early Pliocene Mediterranean stable isotope records. Mar. Micropal., 12: 241-253.

Guerrera, F., Coccioni, R., Loiacono, F., Puglisi, D., & Moretti, E. (1987) Sequenze fliscoide oligo-mioceniche tipo "maurétanien" (sinorogene e tardorogene) della Cordigliera Betica (Spagna) e del Tell orientale (Algeria): confronti nel Rif, nella Catena nord-siciliana e nell'Apennino meridionale. Mem. Soc. Geol. It., 38: 521-550.

Guerrera, F., Loiacono, F., & Grasso, M. (1986) Dati preliminari sulle successioni oligo-mioceniche "miste" affioranti lungo la Catena Betico-Maghrebide-Apennino meridionale: una famiglia di flysch con evidenti implicazioni paleogeografiche e paleotettoniche. Boll. Soc. Geol. It., 105: 99-110.

Guerrera, F., Loiacono, F., Puglisi, D., & Moretti, E. (1992) The Numidian nappe in the Maghrebian Chain: state of the art. Boll. Soc. Geol. It., 111: 217-253.

Guerrera, F., & Wezel, F.C. (1974) Nuovi dati stratigrafici sui flysch oligo-miocenici siciliani e considerazioni tettoniche relative. Riv. Miner. Sicil., 145-147: 27-51.

Hadley, G. (1961) Linear algebra. Addison-Wesley Publ. Co., Reading, Massachusetts, 290 pp.

Hamann, I.M., & Herzfeld, U.C. (1991) On the effects of pre-analysis standardization. J. Geol., 99: 621-631.

Harrell, J., & Blatt, H. (1978) Polycrystallinity: effect on the durability of detrital quartz. J. Sed. Petrol., 48: 25-30.

Harvey, P.K., & Lovell, M.A. (1992) Downhole mineralogy logs: mineral inversion methods and the problem of compositional colinearity. In: Geological applications of wireline logs II (A. Hurst, C.M. Griffiths & P.F. Worthington, eds.), Geol. Soc. Spec. Publ. 65, pp. 361-368.

Haseldonckx, P. (1973) The palynology of some Palaeogene deposits between the Rio Esera and the Rio Segre, Southern Pyrenees, Spain. Leidse Geol. Meded., 49: 145-165.

Haughton, P.D.W., Todd, S.P., & Morton, A.C. (1991) Sedimentary provenance studies. In: Developments in sedimentary provenance studies (A.C. Morton et al., eds.), Geol. Soc. Spec. Publ. 57, pp. 1-11.

Hayes, J.R. (1962) Quartz and feldspar content in South Platte, Platte, and Missouri river sands. J. Sed. Petrol., 32: 793-800.

Heath, G.R., & Dymond, J. (1977) Genesis and transformation of metalliferous sediments from the East Pacific Rise, Bauer Deep, and Central Basin, northwest Nazca plate. Geol. Soc. Am. Bull., 88: 723-733.

Hein, F.J. (1984) Deep-sea and fluvial braided channel conglomerates: A comparison of two case studies. In: Sedimentology of Gravels and Conglomerates (E.H. Koster & R.J. Steel, eds.), Can. Soc. Petrol. Geol. Mem. 10, pp. 33-49.

Hein, F.J., & Walker, R.G. (1977) Bar evolution and development of stratification in the gravelly, braided, Kicking Horse River, British Columbia. Can. J. Earth Sci., 14: 562-570.

Heller, P.L., Renne, P.R., & O'Neill, J.R. (1992) River mixing rate, residence time, and subsidence rates from isotopic indicators: Eocene sandstones of the U.S. Pacific Northwest. Geology, 20: 1095-1098.

Hendershott, M.C., & Rizzoli, P. (1976) The winter circulation of the Adriatic Sea. Deep-Sea Res., 23: 353-370.

Herron, M.M. (1986) Mineralogy from geochemical well logging. Clays & Clay Min., 34: 204-213.

Hilgen, F.J. (1987) Sedimentary rhythms and high-resolution chronostratigraphic correlations in the Mediterranean Pliocene. Newsl. Stratigr., 17: 109-127.

Hilgen, F.J. (1991) Extension of the astronomically calibrated (polarity) time scale to the Miocene/Pliocene boundary. Earth Planet. Sci. Lett., 107: 349-368.

Hilgen, F.J., & Langereis, C.G. (1989) Periodicities of $CaCO_3$ cycles in the Pliocene of Sicily: discrepancies with the quasi-periods of the Earth's orbital cycles? Terra Nova, 1: 409-415.

Hodgson, M., & Dudeney, A.W.L. (1984) Estimation of clay proportions in mixtures by X-ray diffraction and computerized chemical mass balance. Clays & Clay Min., 32: 19-28.

Hsü, K.J. (1960) Texture and mineralogy of the recent sands of the Gulf coast. J. Sed. Petrol., 30: 380-403.
Hubert, J.F. (1971) Analysis of heavy-mineral assemblages. In: Procedures in sedimentary petrology (R.E. Carver, ed.), Wiley-Interscience, New York, pp. 453-478.
Hubert, J.F., & Neal, W.J. (1967) Mineral composition and dispersal patterns of deep-sea sands in the western North Atlantic petrologic province. Geol. Soc. Am. Bull., 78: 749-772.

Ibbeken, H., & Schleyer, R. (1991) Source and sediment: a case study of provenanee and mass balance at an active plate margin (Calabria, southern Italy). Springer-Verlag, Berlin, 286 pp.
Illing, V.C. (1916) The oilfields of Trinidad. Proc. Geol. Ass., 27: 115.
Imbrie, J. (1963) Factor and vector analysis programs for analyzing geologic data. Office of Naval Research, Geography Branch, Technical Report 6, ONR Task No. 389-135, 83 pp.
Imbrie, J., & Poldervaart, A. (1959) Mineral compositions calculated from chemical analyses of sedimentary rocks. J. Sed. Petrol., 29: 588-595.
Imbrie, J., & Purdy, E.G. (1962) Classification of modern Bahamian carbonate sediments. In: Classification of carbonate rocks - A symposium (W.E. Ham, ed.), Am. Ass. Petrol. Geol. Mem. 1, pp. 253-272.
Imbrie, J. & Van Andel, T.H. (1964) Vector analysis of heavy mineral-data. Geol. Soc. Am. Bull., 75: 1131-1156.
Ingersoll, R.V. (1978) Petrofacies and petrologic evolution of the Late Cretaceous fore-arc basin, northern and central California. J. Geol., 86: 335-352.
Ingersoll, R.V. (1983) Petrofacies and provenance of Late Mesozoic forearc basin, Northern and Central California. Am. Ass. Petrol. Geol. Bull., 67: 1125-1142.
Ingersoll, R.V. (1990) Actualistic sandstone petrofacies: Diseriminating modern and ancient source rocks. Geology, 18: 733-736.
Ingersoll, R.V., Bullard, T.F., Ford, R.L., Grimm, J.P., Pickle, J.D., & Sares, S.W. (1984) The effect of grain size on detrital modes: a test of the Gazzi-Dickinson point-counting method. J. Sed. Petrol., 54: 103-116.
Ingersoll, R.V., Bullard, T.F., Ford, R.L., & Pickle, J.D. (1985a) The effect of grain size on detrital modes: a test of the Gazzi-Dickinson point-counting method - Reply to discussion of Lee J. Suttner and Abhijit Basu. J. Sed. Petrol., 55: 617-618.
Ingersoll, R.V., Bullard, T.F., Ford, R.L., & Pickle, J.D. (1985b) The effect of grain size on detrital modes: a test of the Gazzi-Dickinson point-counting method - Reply to discussion of John Decker and Kenneth P. Helmold. J. Sed. Petrol., 55: 620-621.
Ingersoll, R.V., Kretchmer, A.G., & Valles, P.K. (1993) The effect of sampling scale on actualistic sandstone petrofacies. Sedimentol., 40: 937-953.
Ito, M., & Masuda, F. (1989) Petrofacies of paleo-Tokyo Bay sands, the upper Pleistocene of Central Honshu, Japan. In: Sedimentary facies in the active plate margin (A. Taira & F. Masuda, eds.), Terra Scientific Publ. Co., Tokyo, pp. 179-196.

Jamet, M. (1982) Étude néotectonique de Corfou et étude paléomagnétique des sédiments néogène des îles de Corfou, Céphalonie et Zanthe. Ph.D. thesis, Université de Paris-sud, Orsay, 184 pp.
Jobstraibizer, P., & Malesani, P. (1973) I sedimenti dei fiumi veneti. Mem. Soc. Geol. It., 12: 411-452.
Johnsson, M.J. (1990a) Tectonic versus chemical-weathering controls on the composition of fluvial sands in tropical environments. Sedimentol., 37: 713-726.
Johnsson, M.J. (1990b) Overlooked sedimentary particles from tropical weathering environments. Geology, 18: 107-110.
Johnsson, M.J., & Meade, R.H. (1990) Chemical weathering of fluvial sediments during alluvial storage: The Macuapanim island point bar, Solimões River, Brazil. J. Sed. Petrol., 60: 827-842.
Johnsson, M.J., & Stallard, R.F. (1989) Physiographic controls on the composition of sediments derived from volcanic and sedimentary terrains on Barro Colorado Island, Panama. J. Sed. Petrol., 59: 768-781.
Johnsson, M.J., Stallard, R.F., & Lundberg, N. (1991) Controls on the composition of fluvial sands from a tropical weathering environment: Sands of the Orinoco River drainage basin, Venezuela and Colombia. Geol. Soc. Am. Bull., 103: 1622-1647.
Johnsson, M.J., Stallard, R.F., & Meade, R.H. (1988) First-cycle quartz arenites in the Orinoco River basin, Venezuela and Colombia. J. Geol., 96: 263-277.
Jöreskog, K.G., Klovan, J.E., & Reyment, R.A. (1976) Geological factor analysis. Methods in geomathematics 1, Elsevier Sci. Publ., Amsterdam, 178 pp.
Joyce, J.E., Tjalsma, L.R.C., & Prutzman, J.M. (1990) High-resolution planktic stable isotope record and spectral analysis for the last 5.35 M.Y.: Ocean Drilling Program site 625 northeast Gulf of Mexico. Paleoceanogr., 5: 507-529.
Judd, J.W. (1886) Report on a series of specimens of the deposits of the Nile delta. Proc. Roy. Soc., 39: 213-227.

Kastens, K., Mascle, J., Auroux, C., Bonatti, E., Broglia, C., Channell, J., Curzi, P., Emeis, K.C., Glaçon, G., Hasegawa, S., Hieke, W., Mascle, G., McCoy, F., McKenzie, J., Mendelson, J., Müller, C., Rehault, J.P., Robertson, A., Sartori, R., Sprovieri, R., & Torii, M. (1988) ODP Leg 107 in the Tyrrhenian Sea: Insights into passive margin and back-arc basin evolution. Geol. Soc. Am. Bull., 100: 1140-1156.

Kelley, J.C., & Whetten, J.T. (1969) Quantitative statistical analyses of Columbia River sediment samples. J. Sed. Petrol., 39: 1167-1173.

Kelling, G., Sheng, H., & Stanley, D.J. (1975) Mineralogic composition of sand-sized sediment on the outer margin off the Mid-Atlantic States: assessment of the influence of the ancestral Hudson and other fluvial systems. Geol. Soc. Am. Bull., 86: 853-862.

Kelsey, C.H. (1965) Calculation of the CIPW norm. Mineral. Mag., 34: 276-282.

Klein, G.DeV. (1963) Analysis and review of sandstone classifications in the North American geological literature, 1940-1960. Geol. Soc. Am. Bull., 74: 555-576.

Klovan, J.E., & Imbrie, J. (1971) An algorithm and FORTRAN-IV program for large-scale Q-mode factor analysis and calculation of factor scores. Math. Geol., 3: 61-77.

Klovan, J.E., & Miesch, A.T. (1976) Extended CABFAC and QMODEL computer programs for Q-mode factor analysis of compositional data. Comput. Geosci., 1: 161-178.

Knott, S.D. (1987) The Liguride Complex of southern Italy - a Cretaceous to Paleogene accretionary wedge. Tectonophys., 142: 217-226.

Komar, P.D. (1977) Selective longshore transport rates of different grain-size fractions within a beach. J. Sed. Petrol., 47: 1444-1453.

Konta, J. (1988) Minerals in rivers. SCOPE/UNEP Sonderband, Mitt. Geol.-Paläont. Inst. Univ. Hamburg, 66: 341-365.

Kotsakis, T. (1984) Problemi paleobiogeografici dei mammiferi fossili Italiani: Le faune oligoceniche. Geol. Romana, 23: 141-155.

Krissek, L.A., & Clemens, S.C. (1991) Mineralogic variations in a Pleistocene high-resolution eolian record from the Owen Ridge, Western Arabian Sea (site 722): implications for sediment source conditions and monsoon history. In: Proc. ODP, Sci. Results 117 (W.L. Prell, N. Niitsuma et al., eds.), pp. 197-213.

Krook, L. (1969) Investigations on the mineralogical composition of the Tertiary and Quaternary sands in northern Surinam. Verh. Kon. Ned. Geol. Mijnb. Gen., 27: 89-100.

Kroonenberg, S.B. (in press) Effect of source rock, sorting and weathering on the geochemistry of fluvial sands from different tectonic and climatic environments. Proc. 29th Int. Geol. Conf., Japan.

Laagland, H. (1990) Cycloclypeus in the Mediterranean Oligocene. Utrecht Mieropal. Bull. 39, 171 pp.

Lawson, C.L., & Hanson, R.J. (1974) Solving least squares problems. Prentice-Hall, Englewood Cliffs, 340 pp.

Leeder, M.R. (1991) Denudation, vertical crustal movements and sedimentary basin infill. Geol. Rundsch., 80: 441-458.

Leeder, M.R., & Gawthorpe, R.L. (1987) Sedimentary models for extensional tilt-block/half-graben basins. In: Continental Extensional Tectonics (M.P. Coward, J.F. Dewey & P.L. Hancock, eds.), Geol. Soc. Spec. Publ. 28, pp. 139-152.

Leinen, M., & Pisias, N. (1984) An objective technique for determining end-member compositions and for partitioning sediments according to their sources. Geochim. Cosmochim. Acta, 48: 47-62.

Leinen, M., & Pisias, N. (1986) Reply to critical comment on "An objective technique for determining end-member compositions and for partitioning sediments according to their sources". Geochim. Cosmochim. Acta, 50: 1305-1306.

LeMaitre, R.W. (1979) A new generalized petrological mixing model. Contrib. Mineral. Petrol., 71: 133-137.

LeMaitre, R.W. (1981) GENMIX - A generalized petrological mixing model program. Comput. Geosci., 7: 229-247.

Lentin, J.K., & Williams, G.L. (1989) Fossil dinoflagellates: index to genera and species, 1989 edition. Am. Ass. Stratigr. Palynol. Spec. Publ. 20, 451 pp.

Lentini, F. (1975) Le successioni mesozoico-terziarie dell'Unità di Longi (complesso calabride) nei Peloritani occidentali (Sicilia). Boll. Soc. Geol. It., 94: 1477-1503.

Lentini, F., Carbone, S., Catalano, S., Grasso, M., & Monaco, C. (1990) Principali elementi strutturali del thrust belt Appenninico-Maghrebide in Sicilia centro-orientale. Mem. Soc. Geol. It., 45: 495-502.

Lentini, F., & Vezzani, L. (1975) Le unità Meso-Cenozoiche della copertura sedimentaria del basamento cristallino peloritano (Sicilia nord-orientale). Boll. Soc. Geol. It., 94: 537-554.

Lentini, F., & Vezzani, L. (1978) Tentativo di elaborazione di uno schema strutturale della Sicilia orientale. Mem. Soc. Geol. It., 19: 495-500.

Le Pichon, X., & Alvarez, F. (1984) From stretching to subduction in back-arc regions: dynamic considerations. Tectonophys., 102: 343-357.

Linssen, J.H. (1991) Properties of Pliocene sedimentary geomagnetic reversal records from the Mediterranean. Geologica Ultraiectina 80, 231 pp.

Lister, G.S., Banga, G., & Feenstra, A. (1984) Metamorphic core complexes of Cordilleran type in the Cyclades, Aegean Sea, Greece. Geology, 12: 221-225.

Loiacono, F., & Puglisi, D. (1983) Studio sedimentologico-petrografico del Flysch di Reitano (Oligocene-Miocene inferiore, Sicilia). Boll. Soc. Geol. It., 102: 307-328.

Lorenz, C. (1984) Les silexites et les tuffites du Burdigalien, marqueurs volcano-sédimentaires: corrélations dans le domaine de la Méditerranée occidentale. Bull. Soc. geol. Fr. (7), XXVI: 1203-1210.

Lowe, D.R. (1982) Sediment gravity flows, II: depositional models with special reference to the deposits of high-density turbidity currents. J. Sed. Petrol., 52: 279-297.

Luciani, V., Minzoni, N. & Ungaro, S. (1992 in press) Età e significato paleogeografico-strutturale della successione "numidica" di Ferruzzano, Calabria meridionale. Atti Accad. Lincei Rend. fis. ?, 000-000 (preprint).

Luciani, V., Minzoni, N., & Negri, A. (1994 in press) New biostratigraphic data on the "Capo d'Orlando Formation" in central-southern Calabria: geotectonic consequences (manuscript).

Ludwig, R. (1874) Geologische Bilder aus Italien. Bull. Soc. Imprim. Nat. Moscou, 48: 42-131.

Lundberg, N. (1991) Detrital record of the early Central American magmatic arc: Petrography of intraoceanic forearc sandstones, Nicoya Peninsula, Costa Rica. Geol. Soc. Am. Bull., 103: 905-915.

Mack, G.H. (1978) The survivability of labile light-mineral grains in fluvial, aeolian, and littoral marine environments: the Permian Cutler and Cedar Mesa formations, Moab, Utah. Sedimentol., 25: 587-604.

Mack, G.H. (1981) Composition of modern stream sand in a humid climate derived from a low-grade metamorphic and sedimentary foreland fold-thrust belt of North Georgia. J. Sed. Petrol., 51: 1247-1258.

Mack, G.H. (1984) Exceptions to the relationship between plate tectonics and sandstone composition. J. Sed. Petrol., 54: 212-220.

Mack, G.H., & Jerzykiewicz, T. (1989) Detrital modes of sand and sandstone derived from andesitic rocks as a paleoclimatic indicator. Sediment. Geol., 65: 35-44.

Mackie, W. (1899a) The sands and sandstones of eastern Moray. Trans. Edinburgh Geol. Soc., 7: 148-172.

Mackie, W. (1899b) The feldspars present in sedimentary rocks as indicators of the conditions of contemporaneous climates. Trans. Edinburgh Geol. Soc., 7: 443-468.

Mahaney, W.C., & Halvorson, D.L. (1986) Rates of mineral weathering in the Wind River mountains, western Wyoming. In: Rates of chemical weathering of rocks and minerals (S.M. Colman & D.P. Dethier, eds.), Academic Press Inc., Orlando, pp. 147-167.

Malinverno, A., & Ryan, W.B.F. (1986) Extension in the Tyrrhenian Sea and shortening in the Apennines as result of arc migration driven by sinking of the lithosphere. Tectonics, 5: 227-245.

Mann, W.R., & Cavaroc, V.V. (1973) Composition of sand released from three source areas under humid, low relief weathering in the North Carolina piedmont. J. Sed. Petrol., 43: 870-881.

Manson, V., & Imbrie, J. (1964) FORTRAN program for factor and vector analysis of geologic data using an IBM 7090 or 7094/1401 computer system. Kansas Geol. Surv. Sp. Dist. Publ. 13, 46 pp.

Marsaglia, K.M. (1991) Provenance of sands and sandstones from a rifted continental arc, Gulf of California, Mexico. In: Sedimentation in volcanic settings (R.V. Fischer & G.A. Smith, eds.), Soc. Econ. Paleont. Mineral. Spec. Publ. 45, pp. 237-248.

Marsaglia, K.M., & Ingersoll, R.V. (1992) Compositional trends in arc-related, deep-marine sand and sandstone: a reassessment of magmatic-arc provenance. Geol. Soc. Am. Bull., 104: 1637-1649.

McBride, E.F., & Picard, M.D. (1987) Downstream changes in sand composition, roundness, and gravel size in a short-headed, high-gradient stream, northwestern Italy. J. Sed. Petrol., 57: 1018-1026.

McLaren, P. (1981) An interpretation of trends in grain size measures. J. Sed. Petrol., 51: 611-624.

McLaren, P., & Bowles, D. (1985) The effects of sediment transport on grain-size distributions. J. Sed. Petrol., 55: 457-470.

Medak, F., & Cressie, N. (1991) Confidence regions in ternary diagrams based on the power-divergence statistics. Math. Geol., 23: 1045-1057.

Menke, W. (1984) Geophysical data analysis: discrete inverse theory. Academic Press, Orlando, 260 pp.

Merodio, J.C., Spalletti, L.A., & Bertone, L.M. (1992) A FORTRAN program for the calculation of normative composition of clay minerals and pelitic rocks. Comp. & Geosci., 18: 47-61.

Messina, A., Compagnoni, R., De Francesco, A., Giacobbe, A., & Russo, S. (1990) Alpine metamorphic overprint in the Aspromonte Nappe of northeastern Peloritani Mts. (Calabria-Peloritani Arc, southern Italy). Boll. Soc. Geol. It., 109: 655-673.

Messina, A., Russo, S., Stagno, F., & Calandra, M. (1988) Petrochemistry and mineralogy of Monte Cacciagrande granite, Stilo Unit (Calabrian-Peloritan Arc, Southern Italy). Rend. Soc. It. Mineral. Petrol., 43: 569-586.

Meulenkamp, J.E., Hilgen, F., & Voogt, E. (1986) Late Cenozoic sedimentary-tectonic history of the Calabrian Arc. Giorn. Geol. (3a), 48: 345-359.

Meulenkamp, J.E., Wortel, M.J.R., Van Wamel, W.A., Spakman, W., & Hoogerduyn Strating, E. (1988) On the Hellenic subduction zone and the geodynamic evolution of Crete since the late Middle Miocene. Tectonophys., 146: 203-215.

Meunier, S. (1877) Composition et origine du sable diamantifère de Du Toit's Pan (Afrique australe). C. R. Acad. Sci. Paris, 84: 250-252.

Mezzadri, G., & Saccani, E. (1989) Heavy mineral distribution in late Quaternary sediments of the southern Aegean Sea: implications for provenance and sediment dispersal in sedimentary basins along active margins. J. Sed. Petrol., 59: 412-422.

Miall, A.D. (1977) A review of the braided-river depositional environment. Earth-Sci. Rev., 13: 1-62.

Michel Lévy, A. (1878) Note sur quelques minéraux contenus dans les sables du Mesvrin, près Autun. Bull. Soc. Mineral. Fr., 1: 39-41.

Middleton, G.V. (1962) A multivariate statistical technique applied to the study of sandstone composition. Trans. Roy. Soc. Can., 56: 119-126.

Miesch, A.T. (1962) Computing mineral compositions of sedimentary rocks from chemical analyses. J. Sed. Petrol., 32: 217-225.

Miesch, A.T. (1976a) Q-mode factor analysis of geochemical and petrologic data matrices with constant row sums. U.S. Geol. Surv. Prof. Pap. 574-G, 47 pp.

Miesch, A.T. (1976b) Q-mode factor analysis of compositional data. Comput. Geosci., 1: 147-159.

Miesch, A.T. (1976c) Interactive computer programs for petrologic modeling with extended Q-mode factor analysis. Comput. Geosci., 2: 439-492.

Miesch, A.T. (1980) Scaling variables and interpretation of eigenvalues in principal component analysis of geologic data. Math. Geol., 12: 523-538.

Miesch, A.T. (1981) Computer methods for geochemical and petrologic mixing problems. In: Computer applications in the earth sciences, an update of the 70s (D.F. Merriam, ed.), Plenum Press, New York, pp. 243-265.

Milliman, J.D., & Summerhayes, C.P. (1975) Upper continental margin sedimentation off Brazil. Contrib. Sedimentol. 4, 175 pp.

Milliman, J.D., & Syvitsky, J.P.M. (1992) Geomorphic/tectonic control of sediment discharge to the ocean: the importance of small mountainous rivers. J. Geol., 100: 525-544.

Milner, H.B. (1922) The nature and origin of the Pliocene deposits of the county of Cornwall and their bearing on the Pliocene geography of the South-West of England. Quart. J. Geol. Soc., 78: 348-377.

Milner, H.B. (1962) Sedimentary petrography, 4th revised edition. Vol II: principles and applications. Allen & Unwin, London, 715 pp.

Minnis, M.M. (1984) An automatic point-counting method for mineralogical assessment. Am. Ass. Petrol. Geol. Bull., 68: 744-752.

Minzoni, N. (1992 in press) Falde paleogeniche Ovest-vergenti nella Calabria meridionale. Atti Accad. Lincei Rend. fis. 82, 000-000 (preprint).

Minzoni, N. (1993) Le catene Alpina e Appenninica nella Calabria centro-meridionale: Possibili rapporti con la Calabria settentrionale e con i Monti Peloritani (Sicilia). Boll. Soc. Geol. It., 112: 15-30.

Minzoni, N., Garavello, A., Luciani, V., Negri, A., & Ungaro, S. (1992) La Calabria ercinica negli orogeni Alpino e Appenninico-Maghrebide: Guida all III escursione del Gruppo Lavoro Paleozoico Calabria-Aspromonte 25-26 Settembre 1990. Boll. Soc. Geol. It., 111: 131-145.

Mitchell, A.H.G., & Reading, H.G. (1986) Sedimentation and tectonics. In: Sedimentary environments and facies, second edition (H.G. Reading, ed.), Blackwell Sci. Publ., Oxford, pp. 471-519.

Molinaroli, E., Blom, M., & Basu, A. (1991) Methods of provenance determination tested with discriminant function analysis. J. Sed. Petrol., 61: 900-908.

Monopolis, D., & Bruneton, A. (1982) Ionian Sea (Western Greece): Its structural outline deduced from drilling and geophysical data. Tectonophys., 83: 227-242.

Montanari, L. (1986) Aspetti tettono-sedimentari dell'Oligocene e Miocene in Sicilia e aree contigue. Giorn. Geol. (3a), 48: 99-112.

Montanari, L. (1987) Lineamenti stratigrafico-paleogeografici della Sicilia durante il ciclo alpino. Mem. Soc. Geol. It., 38: 361-406.

Montanari, L. (1989) Assetto geologico degli affioramenti mesozoici peloritani. Suppl. 1, Att. Accad. Pelor. Pericol. (I), 67: 9-26.

Montigny, R., Edel, J.B., & Thuizat, R. (1981) Oligo-Miocene rotation of Sardinia: K-Ar ages and paleomagnetic data of Tertiary volcanics. Earth Planet. Sci. Lett., 54: 261-271.

Morris, W.J., & Fan, P.F. (1962) Abrasion effects on arkose mixtures. J. Sed. Petrol., 32: 226-230.

Morton, A.C. (1985) Heavy minerals in provenance studies. In: Provenance of arenites (G.G. Zuffa, ed.), Reidel Publ. Co., Dordrecht, pp. 249-277.

Morton, A.C. (1991) Geochemical studies of heavy minerals and their application to provenance research. In: Developments in sedimentary provenance studies (A.C. Morton et al., eds.), Geol. Soc. Spec. Publ. 57, pp. 31-45.

Moss, A.J. (1972) Initial fluviatile fragmentation of granitic quartz. J. Sed. Petrol., 42: 905-916.

Moussat, E., Angelier, J., Mascle, G., & Rehault, J.P. (1986) L'ouverture de la Mer Tyrrhénienne et la tectonique de faille néogène quaternaire en Calabre. Giorn. Geol. (3a), 48: 63-75.

Muñoz, J.A. (1992) Evolution of a continental collision belt: ECORS-Pyrenees crustal balanced cross-section. In: Thrust tectonics (K.R. McClay, ed.), Chapman & Hall, London, pp. 235-246.

Murray, J.W. (1973) Distribution and ecology of living benthic foraminiferids. Crane, Russak & Co., New York, 274 pp.

Mutti, E. (1985) Turbidite systems and their relations to depositional sequences. In: Provenance of arenites (G.G. Zuffa, ed.), Reidel Publ. Co., New York, pp. 65-93.

Mutti, E., & Normark, W.R. (1987) Comparing examples of modern and ancient turbidite systems: Problems and concepts. In: Marine clastic sedimentology (J.K. Leggett & G.G. Zuffa, eds.), Graham and Trotman, London, pp. 1-38.

Mutti, E., Remacha, E., Sgavetti, M., Rosell, J., Valloni, R., & Zamorano, M. (1985) Stratigraphy and facies characteristics of the Eocene Hecho Group turbidite systems, South-Central Pyrenees. In: Int. Ass. Sediment., 6th European Regional Meeting, Lleida, Spain, Excursion Guidebook, pp. 519-576.

Mutti, E., Séguret, M., & Sgavetti, M. (1988) Sedimentation and deformation in the Tertiary sequences of the Southern Pyrenees. Am. Ass. Petrol. Geol. Mediterranean Basins Conference, Spec. Publ. Inst. Geol. Univ. Parma, Italy, 157 pp.

Nagtegaal, P.J.C., & De Weerd, J.T. (1985) Provenance of Cambro-Ordovician to Oligocene sandstones in the Southern Pyrenees, Spain. Geol. Mijnb., 64: 25-40.

Nelson, B.W. (1970) Hydrography, sediment dispersal, and recent historical development of the Po River delta, Italy. In: Deltaic sedimentation: modern and ancient (J.P. Morgan, ed.), Soc. Econ. Paleont. Mineral. Spec. Publ. 15, pp. 152-184.

Nemec, W., & Steel, R.J. (1984) Alluvial and coastal conglomerates: Their significant features and some comments on gravelly mass-flow deposits. In: Sedimentology of Gravels and Conglomerates (E.H. Koster & R.J. Steel, eds.), Can. Soc. Petrol. Geol. Mem. 10, pp. 1-31.

Nemec, W., Steel, R.J., Porebski, S.J. & Spinnangr, A. (1984) Domba conglomerate, Devonian, Norway: Process and lateral variability in a mass-flow dominated, lacustrine fan-delta. In: Sedimentology of Gravels and Conglomerates (E.H. Koster & R.J. Steel, eds.), Can. Soc. Petrol. Geol. Mem. 10, pp. 295-320.

Neumann, M., & Truillet, R. (1963) Etude micropaléontologique de la formation de Piedimonte (bordure méridionale des monts Péloritains, Sicile). C. R. somm. Soc. Geol. Fr., pp. 88-90.

Nicholls, G.D. (1962) A scheme for recalculating the chemical analysis of argillaceous rocks for comparative purposes. Am. Mineral., 47: 34-46.

Nicotera, P. (1963) Rilevamento geologico dei bacini lignitiferi di Agnana e Antonimina (Calabria). L'Industria Mineraria, 14: 247-260.

Nigro, F. (1992) L'Unità Longi-Taormina nel settore di S. Agata di Militello (Messina): studio geologico preliminare. Natural. sicil. (IV), 16: 63-89.

Nijman, W. (1993) Cyclicity, basin axis shift and structural control in a nappe-top basin, Tremp-Ager Basin, Eocene, South Pyrenees. Terra Abstr., suppl. to Terra Nova, 5, pp. 668.

Nijman, W., & Nio, S.D. (1975) The Eocene Montañana delta (Tremp-Graus Basin, provinces of Lérida and Huesca, Southern Pyrenees, Spain). In: The sedimentary evolution of the Palcogene South Pyrenean Basin. IX Congr. Sedimentol., Nice, Guidebook Exc. 19, Part B, 56 pp.

Nijman, W., & Puigdefàbregas, C. (1989) The second stage of the foreland basin. In: Alluvial deposits of the successive foreland basin stages and their relation to the Pyrenean thrust sequences (C. Puigdefàbregas, W. Nijman, J.A. Muñoz, et al.). 4th Int. Conf. Fluv. Sediment. Guidebook Series, Serv. Geol. Catalunya, pp. 30-62.

Normark, W.R., & Piper, D.J.W. (1991) Initiation processes and flow evolution of turbidity currents: Implications for the depositional record. In: From shoreline to abyss: Contributions in marine geology in honor of Francis Parker Shepard (R.H. Osborne, ed.), Soc. Econ. Paleont. Mineral. Spec. Publ. 46, pp. 207-230.

Ogniben, L. (1960) Nota illustrativa dello schema geologico della Sicilia nord-orientale. Riv. Miner. Sicil., 11: 183-212.

Ogniben, L. (1973) Schema geologico della Calabria in base ai dati odierni. Geol. Romana, 12: 243-585.

Okada, H. (1971) Classification of sandstone: analysis and proposal. J. Geol., 79: 509-525.

Ori, G.G., & Friend, P.F. (1984) Sedimentary basins formed and carried piggyback on active thrust sheets. Geology, 12: 475-478.

Osborne, R.H., & Yeh, C.C. (1991) Fourier grain-shape analysis of coastal and inner continental-shelf sand samples: Oceanside littoral cell, southern Orange and San Diego counties, Southern California. In: From shoreline to abyss: contributions in marine geology in honor of Francis Parker Shepard (R.H. Osborne, ed.), Soc. Econ. Pal. Mineral. Spec. Publ. 46, pp. 51-66.

Owen, R.M. (1987) Geostatistical problems in marine placer exploration. In: Marine minerals (P.G. Teleki, M.R. Dobson, J.R. Moore & U. von Stackelberg, eds.), D. Reidel Publ. Co., Dordrecht, pp. 533-540.

Packer, B.M., & Ingersoll, R.V. (1986) Provenance and petrology of Deep Sea Drilling Project sands and sandstones from the Japan and Mariana forearc and backarc regions. Sediment. Geol., 51: 5-28.

Paola, C., Heller, P.L., & Angevine, C.L. (1992) The large-scale dynamics of grain-size variation in alluvial basins, 1: Theory. Basin Res., 4: 73-90.

Pearce, T.H. (1971) Short distance fluvial rounding of volcanic detritus. J. Sed. Petrol., 41: 1069-1072.

Pearson, M.J. (1978) Quantitative clay mineralogical analyses from the bulk chemistry of sedimentary rocks. Clays & Clay Min., 26: 423-433.

Pecorini, G., & Pomesano Cherchi, A. (1969) Ricerche geologiche e biostratigrafiche sul Campidano meridionale (Sardegna). Mem. Soc. Geol. It., 8: 421-451.

Peper, T., & De Boer, P.L. (1994) Thrust-tectonic versus climate control on rhythmicities in the Eocene South Pyrenean Tremp-Graus foreland basin: inferences from forward modeling. Tectonophys., in press.

Perlmutter, M.A., & Matthews, M.D. (1989) Global cyclostratigraphy - A model. In: Quantitative dynamic stratigraphy (T.A. Cross, ed.), Prentice-Hall, London, pp. 233-260.
Perry, K. Jr. (1967) An application of linear algebra to petrologic problems: Part I. Mineral classification. Geochim. Cosmochim. Acta, 31: 1043-1078.
Pettijohn, F.J. (1941) Persistence of heavy minerals and geologic age. J. Geol., 49: 610-625.
Pettijohn, F.J., Potter, P.E., & Siever, R. (1972) Sand and sandstone. Springer-Verlag, New York, 618 pp.
Pettijohn, F.J., Potter, P.E., & Siever, R. (1987) Sand and sandstone, second edition. Springer-Verlag, New York, 553 pp.
Pettine, M., La Noce, T., Pagnotta, R., & Puddu, A. (1985) Organic and trophic load of major Italian rivers. Mitt. Geol.-Paläont. Inst. Univ. Hamburg, 58: 417-429.
Philip, G.M., Skilbeck, C.G., & Watson, D.F. (1987) Algebraic dispersion fields on ternary diagrams. Math. Geol., 19: 171-181.
Philip, G.M., & Watson, D.F. (1988a) Determining the representative composition of a set of sandstone samples. Geol. Mag., 125: 267-272.
Philip, G.M., & Watson, D.F. (1988b) Angles measure compositional differences. Geology, 16: 976-979.
Philip, G.M., & Watson, D.F. (1988c) Some geometric aspects of the ternary diagram. J. Geol. Educ., 37: 27-29.
Pigorini, B. (1968) Sources and dispersion of recent sediments of the Adriatic Sea. Mar. Geol., 6: 187-229.
Pilkey, O.H. (1963) Heavy minerals of the U.S. South Atlantic shelf and slope. Geol. Soc. Am. Bull., 74: 641-648.
Pingitore, N.E. Jr., & Shotwell, J. (1976) Composition of sand released from three source areas under humid, low relief weathering in the North Carolina piedmont: a discussion. J. Sed. Petrol., 46: 1041-1047.
Pirkle, F.L., Pirkle, E.C., Pirkle, W.A., & Dicks, S.E. (1985) Evaluation through correlation and principal component analysis of a delta origin for the Hawthorne and Citronelle sediments of peninsular Florida. J. Geol., 93: 493-501.
Pittman, E.D. (1969) Destruction of plagioclase twins by stream transport. J. Sed. Petrol., 39: 1432-1437.
Pivnik, D.A. (1990) Thrust-generated fan-delta deposition: Little Muddy Creek conglomerate, SW Wyoming. J. Sed. Petrol., 60: 489-503.
Platt, J.P. (1986) Dynamics of orogenic wedges and the uplift of high-pressure metamorphic rocks. Geol. Soc. Am. Bull., 97: 1037-1053.
Platt, J.P., & Compagnoni, R. (1990) Alpine ductile deformation and metamorphism in a Calabrian basement nappe (Aspromonte, south Italy). Eclogae geol. Helv., 83: 41-58.
Plumley, W.J. (1948) Black Hills terrace gravels: a study in sediment transport. J. Geol., 56: 526-577.
Pollack, J.M. (1961) Significance of compositional and textural properties of South Canadian river channel sands, New Mexico, Texas, and Oklahoma. J. Sed. Petrol., 31: 15-37.
Postma, G. (1984) Mass-flow conglomerates in a submarine canyon: Abrioja fan-delta, Pliocene, southeast Spain. In: Sedimentology of Gravels and Conglomerates (E.H. Koster & R.J. Steel, eds.), Can. Soc. Petrol. Geol. Mem. 10, pp. 237-258.
Postma, G. (1990) Depositional architecture and facies of river and fan deltas: a synthesis. In: Coarse-Grained Deltas (A. Colella & D.B. Prior, eds.), Spec. Publ. Int. Ass. Sediment. 10, pp. 13-28.
Postma, G., Fortuin, A.R. & Van Wamel, W.A. (in press) Basin-fill patterns controlled by tectonics and climate: The Neogene "forearc" basins of eastern Crete as a case history. In: Sedimentation and tectonics (R.J. Steel & L.A. Frostick, eds.), Spec. Publ. Int. Ass. Sediment. ?, 000-000 (preprint).
Postma, G., Hilgen, F.J., Van Hoof, A.A.M., Langereis, C.G., & Zachariasse, W.J. (1992) Preliminary note on precession punctuated growth of a Late Miocene submarine-fan lobe on Gavdos (Greece). In: Deep water clastics: Dynamics of modern and ancient systems, abstracts (S. Gupta et al., eds.), Workshop British Sedimentological Research Group, Oxford, Great Britain, p. 26.
Postma, G., Nemec, W., & Kleinspehn, K.L. (1988) Large floating clasts in turbidites: a mechanism for their emplacement. Sediment. Geol., 58: 47-61.
Potter, P.E. (1978) Petrology and chemistry of modern big river sands. J. Geol., 86: 423-449.
Potter, P.E. (1986) South America and a few grains of sand: part 1 - beach sands. J. Geol., 94: 301-319.
Preisendorfer, R.W. (1988) Principal component analysis in meteorology and oceanography. Developments in atmospheric science 17, Elsevier Sci. Publ., Amsterdam, 425 pp.
Prell, W.L., & Kutzbach, J.E. (1987) Monsoon variability over the past 150 000 years. J. Geophys. Res., 92: 8411-8425.
Press, W.H., Flannery, B.P., Teukolsky, S.A., & Vetterling, W.T. (1989) Numerical recipes: The art of scientific computing (FORTRAN version). Cambridge University Press, Cambridge, 702 pp.
Principi, P. (1940) Sulla estensione dell'Oligocene nell'Appennino meridionale. Boll. Soc. Geol. It., 59: 167-204.
Prior, D.B., & Bornhold, B.D. (1989) Submarine sedimentation on a developing Holocene fan delta. Sedimentol., 36: 1053-1076.
Provost, A., & Allègre, C.J. (1979) Process identification and search for optimal differentiation parameters from major element data. General presentation with emphasis on the fractional crystallisation process. Geochim. Cosmochim. Acta, 43: 487-501.
Puglisi, D. (1979) Variazioni composizionali nelle arenarie del Flysch di Reitano (monti Nebrodi, Sicilia centro-settentrionale). Miner. Petrogr. Acta, 23: 13-46.

Puglisi, D. (1987a) Le successioni torbiditiche cretacio-terziarie della Sicilia nord-orientale nel quadro dell'evoluzione del settore meridionale dell'Arco Calabro-Peloritano e della Catena Maghrebide siciliana. Giorn. Geol. (3á), 49: 167-185.

Puglisi, D. (1987b) I minerali pesanti delle successione arenacee cretacio-terziarie della Catena Maghrebide siciliana. Rend. Soc. It. Miner. Petrol., 42: 155-163.

Puglisi, D. (1991) Il quarzo come indicatore di provenienza nelle arenarie delle sequenze torbiditiche oligo-mioceniche della Catena Maghrebide siciliana. Acta Natur. Ateneo Parmense, 27: 65-75.

Puglisi, D. (1992) Le successionc torbiditiche "tardorogene" della Sicilia orientale. Giorn. Geol. (3a), 54: 181-194.

Puigdefàbregas, C., Muñoz, J.A., & Vergés, J. (1989) The development of the foreland basin in the Southern Pyrenees. In: Alluvial deposits of the successive foreland basin stages and their relation to the Pyrenean thrust sequences (C. Puigdefàbregas, W. Nijman, J.A. Muñoz et al.). 4th Int. Conf. Fluv. Sediment. Guidebook Series, Serv. Geol. Catalunya, pp. 14-22.

Puigdefàbregas, C., Muñoz, J.A., & Vergés, J. (1992) Thrusting and foreland basin evolution in the Southern Pyrenees. In: Thrust tectonics (K.R. McClay, ed.), Chapman & Hall, London, pp. 247-254.

Puigdefàbregas, C., & Souquet, P. (1986) Tecto-sedimentary cycles and depositional sequences of the Mesozoic and Tertiary from the Pyrenees. Tectonophys., 129: 173-202.

Rehault, J.P., Boillot, G., & Mauffret, A. (1985) The Western Mediterranean Basin. In: Geological evolution of the Mediterranean Basin (D.J. Stanley & F.C. Wezel, eds.), Springer-Verlag, New York, pp. 101-129.

Rehault, J.P., Mascle, J., & Boillot, G. (1984) Evolution geodynamique de la Mediterranée depuis l'Oligocène. Mem. Soc. Geol. It., 27: 85-96.

Rehault, J.P., Moussat, E., & Fabbri, A. (1987) Structural evolution of the Tyrrhenian back arc basin. Mar. Geol., 74: 123-150.

Reid, M.J., Ganearz, A.J., & Albee, A.L. (1973) Constrained least-squares analysis of petrologic problems with an application to lunar sample 12040. Earth Planet. Sci. Lett., 17: 433-445.

Renner, R.M. (1988) On the resolution of compositional datasets into convex combinations of extreme vectors. Institute of Statistics and Operations Research Technical Report 88/02. Victoria University of Wellington, New Zealand, 49 pp.

Renner, R.M. (1991) An examination of the use of the logratio transformation for the testing of endmember hypotheses. Math. Geol., 23: 549-563.

Renner, R.M. (1993a) The resolution of a compositional dataset into mixtures of fixed source compositions. Appl. Statist., 42: 615-631.

Renner, R.M. (1993b) A constrained least-squares subroutine for adjusting negative estimated element concentrations to zero. Comput. Geosci., 19: 1351-1360.

Renner, R.M., Glasby, G.P., Manheim, F.T., & Lane-Bostwick, C.M. (1989) A partitioning process for geochemical datasets. In: Statistical applications in the earth sciences (F.P. Agterberg & G.F. Bonham-Carter, eds.), Geol. Surv. Can. Pap. 89-9, pp. 319-328.

Renner, R.M., & Jurke, S.R. (1992) Endmember graphics. Math. Geol., 24: 287-303.

Retgers, J.W. (1895) Ueber die mineralogische und chemische Zusammensetzung der Dünensande Hollands und über die Wichtigkeit von Flusz- und Meeressand-Untersuchungen im allgemeinen. N. Jb. Min. Geol. Pal., 1: 16-74.

Ricci Lucchi, F. (1986) The Oligocene to recent foreland basins of the northern Apennines. In: Foreland Basins (P.A. Allen & P. Homewood, eds.), Spec. Publ. Int. Ass. Sedimentol. 8, pp. 105-139.

Rice, R.M., Gorsline, D.S., & Osborne, R.H. (1976) Relationships between sand input from rivers and the composition of sands from the beaches of Southern California. Sedimentol., 23: 689-703.

Ripley, B.D. (1990) Unmixing finite mixtures. Report BP Research Sunbury, 16 pp.

Rizzini, A. (1974) Holocene sedimentary cycle and heavy-mineral distribution, Romagna-Marche coastal plain, Italy. Sediment. Geol., 11: 17-37.

Rock, N.M.S. (1987) ROBUST: an interactive FORTRAN 77 package for exploratory data analysis via robust estimates of location and scale, tests for normality and outlier assessment. Comput. Geosci., 13: 463-494.

Rock, N.M.S. (1988) Numerical geology: a source guide, glossary and selective bibliography to geological uses of computers and statistics. Lecture notes in earth sciences 18, Springer-Verlag, Berlin, 427 pp.

Roure, F., Casero, P., & Vially, R. (1991) Growth processes and melange formation in the southern Apennines accretionary wedge. Earth Planet. Sci. Lett., 102: 395-412.

Roure, F., Choukroune, P., Berastegui, X., Muñoz, J.A., Villien, A., Matheron, P., Bareyt, M., Séguret, M., Cámara, P., & Deramond, J. (1989) ECORS deep seismic data and balanced cross-sections: geometric constraints to trace the evolution of the Pyrenees. Tectonics, 8: 41-50.

Roure, F., Howell, D.G., Müller, C., & Moretti, I. (1990) Late Cenozoic subduction complex of Sicily. J. Struct. Geol., 12: 259-266.

Royden, L.H. (1985) The Vienna Basin: a thin-skinned pull-apart basin. In: Strike-slip deformation, basin formation, and sedimentation (K.T. Biddle & N. Christie-Blick, eds.), Soc. Econ. Paleont. Mineral. Spec. Publ. 37, pp. 319-338.

Russell, J.K. (1986) A FORTRAN 77 computer program for the least squares analysis of chemical data in Pearce variation diagrams. Comput. Geosci., 12: 327-338.

Russell, R.D. (1937) Mineral composition of Mississippi River sands. Geol. Soc. Am. Bull., 48: 1307-1348.

Ruxton, B.P. (1970) Labile quartz-poor sediments from young mountain ranges in Northeast Papua. J. Sed. Petrol., 40: 1262-1270.

Saccani, E. (1987) Double provenance of sand-sized sediments in the Southern Aegean forearc basin. J. Sed. Petrol., 57: 736-745.

Savage, K.M., De Cesero, P., & Potter, P.E. (1988) Mineralogic maturity of modern sand along a high-energy tropical coast: Baixada de Jacarepaguá, Rio de Janeiro, Brazil. J. South Am. Earth Sci., 1: 317-328.

Savage, K.M., & Potter, P.E. (1991) Petrology of modern sands of the Rios Guaviare and Inirida, southern Colombia: tropical climate and sand composition. J. Geol., 99: 289-298.

Schick, A.P., LeKach, J., & Hassan, M.A. (1987b) Bed load transport in desert floods: observations in the Negev. In: Sediment transport in gravel-bed rivers (C.R. Thorne et al., eds.), John Wiley & Sons, Chichester, pp. 617-642.

Schick, A.P., Hassan, M.A., & LeKach, J. (1987a) A vertical exchange model for coarse bedload movement: numerical considerations. In: Geomorphological models - Theoretical and empirical aspects (F. Ahnert, ed.), Catena Suppl. 10, pp. 73-83.

Schumm, S.A., & Stevens, M.A. (1973) Abrasion in place: a mechanism for rounding and size reduction of coarse sediments in rivers. Geology, 1: 37-40.

Schwab, F.L. (1975) Framework mineralogy and chemical composition of continental margin-type sandstones. Geology, 3: 487-490.

Schwab, F.L. (1981) Evolution of the Western continental margin, French-Italian Alps: sandstone mineralogy as an index of plate-tectonic setting. J. Geol., 89: 349-368.

Sedimentation Seminar (1988) Comparative petrographic maturity of river and beach sand, and origin of quartz arenites. J. Geol. Educ., 36: 79-87.

Self, R.P. (1975) Petrologic changes in fluvial sediments in the Rio Nautla drainage basin, Veracruz, Mexico. J. Sed. Petrol., 45: 140-149.

Shanmugam, G., Moiola, R.J., & Damuth, J.E. (1985) Eustatic control of submarine fan development. In: Submarine fans and related turbidite systems (A.H. Bouma et al., eds.), Springer-Verlag, New York, pp. 23-28.

Shukis, P.S., & Ethridge, F.G. (1975) A petrographic reconnaissance of sand size sediment: upper St. Francis River, southeastern Missouri. J. Sed. Petrol., 45: 115-127.

Siever, R. (1988) Sand. Scientific American Library, HPHLP, New York, 237 pp.

Slatt, R.M., & Eyles, N. (1981) Petrology of glacial sand: implications for the origin and mechanical durability of lithic fragments. Sedimentol., 28: 171-183.

Solomon, J.D. (1932) The heavy mineral assemblages of the Great chalky boulder-clay and Cannon-shot gravels of East Anglia, and their significance. Geol. Mag., 69: 314-320.

Sorby, H.C. (1880) On the structure and origin of non-calcareous stratified rocks. Proc. Geol. Soc. London, 36: 46-92.

Stanley, D.J., Kelling, G., Vera, J.A., & Sheng, H. (1975) Sands in the Alboran Sea: a model of input in a deep marine basin. Smithson. Contr. Earth Sci. 15, 51 pp.

Stattegger, K. (1986) Die Beziehungen zwischen Sediment und Hinterland: Mathematisch-statistische Modelle aus Schwermineraldaten rezenter fluviatiler und fossiler Sedimente. Jb. Geol. Bundes-Anst., Vienna, 128: 449-512.

Stattegger, K. (1987) Heavy minerals and provenance of sands: modeling of lithological end members from river sands of northern Austria and from sandstones of the austroalpine Gosau formation (Late Cretaceous). J. Sed. Petrol., 57: 301-310.

Stattegger, K., & Morton, A.C. (1992) Statistical analysis of garnet compositions and lithostratigraphic correlation: Brent Group sandstones of the Oseberg field, northern North Sea. In: Geology of the Brent Group (A.C. Morton, R.S. Haszeldine, M.R. Giles & S. Brown, eds.), Geol. Soc. Spec. Publ. 61, pp. 245-262.

Stormer, J.C., & Nicholls, J. (1978) XLFRAC - A program for the interactive testing of magmatic differentiation models. Comput. Geosci., 4: 143-159.

Stow, D.A.V., Howell, D.G., & Nelson, C.H. (1985) Sedimentary, tectonic, and sea-level controls. In: Submarine fans and related turbidite systems (A.H. Bouma et al., eds.), Springer-Verlag, New York, pp. 15-22.

Suttner, L.J. (1974) Sedimentary petrographic provinces: An evaluation. In: Paleogeographic provinces and provinciality (C.A. Ross, ed.), Soc. Econ. Pal. Mineral. Spec. Publ. 21, pp. 75-84.

Suttner, L.J. (1989) Recent advances in study of the detrital mineralogy of sand and sandstone: implications for teaching. J. Geol. Educ., 37: 235-240.

Suttner, L.J., & Basu, A. (1985) The effect of grain size on detrital modes: a test of the Gazzi-Dickinson point-counting method - Discussion. J. Sed. Petrol., 55: 616-617.

Suttner, L.J., & Dutta, P.K. (1986) Alluvial sandstone composition and paleoclimate, I. Framework mineralogy. J. Sed. Petrol., 56: 329-345.

Suttner, L.J., Basu, A., & Mack, G.H. (1981) Climate and the origin of quartz arenites. J. Sed. Petrol., 51: 1235-1246.

Thunell, R., Rio, D., Sprovieri, R., & Raffi, I. (1991) Limestone-marl couplets: Origin of the Early Pliocene Trubi Marls in Calabria, southern Italy. J. Sed. Petrol., 61: 1109-1122.

Thürach, H. (1884) Über das Vorkommen mikroskopischer Zirkone und Titanmineralien in den Gesteinen. Verh. Phys. Med. Ges. Würzburg, 18: 203-284.

Tortosa, A., Palomares, M., & Arribas, J. (1989) Caracterizacion composicional de los depositos arenosos actuales generados en el Sistema Central. Estudios Geol., 45: 205-213.

Trochimczyk, J., & Chayes, F. (1977) Sampling variation of principal components. Math. Geol., 9: 497-506.

Trowbridge, A.C., & Shepard, F.P. (1932) Sedimentation in Massachusetts Bay. J. Sed. Petrol., 2: 3-37.

Truillet, R. (1961) Remarques stratigraphiques et tectoniques sur la région de Novara di Sicilia (monts Péloritaines, Sicile). Bull. Soc. Geol. Fr. (7), III, 559-567.

Truillet, R. (1962) Sur les variations d'âge et de faciès des formations tertiaires sur la bordure méridionale des monts Péloritains (Sicile). Bull. Soc. geol. Fr. (7), IV: 749-753.

Underhill, J.R. (1989) Late Cenozoic deformation of the Hellenic foreland, western Greece. Geol. Soc. Am. Bull., 101: 613-634.

Valloni, R. (1985) Reading provenance from modern marine sands. In: Provenance of arenites (G.G. Zuffa, ed.), Reidel Publ. Co., Dordrecht, pp. 309-332.

Valloni, R., Marchi, M., & Mutti, E. (1985) Studio conoscitivo della moda detritica delle torbiditi eoceniche del Gruppo di Hecho (Spagna). Giorn. Geol. (3a), 46: 45-56.

Valloni, R., & Zuffa, G.G. (1984) Provenance changes for arenaceous formations of the Northern Apennines, Italy. Geol. Soc. Am. Bull., 95: 1035-1039.

Van Andel, T.H. (1950) Provenance, transport and deposition of Rhine sediments. Ph.D. Thesis, Veenman & Zonen, Wageningen, 129 pp.

Van Andel, T.H. (1964) Recent marine sediments of the Gulf of California. In: Marine geology of the Gulf of California - A symposium (T.H. Van Andel & G.G. Shor, eds.), Am. Ass. Petrol. Geol. Mem. 3, pp. 216-310.

Van Andel, T.H., & Poole, D.H. (1960) Sources of Holocene sediments in the northern Gulf of Mexico. J. Sed. Petrol., 30: 91-122.

Van Baren, F.A. (1934) Het voorkomen en de betekenis van kali-houdende mineralen in Nederlandse gronden. Ph.D. Thesis, Veenman & Zonen, Wageningen, 120 pp.

Van Baren, F.A., & Kiel, H. (1950) Contribution to the sedimentary petrology of the southern Sunda shelf. J. Sed. Petrol., 20: 185-213.

Van Bergen, P.F., Janssen, N.M.M., Alfrink, M., & Kerp, J.H.F. (1990) Recognition of organic matter types in standard palynological slides. In: International Symposium on Organic Petrology (W.J.J. Fermont & J.W. Weegink, eds.), Med. Rijks Geol. Dienst 45, pp. 9-21.

Van de Kamp, P.C., & Leake, B.E. (1985) Petrography and geochemistry of feldspathic and mafic sediments of the northeastern Pacific margin. Trans. Roy. Soc. Edinburgh: Earth Sci., 76: 411-449.

Van der Heijden, P.G.M., Mooijaart, A., & De Leeuw, J. (1992) Constrained latent budget analysis. In: Sociological methodology 1992, vol. 22 (C.C. Clogg, ed.), Basil Blackwell, Cambridge, pp. 279-320.

Van der Heijden, P.G.M. (in press) End-member analysis and latent budget analysis (comment on "the resolution of a compositional data set into mixtures of fixed source compositions" by R.M. Renner). Appl. Statist. (preprint).

Van Dijk, J.P. (1991) Basin dynamics and sequence stratigraphy in the Calabrian Arc (Central Mediterranean); records and pathways of the Crotone Basin. Geol. Mijnb., 70: 187-202.

Van Dijk, J.P. & Okkes, F.W.M. (1991) Neogene tectonostratigraphy and kinematics of Calabrian basins: Implications for the geodynamics of the Central Mediterranean. Tectonophys., 196: 23-60.

Van Haeringen, A. (1985) Oligocene to Early Miocene stratigraphy and structural evolution of the Capo Spartivento area, southern Calabria, southern Italy. Int. Rep. Stratigraphy Dept., Inst. Earth Sci., Utrecht Univ., 24 pp. (unpublished).

Van Straaten, L.M.J.U. (1970) Holocene and late-Pleistocene sedimentation in the Adriatic Sea. Geol. Rundsch., 60: 106-131.

Velbel, M.A., & Saad, M.K. (1991) Palaeoweathering or diagenesis as the principal modifier of sandstone framework composition? A case study from some Triassic rift-valley redbeds of eastern North America. In: Developments in sedimentary provenance studies (A.C. Morton, S.P. Todd & P.D. Haughton, eds.), Geol. Soc. Spec. Publ. 57, pp. 91-99.

Vergés, J., & Muñoz, J.A. (1990) Thrust sequences in the southern central Pyrenees. Bull. Soc. Geol. Fr., (8) VI: 265-271.

Vismara Schilling, A., Stradner, H., Cita, M.B., & Gaetani, M. (1976) Stratigraphic investigations on the Late Neogene of Corfou (Greece) with special reference to the Miocene/Pliocene boundary and to its geodynamic significance. Mem. Soc. Geol. It., 16: 279-317.

Wang, C.Y., Hwang, W.T., & Shi, Y. (1989) Thermal Evolution of a Rift Basin: The Tyrrhenian Sea. J. Geophys. Res. (B), 94: 3991-4006.

Watson, D.F. (1990) Reply to comment on "Measures of variability for geological data" by D.F. Watson and G.M. Philip. Math. Geol., 22: 227-231.

Watson, D.F. (1991) Reply to "Delusions of uniqueness and ineluctability" by J. Aitchison. Math. Geol., 23: 278.

Watson, D.F., & Philip, G.M. (1989) Measures of variability for geological data. Math. Geol., 21: 233-254.

Watson, G.S. (1987) Confidence regions in ternary diagrams 2. Math. Geol., 19: 347-348.

Watson, G.S., & Nguyen, H. (1985) A confidence region in a ternary diagram from point counts. Math. Geol., 17: 209-213.

Weedon, G.P., Robinson, S.G., & Jenkyns, H.C. (1991) Magnetic susceptibility as a high-resolution logging tool for Mesozoic mudrocks. In: Orbital forcing and cyclic sedimentary sequences, abstracts (P.L. De Boer, ed.), Utrecht, Netherlands, pp. 29-30.

Weltje, G.J. (1988a) Sediment-petrografische karakteristieken van de Stilo-Capo d'Orlando Formatie in het zuidoostelijk deel van het Aspromonte massief (Zuid-Calabrië, Italië). Int. Rep. Sedimentology Dept., Inst. Earth Sci., Utrecht Univ., 62 pp. (unpublished).

Weltje, G.J. (1988b) De Stilo-Capo d'Orlando Formatie in het zuidoostelijk deel van het Aspromonte massief (Zuid-Calabrië, Italië). Int. Rep. Stratigraphy Dept., Inst. Earth Sci., Utrecht Univ., 113 + 80 pp. (unpublished).

Weltje, G.J. (1992) Oligocene to Early Miocene sedimentation and tectonics in the southern part of the Calabrian-Peloritan Arc (Aspromonte, southern Italy): a record of mixed-mode piggy-back basin evolution. Basin Res., 4: 37-68. (Chapter 5 of this volume).

Weltje, G.J. (1994) End-member modelling of compositional data: numerical-statistical algorithms for solving the mixing problem in sedimentary provenance studies (Chapter 3 of this volume).

Weltje, G.J., & De Boer, P.L. (1990) Astronomically induced signals in pelagic and flysch deposits. In: Tethyan correlations: pelagic and flysch facies (K. Birkenmajer et al., eds.), Abstr. Intern. Geol. Corr. Prog. 262 Meeting, Krakow, Poland, p. 53.

Weltje, G.J., & De Boer, P.L. (1993) Astronomically induced paleoclimatic oscillations reflected in Pliocene turbidite deposits on Corfu (Greece): implications for the interpretation of higher order cyclicity in fossil turbidite systems. Geology, 21: 307-310 (Chapter 8 of this volume).

Wezel, F.C. (1973) Nuovi dati sulla età e posizione strutturale del Flysch di Tusa in Sicilia. Boll. Soc. Geol. It., 92: 193-211.

Wezel, F.C. (1974) Flysch successions and the tectonic evolution of Sicily during the Oligocene and Early Miocene. In: Geology of Italy (C.H. Squyres, ed.), Earth Sciences Soc. Libyan Arabian Republic, Tripoli, pp. 105-127.

Wezel, F.C. (1977) Widespread manifestations of Oligocene-Lower Miocene volcanism around Western Mediterranean. In: International Symposium on the structural history of the Mediterranean basins, Split (Yugoslavia), 1976, (B. Biju-Duval & L. Montadert, eds.), Editions Technip, Paris, pp. 287-302.

Whetten, J.T., Kelley, J.C., & Hanson, L.G. (1969) Characteristics of Columbia River sediment and sediment transport. J. Sed. Petrol., 39: 1149-1166.

Whitehouse, I.E., McSaveney, M.J., Knuepfer, P.L.K., & Chinn, T.J.H. (1986) Growth of weathering rinds on Torlesse Sandstone, Southern Alps, New Zealand. In: Rates of chemical weathering of rocks and minerals (S.M. Colman & D.P. Dethier, eds.), Academic Press Inc., Orlando, pp. 419-435.

Wildi, W. (1985) Heavy mineral distribution and dispersal pattern in penninic and ligurian flysch basins (Alps, northern Apennines). Giorn. Geol. (3a), 47: 77-99.

Williams, D.F., Lerche, I., & Full, W.E. (1988) Isotope chronostratigraphy: Theory and methods. Academic Press Geology series, Academic Press Inc., San Diego, 345 pp.

Williams, G.D. (1985) Thrust tectonics in the south central Pyrenees. J. Struct. Geol., 7: 11-17.

Williams, G.D., & Fischer, M.W. (1984) A balanced section across the Pyrenean orogenic belt. Tectonics, 3: 773-780.

Winkler, W., & Slaczka, A. (1992) Sediment dispersal and provenance in the Silesian, Dukla and Magura flysch nappes (outer Carpathians, Poland). Geol. Rundsch., 81: 371-382.

Wolf, K.H. (1971) Textural and compositional transitional stages between various lithic grain types (with a comment on "Interpreting detrital modes of graywacke and arkose"). J. Sed. Petrol., 41: 328-332.

Woronov, A. (1990) Methods for quantifying, statistically testing, and graphically displaying shifts in compositional abundances across data suites. Comp. Geosci., 16: 1209-1233.

Woronov, A. (1991a) Endmember unmixing of compositional data. Geochim. Cosmochim. Acta, 55: 2351-2353.

Woronov, A. (1991b) Analysis of mixtures, 32 pp. (manuscript, subm. to J. Geol.).

Woronov, A. (1991c) Enigmas and solutions in the analyses of compositional data. J. Geol. Educ., 39: 299-302.

Woronov, A., & Love, K.M. (1990) Quantifying and testing differences among means of compositional data suites. Math. Geol., 22: 837-852.

Wortel, M.J.R., & Cloetingh, S.A.P.L. (1986) On the dynamics of convergent plate boundaries and stress in the lithosphere. In: The origin of arcs (F.C. Wezel, ed.), Elsevier Sci. Publ., Amsterdam, pp. 115-140.

Wright, R. (1978) Neogene paleobathymetry of the Mediterranean based on benthic foraminifera from DSDP leg 42A. In: Initial Reports of the Deep Sea Drilling Project, Vol. 42, pt. 1, (K.J. Hsü, L. Montadert et al., eds.), U.S. Government Printing Office, Washington, pp. 837-846.

Wright, T.L., & Doherty, P.C. (1970) A linear programming and least squares computer method for solving petrologic mixing problems. Geol. Soc. Am. Bull., 81: 1995-2008.

Young, S.W., Basu, A., Mack, G.H., Darnell, N., & Suttner, L.J. (1975) Use of size-composition trends in Holocene soil and fluvial sand for paleoclimatic interpretation. Proc. 9th Int. Congr. Sedimentol., Nice, Theme 1, pp. 201-209.

Zhou, D. (1987) Robust statistics and geochemical data analysis. Math. Geol., 19: 207-218.

Zhou, D., Chen, H., & Lou, Y. (1991) The logratio approach to the classification of modern sediments and sedimentary environments in northern South China Sea. Math. Geol., 23: 157-165.

Zinkernagel, U. (1978) Cathodoluminescence of quartz and its application to sandstone petrology. Contrib. Sedimentol. 8, 69 pp.

Zoetemeijer, R., Cloetingh, S., Sassi, W., & Roure, F. (1993) Modelling of piggyback-basin stratigraphy: record of tectonic evolution. Tectonophys., 226: 000-000 (preprint).

Zuffa, G.G. (1980) Hybrid arenites: their composition and classification. J. Sed. Petrol., 50: 21-29.

Zuffa, G.G. (1985) Optical analyses of arenites: influence of methodology on compositional results. In: Provenance of arenites (G.G. Zuffa, ed.), Reidel Publ. Co., Dordrecht, pp. 165-189.

Zuffa, G.G. (1987) Unravelling hinterland and offshore palaeogeography from deep-water arenites. In: Marine clastic sedimentology (J.K. Leggett & G.G. Zuffa, eds.), Graham and Trotman, London, pp. 39-61.

Zuffa, G.G. (1991) On the use of turbidite arenites in provenance studies: critical remarks. In: Developments in sedimentary provenance studies (A.C. Morton et al., eds.), Geol. Soc. Spec. Publ. 57, pp. 23-29.

Zuppetta, A., & Sava, A. (1987) Nuovi dati sulla geologia dei dintorni di Mandanici (Monti Peloritani - Sicilia). Bol. Soc. Geol. It., 106: 347-349.

Curriculum Vitae

Gerardus Johannes Weltje werd geboren op 24 oktober 1962 te Eindhoven. In 1980 behaalde hij het diploma VWO aan de Gemeentelijke Scholengemeenschap te Doetinchem. In hetzelfde jaar begon hij met de studie Geologie aan de Rijksuniversiteit Utrecht. Het kandidaatsexamen Geologie met Scheikunde en Biologie werd in februari 1985 afgelegd. In november 1988 legde hij het doctoraalexamen Stratigrafie/Paleontologie af met bijvakken Sedimentologie en Exploratie Geofysica. Van 1 januari 1989 tot 1 mei 1989 was hij werkzaam als Toegevoegd Onderzoeker bij de Afdeling Stratigrafie/Paleontologie van de Faculteit Aardwetenschappen van de Rijksuniversiteit Utrecht, waarna hij werd aangesteld als Assistent in Opleiding bij de Afdeling Sedimentologie aan dezelfde Faculteit. Van 1 mei 1993 tot 1 augustus 1993 was hij werkzaam als Toegevoegd Docent aan de Faculteit Aardwetenschappen van de Universiteit Utrecht. Op 1 juli 1994 zal hij als Wetenschappelijk Onderzoeksmedewerker in tijdelijke dienst treden bij de Stichting NWO.